

SHRP-A-367

# **Binder Characterization and Evaluation**

## **Volume 1**

J.C. Petersen, R.E. Robertson, J.F. Branthaver,  
P.M. Harnsberger, J.J. Duvall, S.S. Kim  
Western Research Institute  
Laramie, Wyoming

D.A. Anderson, D.W. Christiansen, H.U. Bahia  
Pennsylvania Transportation Institute  
University Park, Pennsylvania



**Strategic Highway Research Program**  
National Research Council  
Washington, D.C. 1994

SHRP-A-367  
ISBN 0-309-05809-0  
Contract A-002A  
Product nos. 1001, 1008, 1010

Program Manager: *Edward T. Harrigan*  
Project Manager: *Jack S. Youtcheff*  
Program Area Secretary: *Juliet Narsiah*  
Production Editor: *Margaret S. Milhous*

May 1994

key words:

asphalt models  
asphalt rheology  
performance-related test methods  
physical-chemical relationships  
distress modes

Strategic Highway Research Program  
National Research Council  
2101 Constitution Avenue N.W.  
Washington, DC 20418

(202) 334-3774

The publication of this report does not necessarily indicate approval or endorsement by the National Academy of Sciences, the United States Government, or the American Association of State Highway and Transportation Officials or its member states of the findings, opinions, conclusions, or recommendations either inferred or specifically expressed herein.

©1994 National Academy of Sciences

1.5M/NAP/0594

## Acknowledgments

The research described herein was supported by the Strategic Highway Research Program (SHRP). SHRP is a unit of the National Research Council that was authorized by section 128 of the Surface Transportation and Uniform Relocation Assistance Act of 1987.

The A-002A research team—which includes Western Research Institute (WRI), Laramie, Wyoming, as the prime contractor; Pennsylvania Transportation Institute at Pennsylvania State University; SRI International, Menlo Park, California; and the Texas Transportation Institute at Texas A&M University—is indebted to SHRP for the support, advice, and encouragement given throughout this project. Thanks and appreciation are expressed to the A-002A Expert Task Group for its regular review and valuable advice given freely throughout the project.

The authors express their thanks and appreciation to the senior management of WRI for its support and encouragement throughout this project. Further, the authors are greatly indebted and express special thanks to Jackie Greaser, Project Secretary, who has typed and assembled tremendous volumes of the technical documentation of A-002A, and to Dawn Geldien, Project Administrator, who has attended to the substantial volumes of detailed administration of A-002A. Finally, the authors express thanks and appreciation to Dr. John Schabron and his groups at WRI for support of this project in conducting routine analyses. Dr. Keith Ensley conducted the thermochemical measurements and Mr. Hank Plancher conducted the rheological measurements that led to the model discussed in this volume.

# Contents

## Volume 1

|   |      |
|---|------|
| List of Figures   | ix   |
| List of Tables  | xiii |
| Abstract  | 1    |
| Executive Summary   | 3    |
| Chapter 1 Introduction and Discussion of Asphalt Model                                | 9    |
| Problem Statement   | 9    |
| Background  | 10   |
| Asphalt Model: Historical Development from the Chemist's Perspective                  | 11   |
| Introduction  | 11   |
| Asphaltenes in Petroleum and Origin of Colloidal Model                                | 11   |
| Associations of Polar Molecules in Petroleum Residua                                  | 15   |
| The Nature of Asphaltenes in Petroleum Residua  | 17   |
| Model Proposed at the Beginning of the Binder Characterization and Evaluation Program | 19   |
| Colloidal Models and Rheological Behavior   | 21   |
| Micellar Colloidal Model and Rheological Behavior                                     | 21   |
| Summary of Current Colloidal Models as Used in Colloidal Science                      | 23   |
| Applicability of Current Colloidal Models to Asphalt Cement                           | 24   |
| Chapter 2 Performance-Related Test Method and Specification Development               | 27   |
| Need for New Measurements   | 27   |
| Viscosity Measurements  | 27   |
| Shear Susceptibility  | 28   |
| Temperature Susceptibility  | 29   |
| Nomographs and Their Inadequacies   | 31   |
| Aging Indexes   | 31   |
| Need for Improved Properties for Use as Specification Criteria                        | 31   |
| Development of New Specification Test Methods   | 32   |
| Strategy for Selecting Specification Properties                                       | 32   |

|            |   |     |
|------------|---|-----|
|            | Distress Modes Considered . . . . .   | 33  |
|            | Consideration of Rutting in Specification . . . . .                           | 34  |
|            | Consideration of Thermal Cracking in Specification . . . . .                  | 35  |
|            | Consideration of Fatigue Cracking in Specification . . . . .                  | 36  |
|            | Consideration of Aging in Specification . . . . .                             | 37  |
|            | Validation of Pressure-Aging Test . . . . .                                   | 38  |
|            | Consideration of Environmental Effects and Specification Philosophy . . . . . | 38  |
|            | Proposed Specification Tests . . . . .  | 39  |
|            | Selected Test Methods . . . . .   | 40  |
| Chapter 3  | Relationships between Chemical Composition and Physical Properties . . . . .  | 69  |
|            | Physical Properties That Relate to the Microstructural Model:                 |     |
|            | Observed Physical Behavior That Must Be Explained by the                      |     |
|            | Microstructural Model . . . . .   | 69  |
|            | Rheological Model . . . . .   | 72  |
|            | Overall Approach to Development of Physical-Chemical Relationships . . . . .  | 76  |
|            | Physical-Chemical Property Relationship Based on Model Parameters . . . . .   | 77  |
|            | Statistical Evaluation of Extended Asphalt Database . . . . .                 | 77  |
|            | Temperature Dependence Related to Microstructural Parameters . . . . .        | 78  |
|            | Time Dependence Related to Microstructural Parameters . . . . .               | 80  |
|            | Relaxation Spectrum Related to Microstructural Parameters . . . . .           | 82  |
|            | Fracture and Fatigue Properties Related to Microstructural                    |     |
|            | Model Parameters . . . . .  | 83  |
|            | Oxidative Aging Related to Microstructural Model Parameters . . . . .         | 84  |
|            | Specification Properties Predicted from Microstructural Model                 |     |
|            | Parameters . . . . .  | 85  |
|            | Summary of Physical-Chemical Property Relationships . . . . .                 | 85  |
|            | Rheological Evidence for a Microstructural Model . . . . .                    | 86  |
|            | Relationships between Chemical Properties and Rheological                     |     |
|            | Parameters of SHRP Asphalts Emphasizing the Core Asphalts . . . . .           | 88  |
|            | Prediction of Physical Properties from Chemical Data . . . . .                | 91  |
|            | Microstructural Model and Results of Chemical Studies . . . . .               | 92  |
| Chapter 4  | Summary . . . . .   | 139 |
| References | . . . . .   | 145 |

## **Volume 2**

- Chapter 1 Separation of Asphalts by Chemical Functionality
- Chapter 2 Size Exclusion Chromatography Separations of Asphalts
- Chapter 3 Rheological Studies of Mixtures of Model Compounds with Asphalts
- Chapter 4 Potentiometric Titration Studies
- Chapter 5 Polarity of Asphalt
- Chapter 6 Molecular Structuring Studies
- Chapter 7 Oxidation Pathways for Asphalt
- Chapter 8 Aging Studies of Asphalt
- Chapter 9 Characterization of Asphalts by Classical Methods
- Appendix A Supplementary Figures and Tables
- Appendix B List of Tables Available in Database
- Appendix C Lot Number for Resins Used in Ion Exchange Chromatography Separations
- Appendix D Separation of a Quinolone-Enriched Fraction from SHRP Asphalts

## **Volume 3**

- Chapter 1 Linear Viscoelastic Model
- Chapter 2 Rheological Measurements
- Chapter 3 Low-Temperature Physical Hardening
- Chapter 4 Fracture and Fatigue
- Chapter 5 Oxidative Aging Studies
- Chapter 6 Miscellaneous Tests

## **Volume 4**

- Chapter 1    Dynamic Shear Rheometer
- Chapter 2    Bending Beam Rheometer
- Chapter 3    Direct Tension
- Chapter 4    Pressure Aging Vessel Procedure
- Chapter 5    Rotational Viscometry
- Chapter 6    Analyses of Asphalts by Standard Analytical Techniques
- Chapter 7    Separation of Asphalts by Ion Exchange Chromatography
- Chapter 8    Analysis of Nonpolar Fractions of Asphalts by Supercritical Fluid Chromatography
- Chapter 9    Separation and Analysis of Asphalts by Size Exclusion Chromatography
- Chapter 10    Oxidation of Asphalts by Thermal, Catalytic, and High Pressure Methods
- Chapter 11    Potentiometric Titrations of Asphalts
- Chapter 12    Rheological Measurements of Asphalts
- Appendix A    Determining the Rheological Properties of Asphalt Binder Using a Dynamic Shear Rheometer (DSR)
- Appendix B    Determining the Flexural Creep Stiffness of Asphalt Binder Using the Bending Beam Rheometer
- Appendix C    Determining the Fracture Properties of Asphalt Binder in Direct Tension
- Appendix D    Extraction and Recovery of Asphalt Cement for Rheological Testing

## List of Figures

|             |   |    |
|-------------|---|----|
| Figure 2.1  | Shear Rate as a Function of Loading Time in a Creep Test . . . . .  | 41 |
| Figure 2.2  | Time Required to Obtain Steady-State Flow at Different<br>Temperatures in a Creep Test . . . . .  | 42 |
| Figure 2.3  | Illustration of Constant-Power Viscosity (after Schweyer et al. 1976) . . .   | 43 |
| Figure 2.4  | Illustration of Technique for Obtaining Viscosity at Zero Shear Rate<br>(after Puzinauskas 1979) . . . . .  | 44 |
| Figure 2.5  | Penetration Index (Based on Penetration at 25°C [77°F] and Ring and<br>Ball Softening-Point Temperature) versus Rheological Type as Measured<br>by Rheological Index, for Eight Asphalt Types . . . . . | 45 |
| Figure 2.6  | Effect of Aging on Rheological Index . . . . .  | 46 |
| Figure 2.7  | Comparison of Temperature-Susceptibility Parameters Calculated<br>by Different Methods . . . . .  | 47 |
| Figure 2.8  | Isochronal Curves of Extensional Stiffness Modulus, as Measured<br>and as Predicted from van der Poel's Nomograph; SHRP Asphalts<br>AAG-1 (Top) and AAK-1 (Bottom) . . . . .                            | 48 |
| Figure 2.9  | Changes in Master Curve (Extensional Stiffness) for SHRP Asphalt<br>AAD-1 during Laboratory Aging . . . . .   | 49 |
| Figure 2.10 | Aging Indexes Based on Different Loading Times and Test<br>Temperatures . . . . .   | 50 |
| Figure 2.11 | Schematic Illustration of Viscosity-Grading System . . . . .  | 51 |
| Figure 2.12 | Flow Diagram Illustrating Strategy for Developing the<br>SHRP Binder Specification . . . . .  | 52 |



|             |   |    |
|-------------|---|----|
| Figure 2.13 | Ranking of Materials Reference Library Asphalts in Tank<br>Condition: Temperature at Which $G^*/\sin \delta = 1$ kPa at a Loading<br>Frequency of 10 rad/s . . . . .        | 53 |
| Figure 2.14 | Ranking of Materials Reference Library Asphalts after Thin-Film Oven<br>Aging: Temperature at Which $G^*/\sin \delta = 2$ kPa at Loading Frequency<br>of 10 rad/s . . . . . | 54 |
| Figure 2.15 | Loss Compliance versus Wheel-Tracking Test Results (after<br>Bouldin, personal communication, 1992) . . . . .   | 55 |
| Figure 2.16 | Ranking of Materials Reference Library Asphalts in Tank<br>Condition: Temperature at Which Stiffness Is 200 MPa after<br>60 Seconds Loading Time . . . . .                  | 56 |
| Figure 2.17 | Ranking of Materials Reference Library Asphalts after Pressure<br>Aging: Temperature at Which $m = 0.35$ after 120 Seconds<br>Loading Time . . . . .                        | 57 |
| Figure 2.18 | Typical Effect of Polymer Modification on Master Curve of<br>Asphalt Cement . . . . .   | 58 |
| Figure 2.19 | Typical Effect of Polymer Modification on Ultimate Properties of<br>Asphalt Cement . . . . .  | 59 |
| Figure 2.20 | Typical Failure Strain Master Curve Showing Transition to Brittle<br>Region . . . . .   | 60 |
| Figure 2.21 | Ranking of Materials Reference Library Asphalts after Pressure<br>Aging: Temperature at Which Strain-to-Failure Strain = 1 Percent . . . .                                  | 61 |
| Figure 2.22 | Evaluation of Fatigue Performance in Zaca-Wigmore Field Trials . . . . .  | 62 |
| Figure 2.23 | Ranking of Materials Reference Library Asphalts after Pressure<br>Aging: Temperature at Which $G^* \sin \delta = 3$ MPa . . . . .   | 63 |
| Figure 2.24 | Comparison of Rheological Changes in Asphalt during Pressure<br>Aging . . . . .   | 64 |
| Figure 2.25 | Flow Diagram of the Experiment to Validate that the Chemistry and<br>Rheology of Pressure-Aging Vessel Residue Relate to Field Exposure . .                                 | 65 |
| Figure 2.26 | Rheological Behavior Determined in the Laboratory as Compared<br>with Field Data . . . . .  | 66 |
| Figure 2.27 | Complex Modulus at 25°C at Various Road Sections for Field Validation<br>Experiment . . . . .   | 67 |

|             |  |     |
|-------------|--|-----|
| Figure 2.28 | Size Exclusion Chromatography Fraction I at 25°C at Various Road Sections for Field Validation Experiment . . . . .  | 68  |
| Figure 3.1  | Typical Master Curve for Asphalt Cement . . . . .  | 97  |
| Figure 3.2  | Relaxation Spectra for Asphalts AAB-1 and AAG-1 . . . . .  | 98  |
| Figure 3.3  | Failure Strain versus Secant Modulus at Failure . . . . .  | 99  |
| Figure 3.4  | Definition of Rheological Model Used for Predictions . . . . .   | 100 |
| Figure 3.5  | Relationship between Performance, Rheological and Microstructural Models, and Chemistry . . . . .  | 101 |
| Figure 3.6  | Experiment Design to Establish Physical-Chemical Property Relationships . . . . .  | 102 |
| Figure 3.7  | Relationship between Dilatometrically Determined Glass Transition Temperature and Defining Temperature . . . . .   | 103 |
| Figure 3.8  | Predicted versus Measured Values of the Defining Temperature Predicted from Asphaltene Content and Number-Average Molecular Weight . . . . .                       | 104 |
| Figure 3.9  | Predicted versus Measured Values of the Steady-State Viscosity at the Defining Temperature Predicted from Asphaltene and Polar Aromatic Content . . . . .          | 105 |
| Figure 3.10 | Predicted versus Measured Values of the Crossover Frequency Predicted from Asphaltene Content . . . . .  | 106 |
| Figure 3.11 | Predicted versus Measured Values of the Rheological Index Predicted from Number-Average Molecular Weight and Gaestel Index . . . . .                               | 107 |
| Figure 3.12 | Tensile Strength versus Molecular Weight When Failure Strain Is 1 Percent . . . . .  | 108 |
| Figure 3.13 | Values of Complex Modulus Predicted from Microstructural Model Parameters versus Measured Values, 10 rad/s for Materials Reference Library Tank Asphalts . . . . . | 109 |
| Figure 3.14 | Values of Loss Tangent Predicted from Microstructural Model Parameters versus Measured Values, 10 rad/s for Materials Reference Library Tank Asphalts . . . . .    | 110 |

|             |  |     |
|-------------|--|-----|
| Figure 3.15 | Values of Shift Factors Predicted from Microstructural Model Parameters versus Measured Values, 10 rad/s for Materials Reference Library Tank Asphalts . . . . . | 111 |
| Figure 3.16 | Viscosities of Asphalt Cements Measured and Predicted by Chemical Properties . . . . .   | 112 |
| Figure 3.17 | Activation Energy for Viscous Flow Calculated and Predicted by Chemical Properties . . . . .   | 113 |
| Figure 3.18 | Viscosities of Ion Exchange Chromatography Neutrals Measured and Predicted by Chemical Properties . . . . .  | 114 |
| Figure 3.19 | Aging Index (Thin-Film Oven Test) of Asphalt Cements Determined and Predicted by Chemical Properties . . . . .   | 115 |
| Figure 3.20 | Aging Index (Thin-Film Oven Test-Pressure-Aging Vessel Test) of Asphalt Cements Determined and Predicted by Chemical Properties . . .                            | 116 |

## List of Tables

|            |   |     |
|------------|---|-----|
| Table 3.1  | Definitions of Physical and Chemical Parameters . . . . .   | 117 |
| Table 3.2  | Linear Viscoelastic Model Parameters . . . . .  | 118 |
| Table 3.3  | Corbett and Size Exclusion Chromatography Parameters . . . . .  | 119 |
| Table 3.4  | Elemental Analysis . . . . .  | 120 |
| Table 3.5  | Computed Indexes . . . . .  | 121 |
| Table 3.6  | Pearson Correlation Coefficients for Physical-Chemical Data . . . . .   | 122 |
| Table 3.7  | $T_d$ Correlated with Compositional Parameters . . . . .  | 125 |
| Table 3.8  | $R$ Correlated with Compositional Parameters . . . . .  | 127 |
| Table 3.9  | $\log \omega_{cTd}$ Correlated with Composition Parameters . . . . .  | 129 |
| Table 3.10 | $\log \eta_{Td}$ Correlated with Compositional Parameters . . . . .   | 131 |
| Table 3.11 | $H(\tau)_{\text{mode}}$ Correlated with Compositional Parameters . . . . .  | 133 |
| Table 3.12 | $AI_{\text{vis60}}$ Correlated with Compositional Parameters . . . . .  | 134 |
| Table 3.13 | Correlations between Heteroatom Content and Selected Chemical and Physical Properties of Core Asphalts Using Simple Linear Regression . . . . . | 136 |
| Table 3.14 | Correlations between Defining Temperature and Combinations of Chemical Properties of Core Asphalts Using Simple Linear Regression . . . . .     | 136 |
| Table 3.15 | Correlations between Crossover Frequency and Combinations of Chemical Properties of Core Asphalts Using Simple Linear Regression . . . . .      | 137 |

Table 3.16      Correlations Between Rheological Index and Combinations  
of Chemical Properties of Core Asphalts Using Simple Linear  
Regression . . . . . 137

## **Abstract**

This final report, in four volumes, of Strategic Highway Research Program (SHRP) Project A-002A describes intensive investigations of the chemical and physical properties of petroleum asphalts used in the construction of highway pavements. The emphasis in the chemical studies has been to measure and understand the various interactions among molecular species that contribute to a high molecular weight-like behavior that explains the rheological behavior of asphalt. In the measurement of physical properties primary emphasis was given to the characterization of rheological behavior, that is, viscoelastic behavior as a function of temperature and loading rate. The fracture (direct tension) behavior of asphalt cement was also investigated and limited studies were conducted on fatigue behavior and other miscellaneous physical properties. Correlation of chemical and physical properties to explain the nature of asphalt in terms of a self-consistent model has been another major effort, which in the main has been accomplished. The self-consistent description of petroleum asphalt has been used further to develop predictive capability for describing the anticipated performance of asphalts in roadways. The model and predictive capability constitute the major portion of volume 1. The chemical studies and their implications constitute volume 2. Physical property and field validation studies constitute volume 3, and volume 4 contains detailed descriptions of techniques, both established and newly developed, used throughout SHRP Project A-002A.

## Executive Summary

The objectives of Strategic Highway Research Program (SHRP) Project A-002A, "Binder Characterization and Evaluation," were to develop a clear understanding of the fundamental chemical and physical properties of petroleum asphalts and to correlate the effects of variations in composition on physical properties, including those that change with aging, that affect performance of asphalt in roadways. The importance of this undertaking was to be able to describe, or predict, expected behavioral characteristics for any given asphalt. Hence, one should be able to select the most suitable asphalt for a given road construction project.

There are several major products of this research that support meeting the objectives. One important product is the development of a highly refined and self-consistent microstructural model that can be used to describe the wide variety of materials known as *asphalt*. Clearly, the results of this study show that asphalts differ greatly. The compositional studies have revealed major variations in the amount and nature of the polar materials forming some sort of microstructure and major variations in the neutral ("dispersing") materials. These variations in composition affect the rheology, which in turn affects the behavioral characteristics.

The differences among asphalts affect, and can be seen (measured) in, the physical properties. A major tool used in this project to study physical properties was rheometry, in which the viscoelastic properties of asphalt and modified asphalt as a function of temperature are readily measurable. The utility of this method has been demonstrated, and it now is accepted within the asphalt industry. Further, rheological measurements have become a significant part of the new SHRP specifications. Other products are the development of a much clearer understanding of the fracture properties of asphalt and a clear understanding of, and methodology to measure, the effects of prolonged low temperature (*low-temperature physical hardening*).

Aging is a long-recognized but difficult-to-predict process that occurs in asphalts in roadways. Major products of the A-002A research in aging are development of an improved understanding of the mechanism of asphalt oxidation and how oxidation affects aging, identification of changes in newly identified amphoteric compounds upon oxidation, and development of methods to simulate pavement oxidative aging. It is clear now that oxidation and aging are related by way of the strength of the microstructure formed during oxidation and not directly related to concentrations of oxidation products alone. Some

asphalts age greatly with little oxidation, others age little with large amounts of oxidation, and most are between these extremes. Asphalts appear to age by some process involving generation of free radicals, but not by a free radical chain mechanism. Asphalts contain components that react rapidly with oxygen, and these intermediates may subsequently react with other asphalt components.

Still another set of products of the A-002A project is the numerous new, newly applied, or greatly improved laboratory methods to predict the behavioral characteristics of asphalts in pavements. Volume 4 is devoted to details of these methods.

The chemical studies conducted for SHRP have been primarily to validate the existence and nature of a microstructure in petroleum asphalt, and the nature and effects of oxidative aging on this structure. Numerous types of experiments were conducted in support of these efforts, which are referred to collectively as the development of a SHRP chemical model of petroleum asphalt. Volume 2 relates the history and details of the chemical studies in the development of the SHRP model.

Asphalts have been separated into chemically meaningful fractions since the beginning of this project. Ion exchange chromatography (IEC) has been used extensively to separate asphalts into strong and weak acids; strong and weak bases; neutrals; and another significant fraction, *amphoterics*, which are compounds with both acid and base functions in one molecule. Isolating amphoteric and studying their properties have required substantial effort during this project. Significant amounts of analytical data have been acquired for these materials. It is quite clear that acidic and basic functions—especially amphoteric, which contain both functions—have a profound effect on the viscoelastic properties of asphalt. Quantitative and qualitative analyses of basic functions, in whole asphalts, have been achieved separately from IEC using nonaqueous potentiometric titration (NAPT), which measures both quantity and relative strength of bases.

Asphalts exhibit significant elastic character at service temperatures, as shown by their rheologies, and it is inferred from fundamental physical chemistry that high molecular weight species, or species that behave as if they are high molecular weight, are responsible for this property. However, when molecular weights are measured by methods that determine molecular weight at or very near the molecular level, the values are relatively small. Rarely does an asphalt have any true molecular species that is significantly larger than a few thousand daltons (molecular weight units), yet rheological measurements at service temperatures suggest that some species in asphalt behave as if they have molecular weights in the tens of thousands. Hence, the hypothesis put forth in years past that some of the relatively small molecules in asphalt associate so strongly that they act like a high molecular weight material has been tested in detail. This association is also described as a three-dimensional microstructure. This information was needed to determine how changes in observed viscous and elastic properties are driven by changes in the microstructure as a function of temperature and shear.

It is theorized that the observed high molecular weight-like behavior results from both electrostatic and  $\pi$ - $\pi$  bonding, both of which are significantly weaker than covalent bonding. Hence, one expects that high molecular weight, resulting from frequent weak



bonds, will change with temperature and shear. This explains the observed viscoelastic properties as a function of shear or temperature.

Self-assembly of polar molecules into a microstructure requires two or more points of attachment per molecule (as in polymer chemistry). While this might be achieved across the dipole of a functional group, it is more likely that bifunctional species are responsible. So it is likely that multifunctional molecules such as amphoteric have the most profound effect on the physical properties of asphalt. Amphoterics have very high aromatic carbon and hydrogen contents, as shown by nuclear magnetic resonance spectroscopy and elemental analyses, and are assumed to contain condensed aromatic ring units that bond by  $\pi$ - $\pi$  interaction in addition to the known acid-base interactions. Spiking experiments using small amounts of amphoteric in tank asphalts have verified that amphoteric cause disproportionate increases in viscosity and elasticity.

Another important tool for validating the microstructural model has been size exclusion chromatography (SEC). Separation of asphalts by SEC has shown that large units, much larger than the molecular level, do exist and can be isolated from asphalt.

Neutral IEC fractions, as expected, show practically no basic or acidic function by NAPT, but do vary significantly among asphalts. The glass transition data were plotted versus the activation energy of viscous flow ( $E_a$ ) for the core asphalts. There is a very strong correlation; that is, the glass transition temperature may be predicted from  $E_a$  at 25°C and 60°C (77°F and 140°F). The highest  $E_a$  values were among the high-compatibility asphalts, those asphalts whose properties are dominated by the more neutral materials. This observation may also be important in predicting low-temperature cracking propensity.

The understanding of the contribution of any given chemical compound type to the rheology of asphalt, coupled with a rapid method to measure rheology over a wide temperature range, greatly improves and simplifies predicting what types of materials (modifiers) are needed to effect desired changes in asphalt physical properties.

The behaviors of asphalts in terms of the refined chemical model, as described thus far, should be measurable in terms of physical properties. A major effort has been the study of the rheology, or the viscoelastic properties, to determine the effects of shear, shear rate, and temperature. This effort has resulted in description of asphalt in terms of rheological master curves that show the variation in viscous and elastic components with shear and temperature. In general, all asphalts exhibit a glasslike behavior at very low temperature, and are relatively fluid at high temperature, but the pathway from glass to fluid, or vice versa, varies substantially from one asphalt to another. Historically, this variation was known as *temperature susceptibility*, but a single temperature susceptibility is a straight-line relationship of log viscosity between two temperatures. The classic idea of temperature susceptibility was shown to be substantially in error. The master curve shows that there are a series of temperature susceptibilities for each asphalt and that the sets vary among asphalts. The master curve varies with asphalt source. Hence, no two-point measurement can describe the variation in viscoelastic properties for asphalts. Determining rheological master curves in detail is a time-consuming process. During the A-002A project, a set of

three points, at appropriate temperatures, was chosen, and it was demonstrated that a reliable simulation of the master curve for any asphalt could be obtained relatively rapidly.

Fracture properties of asphalts at low temperatures were studied in detail. This study resulted in the development of a relatively simple method to measure tensile strengths of asphalts at low temperatures for prolonged periods. Volume 3 is a detailed account of the various physical property studies.

Another major area of chemical studies during the project has been oxidation (with air) and the accompanying age hardening of asphalt. The research examined three principal areas: (1) the mechanism of oxidation, (2) artificial aging of asphalt with air under pressure in a pressure-aging vessel (PAV), and (3) the effect of aggregate on oxidative aging.

The extensive PAV studies show that asphalts oxidize increasingly with increased time and temperature and that some but not all asphalts experience a very sharp temperature dependence at higher pavement service temperatures (60–85°C [140–185°F]). Aging propensity is dependent on asphalt source. Age hardening in asphalts has been shown to correlate reasonably well with the concentration of ketones formed upon oxidation for asphalt from any given crude oil, regardless of grade, but differs sharply among asphalts from different crudes; the field validation study confirms this finding. The amount of ketones, which are primary viscosity builders, formed in asphalt from one crude oil cannot be used to predict viscosity changes in asphalt from another crude oil solely on the basis of ketone concentration. This method is valuable to demonstrate the age-hardening sensitivity of an asphalt to its own oxidation products.

There were also PAV experiments to age core asphalts on aggregates. The chemistry of aging does not appear to change over limited temperature ranges, whether the asphalt is neat or on aggregate. There are, however, variations in the rate of oxidation on aggregate. Generally, it is observed that the aging propensity of asphalt, though it can be defined well for binder alone, is somewhat scrambled when the binder is oxidatively aged on aggregate. Nonetheless, such testing was necessary to determine whether an oxidative aging test for binder alone is sufficiently reliable to predict aging in asphalt concrete. The results suggest that an aging test on binder alone is sufficient to predict (generally) aging in asphalt concrete.

The effects of oxidation on aging can be explained further in terms of amphoteric. The appearance of new amphoteric formed upon oxidation, as shown by NAPT, should promote development of microstructure, with an accompanying increase in viscosity and elasticity, as was demonstrated by spiking asphalts with IEC-separated amphoteric.

The particular state of alignment, or organization, of polar molecules into a microstructure in whole asphalt appears to be a metastable condition. If the model is correct, this should be the case; that is, various stresses should cause reorientation of self-assembled polars. On the other hand, an asphalt left undisturbed should experience a slow increase in orientation of polars, which should be easily observable in its viscoelastic properties. This type of molecular structuring (historically known as *steric hardening*) was studied at a modest level during the project. Hardening of tank asphalts shows up as rather minor increases in

viscoelastic properties with prolonged storage. However, asphalts that were exposed to PAV conditions showed substantial increases in viscosity upon storage for prolonged periods. In one case, the viscosity of an aged asphalt rose 11 million poise (1.1 million Pa·s) over 7 months while stored at 25°C (77°F).

At one point, it was deemed worthwhile to determine whether there was a linear Arrhenius relationship for oxidation of asphalts as a function of temperature. The research was set up as a limited-size, high-risk effort to determine whether it is or is not probable that the mechanism of oxidation changes drastically with temperature. Values of the rate constant ( $k$ ) for formation of oxidation products versus  $1/T$  were to be plotted for this evaluation. Constant values of  $k$  versus time would be needed first but were found not to exist. This absence indicates that the relative contribution of each reaction (especially oxidation reactions) changes with time, even at constant temperature.

In summary, a highly refined, self-consistent model of asphalt was developed and used to predict how the fundamental physical properties that govern performance should be measured. In turn, extensive studies of fundamental physical properties were performed. The results of these studies were employed extensively by SHRP to develop new, performance-based specifications for asphalts.

## **Introduction and Discussion of Asphalt Model**

### **Problem Statement**

The Strategic Highway Research Program (SHRP) was originally conceived in response to a perception within the highway industry that, after the Arab oil embargo of 1972, the quality of paving-grade asphalt had in many instances deteriorated to an unacceptable level. This perceived deterioration was, and still is, cited as the cause of an unacceptable rate of early pavement failures. Because of this perception, the primary objective of the asphalt-related portion of SHRP was to develop performance-related specifications for asphalt cement binders and asphalt concrete mixtures that protect against early pavement failure.

The existing specification tests for asphalt binders, and their associated test methods, are not performance-related and therefore cannot be used either to relate the chemistry of asphalt cement to performance or to develop performance-related specifications that warrant pavement performance. Performance-related physical and chemical test methods are needed to characterize asphalt binders to properly develop performance-related specifications and to ascertain the quality of current paving-grade asphalts. Further, to determine whether current paving-grade asphalts are deficient in certain components allegedly essential to performance—the so-called goodies or stickies (discussed more fully below)—the basic chemical nature of asphalt must be ascertained and related to the physical properties on which the specifications are based. In summary, the SHRP Binder Characterization and Evaluation Program (A-002A) addressed several major objectives:

- Develop test methods that elucidate the basic chemical structure of asphalt cement.
- Develop methods for testing fundamental physical properties that are related to in-service pavement performance and that can be related to basic chemical structure.

- Develop a conceptual microstructural model that can be used to relate the physical and chemical properties of asphalt cement.
- Use the microstructural model to validate relationships between the chemical and physical properties of asphalt cement.

## Background

There is a general sentiment among highway construction and maintenance personnel that asphalts of commerce have changed since the energy crises of the 1960s and 1970s (Anderson et al. 1983; Button and Epps 1985). Moreover, it is widely believed that these changes have been the principal cause of many performance failures in asphalt concrete mixes in the past two decades. Colloquially, this hypothesis is formulated in the statement that petroleum refiners have taken the goodies or stickies out of asphalts. Furthermore, it is sometimes alleged that this removal of goodies or stickies has been accomplished with such ingenuity that currently employed asphalt specification tests are incapable of detecting the absence of these critical materials. If the hypothesis is valid, methods for detecting goodies and stickies and determining their influence on asphalt performance need to be developed.

It is true that refineries currently process more heavy crudes than formerly. Heavy crudes contain a much smaller proportion of volatile matter than lighter crudes. They also contain more of the heteroatoms nitrogen, sulfur, oxygen, and metals. Heavy crudes also tend to be more naphthenic and aromatic than lighter crudes. For these reasons, they tend to be difficult to process, and refiners employ special methods to convert them into salable products. Some heavy crudes are hydrotreated before fractionation. Others are subjected to solvent treatments (e.g., the ROSE process). While many asphalts are distillation residua, some asphalts of commerce are made by other means. Above all, it should be emphasized that heavy crudes are much more complex than light crudes, and that distillation residua from the two materials may not necessarily have similar properties. Also, distillation residua from different heavy crudes vary substantially in many properties, and many more crudes (in much greater variety) are being processed today than 20 to 30 years ago. This variability in the crude stream has contributed to the perception that asphalt quality has deteriorated (Anderson et al. 1983). So the anxiety that currently available asphalts of commerce might be different from those formerly available is not entirely unfounded. However, the reasons for such differences, if indeed they seriously affect asphalt performance, have been well advertised in the open petroleum literature. Those who employ asphalts as paving materials would be well advised to become familiar with the history of their supply line.

The difficulty with this theory is that it does not readily explain why most pavements do not fail, assuming there are agreed standards of performance. Asphalts from the same crude base are used to make a large number of pavements, with varying observed performance. If goodies and stickies were routinely removed, this variation would not exist. If some refiners removed critical components and others did not, that fact would soon become statistically obvious. If all refiners began removing goodies and stickies from asphalts at one time in the past, then pavements constructed since that time should all exhibit similar performance

problems not observed in previously constructed pavements. Moreover, the hypothesis conflicts with another widely held belief: that in highway construction the overriding consideration is proper mix design, and that compositional differences among asphalts are of little importance as long as certain specifications are met. If asphalt composition is of little importance, then by definition asphalts that meet specifications need not contain crucial property-influencing components such as goodies and stickies, or to put the argument another way, the absence of goodies or stickies from asphalts can hardly matter. The hypothesis that goodies or stickies have been removed is scientifically untestable in its commonly stated form. Pavements that do not fail were properly designed. Pavements that fail are always found to have some critical flaw, previously unrevealed, in their designs.

## **Asphalt Model: Historical Development from the Chemist's Perspective**

### *Introduction*

The following discussion outlines the development of ideas about the relationship between asphalt physical properties and asphalt composition. This survey of historical data includes studies from the refining and geochemical literature, in addition to the asphalt literature. Much of the work was published after SHRP began. In chapter 3, results from experiments performed in the Binder Characterization and Evaluation Program will be discussed and will be compared with results from other studies.

Except for a minor amount of naturally occurring asphalt, commercial asphalts are products of petroleum refining operations. Therefore, the composition of an asphalt must be related to that of the crude oil from which the asphalt is manufactured. Most asphalts are residua from distillation of petroleum, some of which have been subjected to mild air oxidation.

However, most distillation residua from crude oils are not converted into asphalt. Corbett and Schweyer (1981) claimed that of the 1100 crude oil streams refined in North America, about 260 were being used to make paving asphalt. Thus, the distillation residua of most crude oils are further treated to make more transport fuel or are burned as fuel oil. Refining the "bottom of the barrel" materials is not easy, and fossil fuel research laboratories have expended considerable effort to determine the best ways to process heavy feeds. Thus, a great deal of research has been performed on materials that are closely related to commercial asphalts, and much understanding of the nature of petroleum residua has been acquired outside of asphalt science.

### *Asphaltenes in Petroleum and Origin of Colloidal Model*

Very early in the study of crude oils, it was observed that mixing oils with several volumes of normal alkane solvents (propane, *n*-butane, *n*-pentane, *n*-hexane, *n*-heptane) resulted in the precipitation of black, friable solids called *asphaltenes*. These solids are relatively enriched in heteroatoms (nitrogen, oxygen, sulfur, metals) and are more aromatic than their parent oils. Asphaltenes are involatile, so they become concentrated in residual fractions.

Deasphalted oils (otherwise known as *petrolenes* or *maltenes*) differ in properties from whole crude oils; for example, maltenes are much less viscous than whole crudes. Therefore asphaltenes, which normally make up a few mass percentage of crudes, are the principal viscosity-enhancing components, as they are with asphalts. Because asphaltenes are easily isolated from crudes and residua, they have been the subject of a large number of studies by many researchers.

Nellensteyn (1924) introduced the concept that petroleum residua are colloidal dispersions of asphaltenes in maltenes (which serve as a solvent phase) peptized by polar materials called *resins*, which may be isolated from maltenes. Mack (1932) studied rheological properties of asphalts and also concluded that asphalts are colloidal. He proposed that asphaltenes are dispersed throughout the maltene phase as large agglomerations, which are stabilized by association with aromatic components of the maltenes. Labout (1950) proposed that in asphalts having highly aromatic maltene fractions, asphaltenes are well dispersed (peptized) and do not form extensive associations. Such asphalts were designated *sol-type* asphalts. In asphalts with less aromatic maltene fractions, asphaltenes are not well dispersed and form large agglomeration, which in extreme cases can form a continuous network throughout an asphalt. These asphalts were designated *gel-type* asphalts. Pfeiffer and Saal (1940) suggested that asphalt dispersed phases are composed of an aromatic core surrounded by layers of less aromatic molecules and dispersed in a relatively aliphatic solvent phase. They did not claim that there are distinct boundaries between asphalt dispersed and solvent phases, as in soap micelles, but that there is a continuum from low to high aromaticity from the solvent phase to the centers of the entities making up the dispersed phase. Pfeiffer and Saal observed that asphaltenes, which they considered to be the core constituents of dispersed phases, have a marked tendency to absorb aromatic hydrocarbon solvents, and they assumed that the same tendency would prevail in asphalt systems; that is, the asphaltenes would attract smaller aromatic components of maltenes, which would surround and peptize the asphaltenes. The smaller aromatic molecules would be compatible with naphthenic and aliphatic components of the remainder of the maltene phase. Therefore, there is no contact between materials having greatly different surface tensions anywhere in the system, although differences in surface tension between the aromatic asphaltene cores and the more naphthenic and aliphatic solvent may be fairly large. Pfeiffer and Saal considered aromaticity gradients in their model and did not address distributions of heteroatom-containing molecules with polar functional groups. They claimed that asphalt properties are a function of the strength of associations between fundamental components of dispersed phases and the extent to which dispersed phases are peptized by solvent phases.

Traxler (1961) discussed the development of the colloidal model of asphalt structure, emphasizing the rationalization of rheological properties of asphalts. The state of dispersion of an asphalt should, according to the model, govern physical properties. In asphalts in which the presumably high molecular weight asphaltenes are well dispersed (because of the presence of considerable amounts of aromatic compounds in the solvent phase and sufficient amounts of peptizing resins), high temperature susceptibilities, high ductilities, low values of complex flow, low rates of age hardening, and little thixotropy should be observed. Such asphalts are designated *sol-type* asphalts. In poorly dispersed asphalts, low temperature susceptibilities, low ductilities, significant thixotropic properties and elasticities, and rapid age-hardening rates are observed. Such asphalts are designated *gel-type* asphalts. Many

asphalts are between these extremes. Traxler pointed out that gel-type asphalts tend to lose complex flow (a measure of non-Newtonian behavior) upon heating. He claimed that the phenomenon of isothermal, reversible age hardening, which he termed *steric hardening*, was strong evidence for the formation of secondary structures unstable to heat and mechanical agitation, and that asphalts are colloidal (Traxler and Coombs 1937).

Yen et al. (1961), on the basis of X-ray diffraction studies, supported many of the essential features of the colloidal model. They claimed that the predominant interaction in association phenomena in petroleum residua is stacking of condensed aromatic molecules to form larger units. Altgelt and Harle (1975) rationalized asphalt rheological behavior on the basis of stacking of condensed aromatic structures.

The colloidal model has been criticized from the standpoint that although it appears appropriate, it is difficult to substantiate experimentally (Bukka et al. 1991). Significantly, although asphaltenes are the principal viscosity-enhancing component of crude oils, viscosities of heavy residua cannot be accurately predicted from asphaltene contents alone (Hagen et al. 1984). Nevertheless, the colloidal model proposed by Nellensteyn and modified by Mack, Pfeiffer and Saal, and later investigators enjoys widespread support among petroleum scientists. There is a great deal of evidence in favor of its validity. Unfortunately, the simple optical methods that would easily verify or refute the model cannot be used because of the opacity of petroleum and all but its most dilute solutions.

It must be emphasized that notions about the nature of colloids at the time the colloidal model of asphalt structure was developed differed somewhat from contemporary ideas. According to the *McGraw-Hill Encyclopedia of Science and Technology* (1982), a colloidal system is one in which one phase is made up of particles having dimensions of 1 to 1000 nm that are dispersed in another phase. Examples of colloids are smokes, gels, emulsions, aerosols, and foams. When mixed together, the separate components of a colloidal system will not form a colloid spontaneously without energy input; techniques such as comminution or ultrasound must be employed. Properties of colloids are greatly influenced by the large surface areas of dispersed phases. Solutions, on the other hand, are homogeneous throughout (above the molecular level) and form spontaneously when the components are brought into contact.

Three of the most common types of colloids are large molecules (which may be polymeric), suspensions in fluids of small solid particles of more or less uniform composition, and agglomerations of smaller molecules dispersed in liquids. The first two categories do not apply to asphalts, which are neither polymers nor simple suspensions. Examples of the third category are emulsions, gels, and micellar solutions. These three terms have been applied to asphalts, particularly in the older literature. *Emulsions* are defined as mixtures of immiscible liquids, requiring an emulsifying agent for stability. *Gels* are two-phase systems, consisting of a solid and a liquid. *Micellar solutions* are aggregates of *amphipathic* molecules (molecules having both hydrophilic and hydrophobic groups). All these systems are characterized by a dispersing phase and a dispersed phase, with a distinct boundary between the phases.



The model of asphalt structure proposed by Pfeiffer and Saal (1940), which is an elaboration of the model suggested by earlier workers, specifically disavows the existence of a sharp boundary between solvent (maltene) and dispersed (asphaltene) phases in asphalts, but proposes an aromaticity gradient instead. Therefore it may be inappropriate to describe this model as colloidal, because it allows no dispersed-phase surfaces. The term *phase* also may be inappropriate when applied to asphalt components. The results of rheological studies performed during the Binder Characterization and Evaluation Program, reported later in this volume (chapter 3) and in volume 3 of this report, question the existence of separate physical phases in asphalts.

Earlier workers were accustomed to dealing with organic molecules of relatively low molecular weight and simple structure. They observed that properties of petroleum residua could not be rationalized by a model describing asphalts as simple mixtures of small molecules. Asphaltene-like components of crude oils can be separated by centrifugation (Eldib et al. 1960; Ray et al. 1957), but such separation is impossible for simple molecular solutions. Asphalts exhibit some properties similar to those of known colloids and contain substantial amounts of surface-active compounds (e.g., metalloporphyrins), so it was inferred that asphalts were colloidal. At the time, the term *colloid* was used as a general term to describe many materials that were not simple mixtures. Until the 1930s, polymers (which now are known to be high molecular weight molecules formed from the combination of large numbers of smaller molecular units called *monomers*) were referred to as colloids.

Asphalts are composed of a wide range of compound types, differing in molecular size, aromaticity, and polarity. In mixtures such as asphalts under service conditions, purely aliphatic and naphthenic molecules of moderate size do not interact strongly with one another. Molecules with polar functional groups tend to associate at the polar sites, and aromatic molecules attract one another. Thus associations of molecules, some of which may be fairly extensive, may form in asphalts. These associations may be similar to those described by Pfeiffer and Saal (1940) and are of colloidal size, but should not necessarily be described as colloidal. Nevertheless, the term *colloidal* as applied to asphalts is in such wide currency that objection to its use is probably futile. The same considerations apply to the sol-gel categorization of asphalts. The terms are appropriate insofar as they refer to an ensemble of properties normally found together, but not appropriate insofar as they imply that asphalts are gels in the strict sense.

For purposes of discussion in this report, the large, mostly aliphatic and naphthenic portion of asphalt, the existence of which is not in doubt, is referred to as the *solvent moiety*, rather than the *solvent phase*. The aromatic, polar components that are capable of associations are referred to as the *dispersed moiety*. Whether these materials can be identified with and are equivalent to asphaltenes is examined later. The structures formed by molecular association processes, however weakly bonded, will be referred to as *microstructures*. It should be recalled that asphalts are so diverse in composition that there may be many different kinds of associations of polar or aromatic molecules in one asphalt; that is, the various associations may not be at all uniform and may change as a function of temperature and mechanical stress. Therefore referring to the state of dispersion of an asphalt is appropriate. Evidence for the existence of associations of polar, aromatic molecules in petroleum residua is presented below.

## *Associations of Polar Molecules in Petroleum Residua*

Goulon et al. (1984) used X-ray absorption spectroscopy to study vanadium complexes in heavy oils. They concluded that essentially all vanadium is chelated by chlorophyll derivatives known as *porphyrins*. These compounds are characterized by distinctive ultraviolet-visible (UV/VIS) spectra, which form the basis of methods used to quantify them. Porphyrin analyses are usually performed by measuring absorbances at 400 nm of dilute solutions of a petroleum or petroleum fraction. For most residual fractions, or in more concentrated solutions of whole crudes, UV/VIS methods seriously undercount vanadyl porphyrin contents compared with elemental vanadium concentrations in the same materials, which may be accurately determined by a variety of means. If the X-ray studies prove that vanadium in crude oils is largely porphyrinic, then there must be a one-to-one correspondence between molar concentrations of vanadium and vanadyl porphyrins. This apparent failure of UV/VIS methods to accurately measure vanadium porphyrin concentrations in residual materials is attributed to quenching of UV/VIS absorbance by associations of molecules in solution, which have no effect on methods that measure concentrations of elemental vanadium. Other X-ray studies of asphaltenes and residua have been reported by Herzog et al. (1988) and Senglet et al. (1990); both studies found evidence of association of molecules into larger structural units.

Dwiggins (1978), using small-angle X-ray scattering methods, found evidence for what he termed *colloidal particles* in asphaltic crude oils. Ravey et al. (1988) used small-angle neutron scattering to investigate the nature of petroleum residua structures. They concluded that asphaltenes from several crudes are fairly similar and consist of polydisperse ensembles of thin (about 1 nm) sheets whose diameters range from 1 to 10 nm. They emphasize that these dimensions are in accord with those calculated by Dwiggins (1978) using X-ray methods and by Reerink and Lijzenga (1975) using size exclusion chromatography (SEC). Donnet et al. (1977) studied different types of asphalts by electron microscopy and claimed to be able to distinguish between sol- and gel-type asphalts. Overfield et al. (1989) studied aggregation of asphaltenes in deuterated toluene by small-angle neutron scattering. Toluene was chosen as the solvent because its solubility properties are believed to resemble those of petroleum maltenes. Overfield et al. claimed to have verified some aspects of the colloidal nature (in toluene) of asphaltenes, but they also showed that asphaltenes are neither colloids of fixed size nor assemblages of similar small molecules. It was inferred that behavior of asphaltenes in deuterated toluene reflects behavior of the molecules composing asphaltenes in petroleum residua.

Molecular weight determinations of asphaltenes by various methods provide the most direct evidence for association phenomena (Speight et al. 1984). Ultracentrifugation experiments yielded very large molecular weights, while colligative methods such as vapor-phase osmometry (VPO) gave values that were solvent dependent; for example, number-average molecular weight ( $M_n$ ) values for asphaltenes in polar solvents such as nitrobenzene are much lower than in toluene. Boduszynski (1991) succeeded in vaporizing more than 90 percent of the heavy Boscan crude oil and measured absolute molecular weights of the components by mass spectrometry. For the lower-boiling fractions, which are of lower molecular weight, the

mass spectrometric values are similar to  $M_n$  values determined by VPO. However the  $M_n$  values by VPO become progressively larger than mass spectrometric values for higher-boiling fractions (which must have included a substantial amount of Boscan asphaltenes), which is direct evidence for association phenomena. Al-Jarrah and Al-Dujaili (1989) measured  $M_n$  values for asphaltenes from several heavy crudes and also determined intrinsic viscosities for solutions of the same asphaltenes. Degrees of association of asphaltene molecules were calculated from data obtained by both methods and were found to be similar for a given asphaltene.

Parenthetically, it should be noted that molecular weights and distributions of molecular weights greatly influence physical properties of mixtures of organic materials. Relationships between rheological properties and molecular weight have been studied intensively in the polymer field. Molecular weight affects polymer properties in which the largest deformations occur (Severs 1962). Molecular weight distribution influences hardness. Rupture properties, such as ultimate strength and total elongation, are affected by molecular weight and molecular weight distribution. Specifically, brittleness is a function of  $M_n$  for some polymers, while flow properties are controlled by weight-average molecular weight ( $M_w$ ). It is not suggested here that asphalt components are polymeric in dimensions or in strength of bonding within fundamental units, but it is certainly appropriate to examine how the size of asphalt molecular associations (assuming their existence) influences various properties. To do this, asphalts must be separated into appropriately sized components. Such separations were performed in the Binder Characterization and Evaluation Program and are reported in volume 2, chapter 2.

Rogacheva et al. (1980) studied surface tensions of asphaltene solutions in toluene. They concluded that at low concentrations (about 1 percent) true solutions are formed, but microheterogeneity exists in more concentrated solutions. Andersen and Birdi (1991) determined critical micelle concentrations (CMCs) of asphaltene solutions and found these CMCs to be surprisingly low (less than 1 percent). The existence of CMC plateaus is required by any colloidal model and is compatible with the formation of noncolloidal associations. Again it is assumed that molecules composing asphaltenes behave in resids as they do in the solvents employed in these studies; both situations should be governed by the same physical laws. Sheu et al. (1991) studied vacuum resid association phenomena and commented on the slowness of self-association of asphaltene molecules. This slowness may be due to the variety in the size and shape of the larger structural units formed from the molecular associations, which inhibits packing into favored thermodynamic states.

El-Mohamed et al. (1986) investigated diamagnetic properties of asphaltenes and concluded that large condensed nuclear structures are not present in significant amounts; this result indicates that the principal associative interaction may not be aromatic stacking. Rao and Serrano (1986) and Maruska and Rao (1987) studied associations of polar, aromatic species in heavy oils and residua. They showed that for solutions of resids in toluene, log viscosity does not vary linearly with asphaltene concentration. This result supports the idea that molecular associations exist in solutions of asphaltenes. These workers also concluded that associations of individual molecules persist to some degree even at high temperatures. Ensley (1975) has demonstrated a similar phenomenon using microcalorimetric methods.

## *The Nature of Asphaltenes in Petroleum Residua*

Many of the studies described above are of asphaltenes in solutions of common organic solvents. The results have been criticized because asphaltenes in their natural environment may not behave as they do in organic solvents.

The question thus arises whether asphaltenes actually exist in crudes or are only "operational" entities. It has been argued that asphaltenes exist only as a solubility class; that is, the molecules composing asphaltenes after precipitation by alkanes are not associated with one another in the same manner while they are components of crude oils or their resids. This position does not preclude the possibility that polar molecules form some kind of association in petroleum but that the associations are not identical to asphaltenes precipitated from petroleum and its fractions by addition of alkanes. A contrary viewpoint is that asphaltenes exist as identifiable entities in petroleum and are virtually identical in composition to the materials precipitated by alkanes. These viewpoints are argued in *Chemistry of Asphaltenes*, edited by Bunger and Li (1981).

Park and Mansoori (1988) modeled asphaltene precipitation behavior on the basis of both viewpoints, which they designated as the *continuous thermodynamic* and *steric colloidal* models. The continuous thermodynamic model considers crude oils to be solutions of organic materials of widely varying molecular weights and polarities. Mutual solubility is a function of the ratios of polar to nonpolar and high molecular weight to low molecular weight species. When a solvent such as *n*-heptane is added to a crude, both ratios are disturbed, and at a certain point the polar and higher molecular weight molecules begin to associate, and eventually precipitate as asphaltenes. The precipitation behavior of asphaltenes deviates from what would be predicted from regular solution theory and is best described as flocculation (Andersen 1992; Park and Mansoori 1988). Thus, according to the continuous thermodynamic model, adding *n*-heptane to a crude oil changes the system from a homogeneous solution to a colloidal system. Interestingly, early work by Katz and Beau (1945) reported no evidence for the existence of particles of any size when asphalt films were examined by electron microscopy. However, 6.5-nm particles were observed in films of asphalts diluted with benzene. Katz and Beau assumed that the particles corresponded to asphaltenes, so they classified asphaltenes as potential colloids.

In the steric colloidal model, asphaltenes are assumed to exist as associations of polar molecules in crude oils, and the associations are not mobilized by addition of solvents such as *n*-heptane. The associations are stabilized by means of resins, some of which are adsorbed by the polar associations and some of which are dissolved in the aliphatic, low molecular weight solvent. Stability of the system requires that the chemical potential of the solvent (including dissolved resins) be equivalent to the chemical potential of the associations (including adsorbed resins). The adsorbed resins tend to repel one another, preventing coagulation of the associations. Adding solvents such as *n*-heptane is believed to cause desorption of resins from the associations, resulting in coalescence of the polar associations and precipitation. The steric colloidal model of Park and Mansoori resembles the colloidal model of Pfeiffer and Saal in many respects.

It is known that asphaltene composition and yields are a function of the *n*-alkane used to precipitate them (Girdler 1965). This observation supports the continuous thermodynamic model. Moschopedis et al. (1976), Moschopedis and Speight (1976), and Speight and Moschopedis (1977, 1981) published results of molecular weight determinations of asphaltenes by several methods. These investigators showed that for cryoscopic and VPO methods, asphaltene molecular weights depended on temperature, solvent, and concentration. They criticized earlier viscometric molecular weight determinations, claiming that viscometric measurements of asphaltenes in pure solvents cannot be extrapolated to whole crudes or bitumens. From infrared studies and molecular weight determinations of asphaltenes in the presence of phenol, it was concluded that hydrogen bonding is the principal interaction between polar molecules in petroleum. It also was suggested that asphaltene molecules do not extensively associate in petroleum but are solubilized by resins through hydrogen bonding interactions. Long (1981) points out that asphaltenes consist of a continuum of compound types ranging from large, nonpolar hydrocarbons to relatively small, polar molecules. The two extremes are unlikely to associate directly with one another.

Geochemists have long contended (Behar et al. 1984) that asphaltenes closely resemble kerogen fragments from source beds of crudes and that asphaltenes actually exist in petroleum and are not artifacts of precipitation. According to current theories, petroleum is derived from algae and bacteria that grew in ancient bodies of water in which oxygen was deficient. In these bodies of water, organic detritus was not recycled but incorporated into sediments. As sediments became deeply buried and lithified, the associated organic matter was converted into a macromolecular, insoluble material called *kerogen*. When the material was buried deep enough to reach temperatures of 350°C (662°F), kerogen cracking reactions began. The products of these cracking reactions were fluids that migrated out of their source rocks (usually shales) and into permeable reservoir rocks. Bandurski (1982) has summarized some of the evidence for the theory that the asphaltenes of a crude oil resemble oil-bearing portions of the source kerogens more than any other component of the crude. He studied asphaltenes from crude oils and source kerogens from which the crude oils were derived. He lists several chemical similarities and notes that pyrolysates from both materials are similar.

Desbene et al. (1988) separated an atmospheric residuum into defined chemical fractions and then precipitated asphaltenes from each fraction. The researchers also separated asphaltenes precipitated from the residuum into the same chemical fractions by the same method used for the residuum. The fractions obtained were nearly identical by either pathway. It was argued that if asphaltenes were only operational entities, such a result would not have been observed; the individual fractions would not have the same solubility behavior as the whole residuum.

Storm and Sheu (1993) favor the idea that asphaltenes are a distinct species in crude oils and residua. They state that it is the experience of refiners that asphaltenes behave as a distinct species during refining. Storm et al. (1991) measured intrinsic viscosities of petroleum resids diluted with their maltene fractions. The maltenes added to the resids are natural solvents, not model solvents. *Intrinsic viscosities* are reduced specific viscosities of solutions extrapolated to zero solute concentrations and are calculated by measuring specific viscosities of maltene-resid mixtures at various asphaltene concentrations. Intrinsic viscosity measurements are used to estimate molecular weights of high polymers, as the two quantities

are related. For dilute suspensions of spherical particles, the intrinsic viscosity should be 2.5. Storm et al. (1991) measured intrinsic viscosities of 7 to 9 for the maltene-resid mixtures. Thus they claim that there are fairly large molecular associations in the mixtures. In other work, Storm et al. (1990) showed that individual asphaltene molecules have maximum true molecular weights of about 1300 daltons. Therefore, these molecules must exist as associated entities in the resids. Storm and Sheu (1993) analyzed the rheological data on the mixtures by five independent theories and concluded that asphaltenes are distinguishable in the resids. Coupled with X-ray data, they claim, these results show that asphaltenes are organized into charged spherical particles of widely distributed sizes that are solvated by resins and dispersed in the surrounding fluid.

There are difficulties with either of the above positions. Park and Mansoori (1988) commented that the asphaltene problem is elusive. Asphaltenes are composed of a great variety of polar (and some relatively nonpolar) compounds. If asphaltenes exist in crudes as more or less homogeneous entities, they must form associations of a great many compounds, and the associations must therefore be very large. This difficulty may be somewhat resolved by assuming very heterogeneous asphaltene associations and, by inference, kerogen fragments. On the other hand, asphaltenes compose over 20 percent of some asphalts and are always the most polar, aromatic components. At such concentrations, it is difficult to conceive of them not engaging in some kinds of self-assemblies in whatever matrix they may be found. Some polar asphaltene molecules have low enough molecular weights that if they were not part of associations (at least with resin molecules, if not other asphaltene molecules), they should be fairly readily distillable. The matter cannot be said to be resolved as of this writing, but further elaboration is found in chapter 3.

Most of the above work was not reported in the asphalt literature and was oriented toward improving processing of resid fractions. The work supports some sort of model of asphalt structure that involves molecular associations, although many details are not elaborated. The work must be considered in the development of a rational model of asphalt structure-property relationships. It should be emphasized again that many of the studies were published after the beginning of the SHRP Binder Characterization and Evaluation Program (A-002A).

### *Model Proposed at the Beginning of the Binder Characterization and Evaluation Program*

In the original proposal in response to the A-002 (soon after called A002A) solicitation, a model based on that suggested by Pfeiffer and Saal (1940), but with modifications, was described to account for asphalt behavior. The authors designate this model the *microstructural model*. It was suggested that asphalts consist of a solvent phase composed of relatively aliphatic, nonpolar molecules that are low in heteroatoms (save perhaps sulfide and thiophenic sulfur and ether and ester oxygen) and that this phase disperses *microstructures* (structural units formed from molecular associations) consisting of more polar, aromatic, asphaltene-like molecules. Many of the molecules composing the dispersed phase were assumed to be polyfunctional and capable of associating through hydrogen bonds, dipole interactions, and  $\pi$ - $\pi$  interactions. It is these interactions that allow formation of primary

microstructures. It was speculated that the primary microstructures could associate into three-dimensional networks under the proper conditions. These networks, and the primary microstructures themselves, may be broken up by heat and shear stress. It was suggested that three-dimensional structuring is suppressed by an effective solvent phase but promoted by an ineffective solvent phase. Oxidative aging increases the number of polar molecules that become part of the dispersed phase, leading to more structuring, but also increases the solvent power of the dispersing phase.

A consequence of the microstructural model is that the variables that influence asphalt physical properties the most are those that most disturb microstructural systems. Among such variables are properties that cause the solvent components (those materials not part of associations) to be an effective or ineffective solvent and properties that stabilize microstructures or enhance interactions between them. Such properties might not be adequately described by many of the bulk properties commonly measured in whole asphalts. Asphalts contain thousands of individual compounds in varying amounts. Isolating and quantifying each of these components would be an impossibly complicated task. Asphalts with similar bulk properties—such as elemental composition, density, and  $M_n$ —can have very different physical properties, because different assemblages of individual compounds, forming different microstructural systems, occur in asphalts that are characterized by similar (but probably not identical) bulk properties.

The above model rationalizes important physical properties of asphalts, such as non-Newtonian rheological behavior, temperature dependence of viscosity, molecular structuring that causes isothermal reversible age hardening (steric hardening), and many others. According to the model, oxidative aging is rationalized by the buildup of polar molecules as a result of reaction of oxygen with reactive molecules, many of which are nonpolar, and by loss of low molecular weight, nonpolar molecules by volatilization. The result of this process is a decrease in asphalt solvent moieties and an increase in molecular associations to the point that remaining reactive molecules are less accessible to oxygen at any given temperature. Details of the model had not been quantified to the extent that a given value of some structural property may be correlated with a certain range of physical properties. The model proposed is descriptive, not quantitative. Some skepticism has been voiced as to whether the model is so vague as to be of any value at all, or whether it is even valid. Accordingly, one of the major objectives of the Binder Characterization and Evaluation Program has been to verify (or reject) and improve (or replace) the model and to correlate chemical and physical properties of asphalts according to an improved model.

It was stated earlier that the model of asphalt structure described in the original proposal, the microstructural model, was developed partly as a result of asphaltene studies. It has long been known that asphaltenes are responsible for the high viscosities and non-Newtonian rheological properties of petroleum residua but that asphaltene contents alone are not good predictors of these properties (Hagen et al. 1984) or of asphalt performance in general. Asphalts are usually graded according to their viscosities at 60°C (140°F), but asphalts having the same viscosity grade exhibit different asphaltene contents. To better evaluate the implications of the microstructural model, other techniques (in addition to asphaltene precipitation) that should be able to separate the components of asphalts that might form associations from solvent moieties need to be investigated. The microstructural model of

asphalt structure postulates that the more polar, aromatic components of asphalts engage in extensive associations at asphalt service temperatures. Therefore, in the native state, the dispersed associated structural units will be of larger molecular size than the solvent components. It should be possible to separate the two moieties by techniques that separate mixtures according to molecular size. During such a separation, the fundamental asphalt structural units must be bonded strongly enough that they will not be broken up. A candidate technique for this objective is SEC. Because the dispersed associated materials are believed to be significantly more polar than materials that compose the solvent, it must also be possible to separate the two components by techniques that effect chemical separations. Two such candidate techniques are ion exchange chromatography (IEC) and conventional absorption liquid chromatography (LC). If the model is correct, materials isolated by all techniques that correspond to either dispersed or solvent moieties should be similar in properties. If the separations cannot be made, the model is incorrect or needs revision. Inability to perform an effective SEC separation would indicate that association forces are much weaker than predicted. Inability to make meaningful IEC or LC separations would indicate that the residua are more homogeneous than the model will allow.

Early in the Binder Characterization and Evaluation Program, the importance of verifying the presence or absence of stickies or goodies was emphasized. If such materials are present in asphalts, they should be isolable by the techniques described above; if they exist, the materials should be among the most polar aromatic components of asphalts.

Chapter 3 of this report outlines what has been learned about the microstructural model in the Binder Characterization and Evaluation Program and how the model has been used to rationalize relationships between asphalt chemical properties and the physical properties that govern performance.

## **Colloidal Models and Rheological Behavior**

### *Micellar Colloidal Model and Rheological Behavior*

The well-known fact that asphaltene are insoluble in oils prompted Nellensteyn (1924, 1928), to propose that asphalt cements are micellar colloids or dispersions of asphaltene particles in maltenes. Labout (1950) and Mack (1932), in attempts to explain the rheological behavior of asphalt, elaborated on its colloidal nature, proposing that the asphaltene are discrete entities, dispersed throughout the maltene phase as large molecular agglomerations, and are, in some cases, associated with high molecular weight aromatic compounds from the maltene phase. Labout further proposed that in asphalts having a highly aromatic maltene phase, the asphaltene are well dispersed and do not form much structure within the asphalt. Such asphalts were called *sol-type* asphalts. In other asphalts, having a weakly aromatic maltene fraction, he proposed that the asphaltene are not well dispersed, and form large agglomerates, which in extreme cases can form a continuous network of micelles in the asphalt. These asphalts were called *gel-type* asphalts by Pfeiffer and Saal (1940). The terms *sol*, *gel*, and *sol-gel* (representing the intermediate state) are still widely used today to qualitatively describe asphalts of different structure and rheological behavior. It has been



recognized that sol asphalts that are subsequently blown or oxidized in processing will become more gel-like (Labout 1950).

Coincident with the early models of asphalt as a micellar colloid were theories explaining the observed rheology of asphalt cements in terms of a colloidal structure. Traxler provides a good review of the rheological evidence existing at that time for the early model of a colloidal structure (Traxler and Coombs 1937; Traxler and Schweyer 1936). Traxler hypothesized that the non-Newtonian flow of gel-type asphalts can be explained in terms of the breakdown of the colloidal structure. Various early researchers also found that asphalts, in the absence of both oxygen and high temperatures, spontaneously increased in viscosity. This molecular structuring—or steric hardening as Traxler called it—was found to be reversible either by heating to a temperature above the softening point of the asphalt or by prolonged mechanical working. Molecular structuring was attributed to the growth and/or coagulation of micelles to form a more fully developed structure in which the individual micelles form a continuous network. In this traditional microstructural model of asphalt cement, sol-type asphalts are formed when asphaltenes peptized by resins float in a sea of maltenes. Gel-type asphalts, on the other hand, are formed when asphaltenes are insufficiently peptized, which allows the asphaltene-containing micelles to form a continuous network.

Van der Poel (1954) presented a well-developed scheme for characterizing asphalts according to their rheology. Using various means for measuring the stiffness of asphalt cement over a wide range of loading times and temperatures, he developed master stiffness curves for a wide range of asphalt types, and found that sol-type asphalts exhibit a rapid transition from glassy behavior to Newtonian flow, while gel-type asphalts show a much more gradual change. Although van der Poel did not directly attempt to relate these findings to the state of colloidal dispersion of the asphalts, his use of the terms *sol* and *gel* to describe asphalts of different rheological types represents an implicit acceptance of the colloidal model.

Rostler and White (1962) further elaborated on the colloidal model of asphalt microstructure, suggesting that the asphaltenes are peptized by a fraction in the asphalt called the *nitrogen bases* (a fraction of the maltenes). They suggested that a gel structure is developed in asphalts that lack sufficient nitrogen bases in relation to the asphaltene content.

Recent attempts to characterize asphaltenes chemically and to relate their chemistry to the structure of asphalt cement have resulted in new concepts that challenge the existing two-phase micellar model. For example, Speight and Moschopedis (1981) proposed that asphaltenes are not present as large agglomerations or micelles at all, but only as small entities that are well distributed throughout the asphalt as discrete particles. Jennings et al. (1991), as part of the SHRP research, concluded that, as they exist in paving-grade asphalt cement, asphaltenes are not large agglomerations but have dimensions no greater than 50 nm. Yen et al. (1961), on the other hand, on the basis of X-ray diffraction studies, proposed that asphaltenes form stacks of a large number of molecules, ultimately agglomerating into roughly spherical micelles that may be very large. The traditional micellar model for asphalt cement appeared suspect as an explanation for the rheological properties of asphalt cement, and a new or modified microstructural model was sought.

## *Summary of Current Colloidal Models as Used in Colloidal Science*

The science of colloids and related materials has developed rapidly since the 1930s and 1940s when much of the original micellar colloid theory of asphalt microstructure was formulated. This rapid development undoubtedly contributes to the confusion and controversy surrounding the existence and nature of the microstructure of asphalt. Recent developments in the study of colloids and related materials suggest significant revisions to previous theories concerning the structure of asphalt cement. Current colloidal models were examined in search of a microstructural model for asphalt cement.

A large variety of colloidal types have been identified by colloid scientists, and definitions have changed in recent years as the science of colloidal chemistry has grown and matured.

Colloids are generally considered to be dispersions of discrete particles of one material or phase within another, continuous phase. For a true colloid to exist, the dispersed particles must be within a certain size range: 1 to 100 nm. Therefore, colloid particles are normally only visible in an electron microscope (Jirgensons and Straumanis 1962). Many of the colloidal types that have been defined, such as aqueous colloids, are not relevant as models for the microstructure of asphalt cement. Some relevant colloid models follow:

- ***Lyophobic sols.*** In lyophobic sols, the dispersed particles have little or no affinity for the solvent, or continuous phase. Typically, the dispersed phase represents only 1 to 2 percent of the total colloid by volume (Jirgensons and Straumanis 1962).
- ***Gels.*** Gels are colloidal solids having a three-dimensional network of particles or molecules held together by various forces and a fluid contained within the network. Gels generally exhibit highly rubber-elastic behavior in the solid state. On heating a gel generally reverts to a sol at a well-defined temperature; on cooling, the gel will not solidify until some lower temperature is reached, exhibiting what might be called *phase hysteresis* (Vold and Vold 1983).
- ***Micellar solutions.*** These substances are also called *association colloids*. They are dispersions of agglomerations of amphipathic molecules of colloidal size. These agglomerations, called *micelles*, are in a state of rapid equilibrium with individual molecules or ions. A normal micelle is spherical, with the polar heads of the amphipathic molecules facing outward and the nonpolar tails facing inward. In some cases, in nonpolar solvents, reversed micelles can be formed in which the polar heads of the molecules face inward and the nonpolar tails face outward. Reversed micelles are not common (Vold and Vold 1983).
- ***Microemulsions.*** Microemulsions are formed from mixtures of two normally immiscible liquids: a surfactant and a cosurfactant. In some cases, a cosurfactant is not necessary. The dispersed liquid exists as droplets of colloidal size within the continuous phase. Although similar to normal emulsions, microemulsions differ in two important ways: the dispersed droplets are much smaller, and

microemulsions are thermodynamically stable; that is, if left unperturbed, a microemulsion has no tendency to settle or coalesce (Vold and Vold 1983).

- *Liquid crystals.* According to the *Kirk-Othmer Encyclopedia of Chemical Technology* (1981), "liquid crystals are highly anisotropic fluids that exist between the boundaries of the solid and conventional, isotropic liquid phase. The ordered phase is a result of long-range orientational ordering among constituent molecules that occurs within certain ranges of temperature in melts and solutions of many organic compounds" (vol. 14, p. 395). The long-range order is generally a result of polar interactions between rod- or disk-shaped molecules, causing them to align into various morphologies visible under an optical microscope: lamellae or sheets (smectic mesophase), threads (nematic mesophase), or columns (columnar, canonic, or discotic) (Chandrasekhar 1982; *Kirk-Othmer Encyclopedia* 1981).

### *Applicability of Current Colloidal Models to Asphalt Cement*

A critical review of the applicability of colloidal models to asphalt cement, in light of the possible colloid types described above, is now in order. Lyophobic sols typically contain only 1 to 2 percent of the dispersed phase. Asphalts contain a much higher percentage of asphaltenes, so this structure is unlikely. Additionally, such a small amount of a dispersed phase would be unlikely to greatly affect the properties of asphalt. Although the gel-type structure seems plausible, there are several contradictions in this classification. Gels typically exhibit a high degree of rubber elasticity. Upon heating, a gel liquifies at a well-defined temperature, and, when cooled, solidifies at another well-defined temperature. Asphalt cements do not exhibit rubber elasticity and show no well-defined melting or solidification points. Emulsions are a three-phase system consisting of a dispersed liquid, a continuous liquid, and a dispersing agent. In this classic model of asphalt structure, the asphaltenes are the dispersed phase, the oils the continuous phase, and the resins the dispersant. There are, however, several problems with this model. Asphaltenes, except at very high temperatures, are solids, not liquids, and probably agglomerate as small (less than 50 nm) discrete particles showing semicrystalline characteristics. Also, although many attempts have been made to explain the properties of asphalt cement through the relative proportions of asphaltenes and resins, none has been successful. The dispersed droplets in emulsions tend to flocculate into larger, spherical droplets, not into three-dimensional networks. Thus, the apparent structure in some asphalts is not explained by this model.

Micellar solutions may be a more appropriate colloidal model for asphalt cement. Micellar solutions are similar in some respects to emulsions, but the primary dispersed phase consists of amphipathic molecules arranged in micelles, either of the normal type or reversed. In asphalt cement, the micelles would be reversed and in many or all cases would be centered around asphaltene particles. This theory is, unfortunately, similar to the emulsion theory and has many of the same drawbacks. An important question here is whether amphipathic molecules are present in asphalt cement in large enough amounts to produce enough micelles to account for the level of structure present in asphalt. Additionally, there is no evidence that

the micelles in micellar solutions can coalesce into a three-dimensional network. Such coalescence would probably be necessary to explain the steric hardening and oxidative hardening seen in most asphalts.

Microemulsions are very similar to emulsions, but the dispersed droplets are much smaller, and such systems are thermodynamically stable. Besides the problems presented for the emulsion theory, this model has the additional drawback that it cannot explain steric hardening, because of the requirement of thermodynamic stability. Steric hardening is evidence of a thermodynamically metastable state. Additionally, microemulsions, when rendered unstable, do not coalesce into three-dimensional networks but simply form ordinary emulsions.

After reviewing the colloidal literature, the researchers concluded that traditional colloidal systems are not fully consistent with the observed rheological behavior of asphalt cement as a function of temperature, loading time, and aging. Thus, the null hypothesis—that asphalt cement is a relatively homogeneous and randomly distributed collection of molecules differing in polarity and molecular size—must be turned to for an effective description of the microstructure of asphalt cement.

## Performance-Related Test Method and Specification Development

The current specifications for asphalt cement are typically based on measurements of viscosity, penetration, and ductility. These measurements are not adequate for fully describing the linear viscoelastic properties that are needed to relate physical properties to asphalt chemistry, to relate physical properties to performance, to relate asphalt chemistry to performance, and, most important, to develop a performance-related binder specification. Before proceeding to the rheological characterizations that were adopted for these purposes, a short review of the shortcomings of the currently used specification techniques is presented. This review is followed by the rationale used for selecting the physical property tests that were proposed as new specification tests and a ranking of the Strategic Highway Research Program (SHRP) Materials Reference Library (MRL) asphalts according to the proposed specification criteria.

### Need for New Measurements

#### *Viscosity Measurements*

At elevated pavement service temperatures, greater than approximately 60°C (140°F), and at mixing and compaction temperatures, unaged asphalt cement generally behaves as a Newtonian fluid (shear-rate independent) and can be properly characterized by capillary viscometry. Aged binders, even at the upper range of pavement service temperatures, exhibit significant non-Newtonian behavior, so capillary viscometry is less applicable to them (Puzinauskas 1979). Further, even unaged modified binders at mixing and compaction temperatures exhibit significant shear-rate dependence when tested in capillary viscometers (Anderson et al. 1991).

A large number of researchers (e.g., Griffen et al. 1956; Moavenzadeh and Stander 1967; Romberg and Traxler 1947) used steady-state creep measurements to calculate a coefficient of viscosity,  $\eta$ , at intermediate pavement service temperatures, ranging from 0°C to 25°C (32°F to 77°F). To conduct such a measurement, it is necessary to apply a shear stress to the asphalt cement until the strain rate,  $\dot{\gamma} = d\gamma(t)/dt$ , becomes constant (figure 2.1). At temperatures below ambient, long loading times are required before this occurs (figure 2.2). If enough time is allowed for delayed elasticity to be expended and for steady-state flow to occur, very large strains will likely result, causing geometric nonlinearity. At temperatures between ambient and 60°C (140°F), most paving-grade asphalt cements, even when loaded in the linear range, exhibit significant delayed elasticity, and strain rate varies with loading time.

Delayed elasticity and geometric nonlinearity are often either confounded or have gone unrecognized by many researchers, causing researchers to apply nonlinear representations to the stress-strain behavior of asphalt cement. This apparent nonlinearity of asphalt cement has been accounted for by various techniques:

- Using a nonlinear representation of the flow behavior, where  $\eta = \tau^n/\dot{\gamma}$  (Traxler 1947)
- Specifying an apparent coefficient of viscosity,  $\eta_{cp}$ , calculated at a specified power input (figure 2.3) (Romberg and Traxler 1947; Schweyer et al. 1976)
- Assuming that the steady-state strain rate has been attained at a series of shear stress levels and extrapolating the calculated apparent coefficients of viscosity to a zero strain rate (figure 2.4) (Puzinauskas 1967, 1979)

In these methods, the testing is generally conducted in the nonlinear region, and the delayed elastic response exhibited by the asphalt cement is either not considered or considered a nonlinear effect. These problems militate against the use of viscosity measurements to characterize asphalt cement at service temperatures.

### *Shear Susceptibility*

Traxler et al. (1944) were the first to consider the shear susceptibility of paving asphalt. They modeled the flow properties using a power law model, in which the logarithms of the shear stress and shear strain rate are linearly related:

$$\log \tau = c(\log \dot{\gamma}) + B$$

where

- $\tau$  = shear stress
- $\dot{\gamma}$  =  $d\gamma(t)/dt$  shear strain rate
- $c$  = degree of complex flow
- $B$  = constant

A more common representation of shear-rate dependence that uses this power law model is the following function:

$$\eta = \tau/\dot{\gamma}^c$$

The power law model is often used to describe the nonlinear flow behavior of fluids (Majidzadeh and Schweyer 1965; Traxler et al. 1944). For Newtonian materials,  $c$  is, by definition, equal to unity; the value of  $c$  is a measure of the degree of non-Newtonian behavior (complex flow). At very low shear rates or very low stress levels, almost all asphalts exhibit Newtonian behavior, where  $c$  is equal to unity. Non-Newtonian behavior appears gradually as the shear-rate or stress level increases (Anderson et al. 1983). Therefore,  $c$  is not a constant but varies with loading time, temperature, and shear rate, as well as the aging and stress history of the asphalt (Halstead and Zenewitz 1961; Majidzadeh and Schweyer 1965). The degree of complex flow,  $c$ , may, however, be useful in understanding the nature of the molecular interactions in the nonlinear response region. To this extent,  $c$  has been used by other researchers to characterize the effect of oxidative aging on the flow properties of asphalt cement (Halstead and Zenewitz 1961).

### *Temperature Susceptibility*

Temperature susceptibility is defined as the change in consistency, stiffness, or viscosity of a material as a function of temperature and is usually quantified through parameters calculated from consistency measurements made at two different temperatures. Asphalt pavements, and hence asphalt cement binders, are subjected to a wide range of temperatures in service. Because many of the problems observed in pavements clearly result from the large temperature-dependent changes in consistency, temperature-susceptibility parameters have been frequently proposed as a means of characterizing paving-grade asphalt. However, there is a major problem in analyzing and interpreting such parameters.

Because the rheological properties of asphalt cement are functions of both loading time and temperature, temperature-susceptibility parameters must be based on measurements at different temperatures but similar loading times. Otherwise, the temperature-susceptibility parameter will be confounded with loading time as is the case when penetration and viscosity, or softening point and penetration, measurements are combined to create a temperature-susceptibility index such as the penetration index. Ideally, rheological parameters used to characterize asphalt cement should fully separate time and temperature effects and should be largely independent of the time and temperature ranges over which they are calculated. Unfortunately, no commonly used temperature-susceptibility parameter meets these criteria.

Various physical properties have been used by researchers and practitioners to calculate temperature-susceptibility parameters. The viscosity temperature susceptibility (VTS) was defined using capillary viscosity measurements at 60°C and 135°C (140°F and 275°F) (Puzinauskas 1979). For unaged, unmodified asphalt, flow behavior over this temperature range is essentially Newtonian and independent of time of loading. Therefore, this parameter will in many cases accurately characterize temperature dependence above 60°C (140°F).

However, a viscosity-based temperature-susceptibility parameter cannot be extrapolated to describe behavior at temperatures below 60°C (140°F), where the delayed elastic properties of the asphalt cement become significant. Other researchers have proposed the use of low-temperature viscosity measurements to calculate temperature-susceptibility parameters, but this method is unacceptable because of the difficulty of measuring viscosity at low temperatures and because the single parameter, viscosity, neglects the important delayed elastic portion of the stress-strain response.

Temperature-susceptibility parameters based on penetration ratios (Barth 1962) are unacceptable for a performance-related binder specification because penetration is itself an empirical property. This is especially true when different loads and loading times (e.g., 50 g and 5 seconds versus 200 g and 6 seconds) are used at different temperatures. Shear rates in the vicinity of the penetration needle vary greatly with distance from the needle tip, and, in the region being sheared, the strain rates are nonlinear. Further, the shear rate within the asphalt binder varies with the penetration value (shear rates are much greater for a penetration of 200 than for a penetration of 20), further confounding the effects of stress level and shear rate.

The empirical method that has received the most attention is perhaps the use of penetration indexes (PIs) and penetration-viscosity numbers (PVNs). The PI was originally developed by Pfeiffer and van Doormaal (1936) and was later used by van der Poel (1954) in the development of a nomograph for predicting the stiffness of asphalt cement using routine test data. These researchers recognized the confounding of time and temperature effects that was inherent in the calculation of the PI but found that, in most cases, the time dependence or the rheological type of the asphalt was the dominant effect. They therefore concluded that the PI was a reasonable estimate of the rheological type of an asphalt. The relationship between PI and rheologic type as measured by more rigorous means is, however, only a weak one, as is obvious from figure 2.5, in which PI (from penetration at 25°C [77°F] and softening-point temperature) is plotted against the rheological index as measured in this study. The weak correlation seems to be largely a result of the confounding of time and temperature effects as discussed above.

To further complicate matters, the rheological type and temperature dependence change with aging, as illustrated in figure 2.6, and therefore the temperature-susceptibility parameter should also change with aging. As appropriate, the PI values typically change with aging, but PVN values as proposed by McLeod (1972) appear to remain unchanged with aging, further casting suspicion on the validity of PVNs as a measure of temperature susceptibility (Anderson et al. 1983).

Temperature susceptibility is not a single-valued parameter but depends on the temperature range being considered, the time of measurement, and the physical property being measured. This is illustrated in figure 2.7, where PI, PVN, and VTS values for the eight SHRP core asphalts are compared and little agreement between PI, PVN, and VTS is shown. PI, PVN, and VTS represent different temperature regimes (Anderson et al. 1991). On the basis of the above evaluation of the traditional temperature-susceptibility parameters, their use in this project for the characterization of asphalt cement was rejected.



## *Nomographs and Their Inadequacies*

The nomographs developed by various researchers offer one means of calculating the stiffness of asphalt cement at various test temperatures and loading times. The first nomograph for this purpose was developed by van der Poel (1954) using the PI. This nomograph was later updated and revised by McLeod (1972) to accommodate penetration and viscosity measurements. These nomographs provide reasonable estimates of asphalt stiffness at temperatures above room temperature; however, the estimates provided by these nomographs may be in considerable error at lower temperatures and longer loading times, as illustrated in figure 2.8. Given the poor reliability of these nomographs and their uncertain applicability to modified asphalts, a more direct measurement of low-temperature stiffness was sought.

## *Aging Indexes*

The control of premature aging is an important specification function, and aging indexes, either directly or indirectly, have traditionally been used for this purpose. Although a single-point aging index, such as that calculated by dividing aged by unaged viscosity, can effectively describe the increase in stiffness when the response is essentially viscous, such single-point aging indexes will not always accurately reflect changes in stiffness at low temperatures, where delayed elasticity is a significant portion of the response. This is illustrated in figure 2.9, in which are shown master curves for SHRP asphalt AAD-1. Both the hardness, as indicated by  $t_c$ , and the rheological index,  $R$ , change with aging.

As with temperature susceptibility, a single-point measurement is insufficient to characterize the rheological changes that occur with aging. An aging index based on the stiffness at a selected temperature and loading time will vary with the temperature and loading time chosen (figure 2.10) and will differ numerically from an aging index based on viscosity. More properly, the effect of aging on hardness, rheological type, and temperature dependence should be controlled by direct measurement of the rheological properties. The development of an effective accelerated aging procedure and the use of direct rheological measurements has made aging indexes unnecessary in the new SHRP binder specification.

## *Need for Improved Properties for Use as Specification Criteria*

The rheological properties of asphalt cement vary in a nonlinear, asphalt-specific fashion with temperature and loading time below 60°C (140°F) (figure 2.8), so measurements made above 60°C (140°F) cannot adequately be extrapolated to describe the behavior of asphalt cement at lower temperatures. Consequently, to specify the rheological properties below 60°C (140°F), the properties of the asphalt cement must be measured at lower temperatures.

The penetration test and the ductility test are both inappropriate as fundamental measurements for characterizing low-temperature rheology because the stress fields within the test specimens cannot be defined, the strains developed during the test are very large and

vary within the test specimen, and the stress-strain field cannot be easily modeled or calculated. Thus, the continued use of penetration or ductility measurements in the new SHRP specification was considered undesirable, and the tests were replaced by more fundamental tests that can be used to define a rational rheological model for temperatures ranging from 60°C (140°F) to as low as -40°C (-40°F). This change led the researchers to seek more fundamentally sound measures of the rheological properties of asphalt cement binder as described below.

Traditional methods of rheological characterization include capillary viscometry, penetration measurements, and the determination of the softening-point temperature. The last two methods are unacceptable for a rational characterization of viscoelastic behavior, since they are almost completely empirical. Capillary viscometry, although a rational test method, does not provide information on the time dependence of asphalt cement; measurements providing complete rheological information are preferred. Temperature-susceptibility parameters, since they are calculated from penetration, softening-point, and viscosity data, are not rational indicators of rheological behavior. These parameters have the additional, severe shortcoming of confounding time and temperature effects, making a complete and accurate description of viscoelastic behavior impossible with their use. Rational measurements and parameters that accurately describe the time and temperature dependence of the stress-strain response of plain and modified binder are needed to develop an effective performance-related asphalt cement specification.

Current specifications for asphalt cement used in the United States and Canada are based on either viscosity grading or penetration grading. Both specification methods are limited by the penetration test, an empirical method that provides limited rheological information. The viscosity-grading system is also limited in its control over low-temperature properties, since the grading window used in this system is at 60°C (140°F) (figure 2.11). To fully control the potential performance of an asphalt cement, the mechanical properties over the entire range of temperatures to which pavements are subjected must be accurately measured and specified.

## **Development of New Specification Test Methods**

### *Strategy for Selecting Specification Properties*

To satisfy the objectives of the A-002A project, the researchers were required to identify the distress mechanisms that are critical to field performance, select and develop material response parameters that relate to the critical distress mechanisms, and incorporate these response parameters into specification-type test methods and specification criteria. The rationale and strategy employed in providing input to the development of the new specifications is presented in figure 2.12. First, the critical distress modes were identified. Next, the fundamental engineering material properties associated with the critical distress modes were identified. Test methods were then selected that best measure the fundamental material properties. Criteria used for selecting the specification tests included the need for fundamental performance-related properties, ease of performance, cost-effectiveness, timeliness of the test results, and general applicability to the specification process. If the

fundamental material properties and the associated test methods were not appropriate for specification use, surrogate test methods were selected. Surrogate methods were also based on fundamental material properties—empirical measurements were rejected. For a performance-related specification, it is essential that the specification properties be fundamental material properties so that the properties can be related in a mechanistic manner to the pavement response and, in turn, to pavement performance.

### *Distress Modes Considered*

The A-002A research team decided early to let the distress modes of concern in the field drive the development of the new specification test methods, rather than selecting a set of tests and forcing them to fit the distress modes. Therefore, the approach the A-002A research team used was first to identify the distress modes of predominant concern. Researchers and practitioners have identified several distress modes of importance to hot-mix asphalt pavements (Anderson et al. 1990; Vallerga 1980). From these, the research team selected the following for consideration:

- Low-temperature thermal shrinkage cracking
- Thermal fatigue
- Load-associated fatigue cracking
- Plastic deformation in the upper hot-mix asphalt layers that leads to rutting
- Premature aging
- Moisture damage

Of these distress modes, it was concluded that the first four could be effectively addressed in a binder specification by selecting appropriate physical property measurements. Initially, the team identified thermal shrinkage cracking and thermal fatigue as separate mechanisms. Researchers on the A-002A and A-005 projects concluded independently that these distress modes are actually highly related and may in fact be controlled by similar physical properties.

Premature aging and moisture damage are not really distress modes but are results of environmental conditioning that can significantly affect pavement performance. Moisture damage, which includes the classic stripping mechanism as well as other moisture-induced effects, is not addressed in the A-002A project because it is primarily an aggregate-related problem and asphalt-aggregate interactions were addressed in the A-003B project.

## *Consideration of Rutting in Specification*

Rutting in the upper pavement layers is caused by the accumulated plastic deformation in the mixture that results from the repeated application of traffic loading. Although the rutting tendencies of a pavement are influenced primarily by aggregate and mixture properties, the properties of the binder are also important. This is particularly true for polymer-modified asphalts, which are claimed to enhance the rutting resistance of pavements. Because rutting is more prevalent at high temperatures than at intermediate or low temperatures, the properties related to rutting should be measured in the upper range of pavement service temperatures. As asphalt cement ages, it becomes stiffer and enhances the resistance of the mix to rutting. Therefore, it was also decided that the rutting criteria should be based on thin-film oven (TFO) or rolling thin-film oven (RTFO) test residue to the extent that it best represents the asphalt properties early in the life of the pavement.

On the basis of these observations, a measurement of the nonrecoverable deformation of the asphalt at the upper service temperatures and for loading rates commensurate with traffic loading was established as critical to specifying the asphalt with respect to rutting resistance. Therefore, the researchers recommended the viscous component of the stiffness at 0.1-second loading time as the critical specification criterion for rutting resistance. The 0.1-second loading time was chosen as being representative of the loading time within the pavement that results from a pass of a truck tire traveling at 80 km/h (50 mi/h). With sinusoidal loading, 0.1 second corresponds to 10 rad/s (1.6 Hz).

The viscous component of the stiffness was adopted initially as the specification parameter for rutting. Correlation of the viscous component of the stiffness with mixture data showed that it did not give sufficient weight to the elastic portion of the response, and consequently the loss compliance,  $1/J''$ , was adopted as the specification criteria for rutting. The loss compliance is equal to the complex modulus divided by the sine of the phase angle:  $J'' = G^*/\sin \delta$ .

A ranking of 42 of the MRL asphalt cements by  $G^*/\sin \delta$  for tank and TFO aged (ASTM D 1754) asphalts is shown in figures 2.13 and 2.14. The ranking is based on the temperature at which  $G^*/\sin \delta$  is equal to 1 and 2 kPa for tank and aged material, respectively. A plot of  $G^*/\sin \delta$  versus wheel-tracking results (figure 2.15) provided an early confirmation of the choice of  $G^*/\sin \delta$  as the specification criterion for rutting (M. Bouldin, personal communication, 1993). The binders in figure 2.15 include plain and polymer-modified materials.

A requirement that  $G^*/\sin \delta$  be greater than 1 kPa was added to the binder specification to protect against the possibility that the asphalt binder would contribute to tenderness during mixing and laydown. This could occur if the plant is operated so that the aging during mixing and laydown is significantly less than during the TFO (ASTM D 1754) or RTFO (ASTM D 2872) aging. Reduced mixing temperature or wet aggregate can lead to significantly reduced aging during mixing and laydown.

## *Consideration of Thermal Cracking in Specification*

A rigorous evaluation of the thermal cracking problem should include a consideration of the crack-propagation characteristics of the binder and a fracture-mechanics analysis. Although such characterizations were pursued during the basic research phase of the A-002A contract, these characterizations were not considered appropriate for specifications. Binder rheology and direct tension properties were used as surrogates for crack-propagation and -initiation parameters.

Thermal shrinkage cracking is a serious problem in much of the northern United States and in most of Canada. Such cracking occurs when rapid temperature drops lead to thermal stresses that exceed the strength of the binder. Cracking may result from a single temperature excursion to the critical cracking temperature or from repeated cycling to somewhat higher temperatures. The latter condition has been described as *thermal fatigue*, although both conditions involve the propagation of cracks within the binder.

The concept of a critical cracking temperature below which cracking will occur as a result of a single cooling cycle has led to the definition of a limiting stiffness temperature (Haas and Topper 1969; Monismith et al. 1965). According to this concept, when the asphalt binder reaches a critical stiffness value, cracking should result. The temperature at which this stiffness is reached is called the *limiting stiffness temperature*.

Previous researchers have demonstrated the validity of the limiting stiffness temperature in predicting low-temperature thermal shrinkage cracking (Readshaw 1972). (Note: The limiting stiffness temperature is simply the pavement temperature at which a certain stiffness value is reached after a specified loading time; at lower temperatures, the pavement will experience thermal cracking. This criterion was developed with the assumption that cracking occurs after a single excursion to or below the limiting stiffness temperature.) In the early versions of the specification, the limiting stiffness temperature was chosen as the temperature at which a stiffness of 200 MPa is obtained after a loading time of 2 hours (Readshaw 1972).

The A-002A research team also recognized the importance of the time dependence in determining the development of thermal shrinkage stresses (see volume 3). Because the time dependence of asphalts varies widely, the shape of the master curve should also influence the magnitude of the thermal shrinkage stresses that develop during cooling. Thus, the slope of the creep curve,  $m = d \log J(t) / d \log t$ , was also included in the binder specification. A bar chart of the limiting stiffness temperatures for the MRL asphalts is shown in figure 2.16. In this figure, the asphalts have been arranged from lowest to highest predicted cracking temperature. A similar plot, showing the temperature at which  $m = 0.35$ , is given in figure 2.17.

In working with polymer-modified materials, the team observed that adding polymers can significantly affect the low-temperature strain and energy to failure without affecting the rheological properties, as shown in figures 2.18 and 2.19. Thus, the researchers concluded that strain tolerance as well as stiffness must be considered with respect to low-temperature thermal shrinkage cracking. This conclusion was reached on the basis of mixture data and

field experience that shows that polymer modification does enhance resistance to low-temperature thermal shrinkage cracking. The strain at failure at the minimum pavement service temperature was selected as one of the specification criteria to ensure that the pavement will not transcend into the brittle region within its service temperature regime. This transition occurs at approximately 1.0 percent strain to failure and occurs rather rapidly as the temperature is lowered (figure 2.20). The failure strain is specified at an elongation rate of 1.27 mm/min (0.05 in./min). Failure strain data for the MRL asphalts are shown in figure 2.21.

The low-temperature specification test temperature is the minimum pavement temperature plus 10°C (18°F). An analysis of the rheological data showed that all asphalts have a common temperature dependence below the glass transition or defining temperature ( $T_d$ ). If a 2-hour stiffness value, as reported in the literature, is adopted as the specification criterion, the low-temperature testing will become too time consuming. Similarly, a slow rate-of-elongation tensile strength test is not acceptable. The team took advantage of the common temperature dependence, which dictates that the stiffness at  $T_{\min}$  after a 2-hour loading time is very nearly equal to the stiffness after a 60-second loading time at  $T_{\min} + 10^\circ\text{C}$  (18°F).

### *Consideration of Fatigue Cracking in Specification*

The selection of specification criteria to ensure satisfactory resistance to fatigue cracking is perhaps the most difficult challenge presented by the new binder specification. First, fatigue cracking generally occurs late in the life of a pavement, requiring the testing of asphalt that is appropriately aged to simulate the long-term in situ properties of the binder. The selection of appropriate specification criteria is further complicated by conflicting evidence regarding the effect of asphalt properties on fatigue performance. The results of laboratory stress-controlled fatigue tests imply that stiffer binders are more resistant to fatigue cracking (Pell and Cooper 1975). Conversely, laboratory strain-controlled fatigue testing implies that softer binders are more resistant to fatigue cracking (Monismith and Deacon 1969; van Dijk 1975).

Ideally, the fatigue properties of the asphalt and the crack-propagation properties should be included in the binder specification. However, as noted above, these properties are considered too complex for use in a specification. Therefore, surrogate properties must be selected as the specification criteria. Research conducted by others for polymer-type materials has shown that the slope of the log stiffness versus log time curve,  $m = d \log S(T, t) / d \log t$ , can be correlated with the rate at which cracks are propagated during fatigue (Shapery 1973). More recent work in the A-003A contract has shown that the dissipated energy is a valid fatigue criterion and that it can be made relevant to both stress- and strain-controlled fatigue tests.

On the basis of the above information, the initially recommended specification criterion for fatigue was based on the  $m$  value at a loading time of 0.1 second and a temperature equal to the mean annual pavement temperature. Using this criterion,  $m$  was to be less than or equal to 0.5 at the mean annual paving temperature at 0.1 second. Including the pavement

temperature in the specification allows the fatigue criterion to be adjusted according to the climatic region.

At the suggestion of the A-003A researchers, and in light of an evaluation of the fatigue performance in field trials such as Zaca-Wigmore (figure 2.22), the fatigue criterion was changed to reflect the energy dissipated per load cycle. Dissipated energy in a dynamic shear test is appropriately calculated as  $G^* \sin \delta$  (Ferry 1980). Researchers from the A-003A team have related the dissipated energy in mixtures to fatigue life and have shown that it can be made relevant to both controlled-stress and controlled-strain conditions.

The asphalt binder specification criterion for fatigue performance is the loss modulus ( $G'' = G^* \sin \delta$ ) at 10 rad/s (1.6 Hz) loading time, and as before, at a temperature equal to the average pavement temperature in the location of interest. For specification purposes, the value of the loss modulus is limited to a maximum of 3 MPa at the anticipated average annual pavement temperature. The MRL asphalts have been ranked according to fatigue resistance using this criterion; figure 2.23 is a bar chart showing the temperature at which the PAV residue attains a  $G''$  value of 3 MPa. The chart is arranged from lowest to highest temperature.

### *Consideration of Aging in Specification*

The criteria in a true performance-related specification must be representative of the material in the pavement. Aging or hardening of asphalt cement occurs during the mixing and laydown process and during service. The existing aging methods, the TFO test (ASTM D 1754) and the RTFO test (ASTM D 2872), were reviewed, and questions were raised about the calibration of these methods for different plants, operating conditions, asphalt sources, aggregate types, and moisture conditions. An in-depth study to validate and cross-correlate the two test methods was considered; however, a comprehensive evaluation of the TFO test or RTFO test would have consumed too much of the project resources. Therefore, further study of the two methods was discounted, and attention was given to long-term field aging, which is not addressed in the current specifications.

To simulate long-term exposure in the field, the pressure-aging test was adopted. This test has been used by other researchers and has been modified for the new SHRP binder specification (Kim et al. 1987; Lee 1968). In its initial form, as used in the project, standard TFO test pans were placed in a pressure-aging vessel (PAV) that contained air at 2 MPa. The pans were held in the PAV for 6 days at 60°C to 80°C (140°F to 176°F) to simulate long-term field exposure. Both long-term field exposure and PAV exposure cause complex changes in the rheology of the asphalt. The shape of the master curve and the hardness of the asphalt are both affected by long-term aging as illustrated in figure 2.9. Therefore, a simple shift factor such as an aging index based on 60°C (140°F) viscosity is insufficient to determine the rheological properties of aged asphalt. Such a viscosity-based aging index merely shifts the master curve to longer loading times and does not account for changes in the shape of the master curve, which in turn reflects changes in the time dependence of the

asphalt binder. Aging does not appear to significantly alter the temperature dependence of the asphalt binder.

### *Validation of Pressure-Aging Test*

Considerable objection was voiced to the length of time required for the initial PAV test. Therefore, the temperature was raised to 100°C (212°F) and the time reduced to 20 hours. The aging produced with 6 days at 71°C (160°F) is nearly identical to that produced with 20 hours at 100°C (212°F), as shown by figure 2.24. When aging in the desert was compared with other climates (R. Reese, personal communication, 1992), it became obvious that several aging temperatures would be necessary. Therefore, the PAV aging is performed at 90°C, 100°C, or 110°C (194°F, 212°F, or 230°F), depending on the asphalt grade.

A detailed experiment was developed to validate that the chemistry and rheology of the residue from the PAV test replicate the chemistry and rheology of long-term field exposure (see figure 2.25). Unfortunately, resources needed to complete the experiment were directed to other tasks, and much of the data specified in figure 2.25 were not obtained. The results that were obtained do verify that similar rheological behavior is obtained in the laboratory and field, as illustrated by figure 2.26. Values of  $G^*$  and size exclusion chromatography (SEC) fraction I that were obtained from several original laboratory-aged and field-aged binders are compared in figures 2.27 and 2.28. Overall, the results validate the hypothesis that the PAV test successfully mimics field aging.

It should be emphasized that results obtained by researchers at Western Research Institute as part of this study (see volume 2) strongly indicate that when accelerated aging temperatures exceed approximately 120°C (248°F), the chemistry of the aging process is dramatically altered. As a consequence, increasing the aging temperature above the 90°C, 100°C, or 110°C (194°F, 212°F, or 230°F) selected for the specification should be strongly discouraged as a means for accelerating the aging process in accelerated aging tests.

### *Consideration of Environmental Effects and Specification Philosophy*

The new SHRP binder specification is based on fundamental measurements obtained at pavement temperatures representative of the upper, middle, and lower ranges of service temperatures. The measurements are in keeping with the distress mechanisms that occur or dominate at these temperatures. In early versions of the specification, measurements at two test temperatures were used with a linear viscoelastic master curve to predict, through a hyperbolic-like rheological model for the asphalt cement, properties at the service temperatures. Such prediction became impossible when it was required that the specification include plain as well as modified asphalt cement. Whereas a simple hyperbolic-shaped model can be developed to characterize plain asphalt with measurements at only two test temperatures, no such model can be developed for many modified asphalt cement binders.



The SHRP binder specification is performance-related, and the grades of asphalt cement binder are designed to serve specific climates. The specification tolerance values or limits are the same across all the grades, but the tolerance values are obtained at different temperatures according to the grade and climate served. For example, the criterion for rutting is that  $G^* \sin \delta$  be less than 2.0 kPa, but this value must be obtained at different temperatures according to the grade specified. In contrast, in the current viscosity-graded specification, viscosity measurements are all made at 60°C (140°F), but the tolerance value differs for each grade. This implies, of course, the assumption that the temperature dependence of all plain and modified asphalt cements is similar, and this is simply not correct.

### *Proposed Specification Tests*

In the new SHRP binder specification the binder is tested in its original condition, after RTFO or TFO exposure, and after RTFO + PAV or TFO + PAV exposure. The original material is tested for safety, to ensure pumpability of the binder in the mix plant, and to be certain that the original material is stiff enough that tenderness is not encountered when minimal hardening occurs in the hot-mix plant.

Because rutting occurs early in the life of a pavement, the specification criterion for rutting is based on RTFO or TFO residue. Fatigue cracking resulting from excessive aging, as opposed to fatigue caused by a base or design failure, occurs late in the life of the pavement, after the asphalt binder has aged appreciably. The most critical time for thermal shrinkage cracking is also after field aging, and therefore both fatigue and thermal shrinkage cracking criteria are based on PAV residue.

In summary, the key elements of the new tests proposed for specification use are as follows:

- New physical property tests that are fundamental and that can be related to the critical distress modes and field performance through rational models
- An accelerated laboratory aging test that mimics the field aging process to produce aged material with fracture and rheological characteristics similar to those of field-aged material

### *Selected Test Methods*

In the process of selecting the test methods that were proposed for the new binder specification, several factors were considered:

- The test methods and test criteria should address the primary modes of pavement distress, thermal cracking at low temperature and permanent deformation (rutting) at high temperature, and fatigue properties.

- The test methods should provide enough information to control the hardness of the asphalt cement, the spectrum width (rheological type), and the temperature dependency.
- The specification tests should be constructed so that a wide array of rheological information—such as the glass transition temperature, spectrum width, and shape of the master curve—can be accurately estimated for use in pavement performance models.
- The specification tests should be reasonably quick and easy to perform at a state highway laboratory or a commercial testing laboratory.

In view of these considerations, the SHRP A-002A research team proposed the following tests for specifying paving-grade asphalt cement binders, including both unmodified and modified asphalt cement:

- Dynamic mechanical measurements in both the intermediate and high pavement temperature ranges using parallel-plate geometry at 10 rad/s (1.6 Hz)
- The bending beam test at the minimum pavement temperatures at which the capacity of the dynamic shear rheometer in parallel-plate geometry is exceeded
- The direct tension test at low temperatures to determine the tensile strain to failure
- The PAV test to simulate long-term in-service aging
- The Brookfield rheometer test (ASTM D 4402)

See volumes 2, 3, and 4 for details regarding these test procedures and their development.

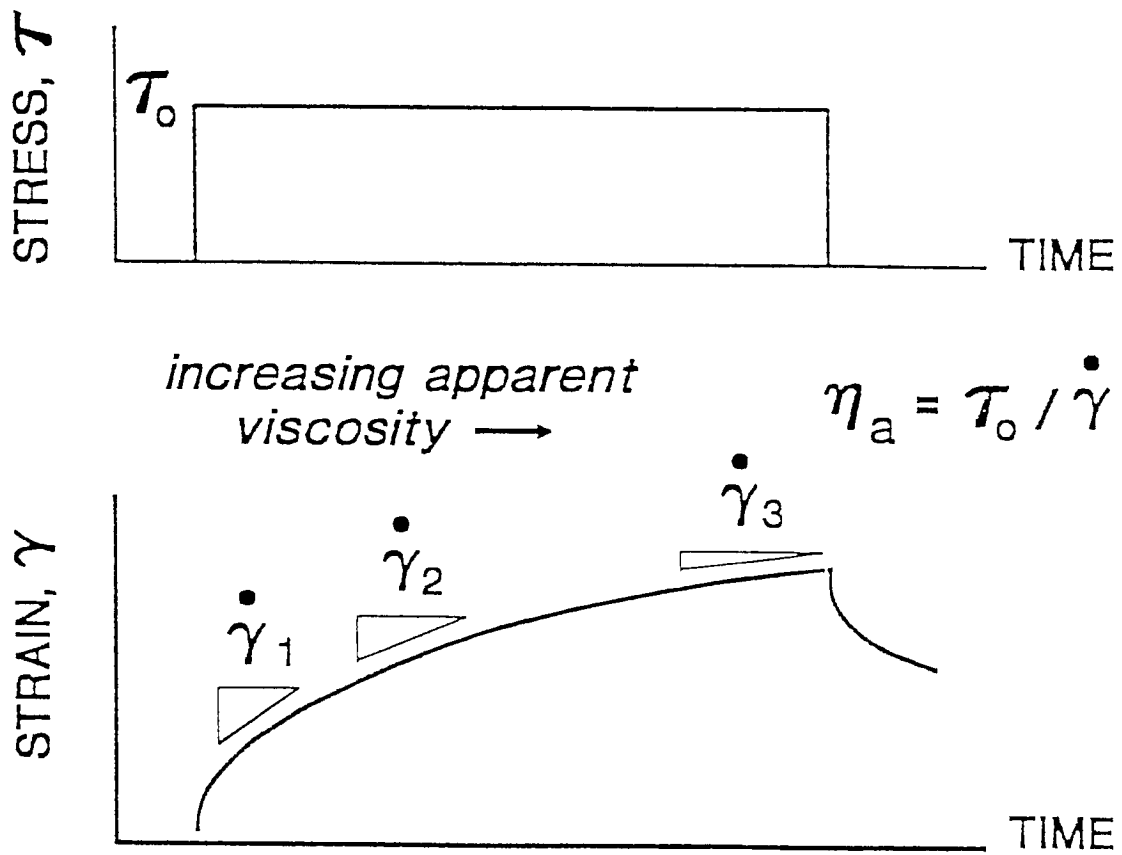
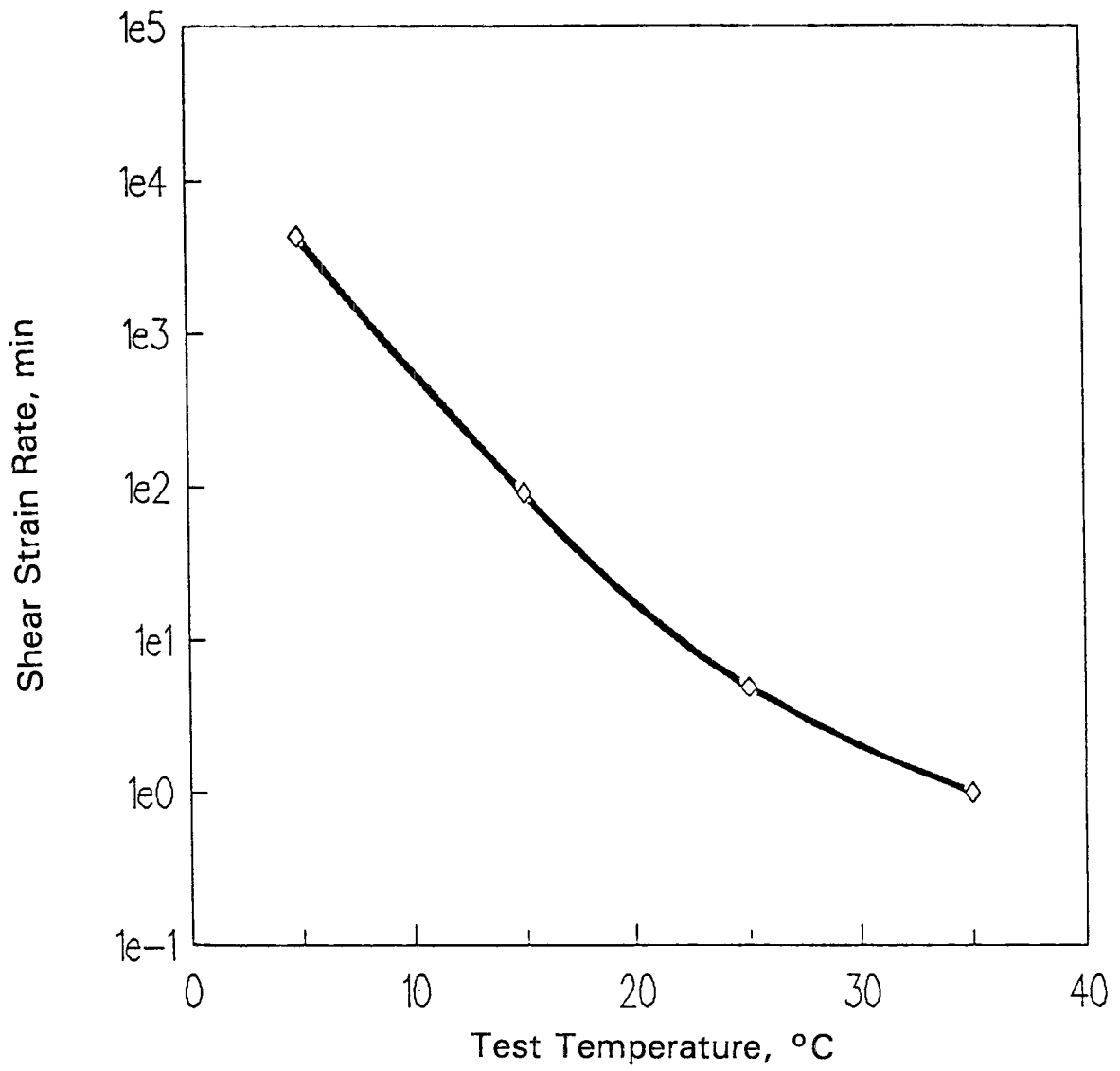


Figure 2.1 Shear Rate as a Function of Loading Time in a Creep Test



**Figure 2.2 Time Required to Obtain Steady-State Flow at Different Temperatures in a Creep Test**

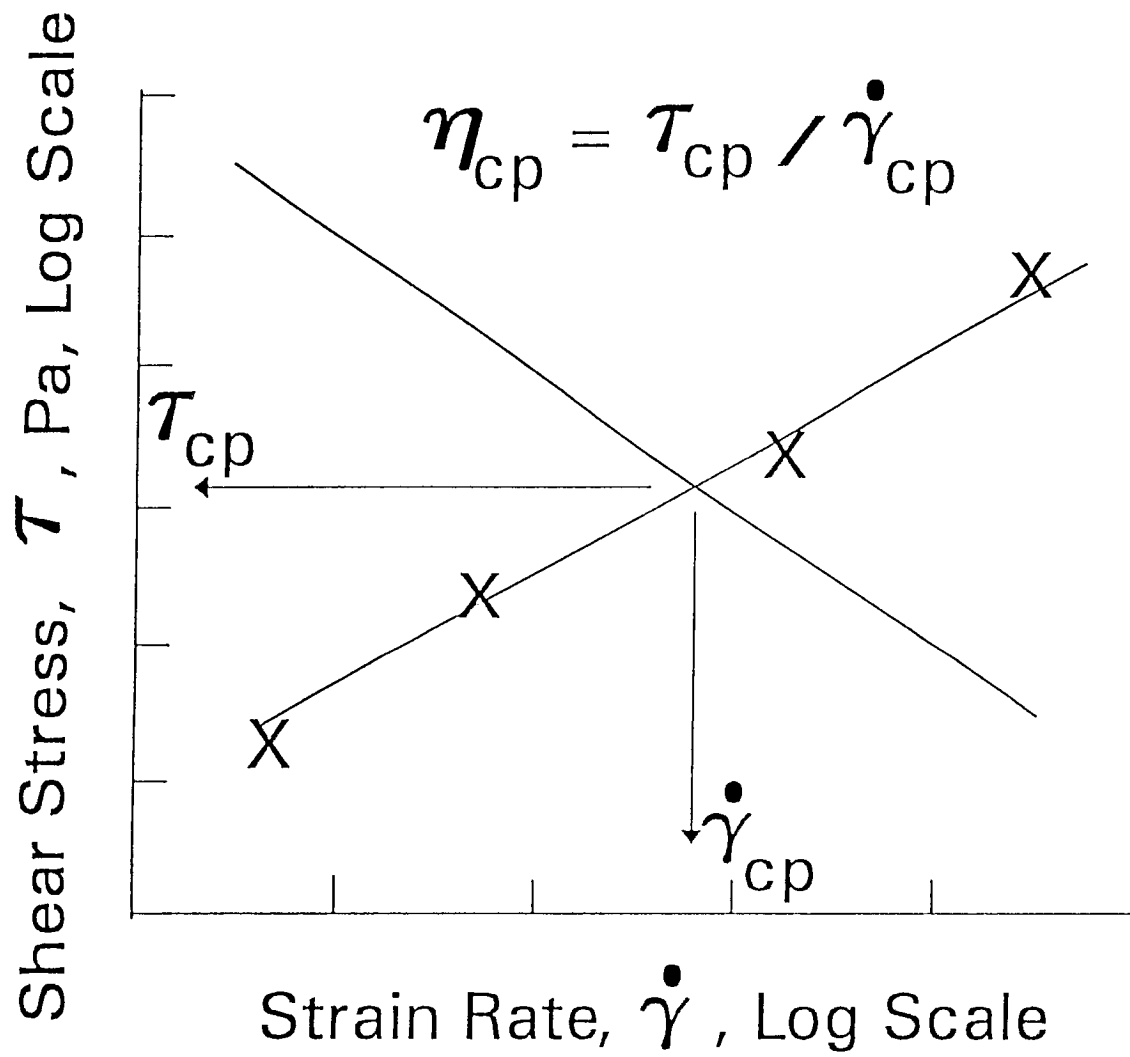
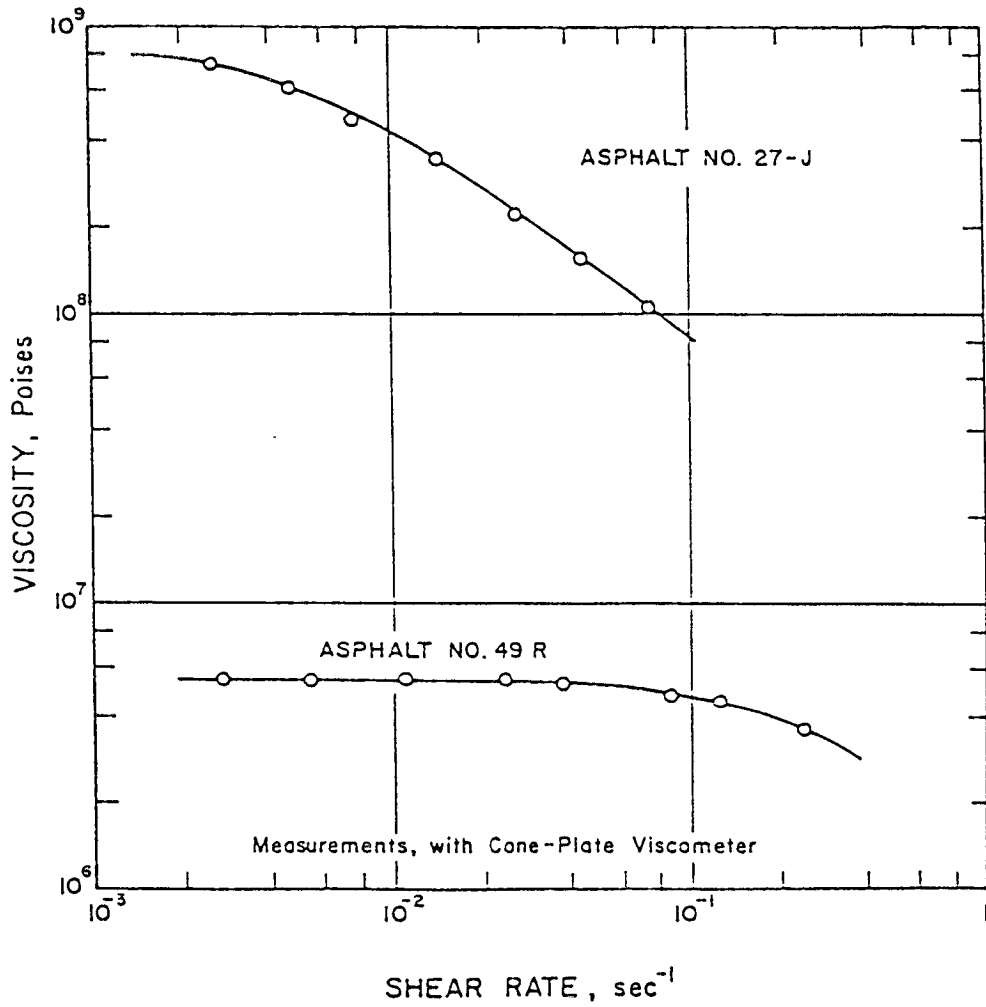
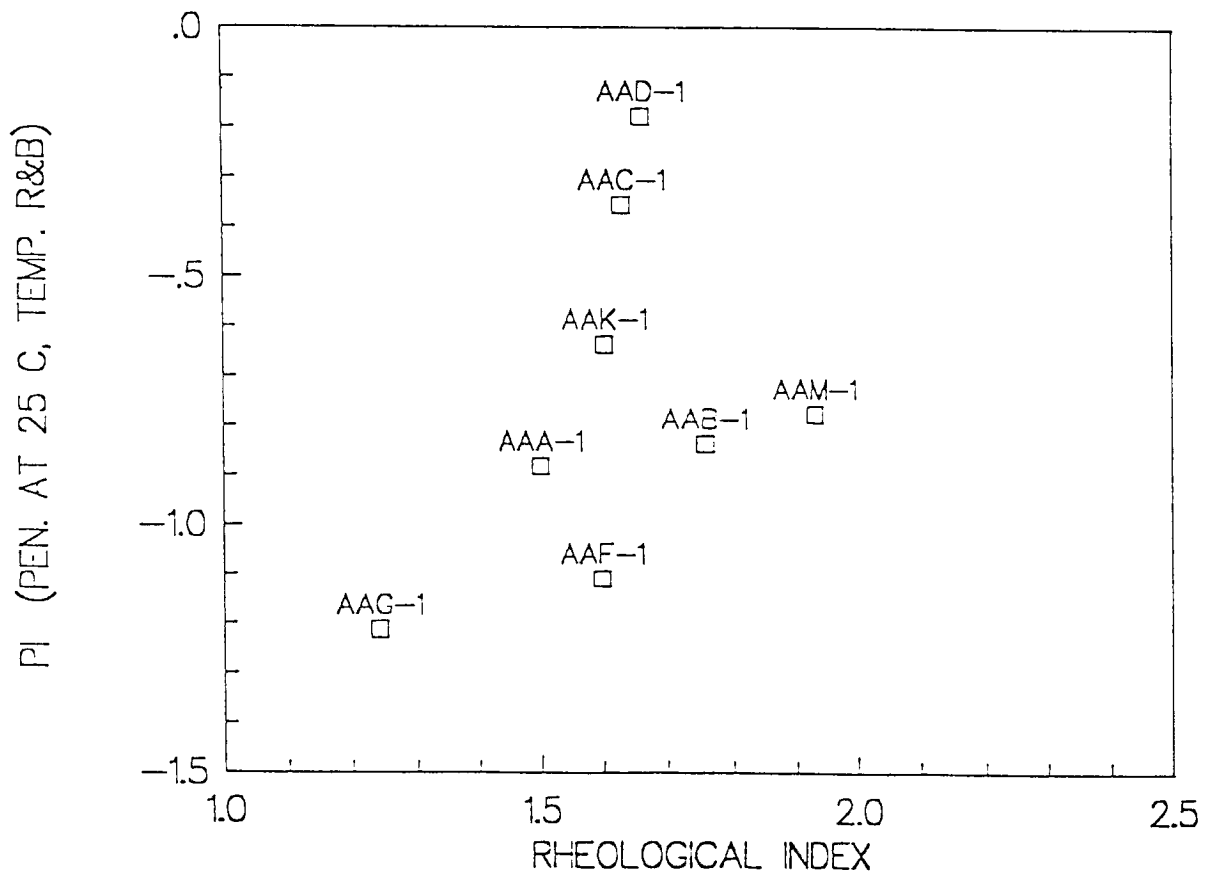


Figure 2.3 Illustration of Constant-Power Viscosity (after Schweyer et al. 1976)



**Figure 2.4 Illustration of Technique for Obtaining Viscosity at Zero Shear Rate (after Puzinauskas 1979)**



**Figure 2.5 Penetration Index (Based on Penetration at 25°C [77°F] and Ring and Ball Softening-Point Temperature) versus Rheological Type as Measured by Rheological Index, for Eight Asphalt Types**

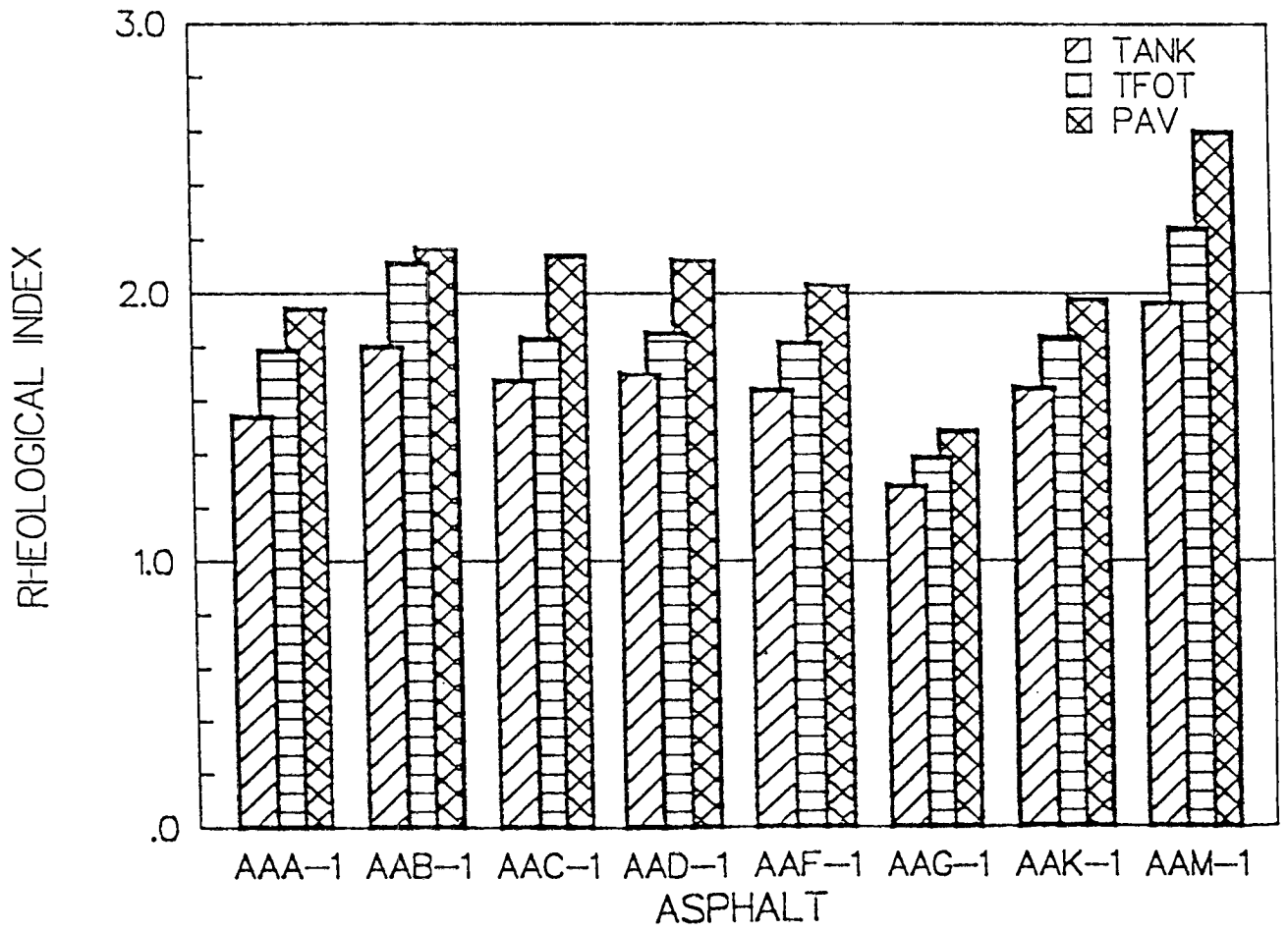
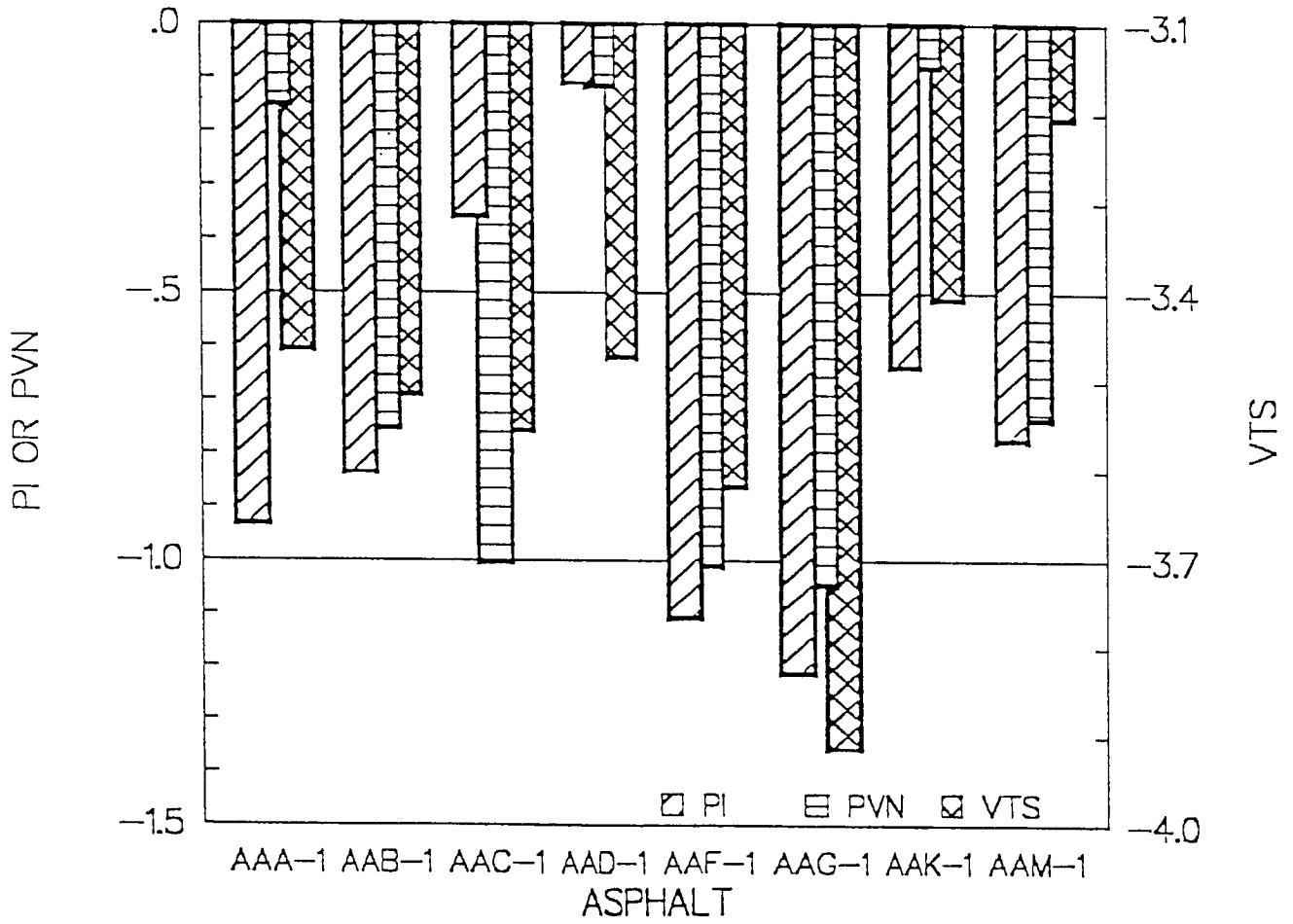
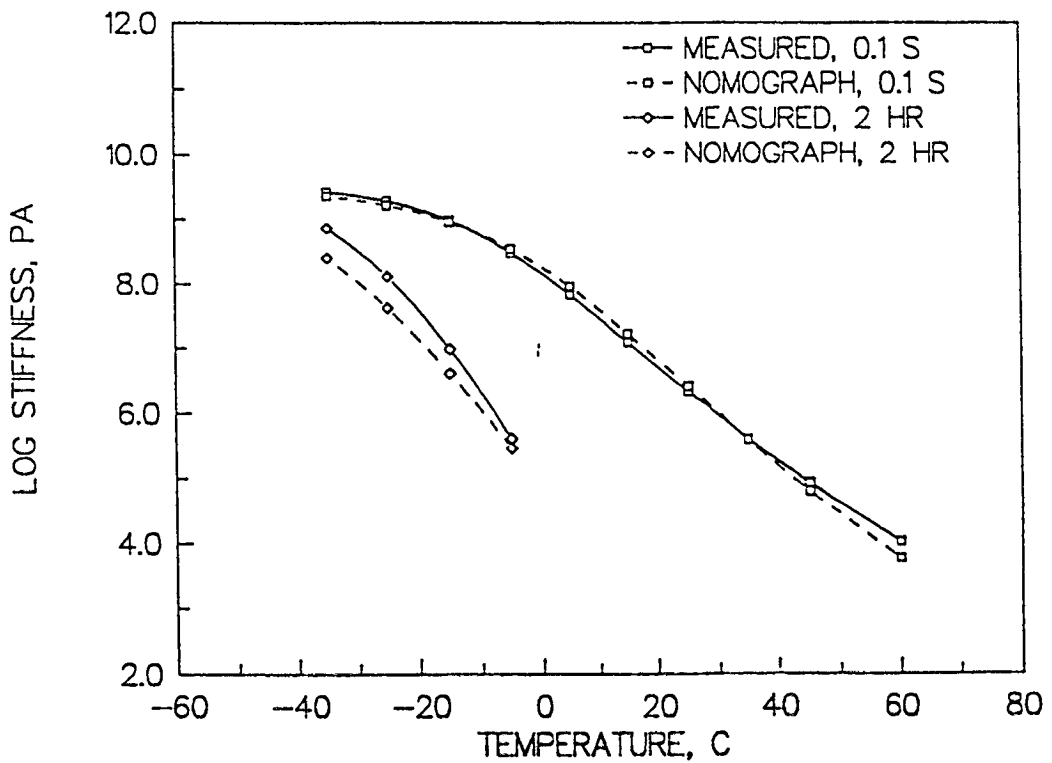
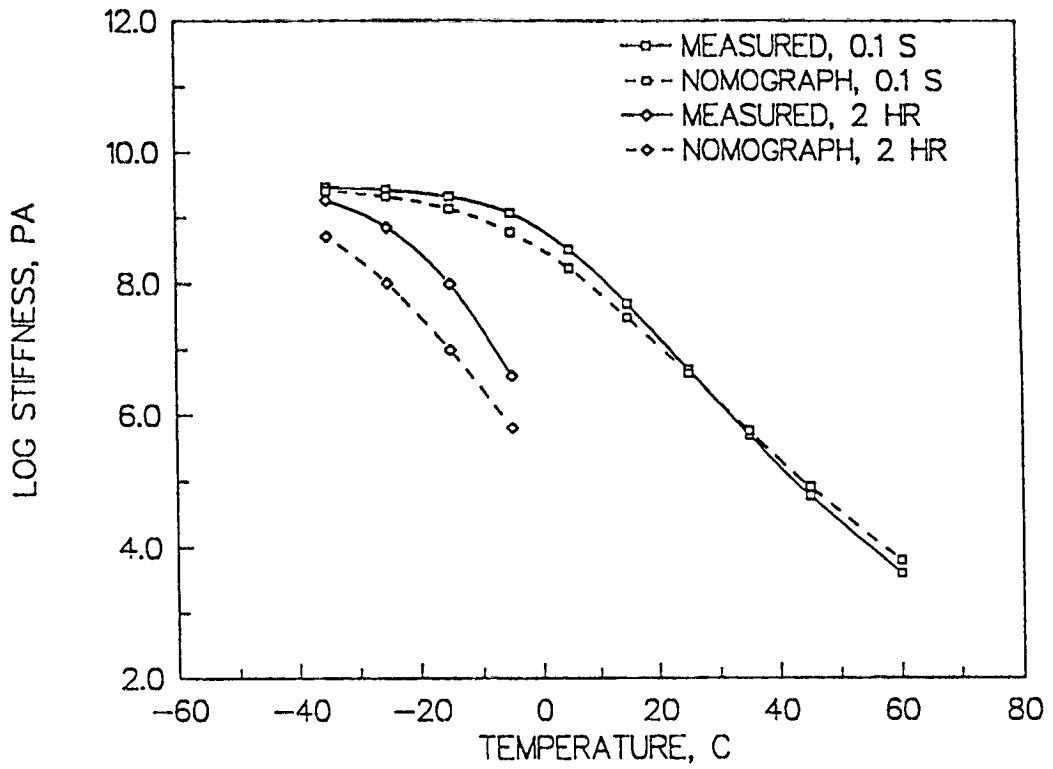


Figure 2.6 Effect of Aging on Rheological Index





**Figure 2.7 Comparison of Temperature-Susceptibility Parameters Calculated by Different Methods**



**Figure 2.8 Isochronal Curves of Extensional Stiffness Modulus, as Measured and as Predicted from van der Poel's Nomograph; SHRP Asphalts AAG-1 (Top) and AAK-1 (Bottom)**

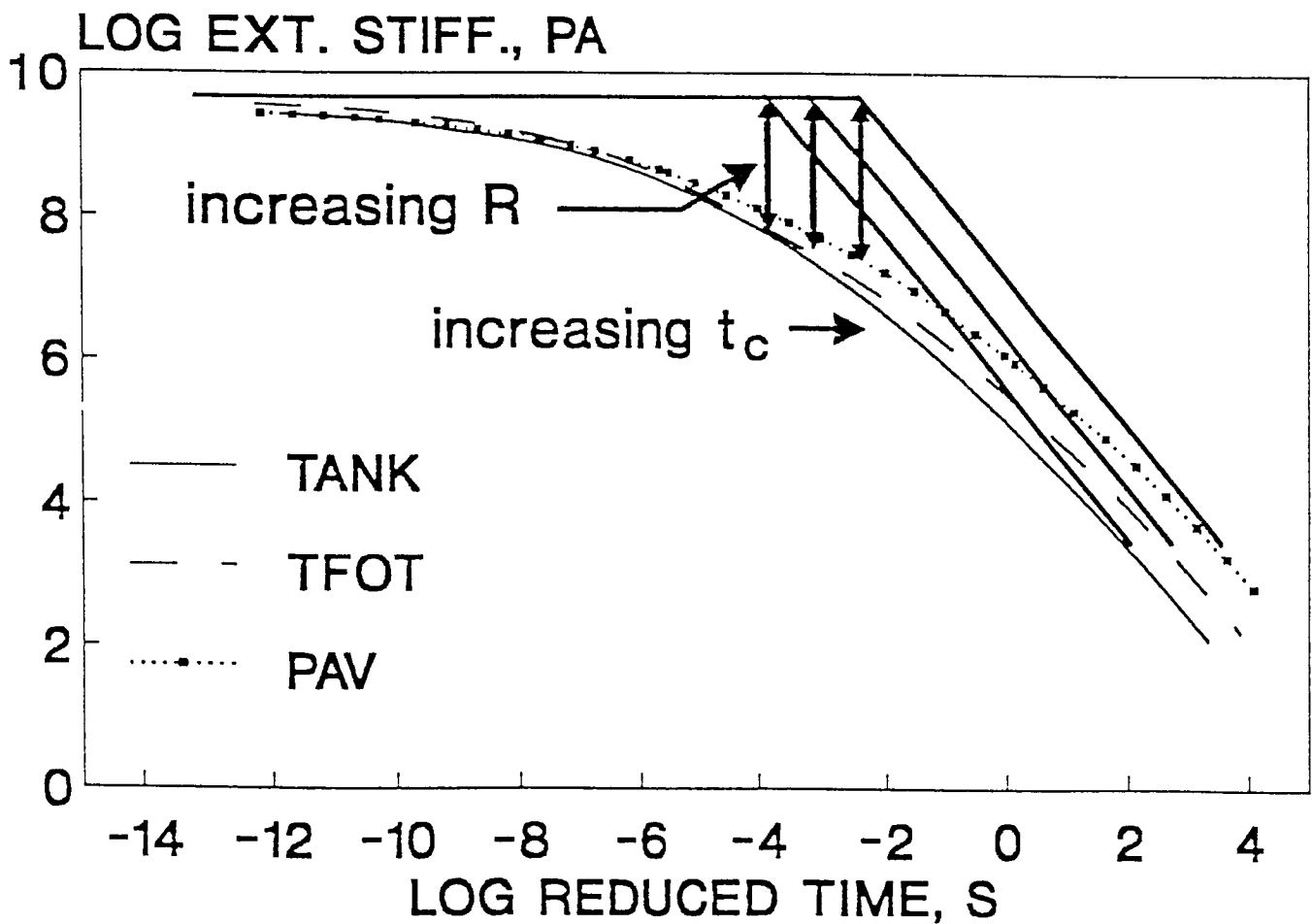


Figure 2.9 Changes in Master Curve (Extensional Stiffness) for SHRP Asphalt AAD-1 during Laboratory Aging

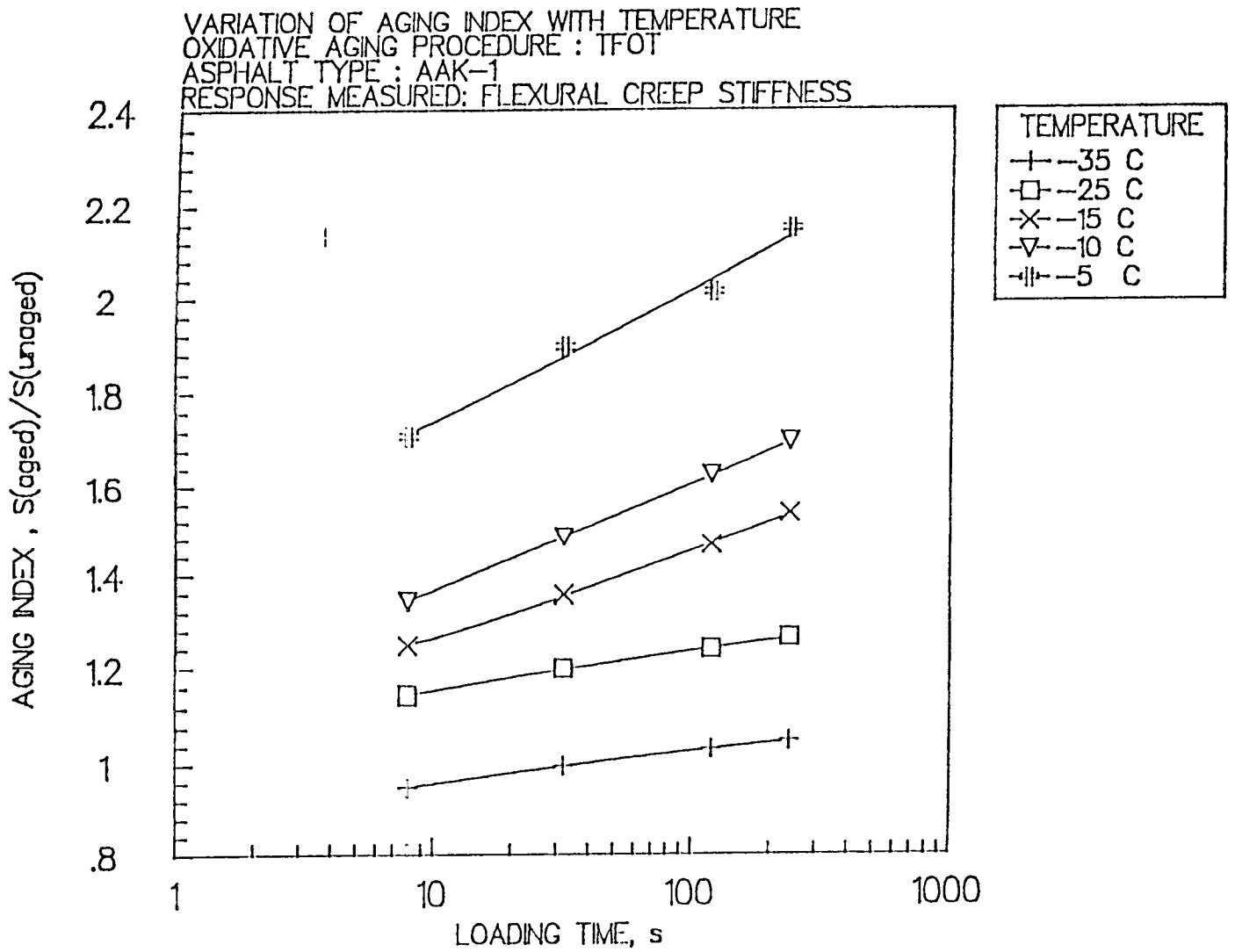


Figure 2.10 Aging Indexes Based on Different Loading Times and Test Temperatures

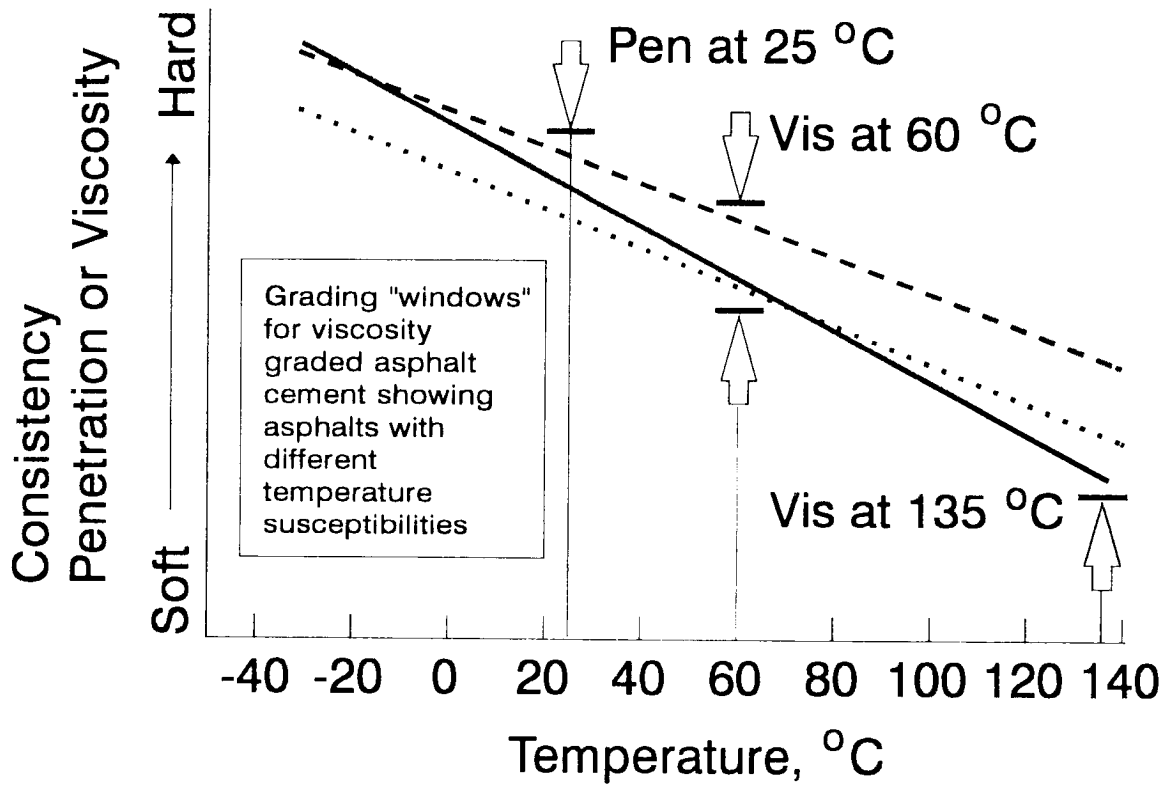


Figure 2.11 Schematic Illustration of Viscosity-Grading System

# Strategy for Specification Development

---

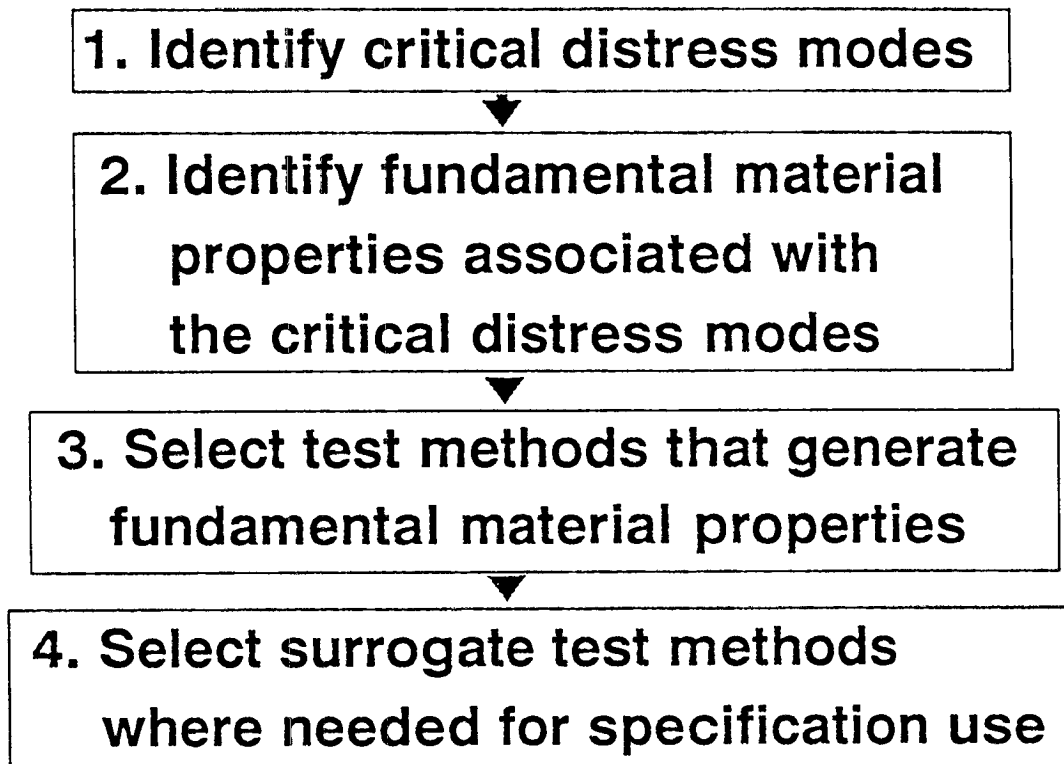
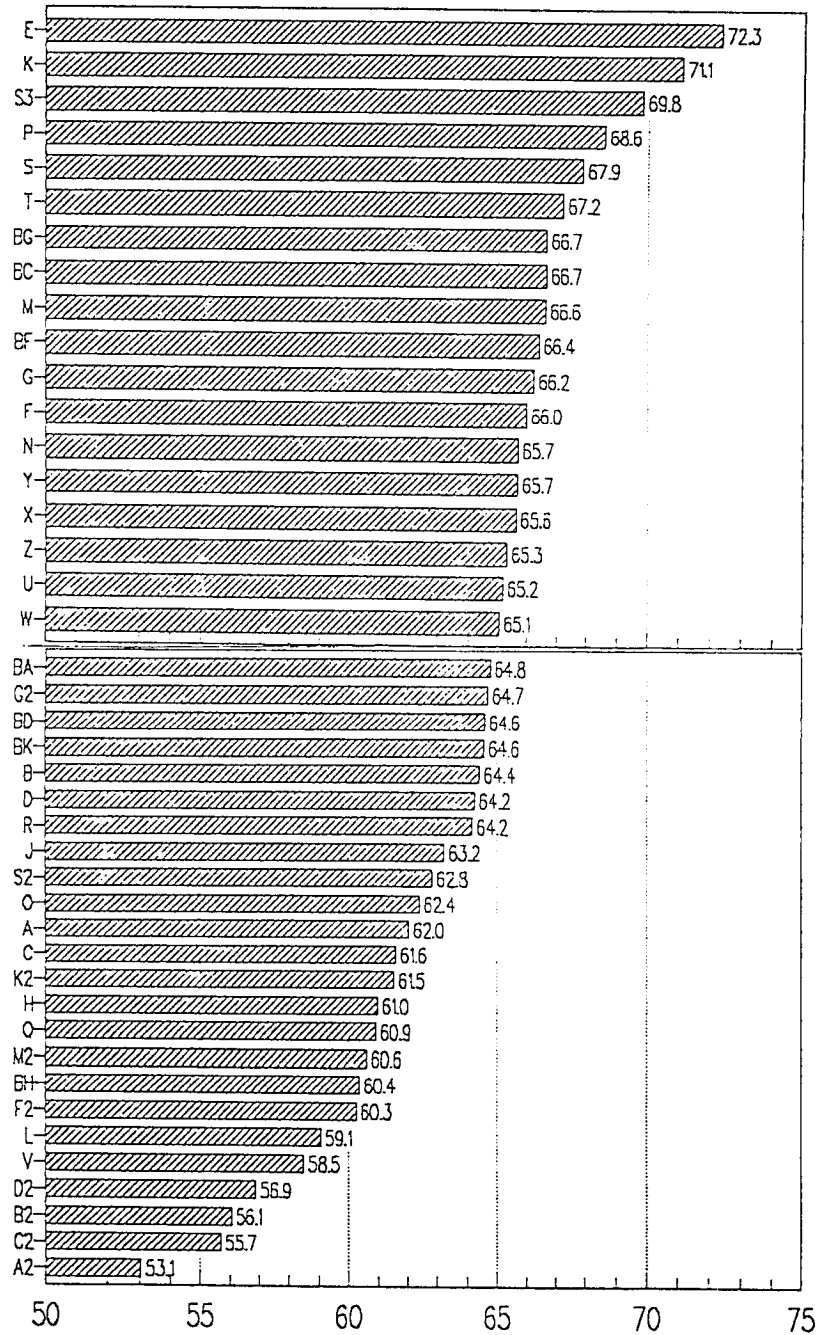


Figure 2.12 Flow Diagram Illustrating Strategy for Developing the SHRP Binder Specification

MRL asphalts tank condition  
 Temperature at which  $G^*/\sin \delta$  at 10 rad/s = 1 KPa



**Figure 2.13 Ranking of Materials Reference Library Asphalts in Tank Condition: Temperature at Which  $G^*/\sin \delta = 1$  kPa at Loading Frequency of 10 rad/s**

MRL asphalt's TFOT aged condition  
 Temperature at which  $G^*/\sin \delta$  at 10 rad/s = 2 kPa

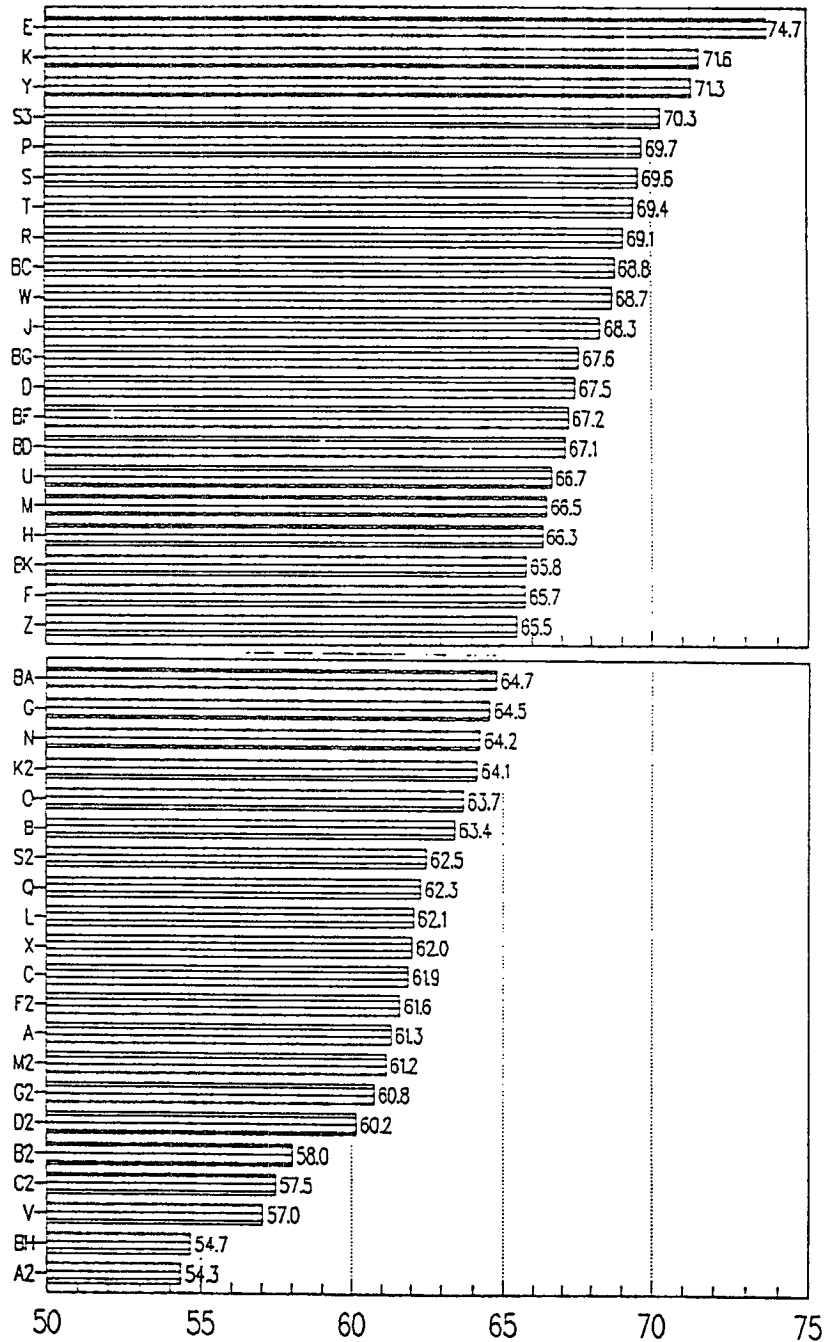
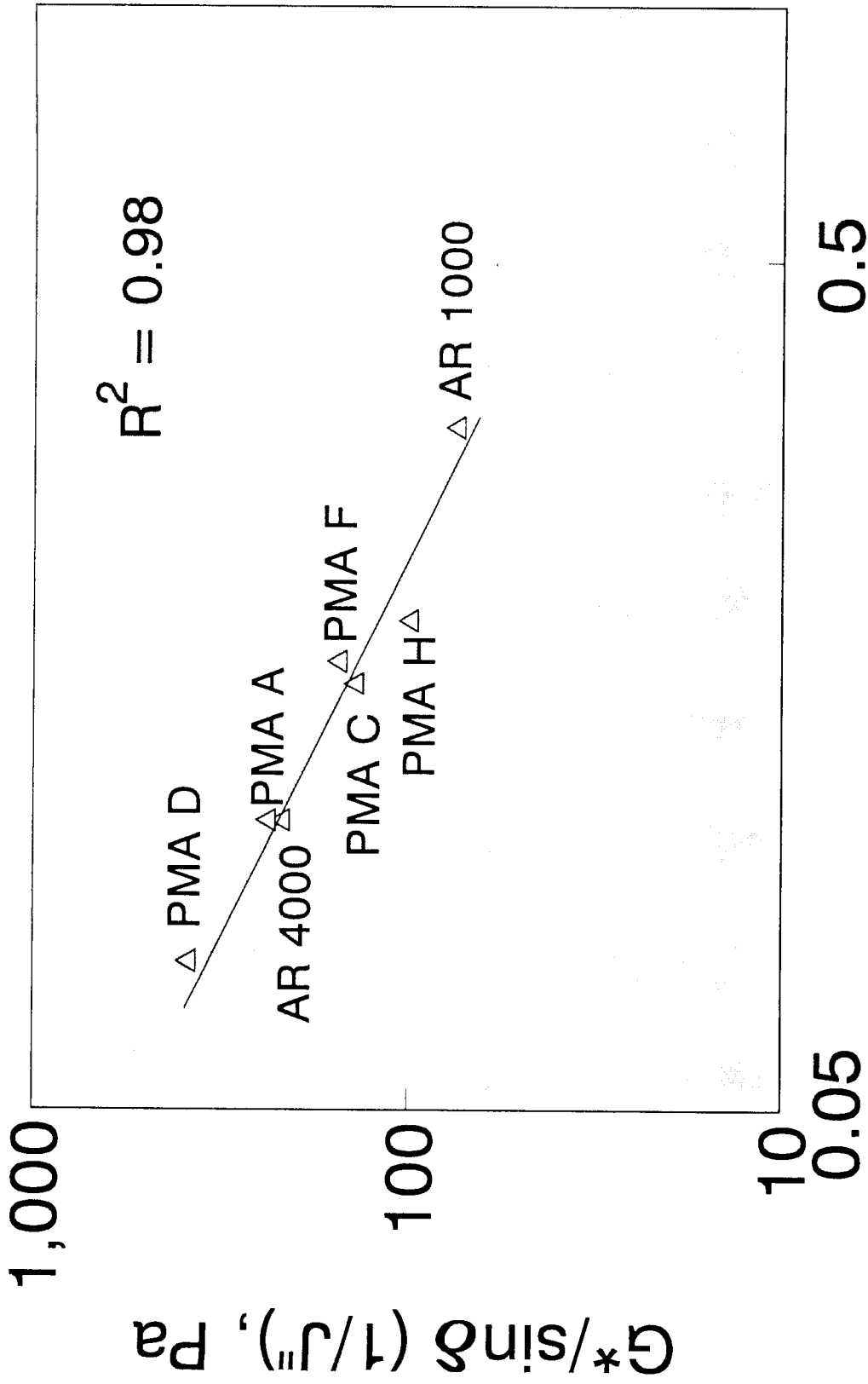


**Figure 2.14 Ranking of Materials Reference Library Asphalts after Thin-Film Oven Aging: Temperature at Which  $G^*/\sin \delta = 2$  kPa at Loading Frequency of 10 rad/s**





## Rutting rate mm/1,000 cycles

Figure 2.15 Loss Compliance versus Wheel-Tracking Test Results  
(after Bouldin, personal communication, 1992)

MRL asphalts after PAV treatment  
 Temperature at which  $S$  at 60 s = 200 MPa , C

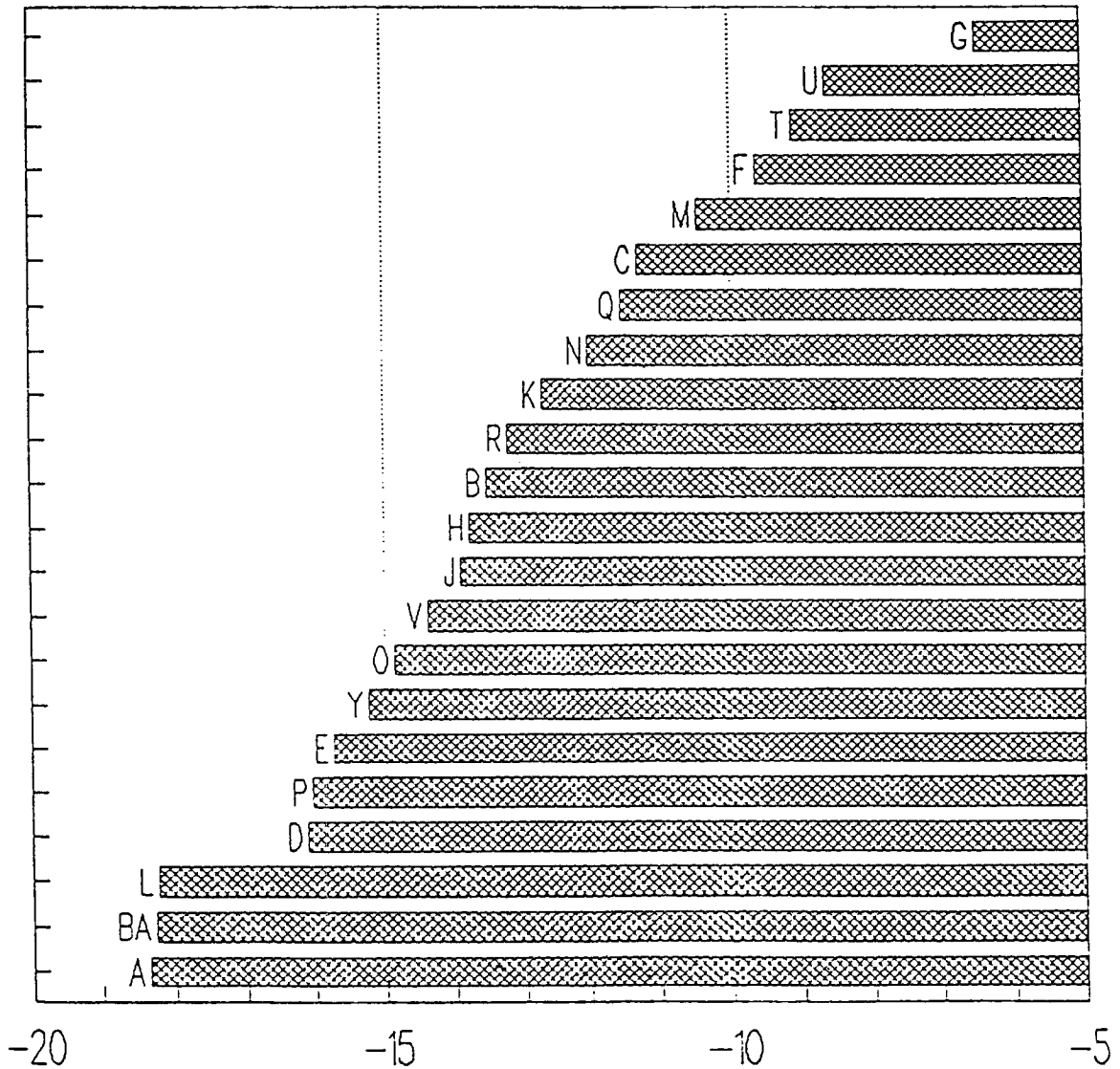


**Figure 2.16 Ranking of Materials Reference Library Asphalts in Tank Condition:  
 Temperature at Which Stiffness Is 200 MPa after 60 Seconds Loading Time**

MRL asphalts after PAV treatment  
 Temperature at which  $m$  at 120 s = 0.35 C

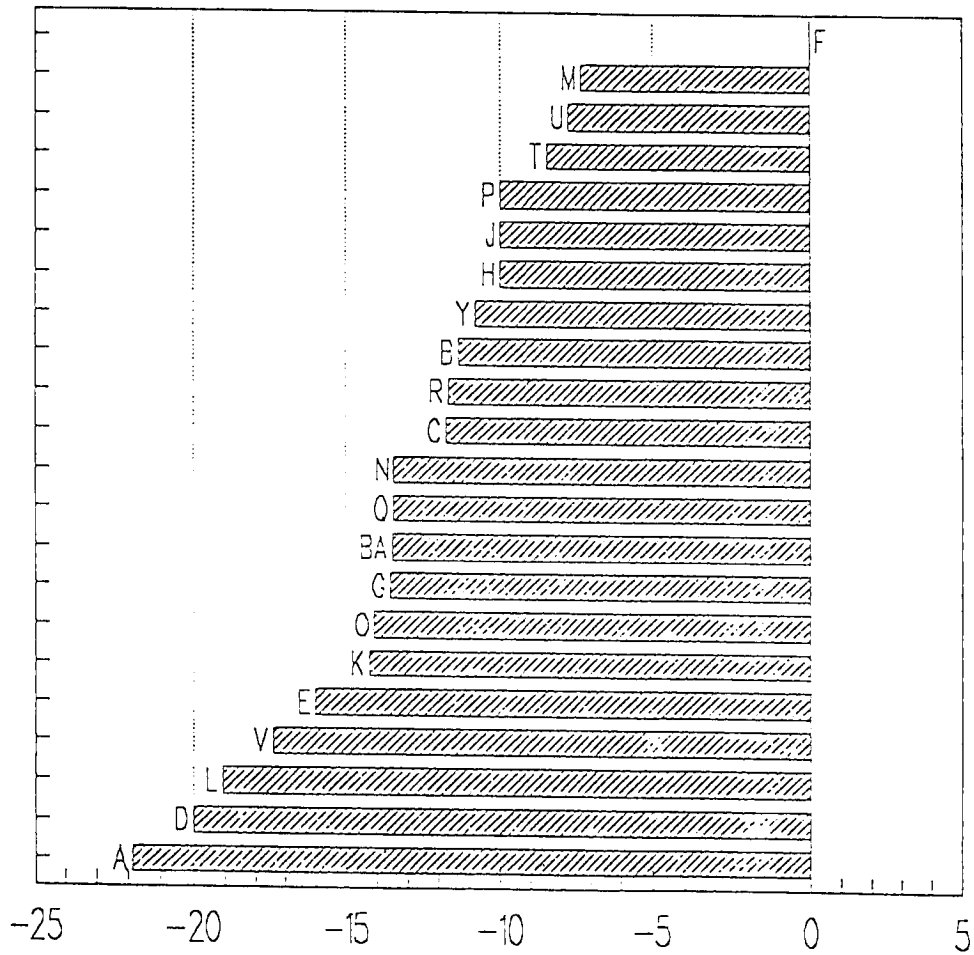


**Figure 2.17 Ranking of Materials Reference Library Asphalts after Pressure Aging: Temperature at Which  $m = 0.35$  after 120 Seconds Loading Time**

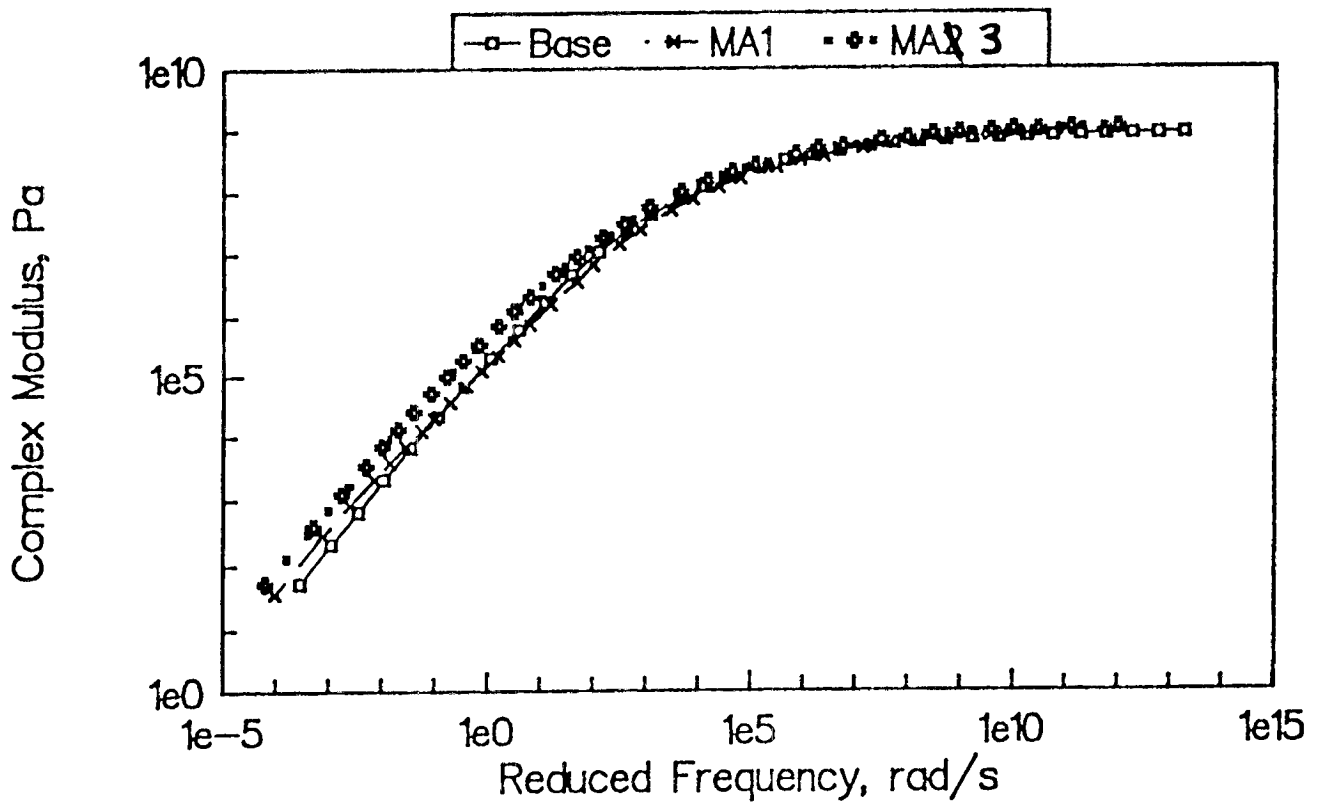


Figure 2.18 Typical Effect of Polymer Modification on Master Curve of Asphalt Cement

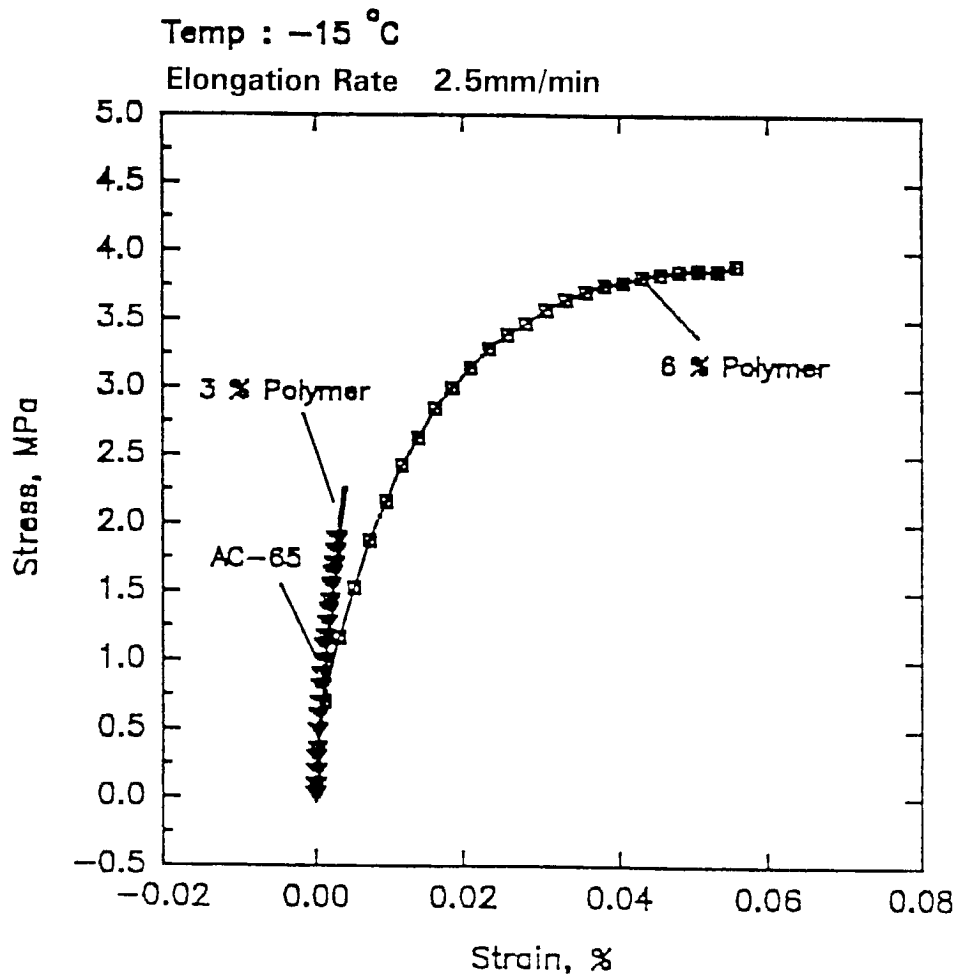


Figure 2.19 Typical Effect of Polymer Modification on Ultimate Properties of Asphalt Cement

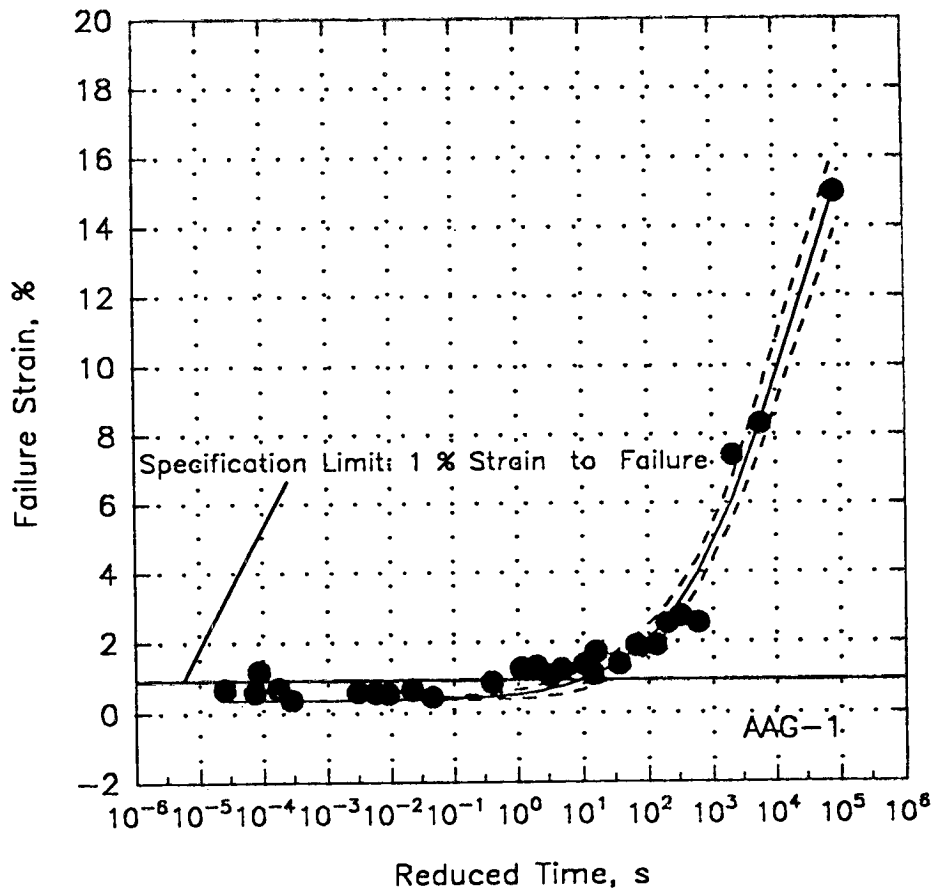
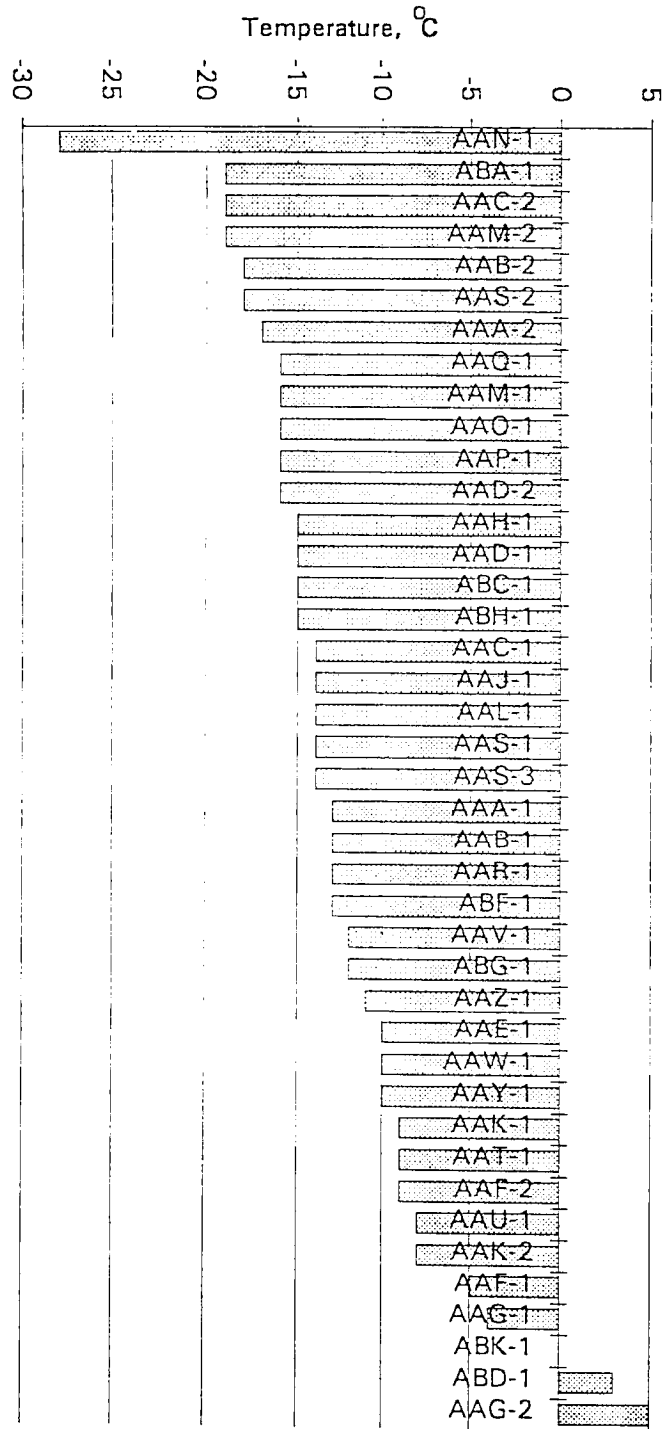


Figure 2.20 Typical Failure Strain Master Curve Showing Transition to Brittle Region



**Figure 2.21 Ranking of Materials Reference Library Asphalts after Pressure Aging: Temperature at Which Strain-to-Failure Strain = 1 Percent**

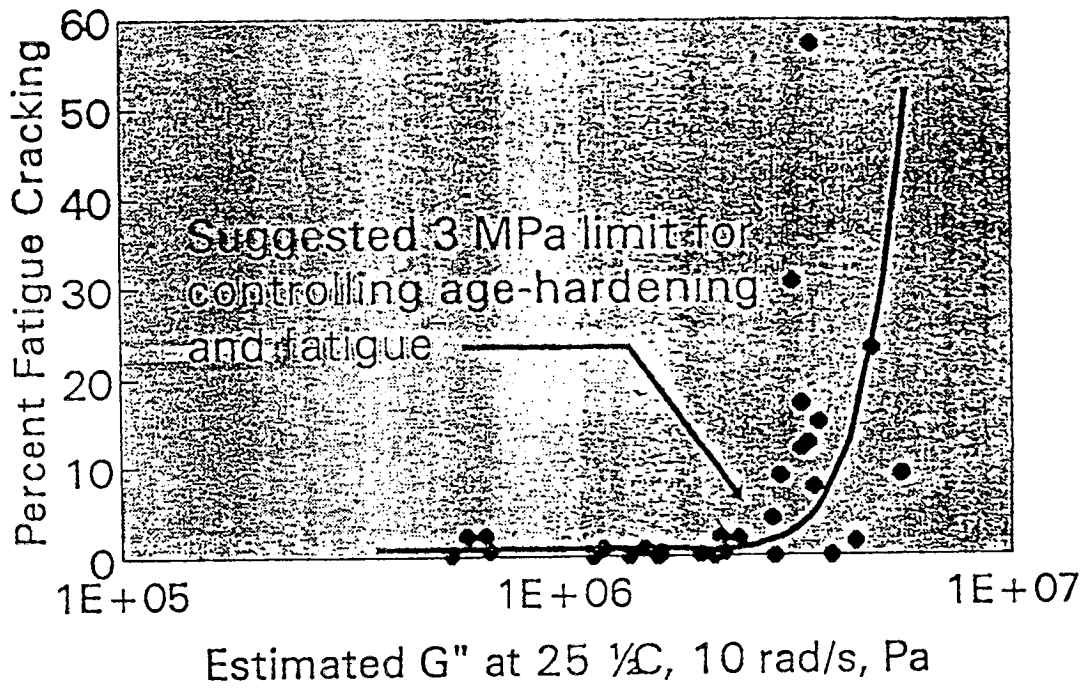


Figure 2.22 Evaluation of Fatigue Performance in Zaca-Wigmore Field Trials



MRL asphalts after PAV treatment  
 Temperature at which  $G' = 3 \text{ MPa}$

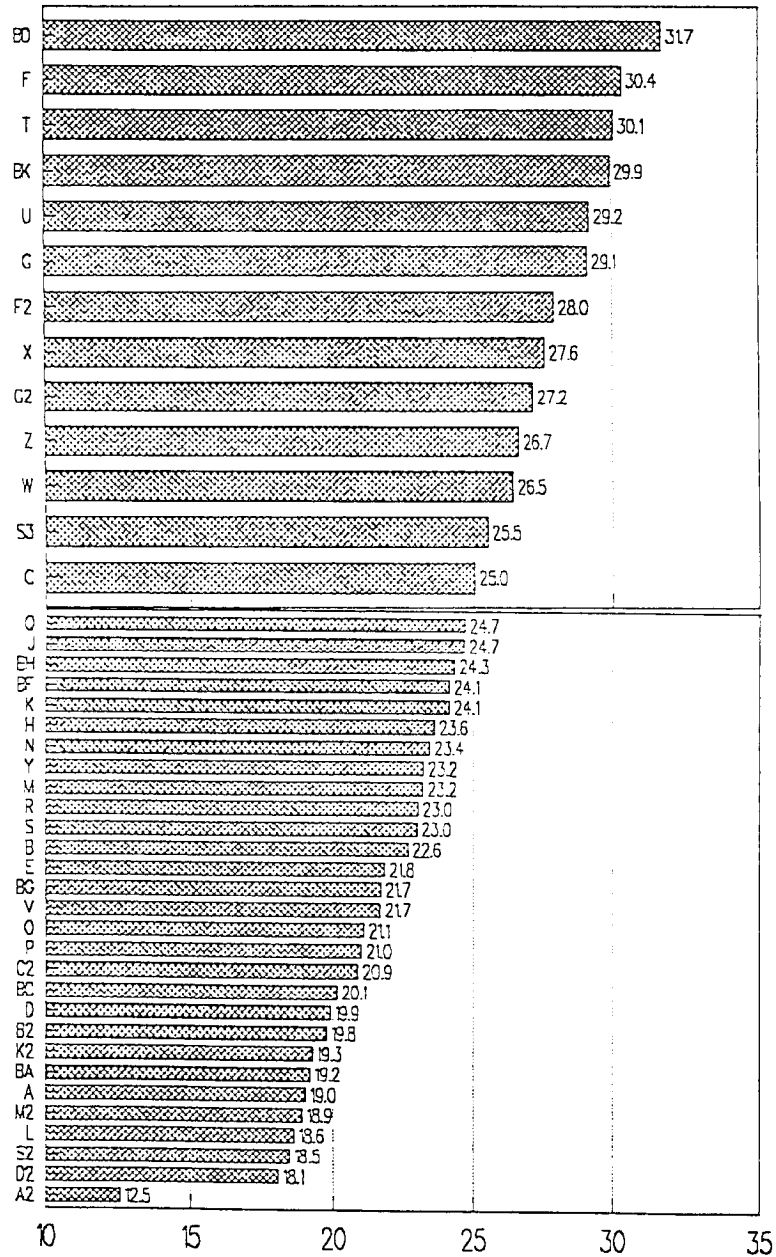
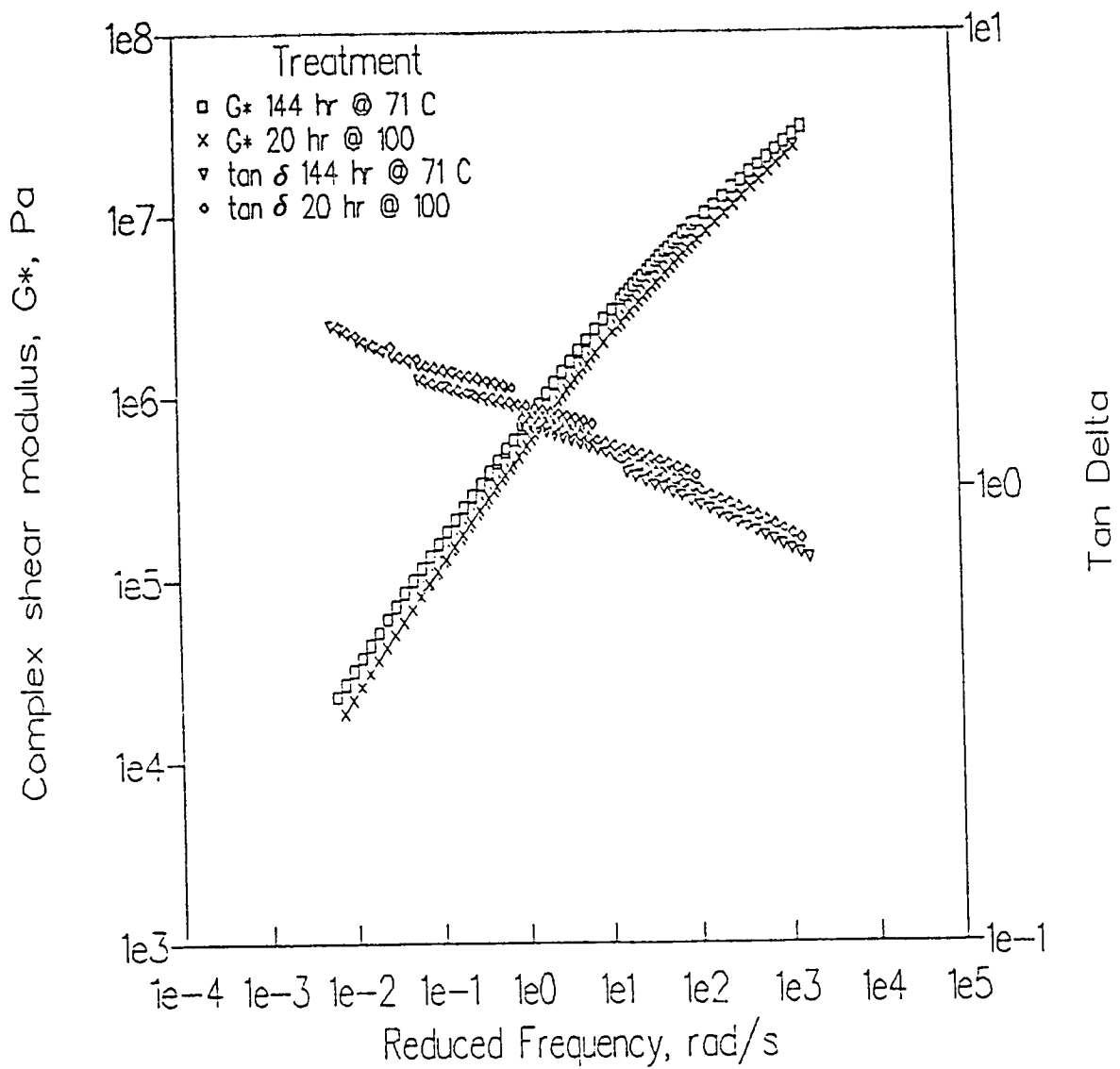


Figure 2.23 Ranking of Materials Reference Library Asphalts after Pressure Aging:  
 Temperature at Which  $G' \sin \delta = 3 \text{ MPa}$



**Figure 2.24 Comparison of Rheological Changes in Asphalt during Pressure Aging**

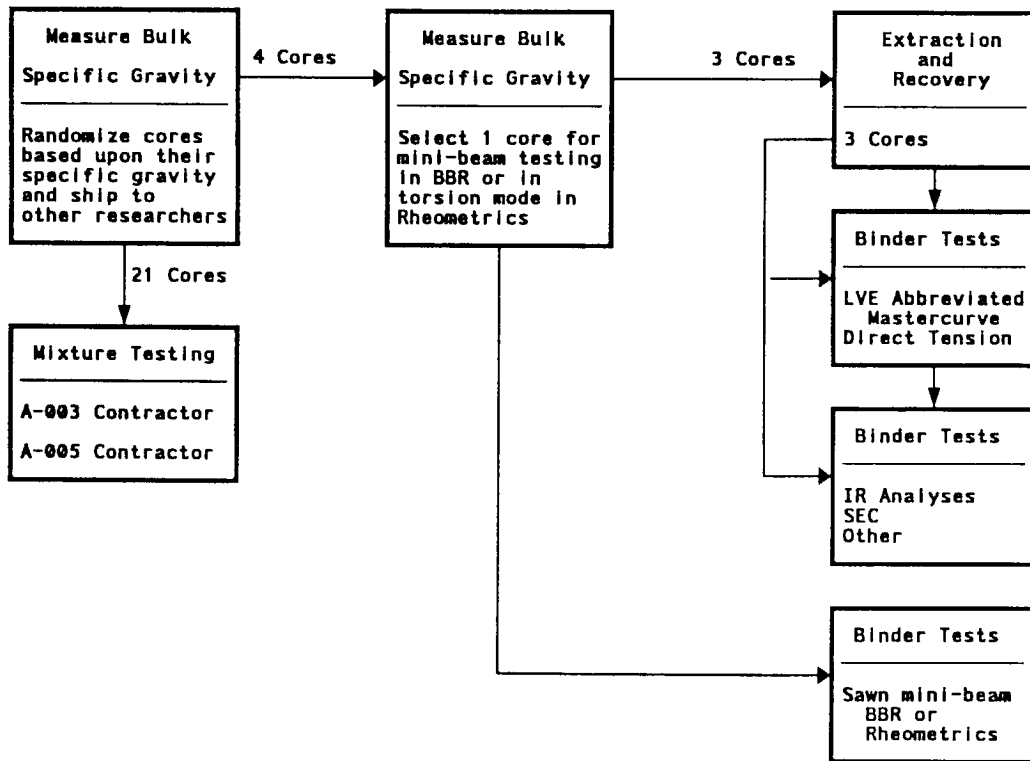


Figure 2.25 Flow Diagram of the Experiment to Validate That the Chemistry and Rheology of Pressure-Aging Vessel Residue Relate to Field Exposure

A-002A Field Validation of Binder Aging  
 WA sr-522, F19

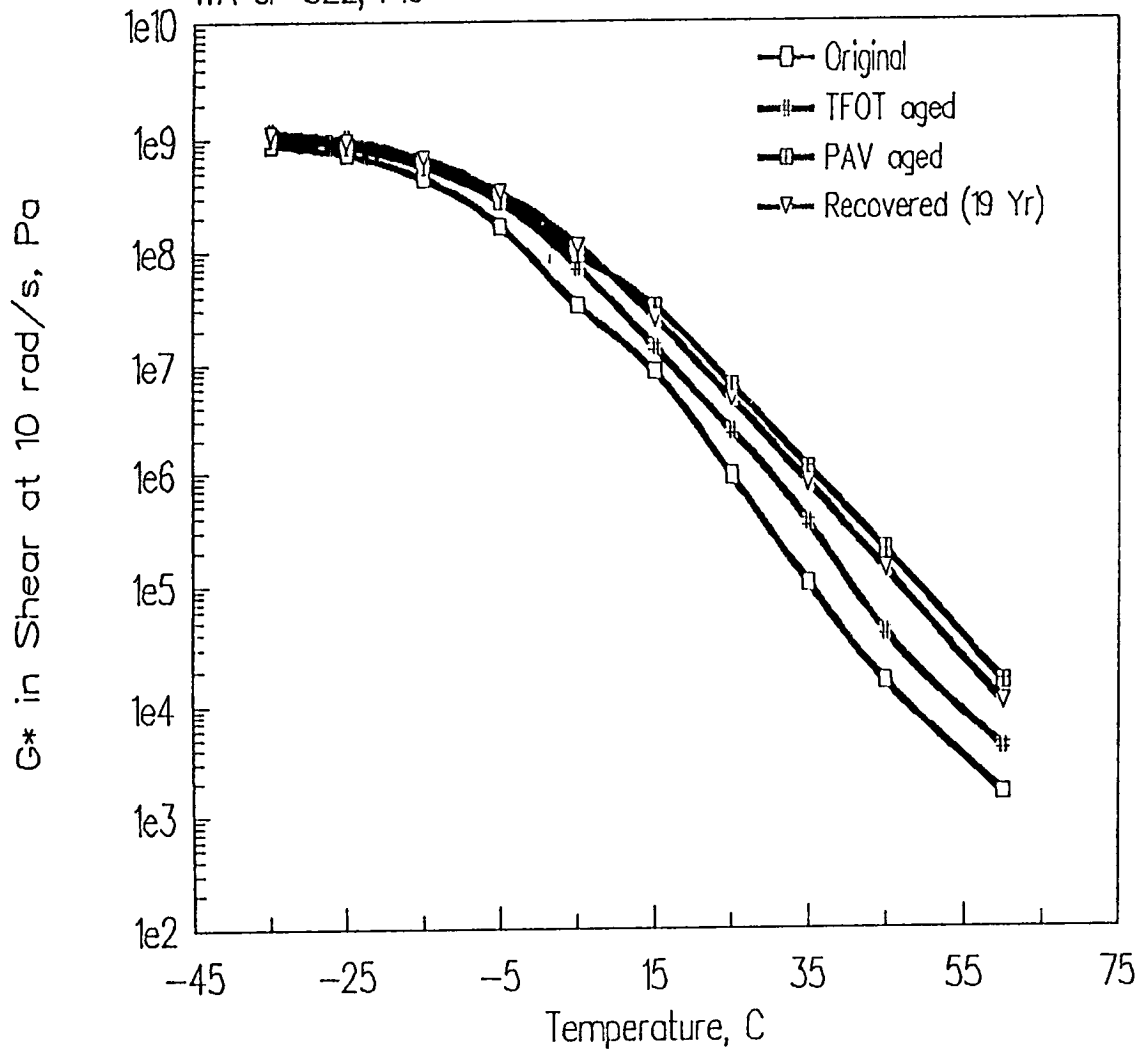
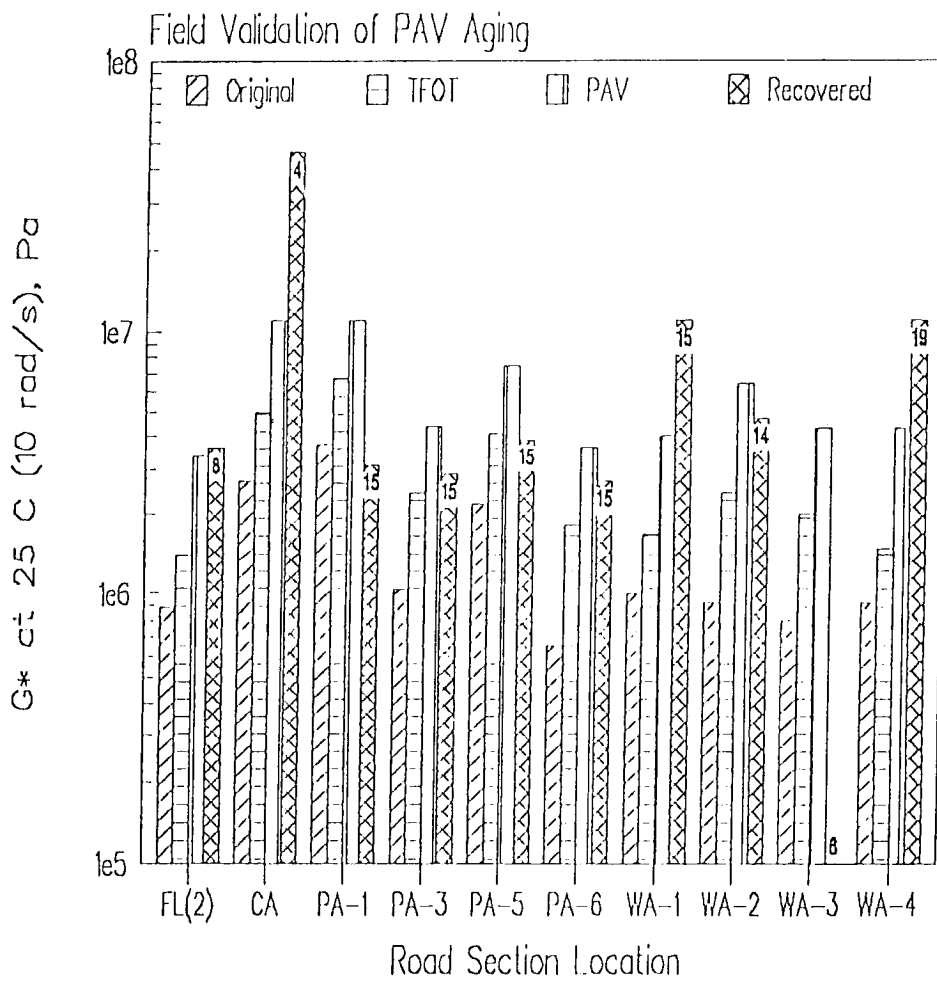
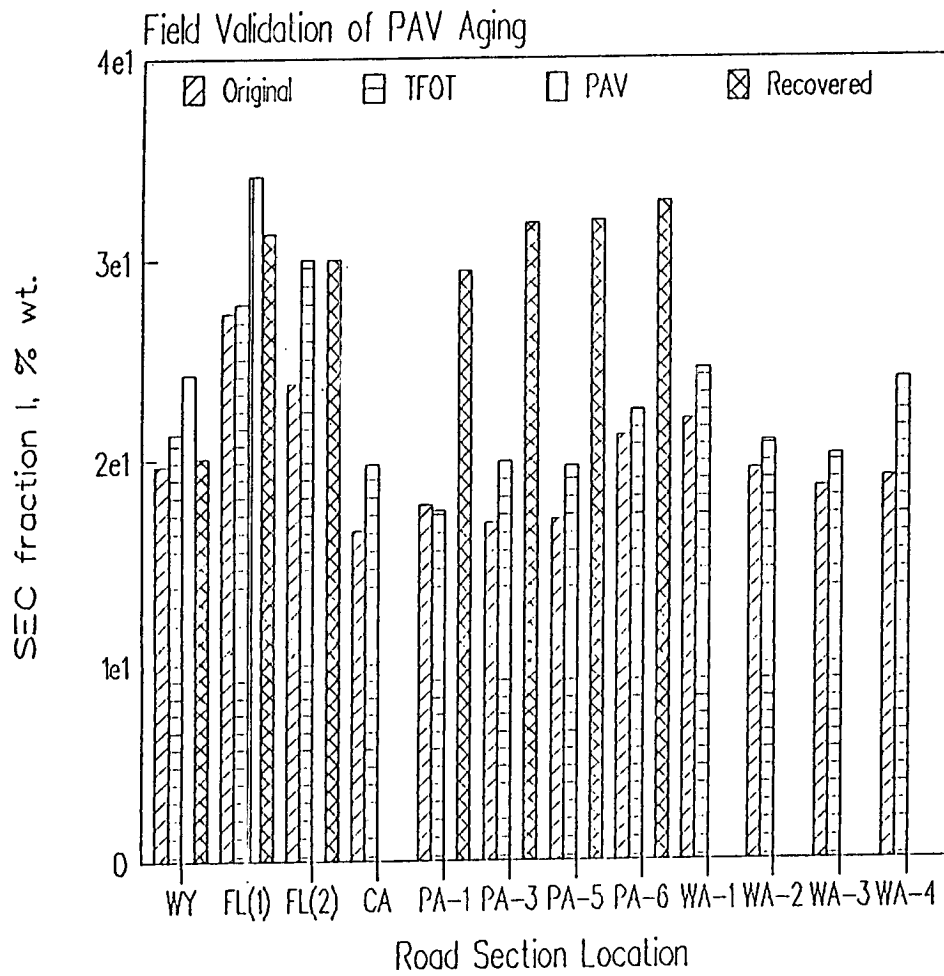


Figure 2.26 Rheological Behavior Determined in the Laboratory  
 as Compared with Field Data



**Figure 2.27 Complex Modulus at 25°C at Various Road Sections for Field Validation Experiment**



**Figure 2.28 Size Exclusion Chromatography Fraction I at 25°C at Various Road Sections for Field Validation Experiment**

### 3

## **Relationships between Chemical Composition and Physical Properties**

### **Physical Properties That Relate to the Microstructural Model: Observed Physical Behavior That Must Be Explained by the Microstructural Model**

Various physical characterizations were performed at Pennsylvania State University to characterize the physical properties of tank, thin-film oven (TFO; ASTM D 1754), and TFO + pressure-aging vessel (PAV) residue. The largest quantity of data was obtained using dynamic mechanical analysis. Other rheological tests performed included flexural creep with the bending beam rheometer and direct tension tests. From these data, various observations can be made about the physical properties of asphalt cement as measured during the project.

The flow properties, as evidenced by the dynamic mechanical properties, follow a regular form as demonstrated in figure 3.1, where a typical master curve is shown, in this case for asphalt AAB-1 as measured in the tank condition. As is the normal convention for representing dynamic mechanical data for asphalt cements and similar viscoelastic materials, a log-log scale is used to plot modulus versus time or frequency. At high frequencies or low temperatures, the modulus changes only slightly with frequency, which is typical for viscoelastic materials in the glassy region. At intermediate frequencies, the modulus decreases with decreasing frequency at an increasing rate, until the log-log plot reaches a slope of 1, denoting that pure viscous flow is reached at long loading times or high temperatures. There is a certain amount of symmetry in the behavior, and no abrupt changes in the complex modulus are observed as a function of either time or temperature. Additionally, no equilibrium modulus is observed, clearly indicating that there is no significant network of covalent bonds or chain entanglements. Asphalt cement, from a rheological standpoint, should therefore be classified as a viscoelastic fluid, rather than a viscoelastic solid.

An important characteristic of the viscoelastic behavior of asphalt cement is the wide range of relaxation times observed in the relaxation processes. For a homogeneous viscoelastic material (e.g., polyethylene), or for most simple viscoelastic solutions, there is normally a narrow time range during which the bulk of the relaxation processes occur. This follows from various molecular theories of viscoelasticity. For asphalt cement, the relaxation processes are normally spread out over five to ten decades of time, indicating that a large array of molecular processes are responsible for the viscoelastic properties of asphalt cements. Additionally, the smooth shape of the relaxation spectrum (see figure 3.2) suggests that the relaxation processes can be modeled with statistical distribution functions. Other researchers have developed empirical models to describe the relaxation spectra of asphalt cements (Jongepier and Kuilman 1969).

The relaxation spectra for two asphalts are shown in figure 3.2. The shape of the spectrum does in fact resemble a "bell curve," although more rigorous analysis of the spectra of a wide range of asphalts indicates that a normal or log-normal distribution is generally not strictly applicable, since the distribution of relaxation times is somewhat skewed for some asphalts, as pointed out by Dickinson and Witt (1974). This skewness is shown by asphalt AAG-1 in figure 3.2. Since a log-normal spectrum is perfectly symmetrical, it is apparent that such a function would not apply to this and similar asphalts over the entire time range of interest.

Upon aging, in-service asphalt cement becomes stiffer, but its temperature dependence and rheological type also change, suggesting gradual but systematic microstructural changes (figure 2.9). Upon aging, the relaxation spectrum broadens, which also suggests gradual but systematic changes in the microstructure of the asphalt. During service, reversible changes in the rheology, called *steric hardening* by earlier researchers and *molecular structuring* and *isothermal, reversible age hardening* in the Strategic Highway Research Program (SHRP), are also observed, and these must be accommodated by the microstructural model.

Testing during this study led to the important discovery that asphalt cements undergo time-dependent isothermal volume changes at temperatures below ambient. This newly reported phenomenon, which has been termed *physical hardening*, is identical to the physical aging seen in many other viscoelastic materials (Bahia and Anderson 1992; Struik 1978). Physical hardening can result in an increase in stiffness that equals or exceeds that caused by long-term, in-service oxidative aging. The term *physical hardening* has been used because the term *aging* is widely used among asphalt technologists to mean oxidative hardening, which is completely different from low-temperature isothermal physical hardening.

Physical hardening of asphalt cement, as with other materials, can be explained by means of free-volume concepts as follows. As asphalt cement is cooled within the temperature range for which the molecular processes are relatively rapid (e.g., above the softening-point temperature or in the Newtonian flow region), the change in volume with temperature is relatively instantaneous, and no time-dependent volume change is observed. However, as the temperature is further depressed, the volume change does not occur instantaneously but over a nonzero time. This time-dependent volume change is called *isothermal physical hardening* because the volume change causes a concomitant time-dependent increase in the stiffness of the asphalt. The temperature at which the molecular processes slow enough that the volume



change is not instantaneous but time dependent is called the *glass transition temperature*. The glass transition temperature is, however, not uniquely defined but is dependent on the rate of cooling and other aspects of thermal history. The performance-related significance of physical hardening has not yet been determined, although it is certainly an important aspect of behavior that must be considered in the laboratory characterization of asphalt cements and mixtures at low temperatures.

Physical hardening has also been attributed to the formation of organized domains of aliphatic or waxlike molecules, and a strong correlation between wax content and physical hardening has been observed (King et al. 1992; also see volume 3, chapter 3). Asphalts do not exhibit first-order phase transitions, as verified by the change in rheological properties or specific volume. Asphalt cement is known to contain small percentages of aliphatic or paraffinic materials that have melting points somewhat above ambient temperatures. However, no distinct changes in physical properties are reflected by these melting points. The melting point of the wax is approximately 30°C to 60°C (86°F to 140°F); however, the physical hardening is observed at temperatures typically below 0°C (32°F), implying that the melting point of the wax is depressed by as much as 30°C to 60°C (54°F to 108°F). The cause-effect relationship between physical hardening and free volume collapse or wax crystallization and domain formation has not been established but must be accommodated in the microstructural model.

The results of the direct tension tests (volume 3, chapter 4) are in general consistent with the findings of Heukelom (1966). The observed failure strain for a wide range of asphalt cements, as noted by Heukelom, appears to be strongly related to the modulus: the higher the modulus, the lower the failure strain. This simple empirical relationship is illustrated in figure 3.3, in which failure strain is plotted versus secant modulus for the eight core asphalts. Rheologically, the secant modulus in a strain-controlled test is approximately equivalent to the inverse of the creep compliance at identical loading times. The failure strains for asphalt cement in the brittle failure zone range from approximately 10 to 15 percent at the brittle-ductile transition to about 0.1 percent or less as the glassy modulus is approached. This range is also consistent with Heukelom's findings. The failure stresses in the brittle zone do not vary nearly as much as the failure strains and tend to reach a maximum immediately after the brittle-ductile transition and decrease as the asphalt becomes more brittle. Typical failure stresses for paving-grade asphalts range from 1 to 3 MPa. These tensile strengths are much lower than for polymers and represent an important observation concerning the engineering properties of asphalt cements.

In summary, the major aspects of the mechanical behavior relevant to the development of a conceptual molecular model are as follows:

- The limiting (glassy) modulus of all asphalt cements is very close to 1 GPa in shear.
- The complex modulus smoothly and monotonically decreases from the limiting value of 1 GPa with decreasing frequency, until viscous flow is reached, at which point the log-log slope of the complex modulus with respect to frequency is unity.

- The relaxation processes for asphalt cements are very dispersed and approximately follow a log-normal distribution, though skewness is apparent to varying degrees in the spectra of different asphalt cements.
- The temperature dependence of asphalt cement is due almost entirely to free-volume effects and should thus be a function of molecular weight.
- The failure strain of asphalt cement is strongly related to the time-dependent modulus at the temperature and time to failure.
- The tensile strength of asphalt is quite low compared with that of most other engineering materials, on the order of 1 to 3 MPa.
- At low temperatures, there is no evidence of large amounts of nonlinear behavior, even up to the point of fracture for most asphalt cements.
- Asphalt cements undergo physical hardening when conditioned isothermally at low temperatures. This hardening is caused by a free-volume collapse that leads to increased resistance to flow under stress.
- There is no equilibrium modulus in conventional asphalts. This lack indicates that there is no network of covalent bonds or entanglements and that asphalt cement should therefore be classified as a viscoelastic fluid.
- With aging, the viscoelastic model parameters change gradually and systematically from the tank to the long-term aged condition.
- The flow properties of asphalt cements are exceedingly temperature dependent when compared with those of other organic or polymeric materials.
- At intermediate temperatures, molecular structuring (previously called *steric hardening*) occurs at varying degrees in most paving-grade asphalts.

Any microstructural model, if it is to be useful to paving technologists, asphalt chemists, and asphalt producers, must account for all these aspects of the observed mechanical behavior in a straightforward manner that can be at least partially quantifiable, if only on an empirical basis. Such considerations place certain constraints on the plausible molecular structures for asphalt cement, as discussed in the following section.

## Rheological Model

To provide meaningful parameters from relationships developed between binder rheology and microstructural model or chemical parameters, a quantitative description of the rheological behavior of the asphalt cement was needed. Dickinson and Witt (1974), Dobson (1972), Jongepier and Kuilman (1969), Maccarrone (1987), and others have developed such models,

and these models were further refined as described in volume 3, chapter 1. The model that was finally adopted, developed by Christensen and Anderson (1992), assumes a hyperbolic shape when the log of complex modulus or creep compliance is plotted versus the log of frequency or time.

The linear viscoelastic (LVE) model developed by Christensen and Anderson (1992) requires four parameters for a complete description of the behavior of a selected asphalt: (1) the defining temperature,  $T_d$ ; (2) the viscosity at the defining temperature,  $\eta_{Td}$ ; (3) the crossover frequency at the defining temperature,  $\omega_{cTd}$ ; and (4) the rheological index,  $R$ . Emphasis was placed on using these parameters for developing physical-chemical relationships as opposed to the specification criteria. In this manner the rheological model parameters can then be used in the physical correlation equations to calculate the complex modulus, the phase angle, and other viscoelastic functions.

As a brief review, the equations for calculating the complex modulus and the phase angle from the LVE parameters are given below:

$$G^*(T_d, \omega) = G_g \{1 + (\omega_{cTd}/\omega_r^d)^{[\log(2)]/R}\}^{R/\log(2)} \quad (3-1)$$

$$\delta = 90/\{1 + (\omega_r^d/\omega_{cTd})^{[\log(2)]/R}\} \quad (3-2)$$

where

- $G^*(T_d, \omega)$  = complex modulus at the defining temperature  $T_d$  and frequency  $\omega$
- $G_g$  = glassy modulus, assumed to be 1 GPa
- $\omega_{cTd}$  = crossover frequency at the defining temperature, rad/s
- $\omega_r^d$  = loading frequency, rad/s
- $R$  = rheological index
- $\delta$  = phase angle, deg.

Equations 3-1 and 3-2 allow the calculation of the complex modulus or phase angle at the defining temperature at any frequency  $\omega$ . A schematic illustration of the role played by each parameter in defining the rheological properties is given in figure 3.4. The exponential term in the model has the effect of reducing the modulus as the frequency is increased. The relative decrease in the modulus as the frequency is reduced is governed by the location parameter  $\omega_{cTd}$  and the rheological index  $R$ . To determine the frequency-temperature equivalence of a given modulus or phase angle, the modulus or phase angle may be shifted to some new frequency at a second temperature by applying a time-temperature shift function,  $a(T)$ . The new frequency is found by multiplying the reference temperature frequency by the shift factor.

The value of  $\log a(T)$  can be found from two equations relating the temperature dependence to the defining temperature. For  $T > T_d$  and below the Newtonian flow region,

$$\log a(T) = -19(T - T_d)/(92 + T - T_d) \quad (3-3)$$

and for  $T \leq T_d$ ,

$$\log a(T) = 13,000(1/T - 1/T_d) \quad (3-4)$$

where

- $a(T)$  = shift factor at temperature  $T$  relative to the defining temperature  $T_d$
- $T$  = selected temperature, °C or K in equation 3-3, K in equation 3-4
- $T_d$  = defining temperature, °C or K in equation 3-3, K in equation 3-4

Equation 3-3 represents the Williams-Landers-Ferry (WLF) equation with coefficients suitable for most paving-grade asphalts; this equation is only applicable above the defining temperature and below temperatures where Newtonian flow is realized. Equation 3-4 is an Arrhenius equation applicable to data at or below the defining temperature. In the Newtonian flow region, it is necessary to invoke an Arrhenius equation; the WLF equation is not valid in this region. This implies that in the Newtonian flow region free volume does not control the flow processes. This is reasonable given the extreme temperature dependence shown by asphalts in the Newtonian flow region and suggests that polar interactions must play a large role in or even dictate temperature dependence in the Newtonian flow behavior.

The complete LVE model is based on these equations, but some complexities are not mentioned here in the interest of brevity. These details are discussed in volume 3, chapter 1.

Briefly, the parameters of this model that are of primary importance are as follows:

- **Glassy Modulus,  $G_g$ .** This represents the limiting modulus in shear at high frequencies and/or low temperatures. The value of the glassy modulus for most paving-grade asphalts is very close to 1 GPa.
- **Crossover Frequency,  $\omega_{cTd}$ .** This is the frequency in radians per second, at a specified reference temperature, at which the loss tangent is equal to 1; it is indicative of the location of the master curve with respect to frequency and decreases with increasing hardness. Typical values for  $\log \omega_{cTd}$  at 25°C (77°F) range from about 0 (1 rad/s) for hard, highly aged asphalts to more than 4 (10,000 rad/s) for soft, unaged materials. The crossover frequency may be thought of as a location parameter.
- **Rheological Index,  $R$ .** This is the log of the glassy shear modulus divided by the modulus in shear at the crossover frequency and is indicative of the rheological type or spectrum width. As the relaxation spectrum becomes broader,  $R$  increases. Typical values for  $R$  for paving-grade asphalts range from 1.2 to 3.0 for highly aged asphalts. The rheological index may be thought of as a shape parameter.
- **Steady-State Viscosity,  $\eta_0$ .** This is the Newtonian viscosity under steady flow conditions and, like the crossover frequency, is indicative of the overall hardness

of the asphalt at the specified reference temperature. For many asphalt cements,  $\eta_0 \approx G_g/\omega_{cTd}$ , but this assumption is not always accurate.

The LVE behavior under sinusoidal loading can be accurately estimated from these four parameters using empirical formulas explained in more detail below. In other words, these parameters are necessary and sufficient to describe the LVE response. One of the major purposes in developing this LVE model was to reduce the number of response variables needed to describe the mechanical behavior so that relatively simple and direct relationships could be developed between the rheological behavior and various compositional parameters.

From the literature review on the molecular theories of viscoelasticity applicable to polymers and other similar materials, and within the context of the microstructural model described above, several important physical-chemical property relationships can be postulated:

- The glassy modulus should be inversely proportional to the average molecular weight. Since the frequency response of most viscoelastic materials having disperse molecular weight distributions is generally controlled by higher molecular weight fractions, the weight-average molecular weight should correlate more closely with  $G_g$  than the number-average molecular weight does.
- The viscosity at a given temperature should be related to the fractional free volume and intermolecular friction. The intermolecular friction should be strongly influenced by the amount of highly polar material in the asphalt. Therefore, viscosity should correlate with such parameters as the asphaltene content, the weight percent of size exclusion chromatography (SEC) fraction I material (volume 2, chapter 2), and the percentage of amphoteric. However, to develop such correlations, the correlations must be done at similar free volumes. To the extent that the free volume is constant at the defining temperature, the viscosity at the defining temperature should correlate with various indicators of overall polarity.
- Following similar reasoning, the crossover frequency  $\omega_{cTd}$  at the defining temperature should also correlate with such parameters as asphaltene content and percentage of amphoteric.
- The rheological index should increase with increasing molecular weight and with increasing dispersion in polarity. The increase in  $R$  with molecular weight should occur because of the general tendency of the storage and loss moduli at a selected rheological reference point to decrease with increasing molecular weight. Additionally, some limited data suggest that higher molecular weight asphalts, such as AAM-1, will normally also have a broader distribution of molecular weights (Robertson et al. 1991). A broader distribution would lead to a broader relaxation spectrum and a higher value of  $R$ .

In addition to establishing physical-chemical property relationships between chemical parameters and LVE properties, it is also essential to understand how asphalt chemistry affects fracture properties and fatigue resistance. To a certain extent, the fracture and fatigue

behavior should be related to LVE properties, since these properties will determine to a large degree the stress-strain behavior during deformation, at least until significant nonlinearity is encountered. In addition to the stress-strain behavior, fracture and fatigue properties will also depend on the ultimate properties, such as stress and strain at failure. For polymers, the stress and strain at failure are both in general directly proportional to molecular weight.

## **Overall Approach to Development of Physical-Chemical Relationships**

The general strategy adopted by the A-002A research team in the development of relationships between the physical and chemical properties of asphalt cement was to first conduct scoping experiments in which the important chemical and physical properties of the asphalt cements were identified. These scoping experiments were conducted on the eight Materials Reference Library (MRL) core asphalt cements, primarily in the unaged tank condition, although some experiments were also conducted on aged materials. From these scoping experiments, a subset of the more important chemical and physical properties was to be identified and determined for the entire set (30 in total) of the MRL asphalts in the tank condition, after TFO aging (ASTM D 1754) and after PAV aging by the new SHRP pressure-aging method.

Western Research Institute conducted extensive chemical scoping experiments to identify key chemical parameters that describe the microstructure and performance of asphalt cement. Test methods that characterize both the molecular weight and the polarity of the asphalt cement were identified during these experiments. Similar physical property experiments and test method evaluations were conducted at Pennsylvania State University to determine the key physical properties.

The original goal of the physical-chemical correlations was to relate asphalt chemistry to pavement performance. This goal was found to be exceedingly optimistic and unrealistic. Physical properties determine the response of a pavement to traffic loading, and there are endless combinations of chemistries that can result in a given value for any of the performance-related binder physical properties. Thus, although it may be possible to define the physical properties needed to provide a certain level of performance, there are innumerable asphalt chemistries that can produce the desired asphalt physical properties. Relationships between asphalt chemistry and pavement performance could undoubtedly be developed empirically by simply correlating chemical properties with percent cracking and other performance-related properties, but this would provide little basic understanding of the real role of asphalt chemistry in determining binder performance. Instead, an indirect route between asphalt chemistry and pavement performance was pursued, as illustrated in figure 3.5.

The experiment shown in figure 3.6 was designed to develop the data needed to establish relationships between the physical and chemical properties of the 30 MRL asphalt cements. The experiment included tank, TFO residue (ASTM D 1754), and TFO + PAV residue. To be valid, the relationships between the physical and chemical properties of asphalt materials must be equally applicable to aged and unaged materials. Unfortunately, resource availability

did not permit the completion of the experiment illustrated in figure 3.6. Consequently, the statistical analyses in this experiment were confined to the variables described in table 3.1 and measured for 18 to 28 (depending on the variable measured) of the MRL core asphalts in the tank condition only. The resulting extended asphalt database (tables 3.2 through 3.5), was used as described in the next section to develop relationships between the rheological parameters and the compositional parameters.

An extensive database of chemical properties was obtained for a limited number of asphalt cements, and this database provided very significant insight into the structure and composition of asphalt cement. This database is discussed in the section following the one below.

## Physical-Chemical Property Relationship Based on Model Parameters

### *Statistical Evaluation of Extended Asphalt Database*

Pearson correlation coefficients for the database variables were obtained using the SAS statistical analysis program. These coefficients are shown in table 3.6 and identify pairs of variables that have a strong relationship to each other. Each variable is listed and defined in table 3.1. Strong relationships between the rheological model parameters and microstructural or chemical parameters were observed as follows:

$$\begin{aligned}
 R: & \quad H(\tau)_{\text{mode}}, (-0.87), \text{SECI} (0.73), \text{SPSECI} (0.62) \\
 T_d: & \quad \log \omega_{cTd} (-0.69), \tau_{\text{term}} (-0.79), \log \eta_{Td} (-0.89), A (-0.65), NA (0.69), \\
 & \quad \log \eta_{\text{SECI}25} (0.73), S (-0.63) \\
 \log \eta_{Td}: & \quad \log \omega_{cTd} (0.90), \tau_{\text{term}} (0.75), \text{AI}_{\text{vis}60} (0.67), A (0.72), NA (-0.72), \\
 & \quad \log \eta_{\text{SECI}25} (-0.66), C (-0.66) \\
 \log \eta_{\text{SECI}25}: & \quad \tau_{\text{term}} (-0.83), \text{AI}_{\text{vis}60} (-0.66), A (-0.86), S (-0.78)
 \end{aligned}$$

Two-way correlations with coefficients greater than 0.65 (or less than -0.65, indicating an inverse relationship) are listed above. From these coefficients,  $R$  and the relaxation spectra are highly related, as expected.  $R$  is also correlated with measures of polarity and not strongly related to molecular weight (correlation between  $R$  and  $M_n$  is 0.49). The defining temperature is related to the polarity and the molecular weight to the extent that  $\log \eta_{Td}$  and  $\log \eta_{\text{SECI}25}$  reflect molecular weight. The defining temperature is also related to various indicators of polarity, so polarity must also play a role in temperature dependence. Last, the viscosity of the nonpolar fraction (as represented by SEC fraction II; see volume 2, chapter 2) is related to the asphaltene content but only weakly to the molecular weight (correlation between  $\log \eta_{\text{SECI}25}$  and  $M_n$  is 0.21).

Other observations derived from the data in table 3.6 show the following relationships:

|         |   |
|---------|---|
| SPSECI: | SECI (0.96)   |
| C:      | A (-0.76), H (0.73), S (-0.90)  |
| S:      | A (0.85), H (-0.71)   |
| Ni:     | $AI_{vis60}$ (0.67), NA (-0.71)                                       |
| A:      | SPSECI (0.38), SECI (0.47), $\tau_{term}$ (0.68), $AI_{vis60}$ (0.76) |

Obviously the percent SPSECI and SECI fractions are highly related, and therefore only the SPSECI data were used in the rheological correlations in this section. The asphaltene content is not highly correlated with the percent SECI or SPSECI fractions and therefore should not be expected to be a surrogate for them.

Statistical relationships were developed by regressing the rheological parameters versus the chemical parameters as shown in tables 3.7 through 3.12. The models were developed systematically by first using the molecular weight, asphaltene content, or SPSECI fraction as a single independent variable. Asphaltene content and the SPSECI fraction were considered as measures of the overall polarity of the asphalts. Other parameters that should quantify the distribution in molecular weight or polarity were then added in a stepwise fashion to the models. In general, 25 to 28 measurements were available for most of the regressions. By limiting the number of predictor variables to four or fewer, sufficient degrees of freedom for error were retained so that the regression models retain a reasonable level of reliability.

### *Temperature Dependence Related to Microstructural Parameters*

From the literature review and discussion presented previously, it was expected that the temperature dependence of asphalt cement should be largely controlled by the free volume and by the change in free volume with temperature. For most polymers and similar materials with low molecular weights (less than about 20,000 daltons), free volume is in turn directly related to molecular weight; the glass transition temperature increases as molecular weight increases.

The LVE model developed by the A-002A project team predicts temperature dependence using the WLF equation in the viscoelastic response temperature region and an Arrhenius function at low and high temperatures (see volume 3). The constants for these equations have been found to be essentially the same for all asphalts studied; the only parameter that varies is the defining temperature,  $T_d$ , which also separates the region in which the WLF equation holds from that in which an Arrhenius function is applicable. The defining temperature has also been found to be closely related to the glass transition temperature determined by dilatometric methods (figure 3.7). It was therefore anticipated that  $T_d$  should increase as molecular weight increases, resulting in an effective increase in the temperature dependence.



To evaluate this hypothesis, a regression analysis was performed in which the defining temperature was the dependent variable and the inverse of the number-average molecular weight was the sole predictor:

$$T_d = 18 - 22,000/M_n \quad (3-5)$$

where

$$\begin{aligned} T_d &= \text{defining temperature, } ^\circ\text{C} \\ M_n &= \text{number-average molecular weight (vapor-phase osmometry, in toluene)} \end{aligned}$$

The coefficient of determination,  $R^2$ , for this model was only 0.27 (adjusted for degrees of freedom), which was not considered adequate for predictive purposes, although it does verify that molecular weight plays a significant role in determining temperature dependence. It was found that asphaltene content had a significant influence on temperature susceptibility; a better prediction of  $T_d$  can be made by using both asphaltene content and molecular weight as predictors:

$$T_d = 16 - 0.57A - 12,400/M_n \quad (3-6)$$

where

$$A = \text{asphaltene content (n-heptane), weight percent}$$

and the other variables are as defined in the previous equation. The coefficient of multiple determination for this model ( $R^2$ ), after adjustment for degrees of freedom, was 0.53, which is significantly better than the model using molecular weight alone. It must be remembered that there is a fair amount of variability in the value of  $T_d$  determined from the master curve:  $\pm 3^\circ\text{C}$  ( $5.4^\circ\text{F}$ ) for the average of two measurements and  $\pm 5^\circ\text{C}$  ( $9^\circ\text{F}$ ) for a single determination. Therefore, it is unlikely that correlations significantly better than this can be established. Figure 3.8 is a plot of defining temperature predicted by equation 3-6, using values of  $T_d$  found from analyses of the master curves and related shift factors.

A comment is in order concerning the observed relationship between asphaltene content and the defining temperature. The observed decrease in defining temperature with increasing asphaltene content may well be an artifact of the grading process. Asphalt cements are graded by their properties at either  $60^\circ\text{C}$  ( $140^\circ\text{F}$ ) (viscosity grading) or  $25^\circ\text{C}$  ( $77^\circ\text{F}$ ) (penetration grading). Most of the MRL asphalts fall into a relatively narrow consistency range at these temperatures: most are either AC-10s or AC-20s. If the concepts presented above are correct, the consistency at high temperatures should depend mostly on molecular weight and overall polarity. To achieve a viscosity in the range of 1000 to 2000 poises at  $60^\circ\text{C}$  ( $140^\circ\text{F}$ ), only certain combinations of molecular weight and overall polarity are acceptable. An asphalt having both a high molecular weight and a high concentration of polar molecules would have a viscosity much higher than 2000 poises; an asphalt having both a low molecular weight and low amounts of polar material would have a very low viscosity. In other words, to achieve a viscosity within a narrowly defined range at a given temperature,

the molecular weight must increase with decreasing polarity. The reverse is also true. Therefore, the observed decrease in  $T_d$  with increasing asphaltene content may simply be a result of this grading artifact.

### *Time Dependence Related to Microstructural Parameters*

The main effect of increasing overall polarity in an asphalt, according to the dispersed polar fluid model, which considers asphalts to be a single-phase system (Christensen and Anderson 1992), should be to increase the average intermolecular friction. This greater friction should cause an increase in the viscosity at constant free volume. In fact, increased intermolecular friction should shift the entire response to lower frequency or higher times, so the crossover frequency should decrease. However, to relate the position of the master curve on the time scale to some chemical property such as asphaltene content, it is necessary to make the rheological comparisons at a point of equal free volume, since the resistance to flow will depend strongly on the free volume available for molecular motion.

It is proposed that the defining temperature,  $T_d$ , represents a point of approximately constant fractional free volume among all asphalt cements. To verify that this is the case, refer to the following equations:

$$B = 2.303C_1^0C_2^0\alpha_f \quad (3-7)$$

$$f_0 = C_2^0\alpha_f \quad (3-8)$$

$$= B/2.303C_1^0 \quad (3-9)$$

where

- $B$  = empirical parameter relating viscosity to free volume, generally about 1
- $C_1^0, C_2^0$  = empirical constants in the WLF equation, for a reference temperature of  $T_0$
- $\alpha_f$  = effective volumetric thermal expansion coefficient of the intermolecular free volume
- $f_0$  = fractional free volume at the reference temperature

For asphalt cements, the standard form of the WLF equation is given using the defining temperature  $T_d$  as the reference. In this case,  $C_1^0$  and  $C_2^0$  have values of 19 and 92, respectively, which are reasonably accurate for all asphalt cements. Furthermore, the coefficient of thermal expansion above the glass transition for asphalt cements is typically  $0.00064 \text{ m}^3/\text{m}^3/^\circ\text{C}$ , on a volume basis, while below  $T_g$  it is  $0.00035 \text{ m}^3/\text{m}^3/^\circ\text{C}$  (see volume 3, chapter 3). The values for both of these parameters vary only slightly among the asphalts studied and thus can be assumed to be constant. The parameter  $\alpha_f$  can be estimated as the difference between the volumetric thermal expansion above and below the glass transition. Therefore,  $\alpha_f \approx 0.0003 \text{ m}^3/\text{m}^3/^\circ\text{C}$ . If this value is used in equation 3-7 above, along with values of 19 and 92 for  $C_1^0$  and  $C_2^0$ , respectively, the calculated value of  $B$  is 1.2, which is very close to the often assumed value of 1. If similar substitutions are made in equation 3-8,

the calculated value of the fractional free volume at  $T_d$  is 0.028, which is within the range 0.020 to 0.030 given by Ferry for the fractional free volume at the glass transition (Ferry 1980).

It can be concluded from this analysis that the free-volume explanation of temperature dependence, as developed by Doolittle and Doolittle (1957), Ferry (1980), and others, is applicable to asphalt cements. Furthermore, the defining temperature  $T_d$ , as proposed by the A-002A project team, is approximately equivalent to the glass transition temperature  $T_g$  and, additionally, represents a point at which the fractional free volume is about 0.028.

One of the fundamental hypotheses of the dispersed polar fluid model is that the resistance to flow, at equivalent free volume, should be largely independent of molecular weight and should instead depend largely on the overall polarity of the asphalt. Since asphaltene represent the most polar fraction of the asphalt, it is natural to express the viscosity or crossover frequency in terms of the asphaltene content. For viscosity at the defining temperature, the following relationship was developed, which includes both asphaltene content and content of polar aromatics, which are the next most highly polar of the Corbett fractions:

$$\log \eta_{Td} = 7.42 + 0.094A + 0.036PA \quad (3-10)$$

where

- $\eta_{Td}$  = steady-state viscosity at the defining temperature, Pa·s
- A = asphaltene content (*n*-heptane), weight percent
- PA = polar aromatic content, weight percent

The coefficient of multiple determination ( $R^2$ ) for this model was 0.71. Measured values of  $\eta_{Td}$ , and those predicted from equation 3-10 are shown in figure 3.9. Various other similar models were evaluated during this research, but this particular model gave the highest values of  $R^2$ , and also used the commonly available Corbett fractions as predictors.

A similar model was developed for the crossover frequency. However, polar aromatics were not in this case a significant predictor, and the model relies solely on asphaltene content:

$$\log \omega_{cTd} = -0.79 - 0.55A \quad (3-11)$$

where

- $\omega_{cTd}$  = crossover frequency at the defining temperature, rad/s

and the other variables are as defined above for equation 3-11. The coefficient of determination for this model was found to be only 0.47, adjusted for degrees of freedom. A comparison of values for  $\omega_{cTd}$  calculated from the master curve and predicted from equation 3-11 is given in figure 3.10.

These two relationships, although not exceptionally strong, clearly establish that increased polarity in an asphalt will increase the viscosity at constant free volume and will also tend to shift the entire master curve toward longer times or lower frequencies. This effect has of course been qualitatively known for some time; previous research (Altgelt and Harle 1975) has established that increasing asphaltene content will also increase viscosity. However, the relationships presented here are the first we know of establishing such relationships for a wide range of systems. The reason such comparisons were successful in this case was that the comparisons were made at a point of approximately equal free volume. This is the only valid way of comparing resistance to flow for a such a wide range of asphalt cements.

### *Relaxation Spectrum Related to Microstructural Parameters*

The final major aspect of the dispersed polar fluid model is that it predicts that the relaxation spectrum width should increase with increasing dispersion in both molecular weight and polarity. The LVE model developed by the A-002A project team uses the rheological index to characterize the spectrum width; increasing values of  $R$  indicate greater width. The review presented earlier suggests that the rheological index should increase not only with increasing dispersion in molecular weight, but also with increasing molecular weight. Fortunately, average molecular weight and dispersion in the molecular weight distribution appear to be strongly related for most asphalt cements. Characterization of the ion exchange chromatography (IEC) neutral fraction of the core asphalts by supercritical fluid chromatography (SFC) suggests that the dispersion in molecular weight increases with molecular weight. Asphalt AAM-1, for example, has both the highest average molecular weight and the greatest dispersion in molecular weight of the eight core asphalts. Therefore, average molecular weight alone should relate well to the rheological index or spectrum width; these should both increase with increasing molecular weight.

To characterize the dispersion in polarity of the constituent molecules of a selected asphalt, the Gaestel index was used:

$$GI = \frac{A + SAT}{PA + NA} \quad (3-12)$$

where

- GI = Gaestel index, an empirical parameter characteristic of the degree of dispersion in polarity of an asphalt cement
- A = weight percent asphaltenes
- SAT = weight percent saturates
- PA = weight percent polar aromatics
- NA = weight percent naphthene aromatics

GI is interpreted as being approximately proportional to the dispersion in the polarity of a given asphalt cement's constituent molecules. Increasing values of GI indicate a broader distribution of polar functional groups. According to the dispersed polar fluid model, the rheological index should increase with increasing values of this parameter.

The statistical model used to predict the rheological index from chemical parameters is as follows:

$$R = -0.49 + 0.0018M_n + 1.90GI \quad (3-13)$$

where

- $R$  = rheological index, which is proportional to the width of the relaxation spectrum
- $M_n$  = number-average molecular weight, daltons
- GI = Gaestel index (equation 3-12)

The coefficient of multiple determination for the regression model, corrected for degrees of freedom, was found to be 0.81 for this model, which is a reasonably good correlation. Values of  $R$  calculated from the master curve and values predicted from this empirical relationship are shown in figure 3.11.

### *Fracture and Fatigue Properties Related to Microstructural Model Parameters*

The strain at failure for asphalt cements, as pointed out by Heukelom (1966), is largely a function of modulus at the temperature and time of failure. Simply put, the stiffer a selected asphalt under given loading conditions, the lower will be the failure strain. General agreement with this principle has been found in A-002A research, using the direct tension test. Figure 3.3 graphically demonstrates the reductions in failure strain with increasing modulus (in this case, secant modulus to the point of failure). Additionally, analysis of direct tension data has shown that the tangent modulus at a given temperature and loading time agrees well with estimates of the extensional relaxation modulus found from dynamic shear data (see volume 3, chapter 4). As would be expected, the same relaxation processes are responsible for the viscoelastic properties in extensional testing to failure as are involved in the dynamic shear properties; there is no evidence of extreme nonlinearity during brittle failure. Therefore, it is proposed that the same chemical factors affecting the LVE response, such as molecular weight and overall polarity, will also affect the modulus during loading to failure and will thus affect the fracture properties.

An aspect of fracture that is, however, largely independent of rheology is the failure limits or failure envelope. Since the moduli in fracture testing are similar to those found through linear characterizations, only one failure limit need be specified. That is, specifying the failure stress, for example, under given loading conditions, will also indirectly specify the failure strain. It has been observed that for most polymers, the tensile strength is largely a function of molecular weight. Increasing molecular weight leads to higher tensile strengths. At this

time, tensile strength data are only available on the core asphalts (tank, TFO, and PAV), and molecular weights are only available on the tank materials. Therefore, a comparison of molecular weight and tensile strength is only possible for the eight unaged core asphalts. This comparison is shown in figure 3.12. In this plot, failure stress at 1 percent failure strain is shown as a function of number-average molecular weight. The failure stress at 1 percent failure strain was used because failure stress varies somewhat with loading conditions; this approach normalizes to some extent the differences in strength due to variations in hardness and failure time. Despite much scatter in the data, there appears to be a trend toward higher strength with increasing molecular weight. Because of the small number of points and the scatter in the data, no statistical analysis was performed. More data are needed to quantify this relationship.

The observed trend toward increased tensile strength with increasing molecular weight has significant implications in potential pavement performance. It suggests that attempting to achieve good low-temperature performance by reducing molecular weight may at some point become pointless, since the tensile strength may also be reduced, perhaps to the point where this weakening more than offsets the potential improvement in performance due to a reduction in modulus.

Since it is generally accepted that fatigue life is a function of the fatigue stress or strain as a function of ultimate stress or strain, the increase in tensile strength with increasing molecular weight should also be manifested in fatigue data. Fatigue studies have not yet demonstrated such an increase, however.

### *Oxidative Aging Related to Microstructural Model Parameters*

Although oxidative aging tends to harden asphalt cements most severely at high temperatures, the major effect on potential pavement performance is to harden the asphalt at low to intermediate temperatures, ultimately leading to reduced strain capacity and fatigue cracking. Fatigue life seems to be directly related to energy lost during deformation. Under strain-controlled conditions, energy lost during sinusoidal loading is proportional to the loss modulus,  $G''$ . To evaluate oxidative aging from this perspective, aging indexes were calculated by dividing the loss modulus after PAV aging at 100°C (212°F) for 20 hours by the loss modulus at 25°C (77°F) for the tank material. Both moduli were determined at a frequency of 10 rad/s.

Since such aging ratios normally increase with decreasing original moduli, the statistical analysis used involved predicting the aging ratio from the moduli of the tank asphalt and various other parameters. The only predictor besides the original moduli that was significant in this analysis was the number-average molecular weight:

$$AI_{vis60} = -7.9 + 2.6 \log G''(25, 10) - 0.0042M_n \quad (3-14)$$

where

$AI_{vis60}$  = ratio of the loss modulus at 25°C (77°F) and 10 rad/s after PAV aging at 100°C (212°F) for 20 hours to the loss modulus at 25°C and 10 rad/s, tank

$G''(25, 10)$  = loss modulus at 25°C (77°F) and 10 rad/s, tank asphalt, Pa

$M_n$  = number-average molecular weight, daltons

The coefficient of multiple determination for this model,  $R^2$ , was only 0.47, but was the highest of any such model evaluated. The level of significance for the number-average molecular weight as a predictor in this model was 0.0017, indicating a high level of significance. The reason the original modulus is a significant predictor of the aging index is that the amount of aging that occurs in the PAV (or in field aging), as measured by an aging index, will in general increase for lower moduli. Thus, the original moduli are significant predictors of the aging index. The reason for less severe aging with increased molecular weight is not clear at this time. It can be hypothesized that higher molecular weight asphalts obtain their consistency less from polar functional groups than from molecular weight and thus would be expected to have fewer oxidizable sites. This would render them less prone to aging. Additionally, a high molecular weight would also reduce volatilization during the TFO test, reducing aging due to the loss of low molecular weight compounds.

### *Specification Properties Predicted from Microstructural Model Parameters*

If the values of the LVE parameters predicted from the chemical model are used in the appropriate equations for time and temperature dependence, it is possible to predict values for the complex modulus and other viscoelastic functions. In this way, the overall accuracy and usefulness of the physical-chemical relationships can be evaluated. Three such comparisons are presented here. In the first (figure 3.13), complex moduli predicted from the chemical model are compared with measured values for the eight core asphalts, at temperatures ranging from -35°C (-31°F) to 60°C (140°F). Two similar comparisons are shown in figures 3.14 and 3.15, in which predicted and measured values of the loss tangent and the shift factor are compared. The agreement is quite good, especially considering that the individual relationships for most of the rheological parameters were not particularly strong. The values of  $G^*$  and the loss tangent are predicted to within a factor of 2; a comparable accuracy is seen in the predicted shift factors. These predicted rheological responses are the first made, to our knowledge, based on a unified conceptual, semiquantitative model of chemical and mechanical behavior. Although semi-empirical, this model verifies that the dispersed polar fluid model is indeed a useful picture of asphalt chemistry and that the concept used above in relating physical and chemical properties is an effective one.

### *Summary of Physical-Chemical Property Relationships*

In summary, the following relationships between chemical and physical properties have been established and verify the various conceptual aspects of the dispersed polar fluid model:

- The temperature dependence of asphalt cements is directly related to the defining temperature, which is analogous to the glass transition temperature and represents a point of approximately equal free volume. As molecular weight increases, the defining temperature increases, increasing the magnitude of viscosity changes with temperature. Increased amounts of highly polar material tend to decrease the defining temperature and the temperature dependence, probably because of molecular associations (interactions) that retard the reduction in free volume with decreasing temperature.
- The viscosity of a given asphalt, at constant free volume, depends on the overall level of polarity; as polarity increases, the viscosity at a given free volume increases, and the master curve shifts to lower frequencies or longer times. The asphaltene content and, to a lesser extent, the amount of polar aromatics seem to relate fairly well to viscosity at constant free volume.
- The width of the relaxation spectrum, or rheological type, depends on the dispersion in molecular weight, the average molecular weight, and the dispersion in polarity among an asphalt cement's constituent molecules. The rheological index, which is proportional to the relaxation spectrum, can be predicted with good accuracy from the number-average molecular weight and the Gaestel index, a parameter calculated from the Corbett fractions:  $(\text{asphaltenes} + \text{saturates}) / (\text{polar aromatics} + \text{naphthene aromatics})$ .
- There is some tendency toward increased tensile strength with increasing molecular weight. Thus, high molecular weight asphalts should, at equivalent rheological points of comparison, have superior fracture and fatigue properties. Conversely, low molecular weight asphalts, even though they may have relatively low stiffness at low temperatures, may suffer in performance because of poor ultimate properties.
- Oxidative aging, as indicated by the aging index at 25°C (77°F) calculated from PAV aging at 100°C (212°F) for 20 hours, increases with decreasing binder stiffness. Additionally, low molecular weight asphalts seem to be more prone to age hardening than high molecular weight asphalts.

## **Rheological Evidence for a Microstructural Model**

Several broad conclusions about the microstructure of asphalt cement can be drawn from the observed rheological properties discussed above and the associated statistical analyses. The primary source of instantaneous elastic (glassy) response is the stiffness of the intramolecular carbon-carbon bond. This stiffness results in the more or less constant glassy modulus of 1 GPa, which is similar for many organic materials, including not only asphalts, but almost all polymers as well. Since there is no plateau region or equilibrium modulus, it can be deduced that there is no long-range structure resulting from a substantial network of covalent bonds.



The observed low tensile strengths support this conclusion, since a strong network would lead to significantly higher tensile strengths.

The smooth transition from glassy behavior to viscous flow and the near log-normal distribution of relaxation times suggest that the relaxation processes in asphalt cement result from a complex and essentially continuous array of molecular interactions, rather than a limited number of homogeneous ones. Additionally, the broad distribution of relaxation times indicates similarly broad distributions of molecular characteristics such as molecular weight and polarity that control relaxation processes. These factors considered together, along with the lack of evidence for a two-phase structure that would be typified by the traditional lamellar micelle structure, point to a system in which the different molecular types and sizes are well distributed spatially throughout the system and may at any moment be expected to occupy any point in the system. The rheological evidence presented above for a microstructural model does not *require* the existence of domains with polarity or compositional gradients. Although the evidence does not rule out the possibility of phase separation in certain unusual modified or highly aged asphalts, the rheological data and analyses indicate that most paving-grade asphalts now in use in this country can be treated as essentially single-phase systems.

As with many other organic materials, including most polymers, the temperature dependence of asphalt cements depends on the free volume and the change in free volume with temperature. Because free volume is strongly related to molecular weight (Ferry 1980), the model developed should include molecular weight as an important factor in determining temperature dependence, especially in the region where viscoelastic behavior dominates. Free-volume changes cannot, however, fully account for the extreme temperature dependence exhibited by asphalt cement, and the role of secondary bonding forces must be considered in this regard.

Asphalt cements exhibit low-temperature isothermal physical hardening that is attributed to a time-dependent reduction in free volume similar to that occurring in other organic liquids. Molecular mobility at low temperatures is reduced, so considerable time is required to reach a thermodynamically stable state. Asphalt cements also typically contain a small number of paraffin-like molecules that contain varying numbers of functional groups. These molecules are probably not purely straight-chained, but branched, with limited functional groups. Based on indirect evidence, it is likely that these molecules orient in some manner much like crystalline wax and that this orientation also contributes to physical hardening. Molecular associations (steric hardening), on the other hand, may be simply a result of geometric rearrangements that, while they result in lowered entropy of the system, do not alter the spatial distribution of the molecules.

The observed delayed elastic behavior, frequently cited as evidence for a gel-like structure, is explainable in terms of the relaxation spectrum. Asphalt cements showing a large amount of delayed elastic behavior have a broad relaxation spectrum. In other words, the molecular weights and intermolecular interactions among constituent molecules are broadly distributed. In reality, because the molecular weights of asphalt cements are relatively small compared with commercial polymers, much of the resistance to flow probably results from secondary forces. It has been clearly shown that when the highly polar functional groups are removed

from asphalt cement, the viscosity drops several orders of magnitude and the behavior approaches that of simple, low molecular weight hydrocarbons. The relaxation spectrum, then, is mostly a reflection of the distribution of secondary forces among the molecules in an asphalt cement.

The essential qualities of a microstructural model for asphalt cement, consistent with its rheological properties as described above, can be summarized as follows. The model should be one in which the essential nature of the material is a fluid, with no substantial covalent networks. The relaxation processes should be related to chemical characteristics, such as molecular weight and polarity, which are broadly and continuously distributed for asphalt cements. The effect of secondary bonding forces and free volume and molecular weight on flow processes must also be a primary feature of the model. To describe a microstructural model in which the molecular types are randomly dispersed (distributed) spatially the term *dispersed polar fluid* was coined (Christensen and Anderson 1992). In the dispersed polar fluid model, this distribution of relaxation times is a result of the dispersion in both the molecular sizes present and the secondary forces among the molecules. The smooth shape of the relaxation spectrum and its resemblance to statistical distribution functions also support the theory that relaxation processes in asphalt cement are controlled through interactions of molecules having a broad range of sizes and functionalities. This hypothesis does not preclude the existence of small domains in asphalt cement, such as wax inclusions, stacks of highly aromatic molecules, or aggregations among polars, but the hypothesis does not rely on these factors to explain the rheological behavior of asphalt cement.

## **Relationships between Chemical Properties and Rheological Parameters of SHRP Asphalts Emphasizing the Core Asphalts**

In volume 2, chapter 5, attempts to predict viscosities of asphalts from polarities and molecular weights of various defined chemical fractions are discussed. It was observed that the viscosity of the neutral fractions derived from eight core asphalts by IEC strongly influenced the viscosity of each parent asphalt. The IEC neutral fractions compose 50 to 60 percent of asphalt and may be considered to confer a "base viscosity" on asphalts. The IEC neutral fractions contain aliphatic, naphthenic, and aromatic hydrocarbons, as well as some nonpolar organosulfur compounds, but are virtually free of polar materials, and their viscosities are orders of magnitude lower than tank asphalt viscosities measured under the same conditions. Aromaticities of IEC neutral fractions, as measured by an atomic hydrogen-to-carbon ratio (H/C), vary significantly. Viscosities of the eight IEC neutral fractions are direct functions of number-average molecular weights ( $M_n$ ), which is not true for tank asphalts at service temperatures. The IEC neutral fractions, which are the bulk of each of the core asphalts, behave as relatively simple mixtures with respect to their viscosities at ambient (and higher) temperatures. Therefore, deviations from this ideal behavior, observed in whole asphalts, must be attributed to the presence of polar components. The problems involved in determining  $M_n$  values of mixtures containing polar components are discussed in volume 2, chapter 9.

In volume 2, chapter 5, it is demonstrated that one polar fraction obtained by IEC, the amphoteric, is the main viscosity-enhancing fraction of asphalts. Other polar materials, when combined with IEC neutrals, enhance viscosity somewhat but not nearly as much as the ampherics. The amphoteric fraction consists of those materials that would be expected to engage in the strongest and most extensive intermolecular associations.

In volume 2, chapter 2, the relationship between relative amounts of asphalt fractions obtained by SEC, and the rheological parameter  $\tan \delta_{ct}$  ( $G''/G'$  determined at 25°C [77°F] at constant torque) is discussed. This relationship appears to be valid for all unaged asphalts studied. In general,  $\tan \delta_{ct}$  increases as the amount of lower molecular weight material (corresponding to asphalt solvent moieties) increases. In terms of the microstructural model, the relationship means that more solvent moiety in an asphalt results in less structuring of polar materials and less prominent elastic properties. As stated earlier in this chapter, elastic effects occur because of strong intermolecular interactions. These interactions are more prevalent in asphalts that contain large amounts of polar, associating materials. The  $\tan \delta_{ct}$  parameter is a measure of the relative size of the elastic modulus of an asphalt.

Correlations between global chemical properties of asphalts are discussed in volume 2, chapter 9. For almost all asphalts studied, a positive correlation among sulfur concentration, asphaltene content (determined by precipitation with *n*-heptane), and metal concentrations (principally nickel and vanadium) was observed. This relationship is known to hold for crude oils, tar sand bitumens, and shale oils and would therefore be expected to be valid for asphalts.

Several relationships between chemical properties of asphalts and asphalt fractions determined at Western Research Institute and physical properties measured at Pennsylvania State University were investigated. From the standpoint of the microstructural model, the chemical properties of most interest are those relating to molecular size (number- or weight-average molecular weights,  $M_n$  or  $M_w$ ) and molecular size distribution, polarity (heteroatom content, asphaltene content, fraction distribution by chromatographic methods), and aromaticity (H/C). Rheological parameters are the physical properties of greatest interest, although other physical properties were considered. From prior research, and consideration of the microstructural model, it was not anticipated that many single global chemical properties would be found that would correlate with single physical properties for whole asphalts. The microstructural model predicts that physical properties should be determined by combinations of chemical properties of solvent moieties (principally molecular size, molecular size distribution, and aromaticity) and of dispersed moieties (heteroatom content, aromaticity, asphaltene content, molecular size, and molecular size distribution). Most of the chemical compositional data were obtained for the eight core asphalts, since budgetary constraints precluded detailed chemical studies of the expanded set of asphalts. Consequently, the statistical base of the correlations discussed below is narrow.

Table 3.13 lists linear regression analyses of the relationship between total heteroatom content (calculated as the sum of weight percents of nitrogen, oxygen, and sulfur, each divided by their respective atomic weight) of the core asphalts with several physical properties and one chemical property. The correlation with dielectric constant is very strong, as it must be for any organic material. The heteroatoms are the charge carriers of asphalts,

and dielectric constant will be a function of total number of charge carriers. Association phenomena should not directly influence this property, save perhaps to inhibit charge transfer. Polarity is a function of heteroatom content and also is a function of the distribution of polar functionalities among molecules. Relative viscosity (calculated by dividing the tank asphalt viscosity by the viscosity of its IEC neutral fraction, both measured at 25°C [77°F]) also correlates well with heteroatom content. The correlation with asphaltene content is strong, as was mentioned earlier. These correlations are almost self-evident and follow directly from the microstructural model. Heteroatom content is considered to be a combination of chemical properties.

Table 3.14 lists linear regression analyses of relationships of chemical properties of eight core asphalts with defining temperature,  $T_d$ . This parameter, which can be measured with an accuracy of  $\pm 3^\circ\text{C}$  ( $5.4^\circ\text{F}$ ), correlates fairly well with the activation energy of viscous flow, as would be expected. The relationship between either  $M_w$  or  $M_n$  of tank asphalts and  $T_d$  is not particularly strong, as was found for  $T_d$  and  $M_n$  for all SHRP asphalts. However, the relationship between  $T_d$  and the ratio  $M_w/M_n$  (polydispersity index) is very strong for the core asphalts, indicating that  $T_d$  is a function of molecular size distribution throughout an asphalt. When asphalts are subjected to oxidative aging,  $T_d$  increases, as does  $M_n$ .

Relationships between  $T_d$  and such properties as Heithaus parameters and  $M_n$  of IEC neutral fraction are not strong. The relationship between  $T_d$  and asphaltene content, which is an inverse relationship, is fairly strong. This relationship was observed to hold for all SHRP asphalts. The relationship appears to be confirmed by the stronger relationship with the Gaestel index, obtained from Corbett fraction data.  $T_d$  has moderate to weak relationships to carbon number maximum and distribution of IEC neutral fraction, obtained by SFC. Some combinations of the above factors strongly correlate with  $T_d$ , particularly the polydispersity index combined with both  $M_n$  and H/C of the IEC neutral fraction of each asphalt. Because of the narrow database, correlations with three factors must be viewed with caution.

The crossover frequency ( $\omega_{cTd}$ ) of the core asphalts would be expected to be related to chemical properties involving polarity and aromaticity, because  $\omega_{cTd}$  is a measure of elasticity. In table 3.15, this rheological parameter is observed to correlate weakly with the asphaltene compatibility index (ACI) and with the Heithaus  $P$  parameter. There is a reasonably good correlation with the Heithaus  $p_a$  parameter, which measures asphaltene peptizability. Unfortunately, data are available for only seven asphalts, because one asphalt is too waxy to be analyzed by the Heithaus method. Polydispersity index ( $M_w/M_n$ ) correlates weakly with  $\omega_{cTd}$ . However, a moderately strong correlation of  $\omega_{cTd}$  with the combination of asphaltene content plus H/C (aromaticity) of the IEC neutral fraction is observed. Crossover frequency appears to be influenced mostly by association phenomena, as predicted, because elastic properties result from interactions of polar, aromatic species.

Table 3.16 lists linear regression analyses of the rheological index ( $R$ ) with chemical properties of the core asphalts.  $R$  correlates weakly with individual chemical properties. Some combinations of chemical properties correlate moderately well with  $R$ , such as the pair of chemical properties  $M_n$  and ACI. ACI is a measure of the state of dispersion of an asphalt, which should influence  $R$ . The  $M_n$  and H/C of IEC neutral fractions combined with total

asphalt heteroatom content also correlate well with  $R$ . Again, results of correlations using three factors among eight asphalts should be viewed with caution.

Other single chemical factors or combinations were correlated with the rheological parameters  $T_d$ ,  $\omega_{cTD}$ , and  $R$ , but the regression analyses resulted in low coefficients of determination ( $r^2$  values), so these numbers are not listed in tables 3.14 to 3.16. No good correlations between aging indexes of the core asphalts and  $T_d$ ,  $\omega_{cTD}$ , or  $R$  were observed.

## Prediction of Physical Properties from Chemical Data

Some of the chemical factors discussed above were used in regression equations to predict physical properties of the eight core asphalts. For tank asphalts at 25°C (77°F),

$$\log \eta = 10.9 + 5.64H + 0.0663C - 6.52A \quad (3-14)$$

where

- $H$  = heteroatom content (number of nitrogen, oxygen, and sulfur atoms)
- $C$  = carbon number at peak maximum of SFC spectrum of IEC neutral fraction; this parameter is closely related to  $M_n$
- $A$  = H/C of IEC neutral fraction

Equation 3-14 indicates that asphalt viscosities at 25°C (77°F) increase as asphalt heteroatom content increases, aromaticity of IEC neutral fraction (solvent moiety) increases, and average carbon number of the IEC neutral fraction increases. This carbon number is closely related to the  $M_n$  value of an IEC neutral fraction, and presumably the two parameters are nearly interchangeable. The  $r^2$  value for the eight asphalts using equation 3-14 is 0.950, and the  $P$  value (observed significance level—not to be confused with the Heithaus parameter also designated  $P$ ) is 0.005.

Activation energy of viscous flow ( $E_a$ ), a parameter related to temperature dependence of viscosity, depends on the same factors that appear in equation 3-14, plus a factor measuring carbon number distribution:

$$E_a = 74.4 + 0.937C + 65.6H - 55.5A - 0.204W \quad (3-15)$$

where  $C$ ,  $H$ , and  $A$  are the same quantities defined for equation 3-14, and  $W$  is the peak width at one-half peak height in the SFC spectrum of the IEC neutral fraction.

For the eight core asphalts, using equation 3-15, linear regression yields  $r^2 = 0.996$  and  $P = 0.001$ .

Viscosity of the IEC neutral fraction at 25°C (77°F) depends mostly on molecular weight and to some degree on aromaticity:

$$\log \eta = 5.23 + 0.0606C - 3.69A \quad (3-16)$$

For the eight IEC neutral fractions, using equation 3-16, linear regression yields  $r^2 = 0.971$  and  $P < 0.001$ . The viscosity of the IEC neutral fraction is independent of the heteroatom content of the parent asphalt.

Aging index in the TFO test is a function of polarity parameters:

$$AI_{TFO} = -5.13 + 0.0323C + 2.43A_{\text{tank}} + 9.91H \quad (3-17)$$

where  $C$  and  $H$  are as above and  $A_{\text{tank}}$  is the H/C of the tank asphalt. For the eight core asphalts, using equation 3-17, linear regression yields  $r^2 = 0.925$  and  $P = 0.010$ .

Aging index for TFO-PAV aged asphalts may be calculated as follows:

$$AI_{TFO-PAV} = 82.4 + 1.14C - 65.9A + 138H - 10.6 \log \eta \quad (3-18)$$

where  $\eta$  is the viscosity of the tank asphalt at 25°C (77°F). In the PAV oxidation, viscosity is definitely a factor. For the eight core asphalts, using equation 3-18, linear regression yields  $r^2 = 0.940$  and  $P = 0.035$ .

In figures 3.16 through 3.20, data for the eight core asphalts in equations 3-14 through 3-18 are graphically illustrated.

As mentioned previously, the use of more than two variables to predict properties of eight asphalts must be viewed with caution. Nevertheless, random selections of chemical variables proved to be poor predictors. The variables examined above would be those predicted by the model, so at least the correlations provide some evidence to support it.

## Microstructural Model and Results of Chemical Studies

Research efforts in the SHRP Binder Characterization and Evaluation Program have been governed by the premise that the important performance-related physical properties of asphalts are functions of asphalt composition. It follows from this premise that the chemical composition of an asphalt depends on the composition of the parent crude oil and the method used to manufacture the asphalt. The lines of work pursued have been directed toward determining which chemical and physical properties are the best predictors of asphalt performance, assuming that there is some agreement about what constitutes asphalt performance. If no such properties could be identified for purposes of pavement construction, the hypothesis that all asphalts of a given viscosity grade are alike would be strongly supported.

In chapter 1, the historical development of a model of asphalt structure was described. This model has been referred to as the *microstructural model* and serves to rationalize relationships between physical properties and the diverse compositional data observed in petroleum residua. The microstructural model is a successor to what has been known as the *colloidal* or *micellar* model, enunciated half a century ago by Pfeiffer and Saal (1940) and

many others. The terms *colloid* and *micelle* may not be appropriate when applied to petroleum systems, as discussed in chapter 1. A principal objective of the Binder Characterization and Evaluation Program was the verification of the microstructural model.

The separation of asphalts by IEC into polar (acidic, basic, and amphoteric) and nonpolar (neutral) components demonstrates that materials corresponding in properties to the dispersed and solvent moieties of the microstructural model do exist. It remains to be proved that they behave as the model predicts as parts of whole asphalts. The nonpolar (neutral) components of asphalts consist of aliphatic, naphthenic, and aromatic hydrocarbons and also substantial amounts of organosulfur compounds. The nonpolar compounds vary in molecular weight from about 200 to more than 1500 daltons. Significantly, the viscosities of these materials appear to depend largely on their number-average molecular weights ( $M_n$ ) determined by vapor-phase osmometry (or related parameters such as carbon number of peak maximum in SFC spectrum), as would be expected for a mixture of weakly associating molecules. However, viscosities of whole asphalts do not correlate with their  $M_n$  values.

The IEC separation of four asphalts showed that the predominant polar fraction consists of amphoteric molecules, which are relatively aromatic and contain at least one acidic and one basic functional group. As discussed earlier in this chapter, amphoteric materials are capable of forming associations and are the principal viscosity-enhancing components of asphalts, although all IEC polar fractions enhance viscosity to some degree. The concentrations of amphoterics increase in asphalts as a result of oxidative aging. Other polyfunctional molecules do not appear to exist in asphalts in large amounts.

SEC separations of asphalt yielded results that complement the IEC studies. The SEC separation provides a method for a rough estimation of weight-average molecular weights ( $M_w$ ) of asphalts, a property known to influence rheological properties of all organic materials. The results of SEC separation of asphalts into associating (and possibly high molecular weight) and nonassociating components, each having distinctly different chemical properties, support the microstructural model. By IEC separation, amphoterics compose most of the SEC associating components. Asphalts having relatively few associating components differ in rheological properties from those having large amounts of associating components. Most important, asphaltene content does not always correspond to amount of associating components as determined by SEC. However, asphaltene content is an indicator of total polarity. Polar molecules tend to interact to form larger associations. Weakly polar molecules are only loosely bonded to larger molecular associations. The size (and possibly shape) of the polar associations should be a function of temperature and shear. The individual associations may be very nonuniform, in both composition and size. The molecules containing polar functional groups may be largely aliphatic or aromatic. Therefore, aromatic hydrocarbons may be involved in associations of polar molecules. Many of the aliphatic and naphthenic hydrocarbons in asphalt (which compose a large portion of the total) will not be so strongly attracted to polar associations that they become part of the associations, and these hydrocarbons will behave as a solvent. At service temperatures, polar associations are large enough to be significant hydrodynamic disturbances to the solvent, as measured by intrinsic viscosities. It is important to emphasize that, according to the model, the polar associations have no well-defined boundaries, so there are no abrupt property changes from the outer areas of the associations to the solvent. The associations are not uniform colloids, as has

been shown by other work, discussed in chapter 1. Associations of some strength are necessary to account for elastic effects (D.A. Anderson, personal communication, 1993). Elastic effects also are associated with changes in entropy. If crude oil residua are randomly assembled homogeneous solutions without any preferred polar associations at a given temperature near ambient, the residua are in a state of maximum entropy. Such random assemblies can hardly become much more random, so the entropy will be unlikely to decrease greatly when the system is heated to a somewhat higher temperature. Yet elastic effects, which are governed by entropy, are observed to decrease in residua with temperature increases. Changes in elasticity caused by mechanical stress also require changes in organization of molecular assemblages (i.e., some deviation from a completely random ensemble). The nature of the polar moieties and solvent moieties of asphalts and their relative amounts vary among asphalts and also change as a result of oxidative aging. Properties of asphalts are a function of the interactions of the two moieties. To predict asphalt properties, parameters descriptive of the solvent and the polar moieties are required. Aromaticity, molecular size, and molecular size distribution should suffice to describe solvent moieties. Dispersed moieties should be described by the above three variables and parameters that measure polar interactions.

Service temperature oxidative aging of asphalts proceeds in such a manner that buildup of polar, associated molecules tends to decrease subsequent reactivity with oxygen by incorporating potentially oxidizable molecules in associations. Dialkyl sulfides and aryl-alkyl sulfides, which are relatively nonpolar, react readily to form polar sulfoxides. These naturally occurring sulfur compounds are more reactive toward oxygen than most other asphalt components. As a result, the initial oxidation of an asphalt results in considerable sulfur oxidation but little carbon oxidation. More carbon oxidation occurs later in the aging process, after most sulfur oxidation has been completed. Many reactive sulfur compounds are associated with solvent moieties, so their reaction with oxygen is rapid until their supply is exhausted. Reactive carbon compounds presumably are aromatic molecules with aliphatic side chains, many of which would be associated with polar associations. Thus, low-temperature oxidation of these species might be inhibited by polar association buildup. At higher mix plant temperatures, polar associations are to some extent broken up, and more aromatic species readily undergo oxidation.

The phenomenon of isothermal, reversible age hardening of asphalts (steric hardening) was studied in several asphalts but was not of significant magnitude in one asphalt that contains relatively few associating components. Steric hardening cannot be explained by a simple solution model and must involve a slow progression to a favored thermodynamic state, one in which polars assume more alignment than random orientation.

The above results, and much other data, show that the essential features of the microstructural model are valid. It should be possible, by using the model, to predict important physical properties of asphalts from specific chemical properties and vice versa. For purposes of analysis, asphalts can be considered to be mixtures of solvent moieties and dispersed moieties. Many physical properties of asphalts can be predicted from knowledge of molecular weights and aromaticities of solvent moieties, and polarity factors of dispersed moieties. No single global chemical variable was found to be a good predictor of physical properties.



It was pointed out in chapter 1 that much concurrent work on the nature of asphaltenes in crude oils and residua has been reported since the SHRP Binder Characterization and Evaluation Program began. Many of these studies focused on a limited number of materials. The eight core asphalts chosen for intensive study by SHRP represent the variation in properties exhibited by pavement binders; they are not a group of "pet" asphalts. In volumes 2 and 3, it is shown that many of these asphalts are distinctive in their chemical and physical properties.

In chapter 1, the historical development of models relating asphalt structure to physical properties is described. Two somewhat different concurrent views of asphalt structure are presented. One view, the continuous thermodynamic model, considers asphalts to be more like solutions and contends that asphaltenes have no real existence in asphalt systems but are artifacts of precipitation. The other view, the steric colloidal model, considers asphalts to have some sort of colloidal nature and assumes that asphaltenes (for the most part) have a real existence. The steric colloidal model more closely approximates the microstructural model proposed at the outset of the SHRP Binder Characterization and Evaluation Program. Neither viewpoint precludes the existence in crude oils and crude oil residua of associations of polar molecules. Polar molecules are present in too high a concentration for all of them to exist as solvated monomeric entities. Infrared spectra of thin films of residua demonstrate the existence of hydrogen bonding interactions between carboxylic acids, phenols, and 2-quinolones. At issue are the sizes and shapes of the polar associations and the nature of their solvation. The continuous thermodynamic model contends that the wide variety of asphaltene-forming molecules are individually solvated by less polar resins. The steric colloidal model contends that asphaltenes exist as associations of widely varying size, each association being solvated by resins.

Judging by the results in the SHRP Binder Characterization Program, there may be merit to both viewpoints. Earlier in this chapter, it was asserted that no model as complicated as the microstructural model need be invoked to explain asphalt rheology. From the chemical standpoint, the oxidation behavior of asphalts is best described by the steric colloidal (microstructural) model, with the possible exception of asphalt AAG-1. Indeed, AAG-1 may best be described as more solution-like than any other asphalt studied. It also should be pointed out that AAG-1 exhibits little steric hardening at 25°C (77°F).

On the other hand, all the core asphalts are characterized by substantial intrinsic viscosity values at 25°C and 60°C (77°F and 140°F), indicating that associations of considerable size are present. The phenomenon of steric hardening requires that there be a favored thermodynamic state at a given temperature. The pronounced temperature dependence of viscosity of asphalts and variation of elastic properties with temperature were once considered proofs of the colloidal model, but for the eight core asphalts, temperature dependence is most pronounced with AAG-1. If the steric colloidal model is correct, then shapes of associations will prove to be important determinants of asphalt properties in addition to the sizes of assemblies. We did not directly observe any spherical associations of asphaltene molecules. In one SHRP project (Jennings et al. 1991; Project A-002C), widely separated phases, and presumably highly spherical associations, were ruled out by nuclear magnetic resonance (NMR) evidence. The NMR data conflict with X-ray and other data here. Nevertheless an important result of the SHRP Binder Characterization and Evaluation

Program is that, by considering asphalts to consist of solvent and associating (dispersed) moieties, asphalt aging behavior and asphalt physical properties can be correlated and predicted from a limited number of chemical parameters. These relationships should allow for the rationalization of the physical properties that lead to (or retard) pavement failure modes such as oxidative aging, fatigue cracking, thermal cracking, and permanent deformation. This new understanding has been used to formulate better binder specifications. The SHRP asphalt programs have led to a better understanding of the phenomena involved in pavement failure.

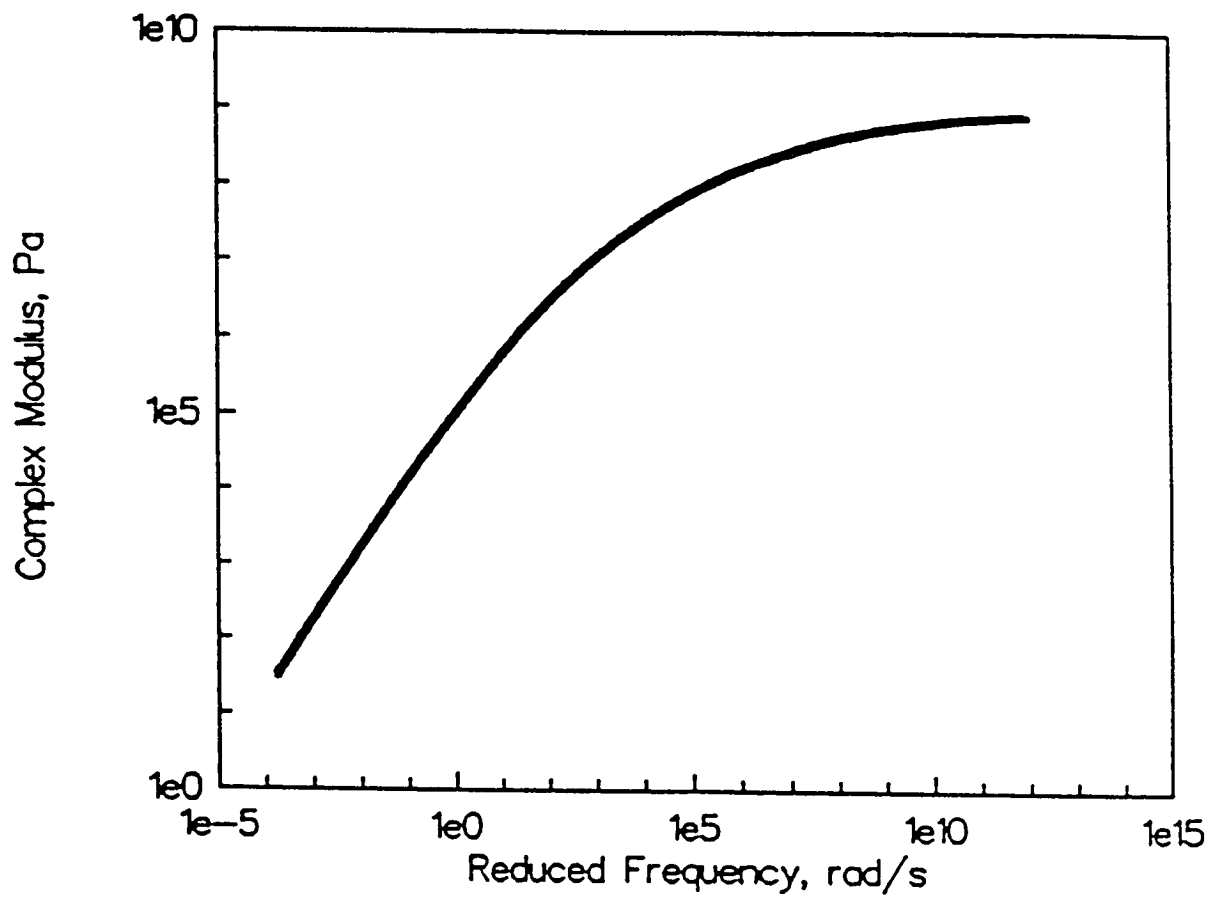


Figure 3.1 Typical Master Curve for Asphalt Cement

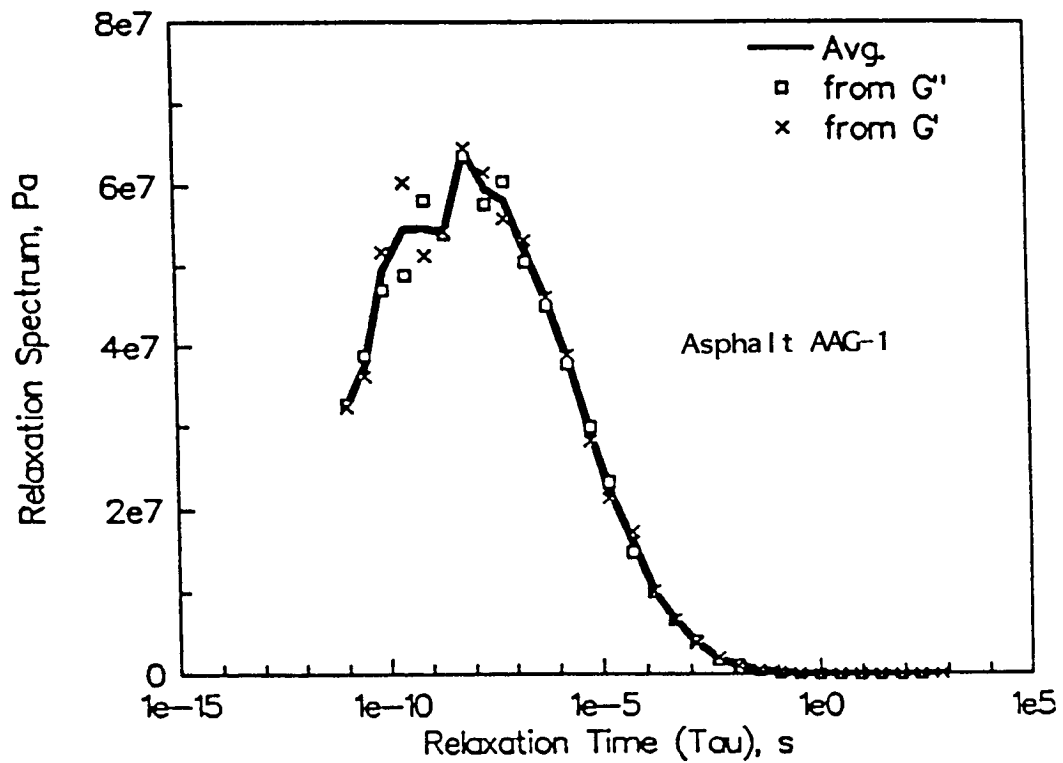
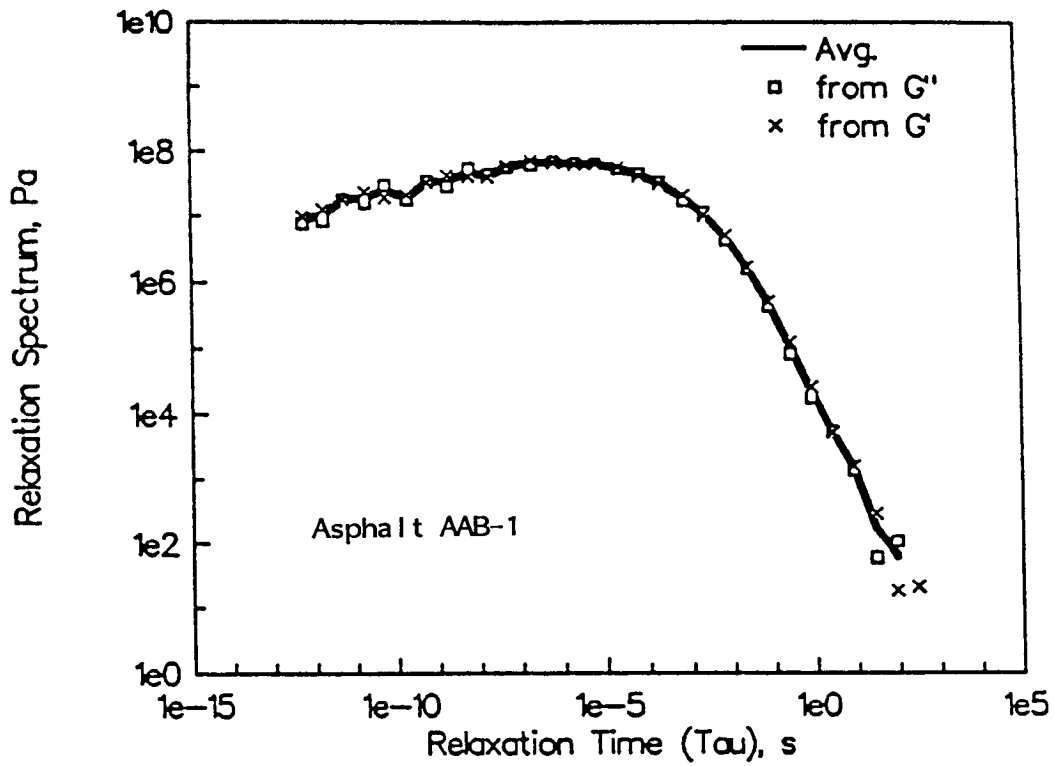


Figure 3.2 Relaxation Spectra for Asphalts AAB-1 and AAG-1

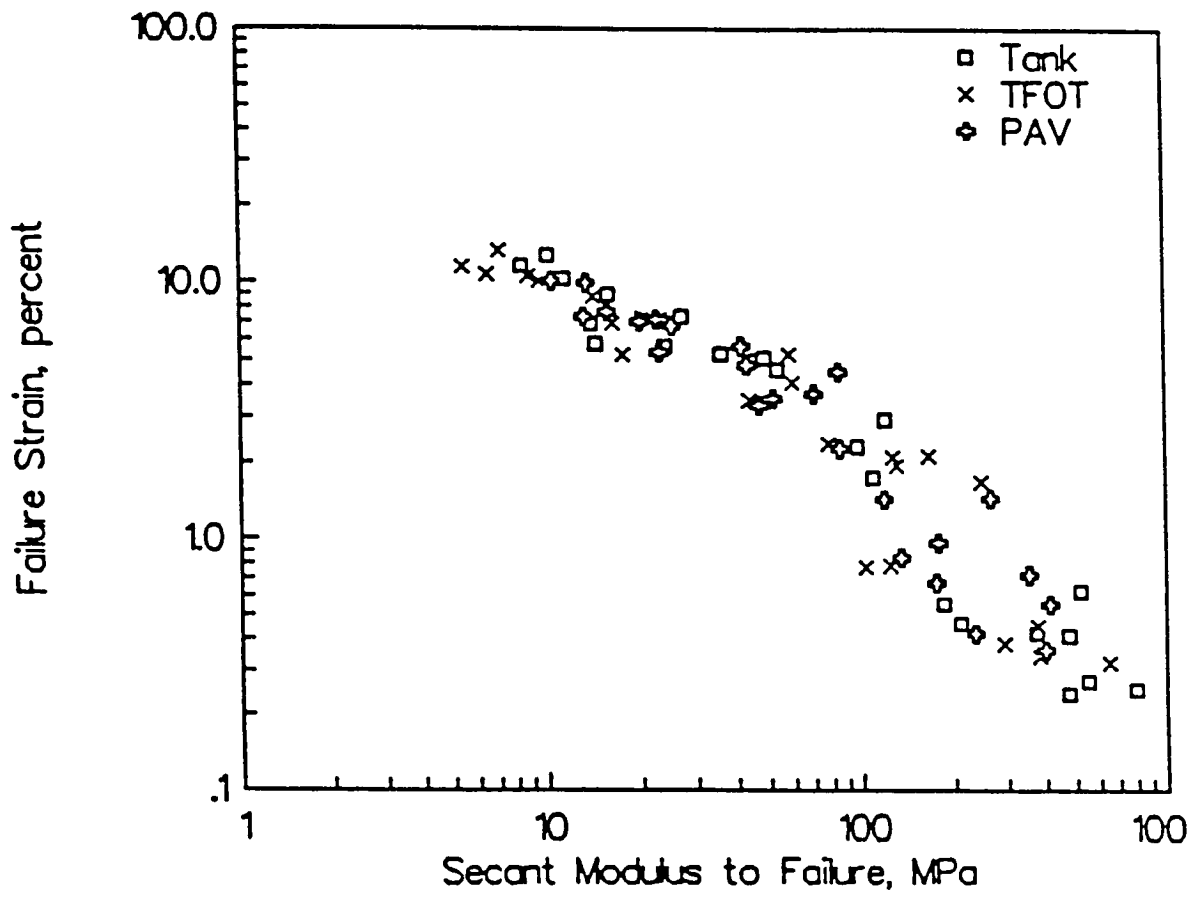


Figure 3.3 Failure Strain versus Secant Modulus at Failure

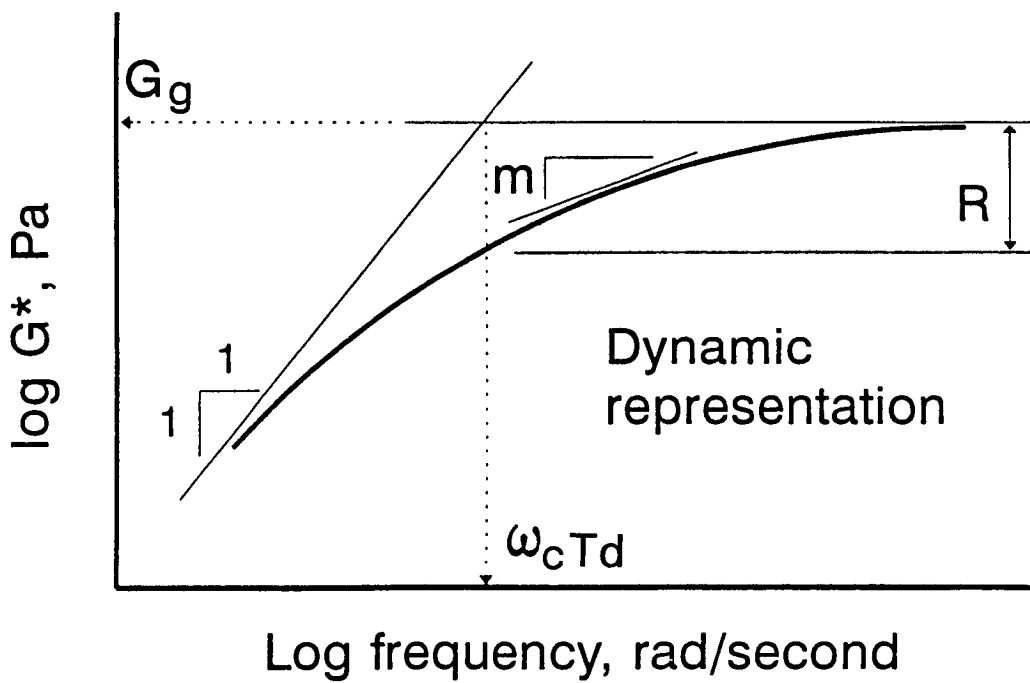
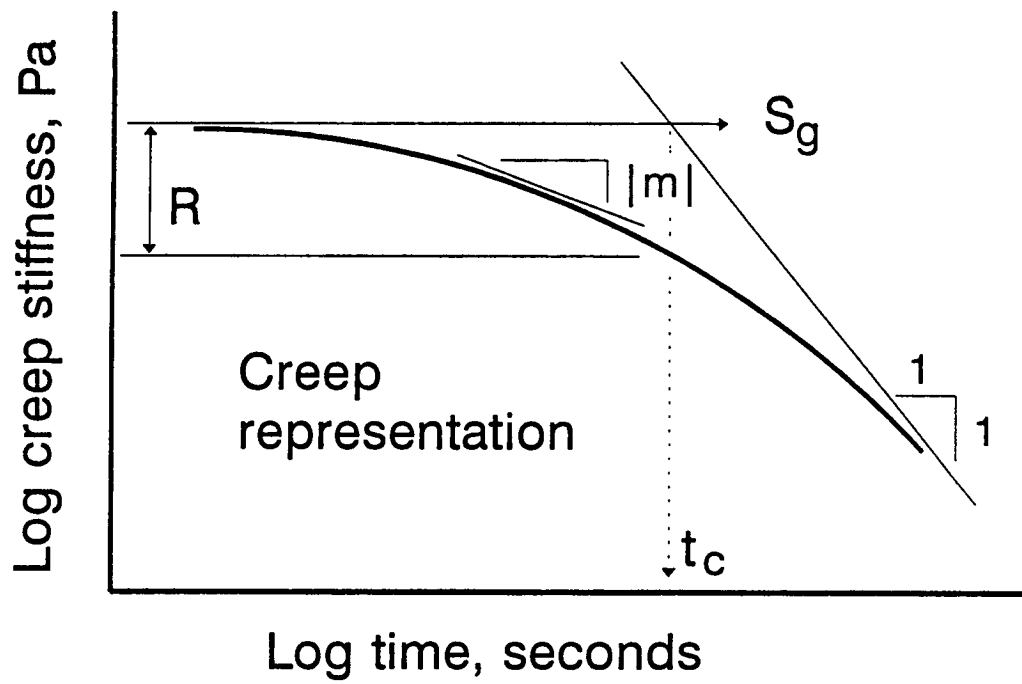
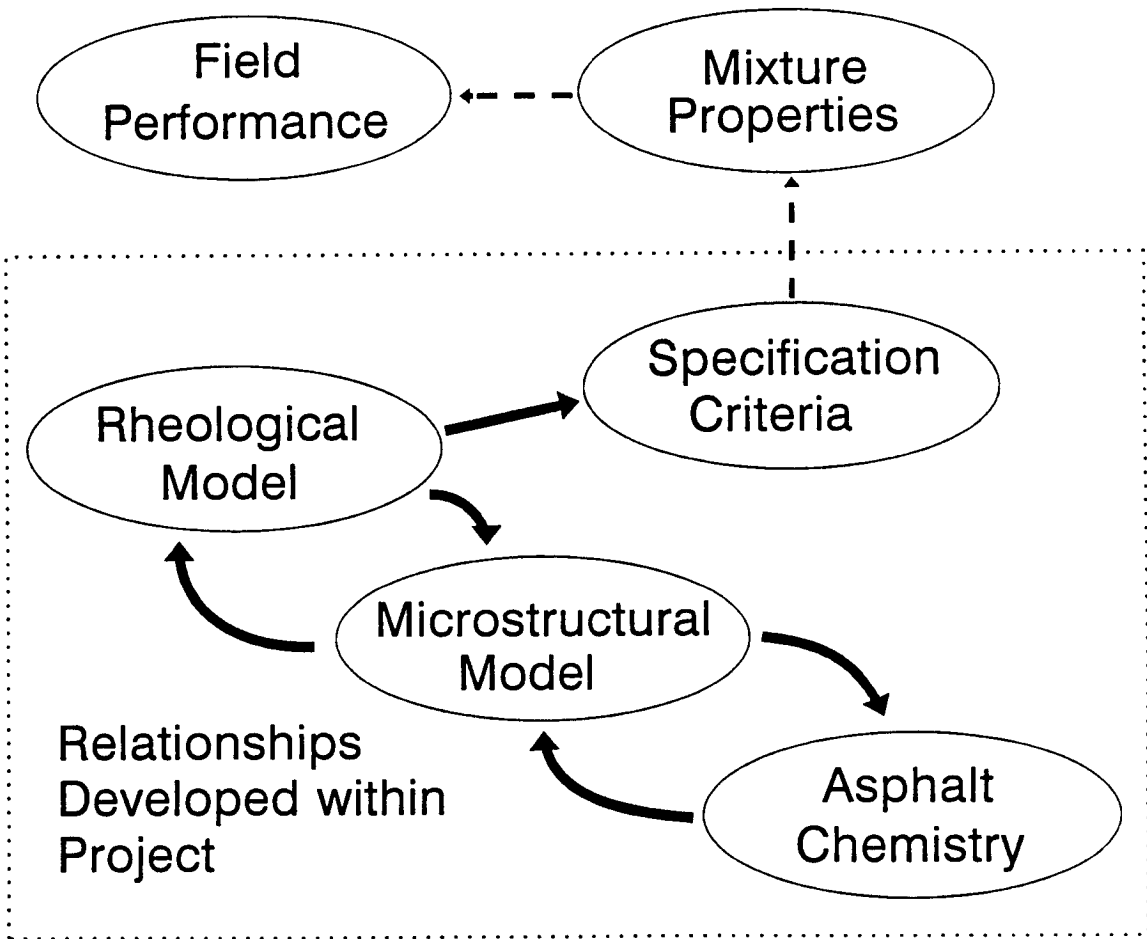
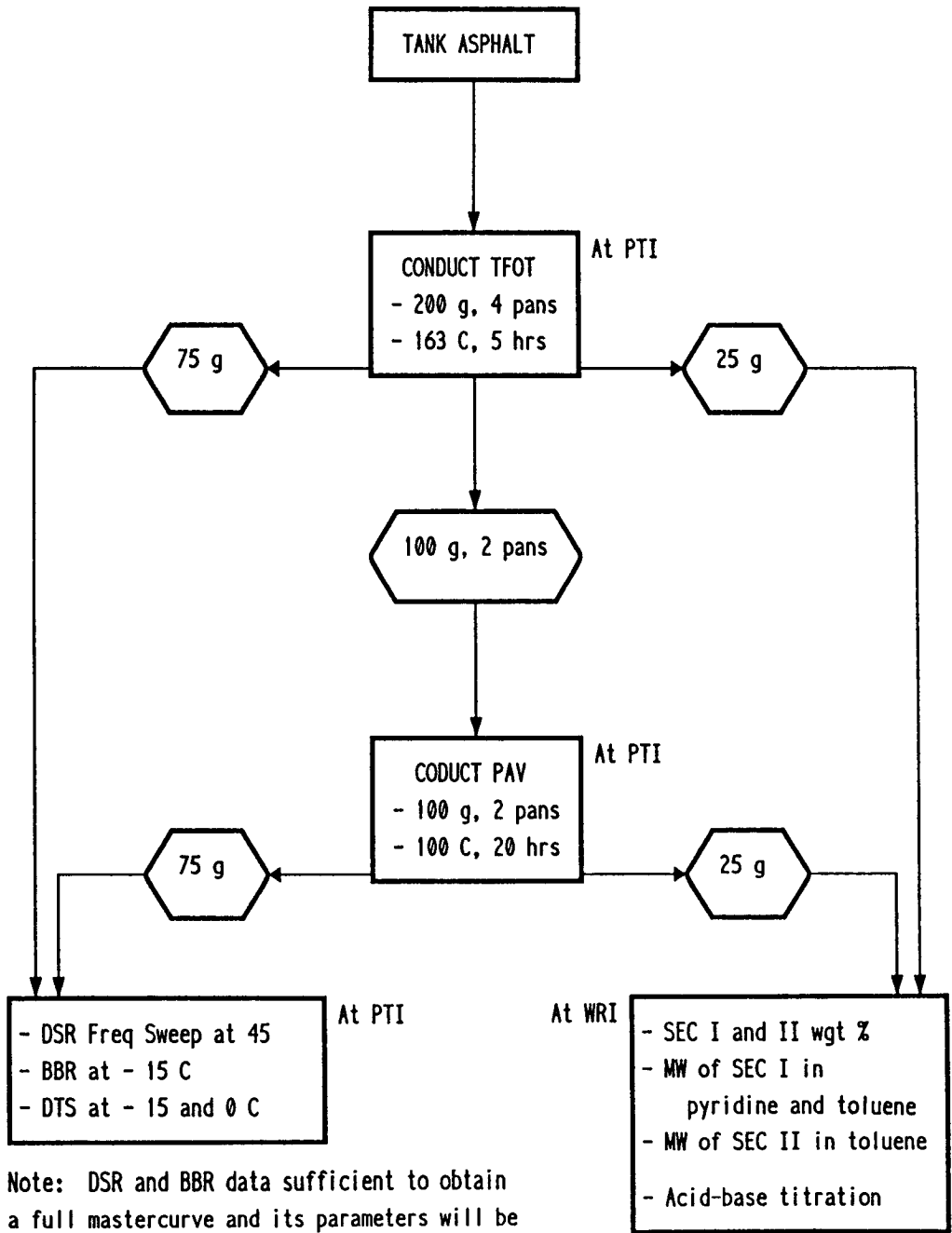


Figure 3.4 Definition of Rheological Model Used for Predictions



**Figure 3.5 Relationship between Performance, Rheological and Microstructural Models, and Chemistry**



Note: DSR and BBR data sufficient to obtain a full mastercurve and its parameters will be obtained. This may necessitate a second DSR measurement at an intermediate temperature.

**Figure 3.6 Experiment Design to Establish Physical-Chemical Property Relationships**



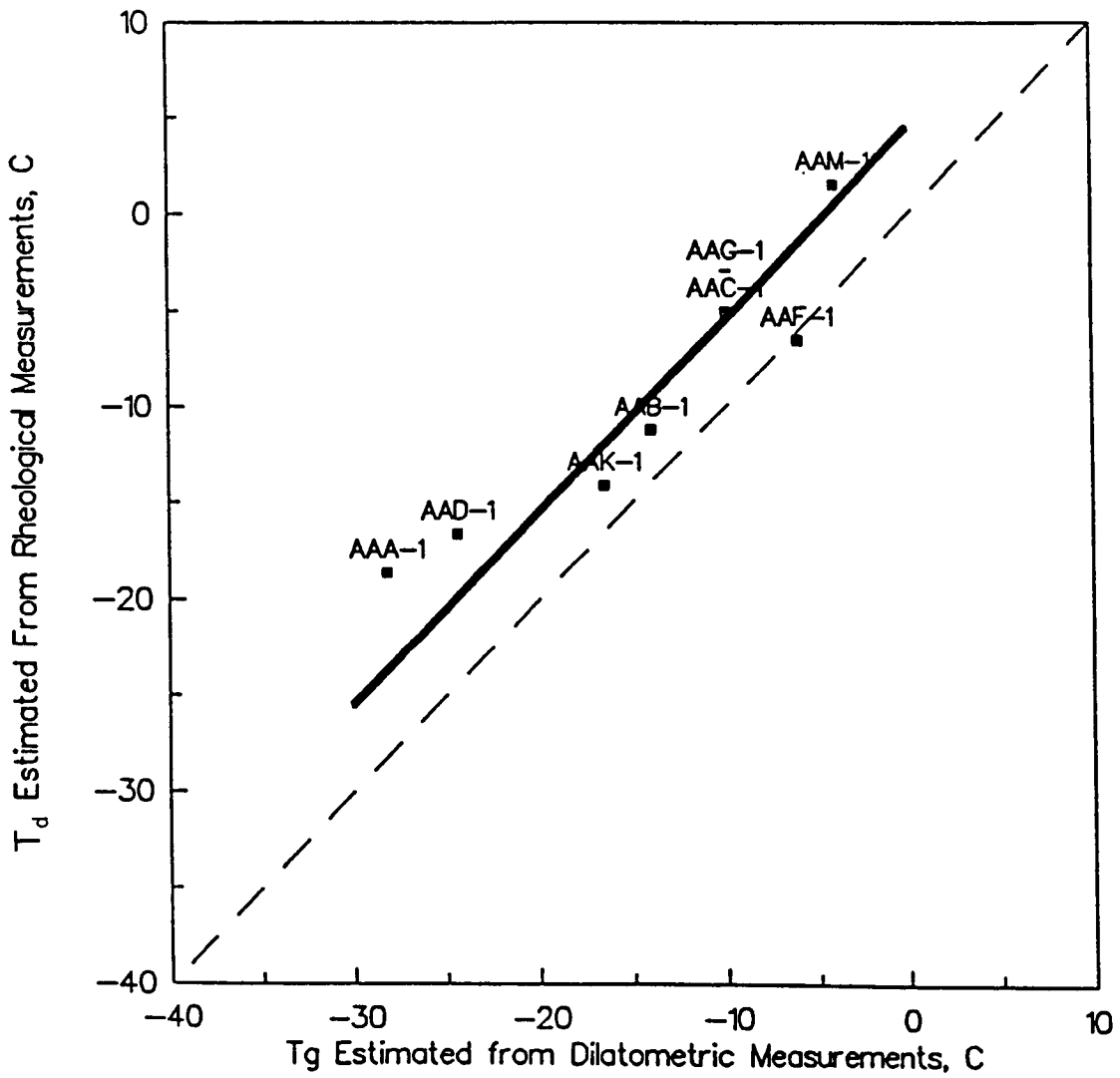


**Figure 3.7 Relationship between Dilatometrically Determined Glass Transition Temperature and Defining Temperature**

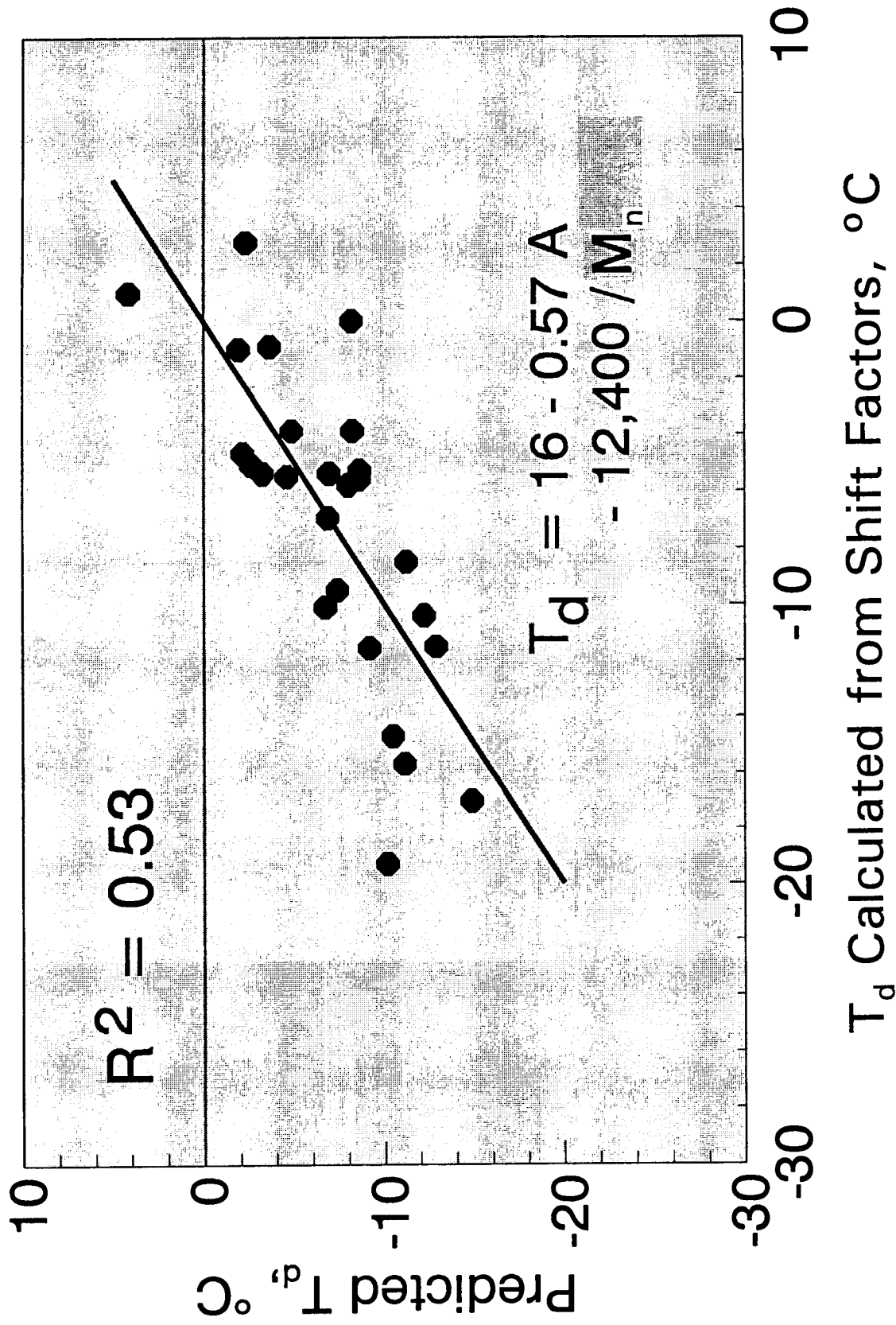


Figure 3.8 Predicted versus Measured Values of the Defining Temperature Predicted from Asphaltene Content and Number-Average Molecular Weight

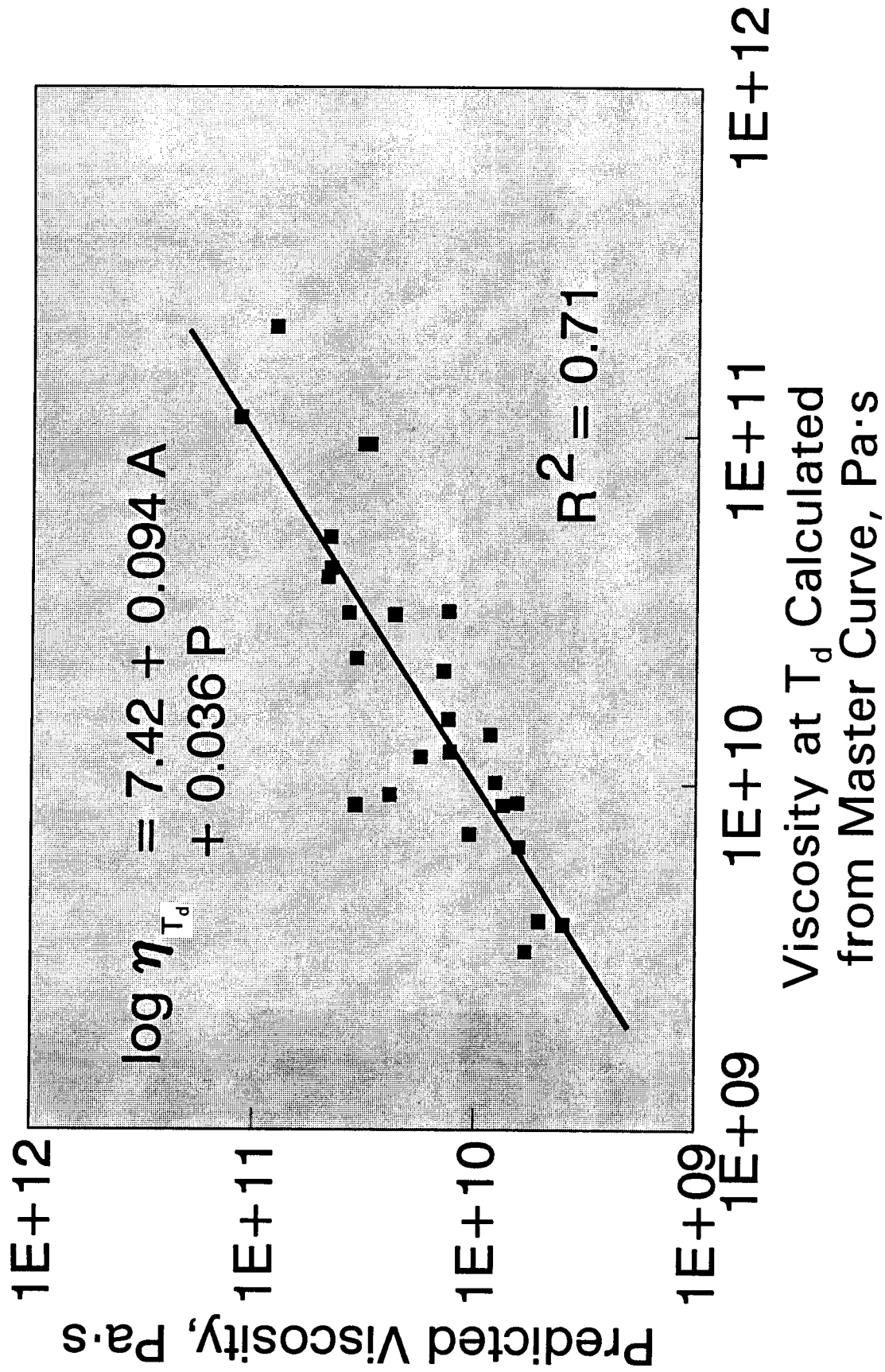


Figure 3.9 Predicted versus Measured Values of the Steady-State Viscosity at the Defining Temperature Predicted from Asphaltene and Polar Aromatic Content

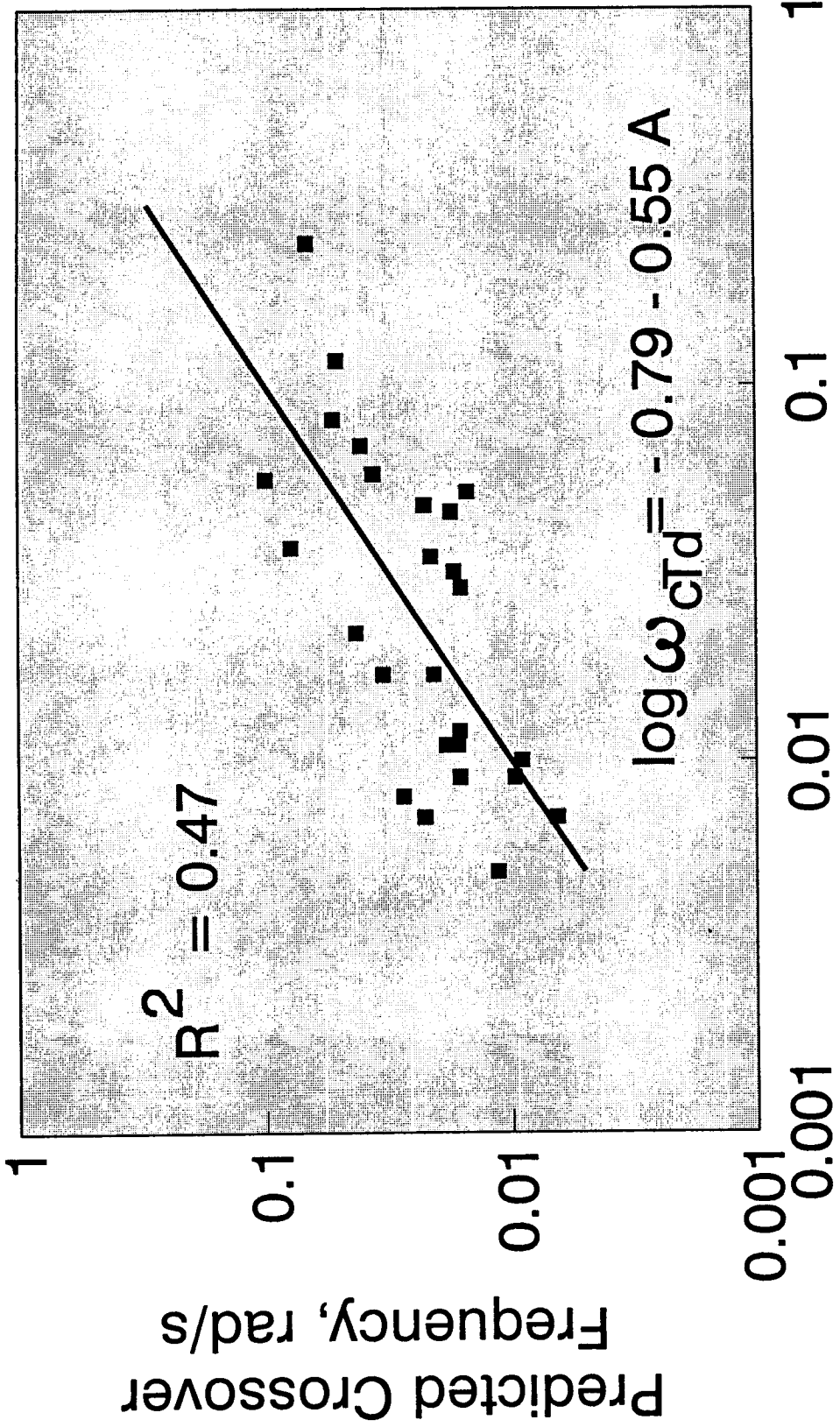
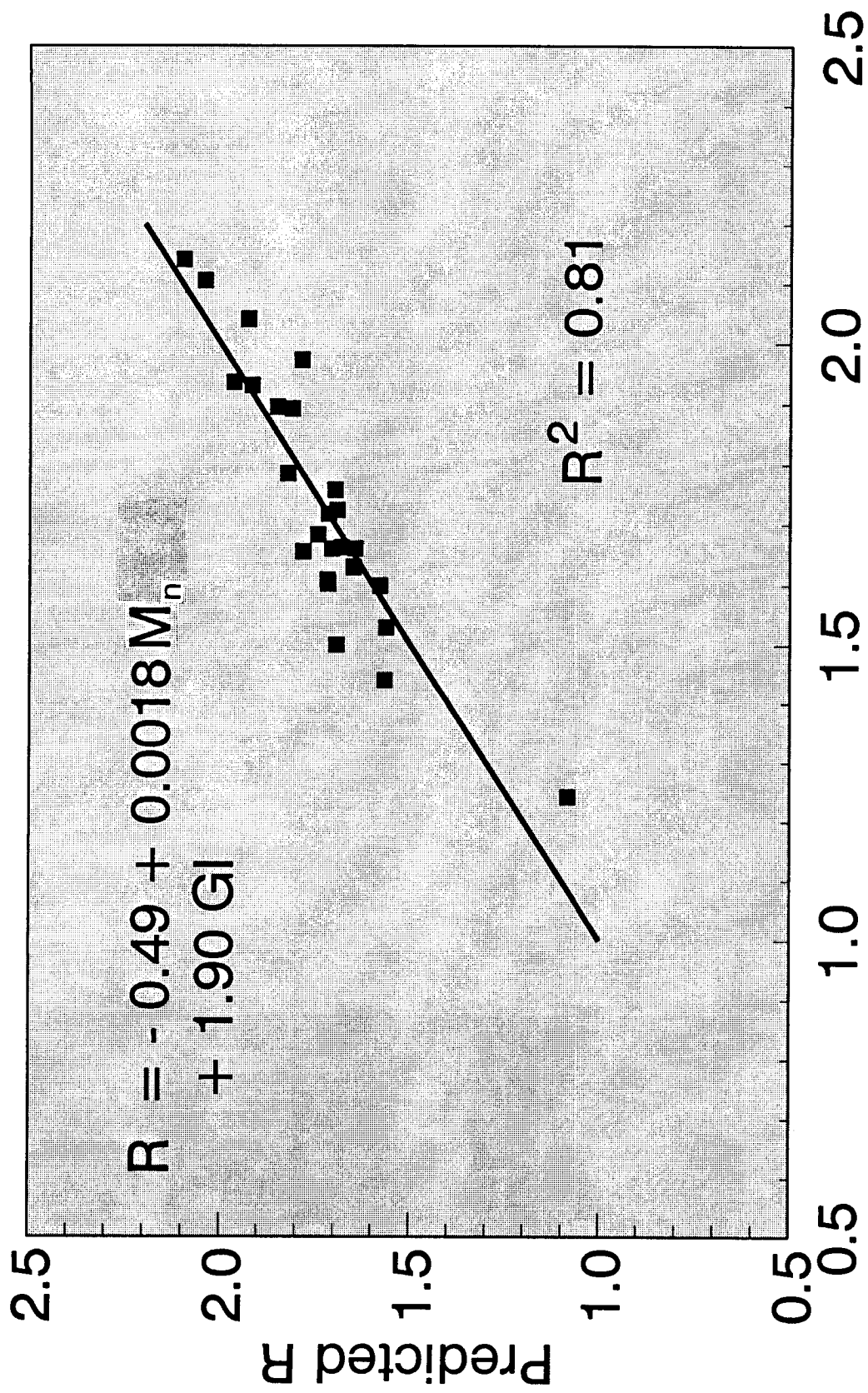


Figure 3.10 Predicted versus Measured Values of the Crossover Frequency Predicted from Asphaltene Content



## R from Master Curve

Figure 3.11 Predicted versus Measured Values of the Rheological Index Predicted from Number-Average Molecular Weight and Gaestel Index

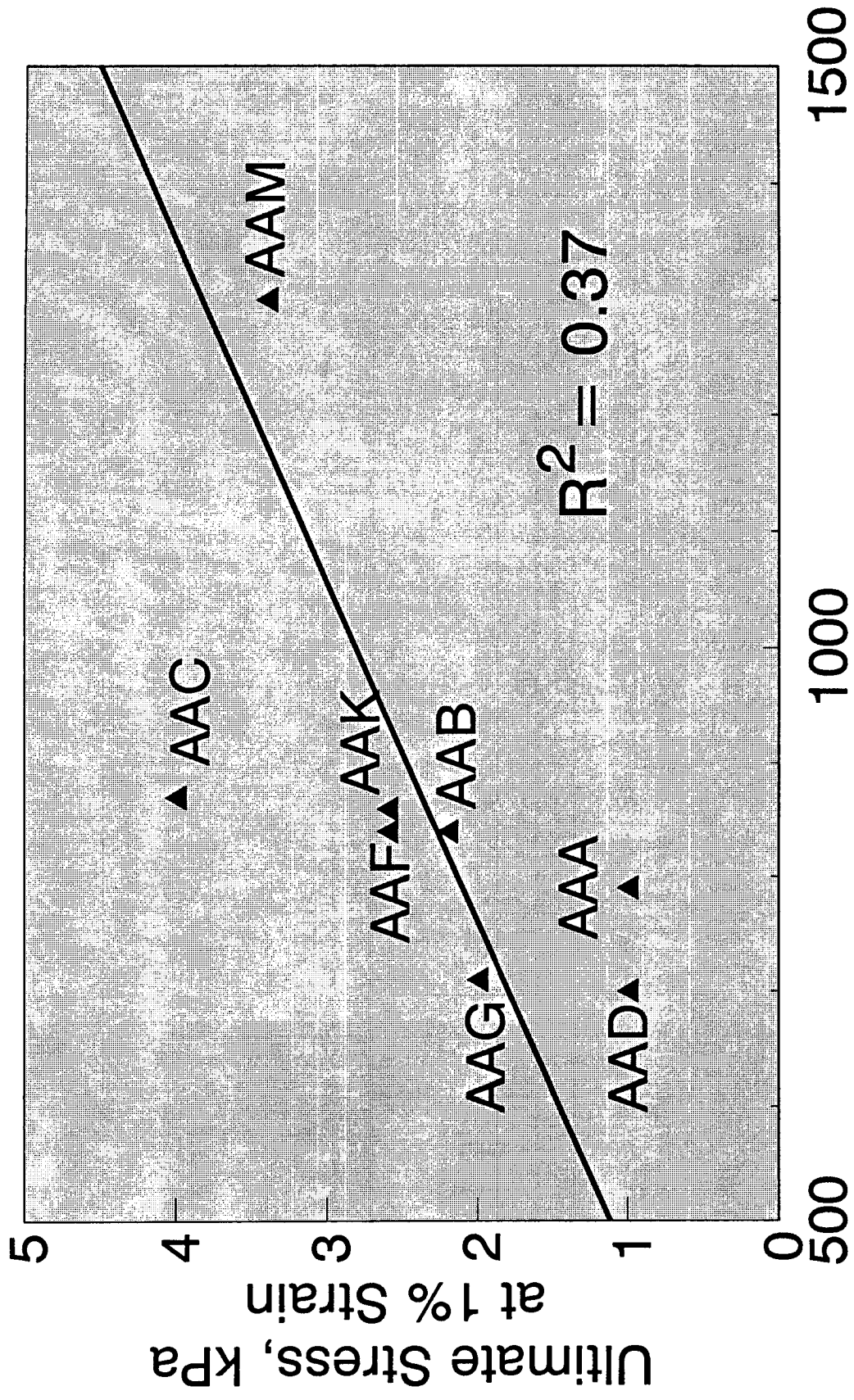


Figure 3.12 Tensile Strength versus Molecular Weight When Failure Strain Is 1 Percent

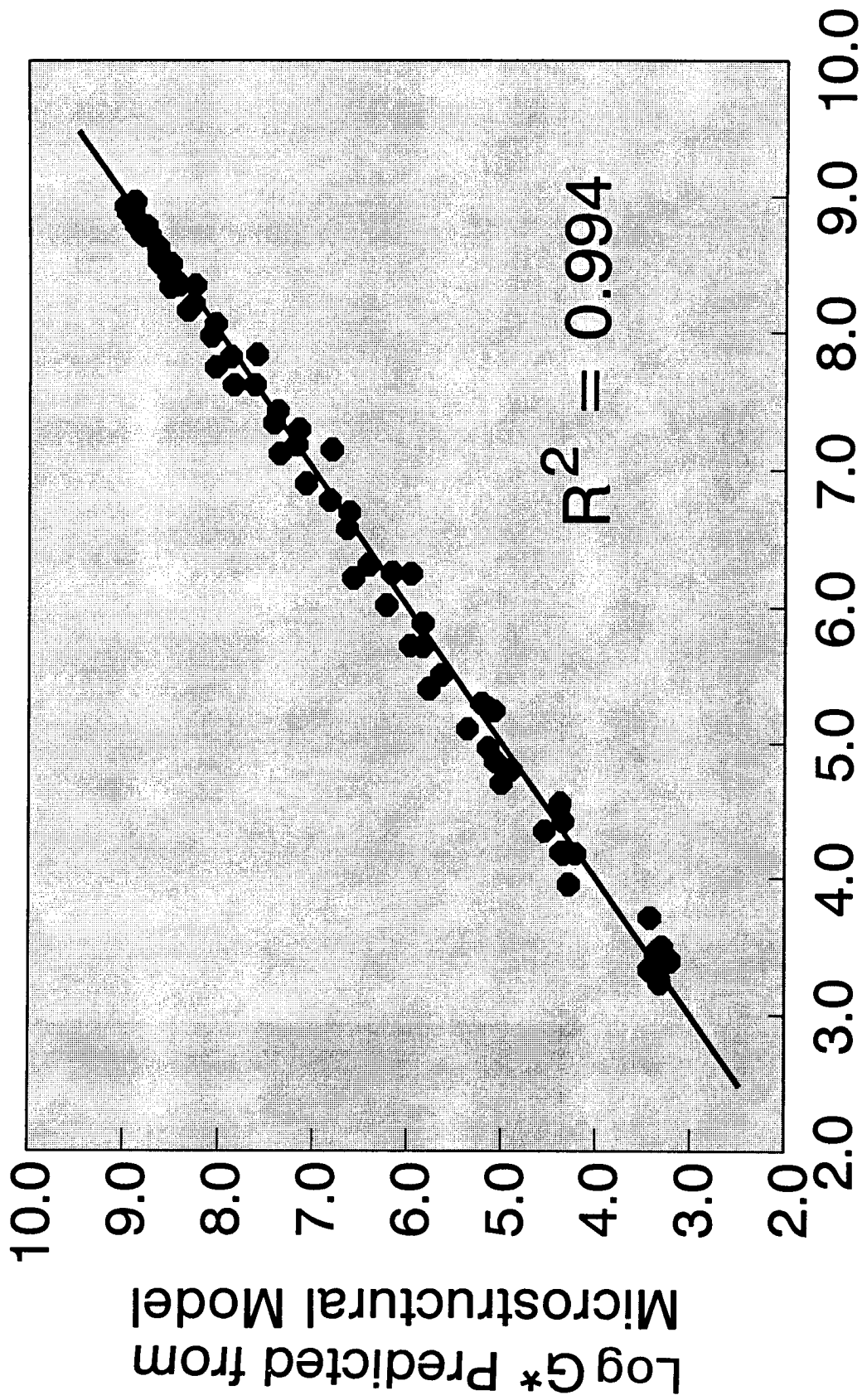


Figure 3.13 Values of Complex Modulus Predicted from Microstructural Model Parameters versus Measured Values, 10 rad/s for Materials Reference Library Tank Asphalts

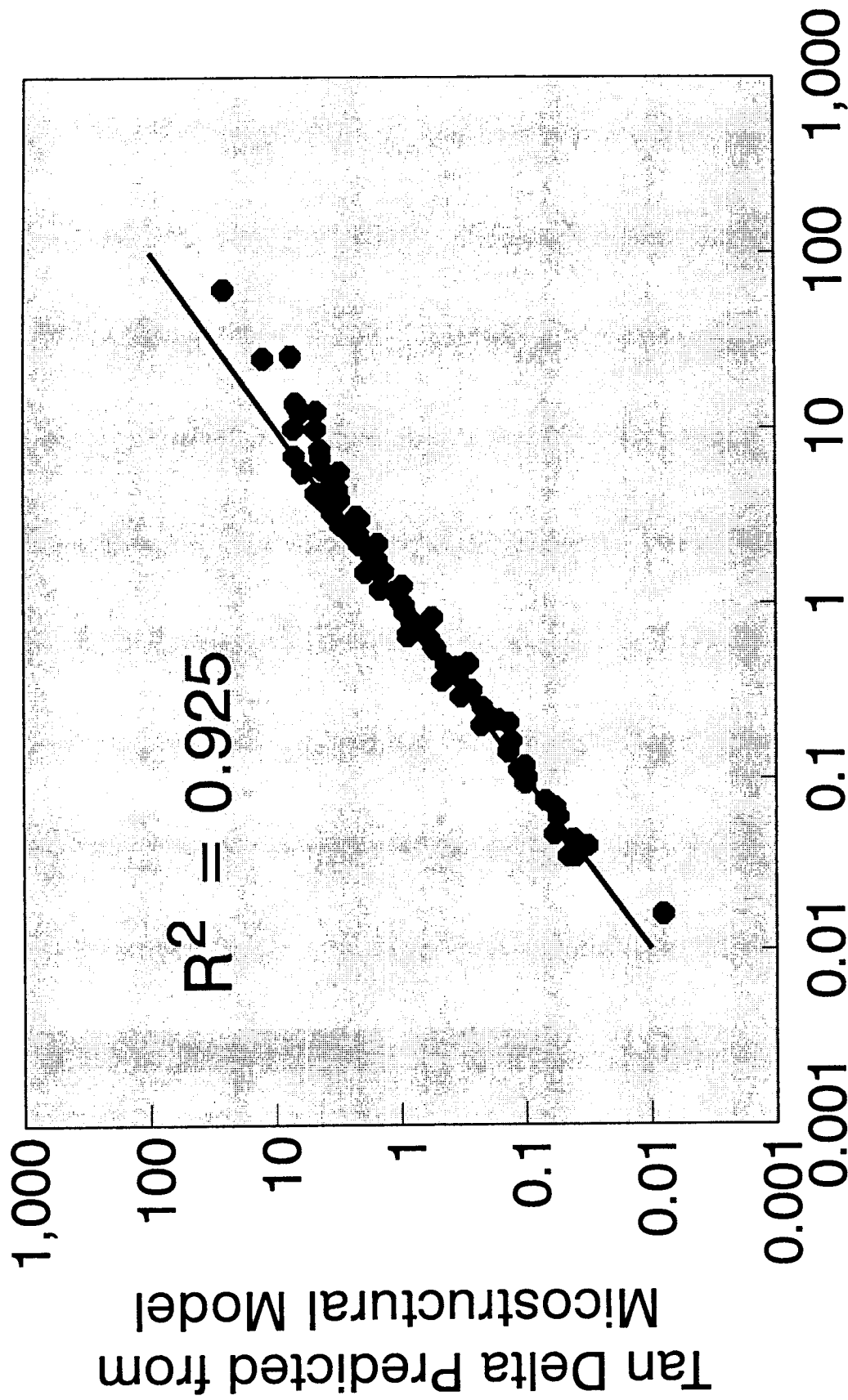
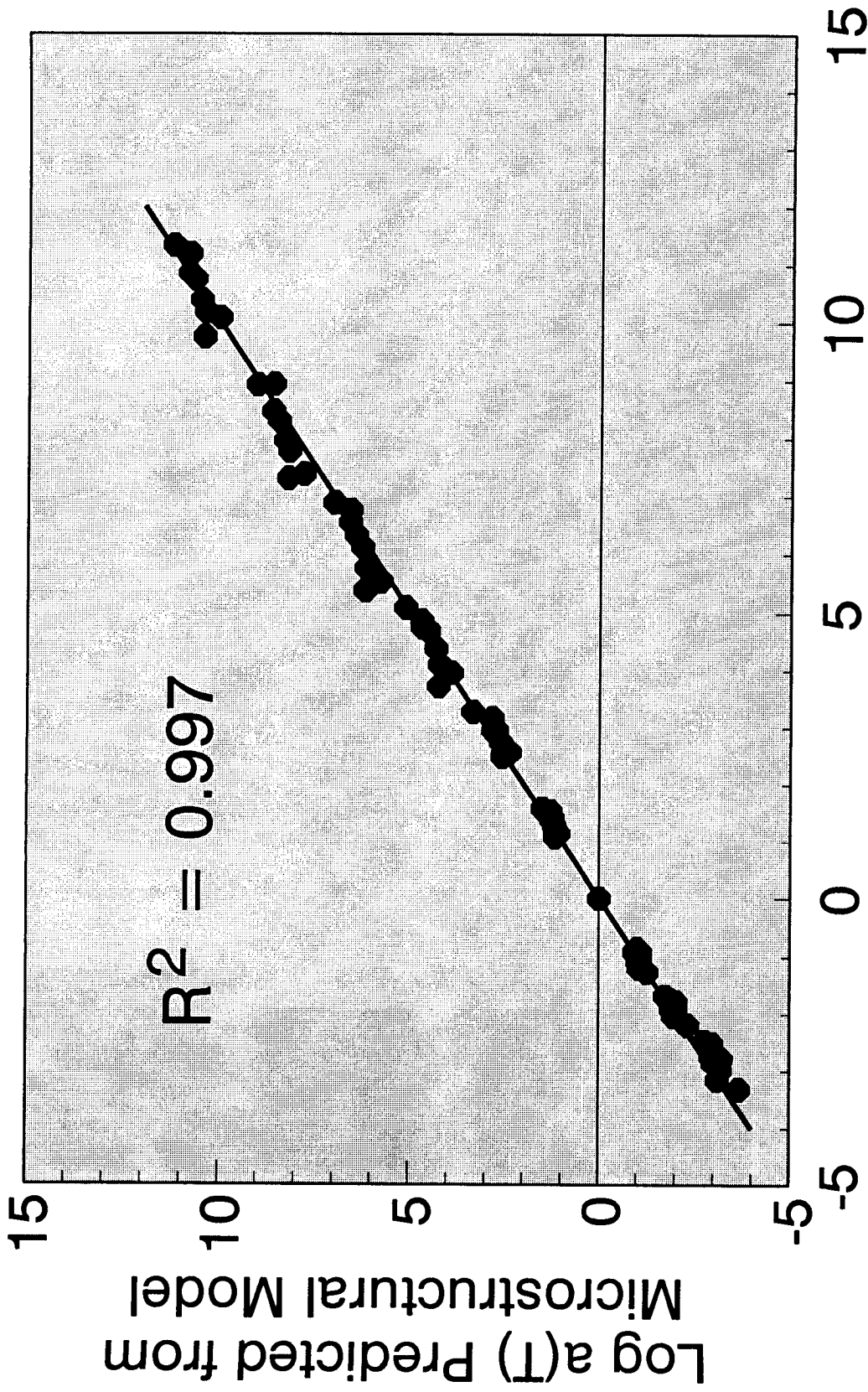


Figure 3.14 Values of Loss Tangent Predicted from Microstructural Model Parameters versus Measured Values, 10 rad/s for Materials Reference Library Tank Asphalts





## Log a(T) from Master Curve

Figure 3.15 Values of Shift Factors Predicted from Microstructural Model Parameters versus Measured Values, 10 rad/s for Materials Reference Library Tank Asphalts

$$\text{Log (Vis of AC)} = 10.9 + 5.64 (H) + 0.0663 (C) - 6.52 (A)$$

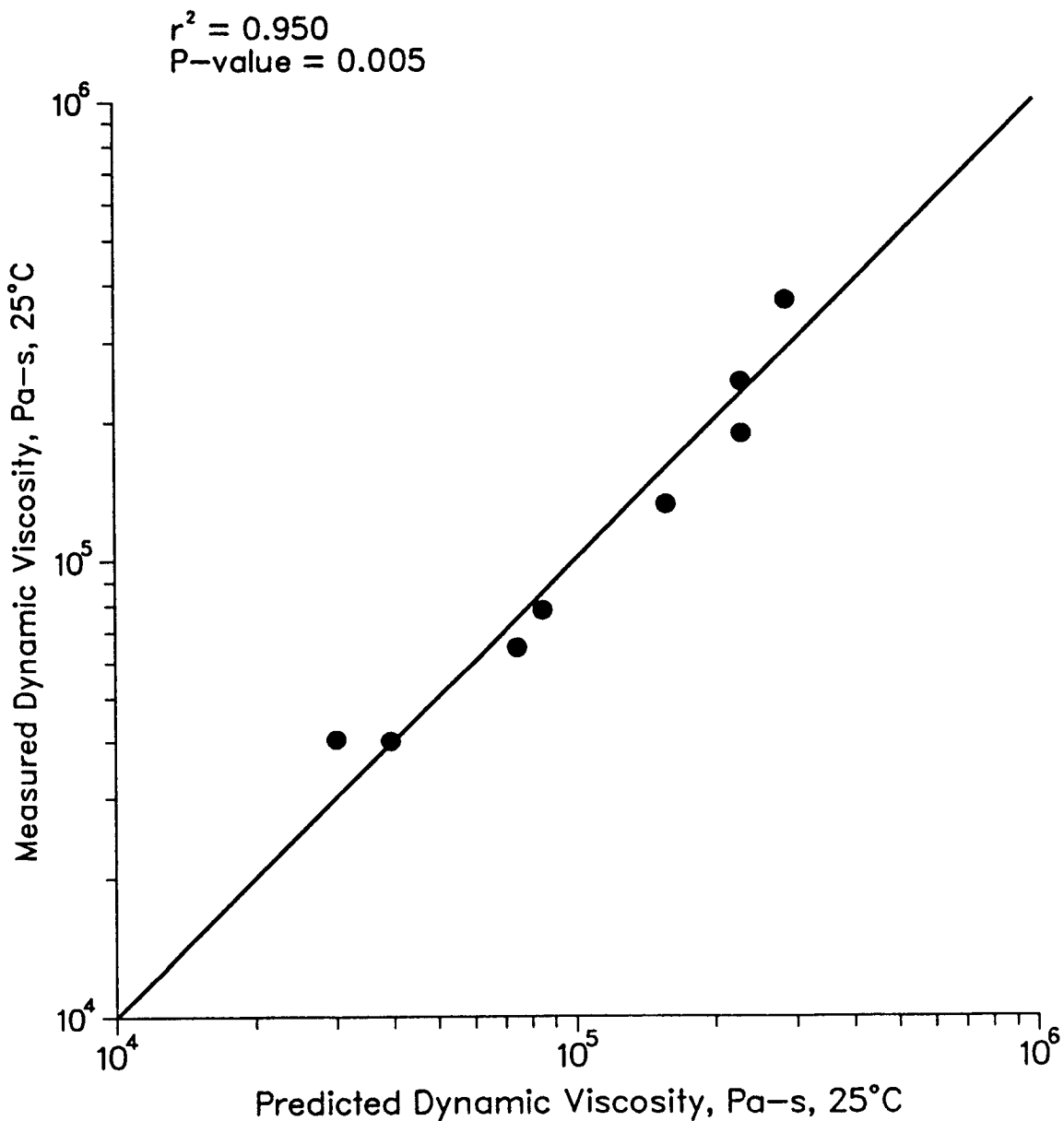


**Figure 3.16 Viscosities of Asphalt Cements Measured and Predicted by Chemical Properties**

$$E_a = 74.4 + 0.937 (C) + 65.6 (H) - 55.5 (A) - 0.204 (W)$$

$r^2 = 0.996$   
P-value = 0.001

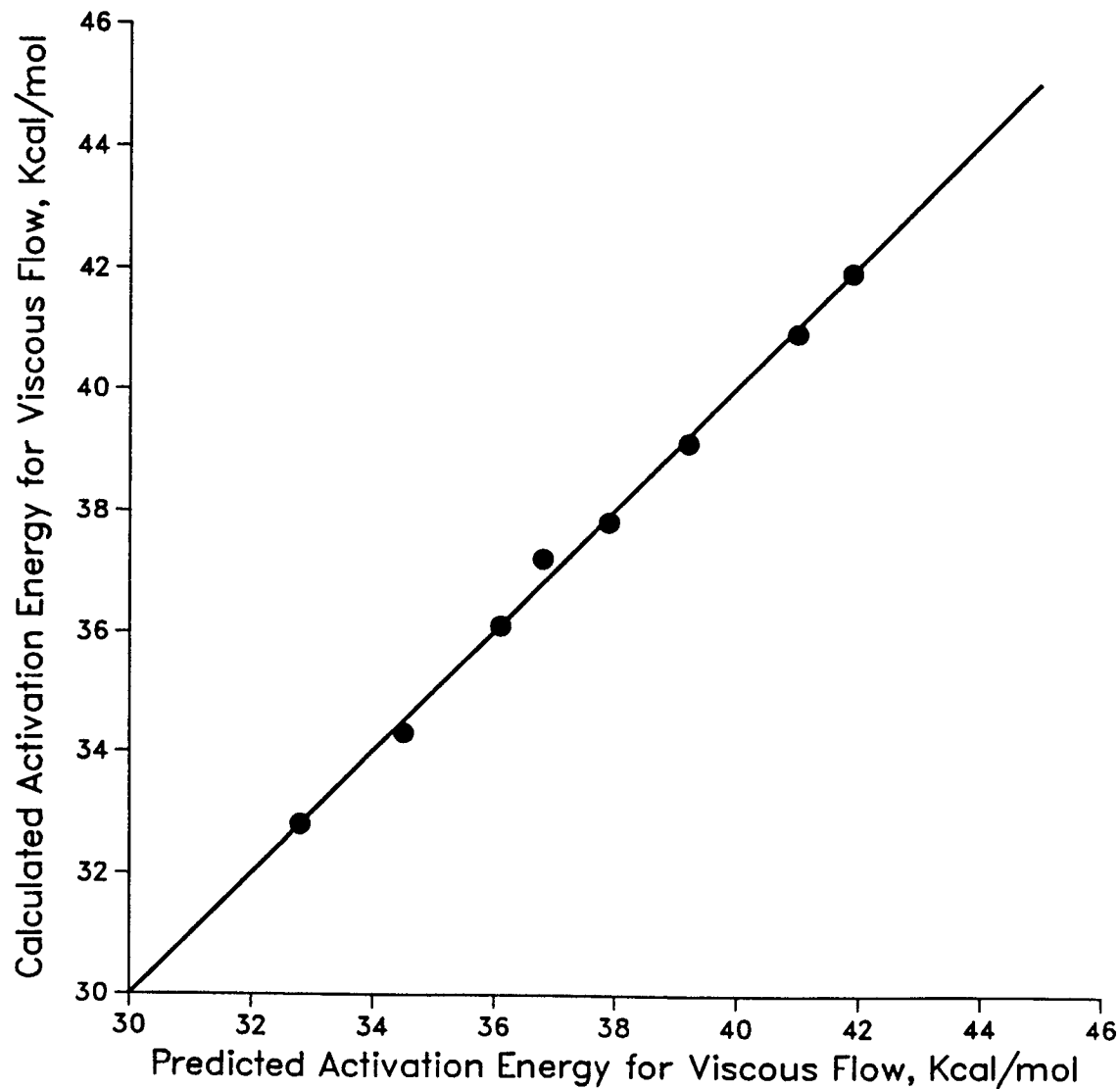


**Figure 3.17** Activation Energy for Viscous Flow Calculated and Predicted by Chemical Properties

$$\text{Log (Vis of IEC N)} = 5.23 + 0.0606 (C) - 3.69 (A)$$

$r^2 = 0.971$   
P-value = 0.000

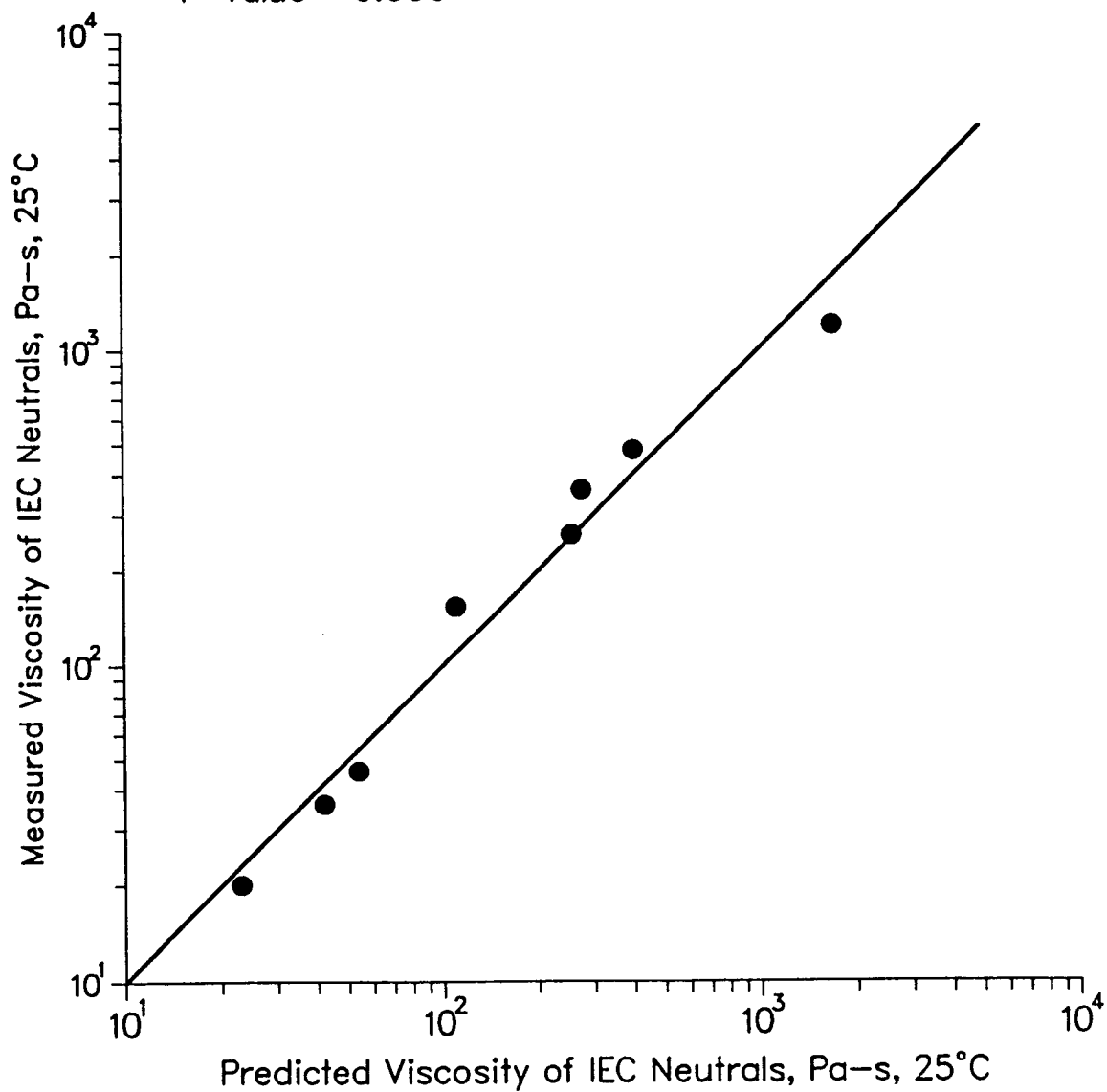


**Figure 3.18** Viscosities of Ion Exchange Chromatography Neutrals Measured and Predicted by Chemical Properties

$$AI(TFOT) = -5.13 + 0.0323 (C) + 2.43 (A)_{\text{tank}} + 9.91 (H)$$

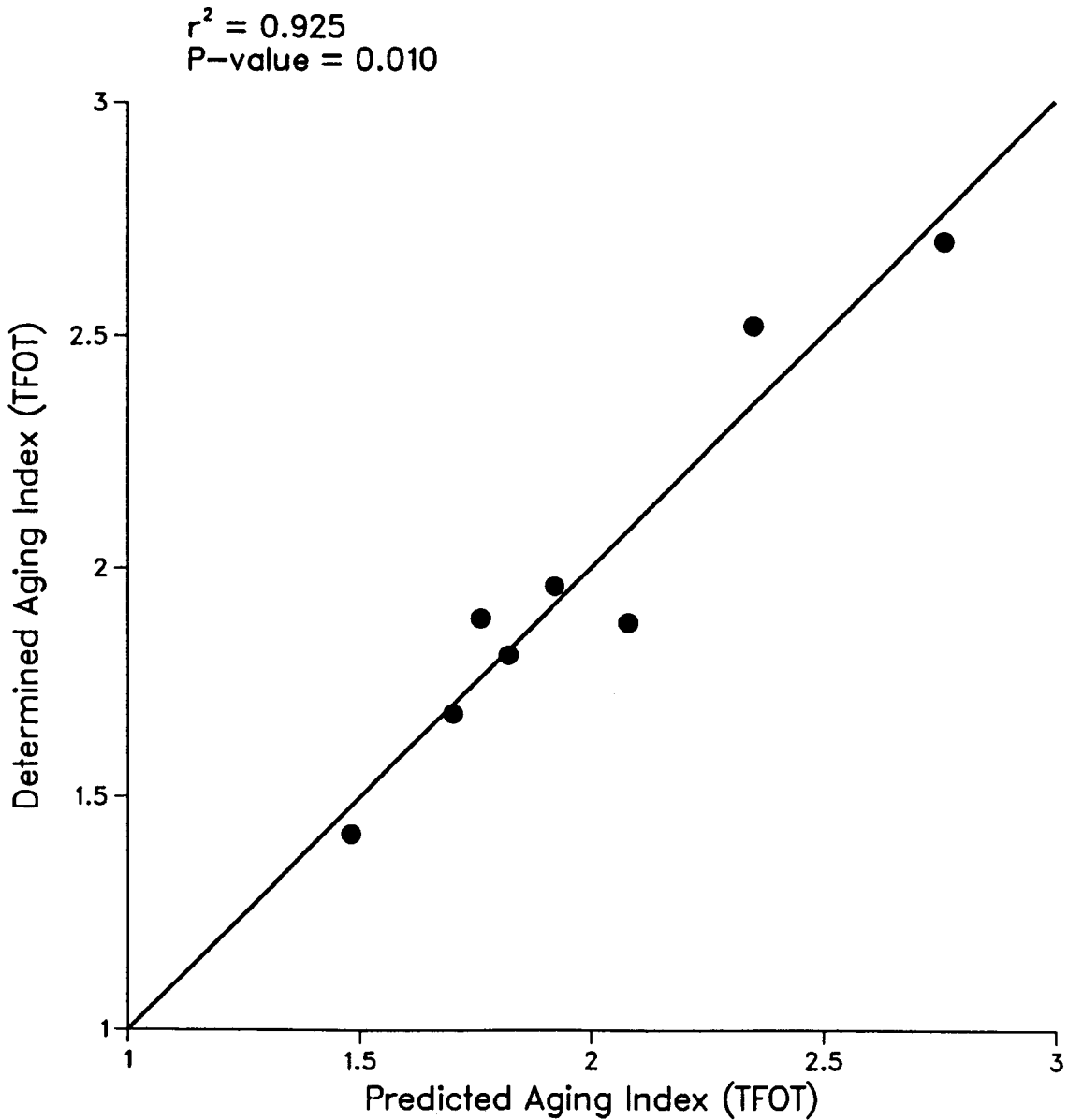


**Figure 3.19 Aging Index (Thin-Film Oven Test) of Asphalt Cements Determined and Predicted by Chemical Properties**

$$AI(\text{TFOT-PAV}) = 82.4 + 1.14 (C) - 65.9 (A) + 138 (H) - 10.6 \text{ Log (V of AC)}$$

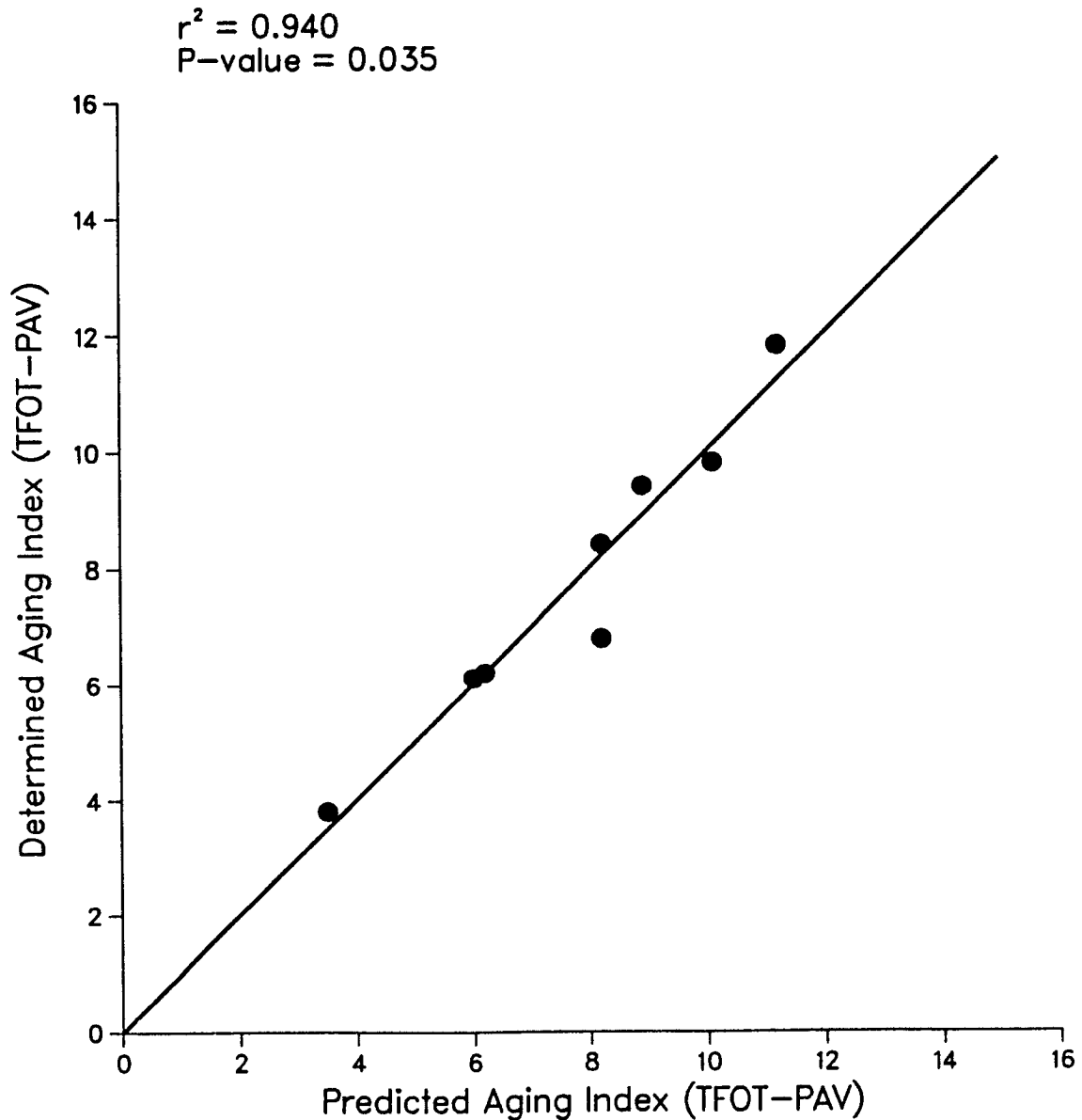


**Figure 3.20 Aging Index (Thin-Film Oven Test-Pressure-Aging Vessel Test) of Asphalt Cements Determined and Predicted by Chemical Properties**

**Table 3.1 Definitions of Physical and Chemical Parameters**

|                             |   |
|-----------------------------|---|
| $T_d$ , °C                  | Defining temperature  |
| $\log G_g$ , Pa             | Log of glassy modulus   |
| $\log \omega_{cTd}$ , rad/s | Log of crossover frequency at defining temperature                        |
| $R$ , Pa                    | Rheological index   |
| $\log H(\tau)_{mode}$ , s   | Log of relaxation time at peak in relaxation spectrum                     |
| $\log \tau_{term}$ , s      | Log of estimated terminal relaxation time                                 |
| $\log \eta_{Td}$ , Pa·s     | Log of estimated viscosity at defining temperature                        |
| $AI_{vis60}$                | Aging index based on capillary viscosity at 60°C, TFO/tank                |
| $M_n$ , daltons             | Number-average molecular weight, vapor-phase osmometry in toluene at 60°C |
| A, %                        | Corbett asphaltenes   |
| PA, %                       | Corbett polar aromatics   |
| NA, %                       | Corbett naphthene aromatics   |
| SAT, %                      | Corbett saturates   |
| SECI, %                     | SEC fraction I (associated material)                                      |
| $\log \eta_{SECI25}$ , Pa·s | Log of viscosity of SEC fraction II (nonassociated material) at 25°C      |
| C, %                        | Weight percent total carbon   |
| H, %                        | Weight percent total hydrogen   |
| N, %                        | Weight percent total nitrogen   |
| S, %                        | Weight percent total sulfur   |
| O, %                        | Weight percent total oxygen   |
| Ni, ppm                     | Nickel content  |
| V, ppm                      | Vanadium content  |
| SPSECI, %                   | Streamlined preparative SEC fraction I (associated material)              |

**Table 3.2 Linear Viscoelastic Model Parameters**

| Asphalt | $T_d$<br>(°C) | $G_g$<br>(Pa) | $\log \omega_c \tau_d$<br>(rad/s) | $R$<br>(Pa) | $H(\tau)_{mode}$<br>(s) | $\tau_{term}$<br>(s) | $\log \eta_{Td}$<br>(Pa·s) | $AI_{vis60}$ |
|---------|---------------|---------------|-----------------------------------|-------------|-------------------------|----------------------|----------------------------|--------------|
| AAA-1   | -19.3         | 8.99          | 2.03                              | 1.50        | -1.49                   | 9.49                 | 10.98                      | 2.20         |
| AAB-1   | -11.6         | 8.95          | 1.97                              | 1.76        | -2.52                   | 5.14                 | 10.57                      | 2.31         |
| AAC-1   | -5.5          | 8.97          | 1.16                              | 1.63        | -2.83                   | 3.95                 | 9.82                       | 2.42         |
| AAD-1   | -17.1         | 9.04          | 2.01                              | 1.66        | -2.10                   |                      | 11.05                      | 3.24         |
| AAE-1   | -10.4         | 9.09          | 1.98                              | 2.11        | -3.93                   | 5.76                 | 10.60                      | 3.19         |
| AAF-1   | -7.0          | 8.96          | 2.07                              | 1.60        | -1.80                   | 3.28                 | 10.50                      | 2.45         |
| AAG-1   | -3.9          | 8.94          | 1.43                              | 1.24        | -1.17                   | 1.44                 | 9.95                       | 1.75         |
| AAH-1   | -18.4         | 8.66          | 3.23                              | 1.74        | -1.21                   | 5.45                 | 11.43                      | 2.66         |
| AAJ-1   | -4.7          | 8.98          | 1.67                              | 1.90        | -3.38                   | 3.55                 | 10.00                      | 2.28         |
| AAK-1   | -14.7         | 8.98          | 2.33                              | 1.60        | -1.56                   |                      | 11.31                      | 2.98         |
| AAL-1   | -15.7         | 9.20          | 1.28                              | 1.61        | -2.63                   | 6.33                 | 10.37                      | 2.73         |
| AAM-1   | 1.0           | 8.88          | 1.26                              | 1.93        | -3.93                   | 3.85                 | 9.60                       | 1.98         |
| AAN-1   | -5.4          | 8.99          | 1.32                              | 1.68        | -2.88                   | 5.33                 | 10.09                      | 2.12         |
| AAO-1   | -10.1         | 8.83          | 1.78                              | 1.66        | -2.32                   | 5.00                 | 10.33                      | 2.03         |
| AAP-1   | -5.1          | 9.00          | 1.77                              | 2.14        | -4.29                   | 4.70                 | 10.14                      | 2.55         |
| AAQ-1   | -5.6          | 8.94          | 1.46                              | 1.66        | -2.65                   | 3.33                 | 9.94                       | 1.88         |
| AAR-1   | -5.3          | 8.95          | 1.54                              | 1.89        | -3.49                   | 4.82                 | 10.08                      | 2.23         |
| AAS-1   | -9.5          | 8.95          | 1.93                              | 1.79        | -2.67                   | 4.89                 | 10.49                      | 2.21         |
| AAT-1   | -5.8          | 8.94          | 1.96                              | 1.72        | -2.40                   | 4.49                 | 10.50                      | 2.53         |
| AAU-1   | -3.9          | 9.06          | 1.34                              | 1.72        | -3.00                   | 3.52                 | 9.94                       | 2.67         |
| AAV-1   | -5.4          | 8.97          | 0.93                              | 1.53        | -2.69                   | 3.39                 | 9.60                       | 1.85         |
| AAW-1   | 0.0           | 9.04          | 1.50                              | 1.97        | -3.86                   | 4.03                 | 9.97                       | 2.47         |
| AAX-1   | -0.9          | 9.04          | 1.24                              | 1.66        | -2.88                   | 3.38                 | 9.85                       | 2.12         |
| AAZ-1   | -8.5          | 8.98          | 2.07                              | 2.04        | -3.57                   | 5.94                 | 10.62                      | 2.95         |
| AAZ-1   | -1.0          | 8.92          | 1.09                              | 1.44        | -2.20                   | 1.78                 | 9.52                       | 1.65         |
| ABA-1   | -3.5          | 9.00          | 2.16                              | 2.49        | -5.39                   | 4.68                 | 10.19                      |              |
| ABC-1   | -11.5         | 8.93          | 2.16                              | 1.94        | -3.05                   | 5.91                 | 10.71                      |              |
| ABD-1   | 2.8           | 8.92          | 0.63                              | 1.15        | -1.66                   | 1.11                 | 9.27                       |              |



**Table 3.3 Corbett and Size Exclusion Chromatography Parameters**

| Asphalt | $M_n$<br>(daltons) | A<br>(%) | PA<br>(%) | NA<br>(%) | SAT<br>(%) | SECI<br>(%) | log<br>$\eta_{SECI125}$ | SPSECI<br>(%) |
|---------|--------------------|----------|-----------|-----------|------------|-------------|-------------------------|---------------|
| AAA-1   | 790                | 18       | 37        | 32        | 11         | 22          | 3.7                     | 22            |
| AAB-1   | 840                | 18       | 38        | 33        | 9          | 22          | 4.1                     | 20            |
| AAC-1   | 870                | 11       | 37        | 37        | 13         | 14          | 4.9                     | 13            |
| AAD-1   | 700                | 23       | 41        | 25        | 9          | 23          | 3.5                     | 23            |
| AAE-1   | 820                | 23       | 31        | 32        | 13         | 26          | 3.5                     | 25            |
| AAF-1   | 840                | 14       | 38        | 38        | 10         | 14          | 5.7                     | 14            |
| AAG-1   | 710                | 6        | 51        | 33        | 9          | 13          | 5.8                     | 11            |
| AAH-1   | 840                | 16       | 41        | 29        | 13         | 25          | 4.6                     | 22            |
| AAJ-1   | 1030               | 11       | 42        | 36        | 11         | 21          | 4.7                     | 23            |
| AAK-1   | 860                | 21       | 42        | 30        | 5          | 26          | 4.1                     | 25            |
| AAL-1   | 760                | 19       | 37        | 30        | 12         |             |                         | 20            |
| AAM-1   | 1300               | 4        | 50        | 42        | 2          | 31          | 5.4                     | 32            |
| AAN-1   | 890                | 16       | 34        | 40        | 10         | 21          | 4.4                     | 20            |
| AAO-1   | 930                | 16       | 33        | 42        | 9          |             |                         | 19            |
| AAP-1   | 1090               | 13       | 37        | 36        | 13         |             |                         | 21            |
| AAQ-1   | 810                | 16       | 26        | 45        | 13         |             |                         | 15            |
| AAR-1   | 880                | 18       | 31        | 41        | 10         |             |                         | 22            |
| AAS-1   | 960                | 18       | 34        | 40        | 6          | 24          | 4.1                     | 21            |
| AAT-1   | 880                | 17       | 43        | 32        | 8          |             |                         | 20            |
| AAU-1   | 880                | 18       | 41        | 34        | 8          |             |                         | 20            |
| AAV-1   | 890                | 9        | 40        | 39        | 11         | 16          | 4.6                     | 15            |
| AAW-1   | 890                | 18       | 36        | 37        | 9          | 20          | 4.6                     | 22            |
| AAX-1   | 970                | 12       | 41        | 40        | 8          | 18          | 5.1                     | 16            |
| AAZ-1   | 860                | 22       | 31        | 35        | 9          |             |                         | 24            |
| AAZ-1   | 970                | 9        | 42        | 43        | 7          | 15          | 5.4                     | 16            |
| ABA-1   |                    | 16       | 34        | 38        | 11         |             |                         | 22            |
| ABC-1   | 870                |          |           |           |            |             |                         | 27            |
| ABD-1   | 728                | 7        |           |           |            | 11          | 5.8                     | 13            |

**Table 3.4 Elemental Analysis**

| Asphalt | C (%) | H (%) | N (%) | S (%) | O (%) | Ni (ppm) | V (ppm) |
|---------|-------|-------|-------|-------|-------|----------|---------|
| AAA-1   | 84.1  | 10.0  | 0.6   | 5.5   | 0.6   | 86.0     | 174     |
| AAB-1   | 83.4  | 10.0  | 0.6   | 4.7   | 0.8   | 57.0     | 222     |
| AAC-1   | 85.5  | 10.6  | 0.7   | 1.9   | 0.9   | 63.3     | 148     |
| AAD-1   | 81.1  | 10.1  | 0.8   | 6.9   | 0.9   | 141.3    | 308     |
| AAE-1   | 83.8  | 10.1  | 0.7   | 5.2   | 1.0   | 90.8     | 179     |
| AAF-1   | 83.7  | 9.7   | 0.6   | 3.4   | 1.1   | 36.3     | 91      |
| AAG-1   | 85.7  | 9.9   | 1.1   | 1.3   | 1.1   | 95.3     | 37      |
| AAH-1   | 86.3  | 10.1  | 0.8   | 2.8   | 1.0   | 43.1     | 84      |
| AAJ-1   | 86.5  | 10.7  | 0.6   | 1.9   | 0.7   | 74.0     | 148     |
| AAK-1   | 81.0  | 9.6   | 0.7   | 6.4   | 0.8   | 141.0    | 1498    |
| AAL-1   | 83.4  | 10.1  | 0.6   | 5.5   | 1.0   | 97.8     | 244     |
| AAM-1   | 86.6  | 10.8  | 0.6   | 1.2   | 0.5   | 37.3     | 58      |
| AAN-1   | 84.5  | 10.2  | 0.7   | 4.3   | 0.8   | 65.4     | 157     |
| AAO-1   | 83.8  | 10.1  | 0.4   | 5.0   | 0.5   | 45.7     | 163     |
| AAP-1   | 85.9  | 10.9  | 0.6   | 1.7   | 0.8   | 68.1     | 128     |
| AAQ-1   | 85.5  | 10.1  | 0.6   | 3.6   | 0.5   | 51.4     | 127     |
| AAR-1   | 84.1  | 10.1  | 0.7   | 4.6   | 0.6   | 79.0     | 334     |
| AAS-1   | 84.0  | 10.0  | 0.6   | 5.4   | 0.8   | 52.4     | 159     |
| AAT-1   | 83.9  | 10.1  | 0.6   | 5.1   | 0.7   | 80.1     | 201     |
| AAU-1   | 84.4  | 10.2  | 0.8   | 4.0   | 0.7   | 97.6     | 197     |
| AAV-1   | 86.4  | 10.5  | 0.8   | 2.4   | 1.1   | 40.8     | 92      |
| AAW-1   | 84.5  | 10.1  | 0.7   | 4.5   | 0.9   | 80.3     | 334     |
| AAX-1   | 86.6  | 10.4  | 0.8   | 2.4   | 1.1   | 55.9     | 116     |
| AAZ-1   | 83.7  | 10.1  | 0.6   | 5.4   | 0.5   | 88.4     | 439     |
| AAZ-1   | 85.0  | 10.0  | 0.6   | 4.4   | 0.9   | 35.0     | 102     |
| ABA-1   | 86.4  | 10.8  | 0.4   | 2.3   | 1.5   |          |         |
| ABC-1   | 83.2  | 9.9   | 0.3   | 6.4   | 0.4   | 25.1     | 37      |
| ABD-1   | 86.8  | 10.7  | 1.2   | 1.6   | 1.2   | 123.0    | 62      |

**Table 3.5 Computed Indexes**

| Asphalt | Gaestel Index | Carbon/Hydrogen Ratio | Heteroatom Index |
|---------|---------------|-----------------------|------------------|
| AAA-1   | 0.414         | 8.41                  | 0.252            |
| AAB-1   | 0.371         | 8.34                  | 0.240            |
| AAC-1   | 0.321         | 8.07                  | 0.166            |
| AAD-1   | 0.476         | 8.03                  | 0.329            |
| AAE-1   | 0.575         | 8.30                  | 0.275            |
| AAF-1   | 0.311         | 8.63                  | 0.218            |
| AAG-1   | 0.173         | 8.66                  | 0.188            |
| AAH-1   | 0.417         | 8.55                  | 0.207            |
| AAJ-1   | 0.283         | 8.08                  | 0.146            |
| AAK-1   | 0.364         | 8.44                  | 0.300            |
| AAL-1   | 0.460         | 8.26                  | 0.277            |
| AAM-1   | 0.064         | 8.02                  | 0.112            |
| AAN-1   | 0.355         | 8.28                  | 0.234            |
| AAO-1   | 0.329         | 8.30                  | 0.216            |
| AAP-1   | 0.357         | 7.88                  | 0.146            |
| AAQ-1   | 0.403         | 8.47                  | 0.187            |
| AAR-1   | 0.391         | 8.33                  | 0.231            |
| AAS-1   | 0.324         | 8.40                  | 0.262            |
| AAT-1   | 0.330         | 8.31                  | 0.246            |
| AAU-1   | 0.350         | 8.28                  | 0.226            |
| AAV-1   | 0.254         | 8.23                  | 0.201            |
| AAW-1   | 0.375         | 8.37                  | 0.247            |
| AAX-1   | 0.246         | 8.38                  | 0.201            |
| AAZ-1   | 0.470         | 8.29                  | 0.243            |
| AAZ-1   | 0.186         | 8.50                  | 0.237            |
| ABA-1   | 0.380         | 8.00                  | 0.194            |
| ABC-1   |               | 8.40                  | 0.246            |
| ABD-1   |               | 8.11                  | 0.211            |

Table 3.6 Pearson Correlation Coefficients for Physical-Chemical Data

|                                | $T_d$<br>(°C) | $\log \omega_{cTd}$<br>(rad/s) | $R$<br>(Pa) | $H(\tau)_{mode}$<br>(s) | $\tau_{term}$<br>(s) | $\log \eta_{Td}$<br>(Pa·s) | $AI_{vis60}$ | $M_n$<br>(daltons) | $A$<br>(%) | $PA$<br>(%) | $NA$<br>(%) | $SAT$<br>(%) |
|--------------------------------|---------------|--------------------------------|-------------|-------------------------|----------------------|----------------------------|--------------|--------------------|------------|-------------|-------------|--------------|
| $T_d$<br>(°C)                  | 1.00          |                                |             |                         |                      |                            |              |                    |            |             |             |              |
| $\log \omega_{cTd}$<br>(rad/s) | -0.69         | 1.00                           |             |                         |                      |                            |              |                    |            |             |             |              |
| $R$<br>(Pa)                    | 0.00          | 0.41                           | 1.00        |                         |                      |                            |              |                    |            |             |             |              |
| $H(\tau)_{mode}$<br>(s)        | -0.39         | 0.09                           | -0.87       | 1.00                    |                      |                            |              |                    |            |             |             |              |
| $\tau_{term}$<br>(s)           | -0.79         | 0.55                           | 0.38        | -0.12                   | 1.00                 |                            |              |                    |            |             |             |              |
| $\log \eta_{Td}$<br>(Pa·s)     | -0.89         | 0.90                           | 0.19        | 0.28                    | 0.75                 | 1.00                       |              |                    |            |             |             |              |
| $AI_{vis60}$                   | -0.52         | 0.54                           | 0.46        | -0.13                   | 0.48                 | 0.67                       | 1.00         |                    |            |             |             |              |
| $M_n$<br>(daltons)             | 0.42          | -0.12                          | 0.49        | -0.58                   | -0.63                | -0.32                      | -0.31        | 1.00               |            |             |             |              |
| $A$<br>(%)                     | -0.65         | 0.56                           | 0.38        | -0.09                   | 0.68                 | 0.72                       | 0.76         | -0.40              | 1.00       |             |             |              |
| $PA$<br>(%)                    | 0.14          | -0.09                          | -0.40       | 0.35                    | -0.40                | -0.10                      | -0.17        | 0.23               | -0.59      | 1.00        |             |              |
| $NA$<br>(%)                    | 0.69          | -0.54                          | 0.07        | -0.33                   | -0.42                | -0.72                      | -0.73        | 0.54               | -0.48      | -0.30       | 1.00        |              |

(cont'd)

**Table 3.6 Pearson Correlation Coefficients for Physical-Chemical Data (cont'd)**

|                                | $T_d$<br>(°C) | $\log \omega_{cTd}$<br>(rad/s) | $R$<br>(PA) | $H(\tau)_{mode}$<br>(s) | $\tau_{term}$<br>(s) | $\log \eta_{Td}$<br>(Pa·s) | $Al_{vis60}$ | $M_n$<br>(daltons) | $A$<br>(%) | $PA$<br>(%) | $NA$<br>(%) | $SAT$<br>(%) |
|--------------------------------|---------------|--------------------------------|-------------|-------------------------|----------------------|----------------------------|--------------|--------------------|------------|-------------|-------------|--------------|
| SAT (%)                        | -0.26         | 0.14                           | 0.19        | -0.12                   | 0.28                 | 0.10                       | 0.19         | -0.42              | 0.21       | -0.51       | -0.16       | 1.00         |
| SECI (%)                       | -0.44         | 0.55                           | 0.73        | -0.36                   | 0.59                 | 0.54                       | 0.48         | 0.44               | 0.47       | -0.06       | -0.27       | -0.34        |
| $\log \eta_{secl25}$<br>(Pa·s) | 0.73          | -0.49                          | -0.50       | 0.17                    | -0.83                | -0.66                      | -0.66        | 0.21               | -0.86      | 0.61        | 0.56        | -0.24        |
| C (%)                          | 0.62          | -0.38                          | 0.01        | -0.24                   | -0.52                | -0.66                      | -0.61        | 0.40               | -0.76      | 0.17        | 0.48        | 0.22         |
| H (%)                          | 0.51          | -0.39                          | 0.31        | -0.57                   | -0.22                | -0.57                      | -0.17        | 0.53               | -0.50      | 0.08        | 0.27        | 0.20         |
| N (%)                          | 0.26          | -0.38                          | -0.62       | 0.45                    | -0.54                | -0.29                      | -0.00        | -0.40              | -0.34      | 0.48        | -0.36       | -0.01        |
| S (%)                          | -0.63         | 0.39                           | 0.06        | 0.16                    | 0.61                 | 0.64                       | 0.52         | -0.37              | 0.85       | -0.37       | -0.36       | -0.15        |
| O (%)                          | 0.19          | -0.11                          | -0.08       | -0.01                   | -0.37                | -0.17                      | 0.07         | -0.36              | -0.20      | 0.18        | 0.23        | 0.27         |
| Ni (ppm)                       | -0.20         | -0.02                          | -0.20       | 0.19                    | -0.00                | 0.23                       | 0.67         | -0.50              | 0.41       | 0.07        | -0.71       | -0.04        |
| V (ppm)                        | -0.30         | 0.29                           | 0.05        | 0.12                    | 0.39                 | 0.45                       | 0.46         | -0.11              | 0.47       | -0.04       | -0.31       | -0.29        |
| SPSECI (%)                     | -0.29         | 0.44                           | 0.62        | -0.43                   | 0.55                 | 0.42                       | 0.47         | 0.46               | 0.38       | 0.02        | -0.21       | -0.33        |

(cont'd)

Table 3.6 Pearson Correlation Coefficients for Physical-Chemical Data (cont'd)

|                                    | SECI (%) | $\log \eta_{\text{secI}25}$ (Pa s) | C (%) | H (%) | N (%) | S (%) | O (%) | Ni (ppm) | V (ppm) | SPSECI (%) |
|------------------------------------|----------|------------------------------------|-------|-------|-------|-------|-------|----------|---------|------------|
| SAT (%)                            |          |                                    |       |       |       |       |       |          |         |            |
| SECI (%)                           | 1.00     |                                    |       |       |       |       |       |          |         |            |
| $\log \eta_{\text{secI}25}$ (Pa s) | -0.61    | 1.00                               |       |       |       |       |       |          |         |            |
| C (%)                              | -0.33    | 0.62                               | 1.00  |       |       |       |       |          |         |            |
| H (%)                              | -0.06    | 0.27                               | 0.73  | 1.00  |       |       |       |          |         |            |
| N (%)                              | -0.51    | 0.40                               | 0.26  | 0.08  | 1.00  |       |       |          |         |            |
| S (%)                              | 0.41     | -0.78                              | -0.90 | -0.71 | -0.38 | 1.00  |       |          |         |            |
| O (%)                              | -0.67    | 0.38                               | 0.31  | 0.22  | 0.43  | -0.39 | 1.00  |          |         |            |
| Ni (ppm)                           | 0.05     | -0.33                              | -0.43 | -0.10 | 0.51  | 0.27  | 0.22  | 1.00     |         |            |
| V (ppm)                            | 0.33     | -0.35                              | -0.61 | -0.41 | -0.03 | 0.45  | -0.10 | 0.56     | 1.00    |            |
| SPSECI (%)                         | 0.96     | -0.52                              | -0.30 | 0.05  | -0.48 | 0.37  | -0.45 | 0.04     | 0.29    | 1.00       |

Table 3.7  $T_d$  Correlated with Compositional Parameters

| $R^2$ | $N$ | $y$ Intercept | $M_n$<br>(daltons) | Heptane<br>Asphal-<br>tenes<br>(%) | $T_d$ as Dependent Variable: Regression Coefficients for Independent Variables |               |                        |                  |                              |                     |
|-------|-----|---------------|--------------------|------------------------------------|--|---------------|------------------------|------------------|------------------------------|---------------------|
|       |     |               |                    |                                    | SPSECI Fraction  | Volume<br>(%) | $\log \eta$<br>at 25°C | Gaestel<br>Index | Carbon/<br>Hydrogen<br>Ratio | Heteroatom<br>Index |
| 0.46  | 27  | -5.252        | 0.009              | 0.665                              |  |               |                        |                  |                              |                     |
| 0.47  | 25  | -10.64        | 0.0132             | -0.222                             |  |               |                        | -15.75           |                              |                     |
| 0.46  | 26  | 11.5          | 0.0078             | -0.670                             |  |               |                        |                  | -1.88                        |                     |
| 0.46  | 26  | -5.2          | 0.009              | -0.665                             |  |               |                        |                  |                              | -0.1                |
| 0.48  | 27  | -22.3         | 0.0342             |                                    |  | -0.77         |                        |                  |                              |                     |
| 0.57  | 25  | -21.4         | 0.0315             |                                    |  | -5.81         |                        |                  | -8.1                         |                     |
| 0.498 | 27  | 14.0          | 0.0321             |                                    |  | -0.794        |                        |                  |                              | -4.10               |
| 0.489 | 27  | -16.3         | 0.0292             |                                    |  | -0.692        |                        |                  |                              | -14.4               |

(cont'd)

Table 3.7  $T_d$  Correlated with Compositional Parameters (cont'd)

|       |     | $T_d$ as Dependent Variable: Regression Coefficients for Independent Variables |                    |                                    |                 |                        |                  |                              |                     |       |
|-------|-----|--|--------------------|------------------------------------|-----------------|------------------------|------------------|------------------------------|---------------------|-------|
| $R^2$ | $N$ | $y$ Intercept  | $M_n$<br>(daltons) | Heptane<br>Asphal-<br>tenes<br>(%) | SPSECI Fraction |                        | Computed Indexes |                              |                     |       |
|       |     |  |                    |                                    | Volume<br>(%)   | $\log \eta$<br>at 25°C | Gaestel<br>Index | Carbon/<br>Hydrogen<br>Ratio | Heteroatom<br>Index |       |
| 0.18  | 27  | -25.437  | 0.0203             |                                    |                 |                        |                  |                              |                     |       |
| 0.61  | 18  | -47.7  | 0.0136             |                                    | 6.09            |                        |                  |                              |                     |       |
| 0.42  | 27  | 4.106  |                    | -0.747                             |                 |                        |                  |                              |                     |       |
| 0.40  | 26  | 4.18   |                    | -0.248                             |                 |                        | -23.0            |                              |                     |       |
| 0.44  | 27  | 43.5   |                    | -0.73                              |                 |                        |                  |                              | -4.78               |       |
| 0.43  | 27  | 6.76   |                    | -0.577                             |                 |                        |                  |                              |                     | -23.5 |
| 0.08  | 28  | -0.23  |                    |                                    |                 | -0.356                 |                  |                              |                     |       |
| 0.39  | 26  | 5.42   |                    |                                    |                 | -0.083                 |                  |                              |                     | -32.8 |
| 0.19  | 28  | 91.3   |                    |                                    |                 | -0.491                 |                  |                              |                     | -10.7 |
| 0.38  | 28  | 13.2   |                    |                                    |                 | -0.268                 |                  |                              |                     | -68.2 |



**Table 3.8 R Correlated with Compositional Parameters**

| R as Dependent Variable: Regression Coefficients for Independent Variables |    |             |                          |                         |                 |               |               |                       |                  |
|--|----|-------------|--------------------------|-------------------------|-----------------|---------------|---------------|-----------------------|------------------|
| R <sup>2</sup>   | N  | y Intercept | M <sub>n</sub> (daltons) | Heptane Asphaltenes (%) | SPSECI Fraction |               |               | Computed Indexes      |                  |
|  |    |             |                          |                         | Volume (%)      | log η at 25°C | Gaestel Index | Carbon/Hydrogen Ratio | Heteroatom Index |
| 0.73   | 26 | -0.15       | 0.0015                   | 0.0340                  |                 |               |               |                       |                  |
| 0.82   | 25 | -0.50       | 0.0018                   | -0.0027                 |                 |               | 2.04          |                       |                  |
| 0.74   | 26 | 1.42        | 0.0014                   | 0.0336                  |                 |               |               | -0.176                |                  |
| 0.84   | 26 | 0.64        | 0.0011                   | 0.0517                  |                 |               |               |                       | -3.01            |
| 0.52   | 27 | 0.76        | 0.0004                   |                         | 0.0294          |               |               |                       |                  |
| 0.82   | 25 | -0.48       | 0.0017                   |                         | 0.0011          |               | 1.89          |                       |                  |
| 0.53   | 27 | 1.62        | 0.0004                   |                         | 0.0288          |               |               | -0.097                |                  |
| 0.52   | 27 | 0.89        | 0.0003                   |                         | 0.0310          |               |               |                       | -0.30            |

(cont'd)

Table 3.8 *R* Correlated with Compositional Parameters (cont'd)

| $R^2$ | <i>N</i> | <i>y</i> Intercept | $M_n$<br>(daltons) | <i>R</i> as Dependent Variable: Regression Coefficients for Independent Variables |                       |                  |                              |                     |
|-------|----------|--------------------|--------------------|---|-----------------------|------------------|------------------------------|---------------------|
|       |          |                    |                    | Heptane<br>Asphal-<br>tenes<br>(%)  | SPSECI Fraction       | Computed Indexes |                              |                     |
|       |          |                    |                    | Volume<br>(%)   | log $\eta$<br>at 25°C | Gaestel<br>Index | Carbon/<br>Hydrogen<br>Ratio | Heteroatom<br>Index |
| 0.24  | 27       | 0.88               | 0.0009             |   |                       |                  |                              |                     |
| 0.62  | 18       | 1.65               | 0.0011             |   | -2.03                 |                  |                              |                     |
| 0.14  | 27       | 1.43               |                    | 0.0203  |                       |                  |                              |                     |
| 0.11  | 26       | 1.48               |                    | -0.0064   |                       | 1.08             |                              |                     |
| 0.39  | 27       | 7.20               |                    | 0.0227  |                       |                  | -0.701                       |                     |
| 0.59  | 27       | 2.10               |                    | 0.0636  |                       |                  |                              | -6.00               |
| 0.39  | 28       | 1.02               |                    | 0.0362  |                       |                  |                              |                     |
| 0.37  | 26       | 0.97               |                    | 0.0295  |                       | 0.575            |                              |                     |
| 0.45  | 28       | 4.20               |                    | 0.0315  |                       |                  | -0.372                       |                     |
| 0.43  | 28       | 1.25               |                    | 0.0377  |                       |                  |                              | -1.21               |

**Table 3.9  $\log \omega_{cTd}$  Correlated with Compositional Parameters**

|       |     | $\log \omega_{cTd}$ as Dependent Variable: Regression Coefficients for Independent Variables |                    |                                    |                 |                        |                  |                              |                     |
|-------|-----|--|--------------------|------------------------------------|-----------------|------------------------|------------------|------------------------------|---------------------|
| $R^2$ | $N$ | $y$ Intercept  | $M_n$<br>(daltons) | Heptane<br>Asphal-<br>tenes<br>(%) | SPSECI Fraction |                        |                  | Computed Indexes             |                     |
|       |     |  |                    |                                    | Volume<br>(%)   | $\log \eta$<br>at 25°C | Gaestel<br>Index | Carbon/<br>Hydrogen<br>Ratio | Heteroatom<br>Index |
| 0.34  | 26  | 0.19   | 0.0006             | 0.0629                             |                 |                        |                  |                              |                     |
| 0.26  | 25  | 0.67   | 0.0002             | 0.0420                             |                 |                        | 0.54             |                              |                     |
| 0.45  | 26  | -9.08  | 0.0013             | 0.645                              |                 |                        |                  | 1.04                         |                     |
| 0.36  | 26  | 1.05   | 0.0001             | 0.0821                             |                 |                        |                  |                              | -3.29               |
| 0.32  | 27  | 1.83   | -0.0017            |                                    | 0.0678          |                        |                  |                              |                     |
| 0.32  | 25  | 1.51   | -0.0012            |                                    | 0.0458          |                        | 0.99             |                              |                     |
| 0.48  | 27  | -9.28  | -0.0019            |                                    | 0.0754          |                        |                  | 1.25                         |                     |
| 0.32  | 27  | 1.99   | -0.0018            |                                    | 0.0699          |                        |                  |                              | -0.38               |
| 0.23  | 26  | 0.95   |                    |                                    |                 |                        | 2.22             |                              |                     |
| 0.07  | 28  | -4.22  |                    |                                    |                 |                        |                  | 0.713                        |                     |
| 0.09  | 28  | 0.97   |                    |                                    |                 |                        |                  |                              | 3.25                |

(cont'd)

Table 3.9  $\log \omega_{cTd}$  Correlated with Compositional Parameters (cont'd)

|       |     | $\log \omega_{cTd}$ as Dependent Variable: Regression Coefficients for Independent Variables |                    |                                    |                 |                        |                  |                              |                     |       |
|-------|-----|--|--------------------|------------------------------------|-----------------|------------------------|------------------|------------------------------|---------------------|-------|
| $R^2$ | $N$ | $y$ Intercept  | $M_n$<br>(daltons) | Heptane<br>Asphal-<br>tenes<br>(%) | SPSECI Fraction |                        | Computed Indexes |                              |                     |       |
|       |     |  |                    |                                    | Volume<br>(%)   | $\log \eta$<br>at 25°C | Gaestel<br>Index | Carbon/<br>Hydrogen<br>Ratio | Heteroatom<br>Index |       |
| 0.01  | 27  | 2.11   | -0.0005            |                                    |                 |                        |                  |                              |                     |       |
| 0.25  | 18  | 3.78   | -0.0004            |                                    |                 |                        | -.38             |                              |                     |       |
| 0.32  | 27  | 0.80   |                    | 0.0579                             |                 |                        |                  |                              |                     |       |
| 0.25  | 26  | 0.91   |                    | 0.0386                             |                 |                        |                  | 0.58                         |                     |       |
| 0.36  | 27  | -3.59  |                    | 0.0560                             |                 |                        |                  |                              | 0.533               |       |
| 0.37  | 27  | 1.24   |                    | 0.0864                             |                 |                        |                  |                              |                     | -3.95 |
| 0.19  | 28  | 0.71   |                    |                                    | 0.0488          |                        |                  |                              |                     |       |
| 0.29  | 26  | 0.46   |                    |                                    | 0.0282          |                        |                  | 2.00                         |                     |       |
| 0.37  | 28  | -9.60  |                    |                                    | 0.0641          |                        |                  |                              | 1.21                |       |
| 0.25  | 28  | 0.19   |                    |                                    | 0.0454          |                        |                  |                              |                     | 2.67  |

**Table 3.10  $\log \eta_{Td}$  Correlated with Compositional Parameters**

| $\log \eta_{Td}$ as Dependent Variable: Regression Coefficients for Independent Variables |     |             |                    |                                    |                 |                        |                  |                              |                     |      |
|---|-----|-------------|--------------------|------------------------------------|-----------------|------------------------|------------------|------------------------------|---------------------|------|
| $R^2$   | $N$ | y Intercept | $M_n$<br>(daltons) | Heptane<br>Asphal-<br>tenes<br>(%) | SPSECI Fraction |                        |                  | Computed Indexes             |                     |      |
|   |     |             |                    |                                    | Volume<br>(%)   | $\log \eta$<br>at 25°C | Gaestel<br>Index | Carbon/<br>Hydrogen<br>Ratio | Heteroatom<br>Index |      |
| 0.53  | 26  | 9.24        | -0.0001            | 0.0748                             |                 |                        |                  |                              |                     |      |
| 0.49  | 25  | 9.89        | -0.0006            | 0.0734                             |                 |                        | -0.54            |                              |                     |      |
| 0.57  | 26  | 3.57        | -0.0003            | 0.0764                             |                 |                        |                  | 0.636                        |                     |      |
| 0.57  | 26  | 9.21        | -0.0001            | 0.0742                             |                 |                        |                  |                              |                     | 0.11 |
| 0.52  | 27  | 11.2        | -0.0029            |                                    | 0.0821          |                        |                  |                              |                     |      |
| 0.57  | 25  | 11.1        | -0.0027            |                                    | 0.0666          |                        |                  | 0.66                         |                     |      |
| 0.59  | 27  | 3.45        | -0.0025            |                                    | 0.0873          |                        |                  |                              | 0.872               |      |
| 0.53  | 27  | 10.30       | -0.0021            |                                    | 0.0702          |                        |                  |                              |                     | 2.21 |
| 0.38  | 26  | 9.26        |                    |                                    |                 |                        |                  | 2.98                         |                     |      |
| 0.08  | 28  | 3.83        |                    |                                    |                 |                        |                  |                              | 0.776               |      |
| 0.34  | 28  | 8.81        |                    |                                    |                 |                        |                  |                              |                     | 6.53 |

(cont'd)

Table 3.10  $\log \eta_{Td}$  Correlated with Compositional Parameters (cont'd)

| $\log \eta_{Td}$ as Dependent Variable: Regression Coefficients for Independent Variables |     |               |                    |                                    |                 |                        |                  |                              |                     |
|---|-----|---------------|--------------------|------------------------------------|-----------------|------------------------|------------------|------------------------------|---------------------|
| $R^2$   | $N$ | $y$ Intercept | $M_n$<br>(daltons) | Heptane<br>Asphal-<br>tenes<br>(%) | SPSECI Fraction |                        |                  | Computed Indexes             |                     |
|   |     |               |                    |                                    | Volume<br>(%)   | $\log \eta$<br>at 25°C | Gaestel<br>Index | Carbon/<br>Hydrogen<br>Ratio | Heteroatom<br>Index |
| 0.10  | 27  | 11.5          | -0.0014            |                                    |                 |                        |                  |                              |                     |
| 0.48  | 18  | 13.6          | 0.0010             |                                    | -0.523          |                        |                  |                              |                     |
| 0.53  | 27  | 9.1           |                    | 0.0760                             |                 |                        |                  |                              |                     |
| 0.48  | 26  | 9.20          |                    | 0.0737                             |                 |                        | -0.14            |                              |                     |
| 0.57  | 27  | 4.52          |                    | 0.0741                             |                 |                        |                  | 0.556                        |                     |
| 0.53  | 27  | 9.04          |                    | 0.723                              |                 |                        |                  |                              | 0.51                |
| 0.18  | 28  | 9.31          |                    |                                    | 0.0477          |                        |                  |                              |                     |
| 0.43  | 26  | 8.83          |                    |                                    | 0.0248          |                        | 2.79             |                              |                     |
| 0.37  | 28  | -1.52         |                    |                                    | 0.0638          |                        |                  | 1.27                         |                     |
| 0.46  | 26  | 8.12          |                    |                                    | 0.0400          |                        |                  |                              | 6.01                |

**Table 3.11  $H(\tau)_{\text{mode}}$  Correlated with Compositional Parameters (cont'd)**

| $H(\tau)_{\text{mode}}$ as Dependent Variable: Regression Coefficients for Independent Variables |     |             |                    |                                    |                 |                       |                  |                              |                     |      |
|--|-----|-------------|--------------------|------------------------------------|-----------------|-----------------------|------------------|------------------------------|---------------------|------|
| $R^2$  | $N$ | y Intercept | $M_n$<br>(daltons) | Heptane<br>Asphal-<br>tenes<br>(%) | SPSECI Fraction |                       | Computed Indexes |                              |                     |      |
|  |     |             |                    |                                    | Volume<br>(%)   | log $\eta$<br>at 25°C | Gaestel<br>Index | Carbon/<br>Hydrogen<br>Ratio | Heteroatom<br>Index |      |
| 0.009  | 26  | -2.49       |                    |                                    |                 |                       | -0.90            |                              |                     |      |
| 0.253  | 26  | -4.07       |                    |                                    |                 |                       |                  | -4.58                        |                     | 12.8 |
| 0.01   | 27  | -2.49       |                    | -0.0180                            |                 |                       |                  |                              |                     |      |
| 0.03   | 26  | -2.55       |                    | 0.0702                             |                 |                       |                  | -3.88                        |                     |      |
| 0.36   | 27  | -4.67       |                    | -0.158                             |                 |                       |                  |                              |                     | 19.4 |
| 0.19   | 28  | -0.96       |                    |                                    | 0.0903          |                       |                  |                              |                     |      |
| 0.16   | 26  | -0.99       |                    |                                    | -0.0868         |                       |                  |                              | -0.21               |      |
| 0.32   | 28  | -2.46       |                    |                                    | -0.100          |                       |                  |                              |                     | 7.64 |

Table 3.12  $AI_{vis60}$  Correlated with Compositional Parameters

| $R^2$ | $N$ | $y$ Intercept | $M_n$<br>(daltons) | $AI_{vis60}$ as Dependent Variable: Regression Coefficients for Independent Variables |                 |                        |                  | Computed Indexes             |                     |
|-------|-----|---------------|--------------------|---|-----------------|------------------------|------------------|------------------------------|---------------------|
|       |     |               |                    | Heptane<br>Asphal-<br>tenes<br>(%)  | SPSECI Fraction | $\log \eta$<br>at 25°C | Gaestel<br>Index | Carbon/<br>Hydrogen<br>Ratio | Heteroatom<br>Index |
| 0.60  | 25  | 0.89          | 0.0004             | 0.0709  |                 |                        |                  |                              |                     |
| 0.62  | 25  | 0.58          | 0.0006             | 0.0435  |                 |                        | 1.57             |                              |                     |
| 0.67  | 25  | 7.78          | -0.0003            | 0.0629  |                 |                        |                  | -0.738                       |                     |
| 0.60  | 25  | 1.13          | 0.0001             | 0.0768  |                 |                        |                  |                              | -0.96               |
| 0.56  | 25  | 2.97          | -0.0023            |   | 0.0709          |                        |                  |                              |                     |
| 0.68  | 25  | 1.37          | -0.0007            |   | 0.0428          |                        | 2.18             |                              |                     |
| 0.64  | 25  | 9.71          | -0.0027            |   | 0.0623          |                        |                  | -0.747                       |                     |
| 0.57  | 25  | 2.53          | -0.0019            |   | 0.0654          |                        |                  |                              | 1.02                |
| 0.22  | 25  | 2.65          |                    |   | 0.0416          |                        |                  |                              | -0.133              |

(cont'd)



**Table 3.12  $AI_{vis60}$  Correlated with Compositional Parameters (cont'd)**

|       |     | $AI_{vis60}$ as Dependent Variable: Regression Coefficients for Independent Variables |                    |                                    |                 |                        |                  |                              |                     |       |
|-------|-----|---|--------------------|------------------------------------|-----------------|------------------------|------------------|------------------------------|---------------------|-------|
| $R^2$ | $N$ | $y$ Intercept   | $M_n$<br>(daltons) | Heptane<br>Asphal-<br>tenes<br>(%) | SPSECI Fraction |                        | Computed Indexes |                              |                     |       |
|       |     |   |                    |                                    | Volume<br>(%)   | $\log \eta$<br>at 25°C | Gaestel<br>Index | Carbon/<br>Hydrogen<br>Ratio | Heteroatom<br>Index |       |
| 0.10  | 25  | 3.35  | -0.0011            |                                    |                 |                        |                  |                              |                     |       |
| 0.46  | 17  | 4.65  | -0.0006            |                                    |                 | -0.384                 |                  |                              |                     |       |
| 0.58  | 26  | 1.37  |                    | 0.0652                             |                 |                        |                  |                              |                     |       |
| 0.60  | 25  | 1.32  |                    | 0.0444                             |                 |                        | 1.08             |                              |                     |       |
| 0.67  | 25  |   |                    | 0.0663                             |                 |                        |                  | -0.657                       |                     |       |
| 0.60  | 25  | 1.52  |                    | 0.0768                             |                 |                        |                  |                              |                     | -1.47 |
| 0.22  | 25  | 1.50  |                    |                                    | 0.0940          |                        |                  |                              |                     |       |
| 0.67  | 25  | 0.80  |                    |                                    | 0.0325          |                        | 2.71             |                              |                     |       |
| 0.48  | 25  | 0.62  |                    |                                    | 0.0389          |                        |                  |                              |                     | 4.41  |

**Table 3.13 Correlations between Heteroatom Content and Selected Chemical and Physical Properties of Core Asphalts Using Simple Linear Regression**

| Physical Property                | $r^2$ (Coefficient of Determination) | $P$ (Observed Significance Level) |
|----------------------------------|--------------------------------------|-----------------------------------|
| Dielectric Constant <sup>1</sup> | 0.919                                | <0.001                            |
| Polarity <sup>2</sup>            | 0.896                                | 0.053                             |
| Relative Viscosity <sup>3</sup>  | 0.806                                | 0.002                             |
| Asphaltene Content <sup>4</sup>  | 0.848                                | 0.001                             |

Note: Heteroatom content is sum of weight percents of nitrogen, oxygen, and sulfur in an asphalt, each divided by their respective atomic weight.

<sup>1</sup> Determined at Pennsylvania State University.

<sup>2</sup> Discussed in volume 2, chapter 5.

<sup>3</sup> Obtained by dividing viscosities of tank asphalts at 25°C (77°F) by viscosities of their IEC neutral fractions at 25°C (77°F)

<sup>4</sup> Determined by *n*-heptane precipitation.

**Table 3.14 Correlations between Defining Temperature and Combinations of Chemical Properties of Core Asphalts Using Simple Linear Regression**

| Chemical Properties                                    | $r^2$ (Coefficient of Determination) | $P$ (Observed Significance Level) |
|--|--------------------------------------|-----------------------------------|
| Activation energy of viscous flow ( $E_a$ )            | 0.772                                | 0.004                             |
| Polydispersity index ( $M_w/M_n$ ), asphalt            | 0.930                                | <0.001                            |
| $M_w$ , asphalt  | 0.501                                | 0.050                             |
| $M_n$ , asphalt  | 0.380                                | 0.104                             |
| $M_n$ , IEC neutral fraction                           | 0.577                                | 0.029                             |
| Asphaltene content                                     | 0.788                                | 0.003                             |
| Gaestel index  | 0.831                                | 0.002                             |
| Heithaus $P$ value                                     | 0.585                                | 0.045                             |
| Heithaus $p_a$ value                                   | 0.636                                | 0.032                             |
| Carbon number maximum, SFC                             | 0.833                                | 0.002                             |
| Carbon number distribution, SFC                        | 0.699                                | 0.010                             |
| $M_w$ , asphalt, plus Gaestel index                    | 0.934                                | 0.001                             |
| Carbon number maximum, SFC, plus Gaestel index         | 0.916                                | 0.002                             |
| $M_n$ , and H/C, IEC neutral, plus $M_w/M_n$ , asphalt | 0.982                                | 0.001                             |

**Table 3.15 Correlations between Crossover Frequency and Combinations of Chemical Properties of Core Asphalts Using Simple Linear Regression**

| Chemical Properties                                 | $r^2$ (Coefficient of Determination) | $P$ (Observed Significance Level) |
|---|--------------------------------------|-----------------------------------|
| Asphaltene compatibility index (ACI)                | 0.572                                | 0.030                             |
| Heithaus $P$ value                                  | 0.662                                | 0.026                             |
| Heithaus $p_a$ value                                | 0.803                                | 0.006                             |
| Polydispersity index ( $M_w/M_n$ )                  | 0.692                                | 0.010                             |
| Asphaltene content plus H/C of IEC neutral fraction | 0.896                                | 0.004                             |

**Table 3.16 Correlations between Rheological Index and Combinations of Chemical Properties of Core Asphalts Using Simple Linear Regression**

| Chemical Properties  | $r^2$ (Coefficient of Determination) | $P$ (Observed Significance Level) |
|--|--------------------------------------|-----------------------------------|
| H/C of IEC neutral fraction                                      | 0.573                                | 0.030                             |
| $M_n$ plus Heithaus $p_a$ value                                  | 0.838                                | 0.026                             |
| $M_n$ plus ACI value   | 0.795                                | 0.019                             |
| H/C of IEC neutral fraction plus mass fraction of SEC fraction I | 0.772                                | 0.025                             |
| Heteroatom content plus $M_n$ and H/C of IEC neutral fraction    | 0.911                                | 0.014                             |

## Summary

One of the major objectives of this Strategic Highway Research Program (SHRP) project was to develop test methods that could be used to characterize the performance-related physical properties of asphalt cement binders so that a performance-related binder specification could be developed and so that rational relationships could be developed between asphalt chemistry and pavement performance. A linear viscoelastic (LVE) representation was chosen to characterize the rheological properties of asphalt binders, and fracture properties were characterized through a newly developed direct tension test. The LVE characterization allowed development of a rheological model that results in parameters that can be related to the microstructural model parameters and, in turn, to asphalt chemistry. The rheological model that was developed is based on work done by others. Parameters in the model include a shape parameter that describes the sensitivity of the moduli and phase angle to changes in frequency or time of loading, a location parameter that describes overall hardness, and a glassy modulus that is common to all asphalt cement binders.

Temperature dependence was shown to be separable from time dependence, and three regions of temperature dependence were described: a low-temperature region below the defining or glass transition temperature, an intermediate region in which viscoelastic behavior predominates, and the Newtonian region in which the phase angle approximates 90 degrees. The temperature dependence in both the Newtonian region and the low-temperature region is described by Arrhenius equations. In the viscoelastic region, the Williams-Landers-Ferry (WLF) equation appropriately describes the temperature dependence of asphalt cement. The addition of modifiers, especially polymer modifiers, disrupts the behavior of asphalt cement so that the hyperbolic-shaped rheological model described above is no longer valid. Because the plateau-region exhibited by polymer modifiers is reflected in modified asphalt cements, the hyperbolic-shaped model is not valid for polymer-modified asphalt cements. This effect caused researchers to abandon the use of a rheological model in the specifications and, instead, point measurements at critical pavement temperatures were recommended for the specification criteria.

To describe the low-temperature rheological behavior of asphalt cement binders, a new test, the bending beam rheometer, was developed. This test procedure was developed early in the project before the low-cost and widespread applicability of dynamic shear rheometers was realized. The bending beam rheometer is appropriate for testing materials with stiffness

values greater than 1 MPa. Measurements made with the bending beam rheometer are extensional, but they can be related to the shear measurements obtained with the dynamic shear rheometer. Therefore, the dynamic shear rheometer provides useful specification information at intermediate and high temperatures at loading rates of 10 rad/s which are relevant to traffic-induced loadings. The bending beam rheometer is appropriate for creep measurements at low temperatures at which thermal cracking predominates and isothermal physical hardening occurs. Interconvertibility between creep and dynamic shear measurements was demonstrated during the project.

Another new test, the direct tension test, was developed to characterize the low-temperature direct tension failure properties of asphalt cement binders. Using this new test, which is based on a noncontact laser extensometer, failure strains as small as 0.05 percent were recorded. The direct tension test provides a very convenient method of determining the temperature at which the asphalt cement binder exhibits a transformation from brittle-ductile to brittle behavior. This transition, at a given rate of deformation, is typically experienced within a temperature range of 5°C to 10°C (9°F to 18°F). Thus, the direct-tension test is an excellent means of determining the temperature at which the asphalt cement binder undergoes a transition from a brittle to a ductile-brittle failure. Ideally, the pavement service temperature should be above this transition temperature. Previous researchers have shown a unique relationship between the stiffness of asphalt cement and the strain at failure. This unique relationship was verified for plain asphalt cements; however, the relationship was shown to be invalid for many modified asphalt cements.

The pressure-aging vessel (PAV) test as developed by previous researchers was refined for use as a specification test. The test was shortened to 20 hours of exposure time, with exposure temperatures adjusted according to the climate. Specification criteria for fatigue and low-temperature cracking are based on measurements made on PAV residue.

Another major finding during the project was the discovery of low-temperature physical hardening. This phenomenon occurs when the time-dependent volume shrinkage of the asphalt cement is delayed so that equilibrium free volume is not obtained instantaneously. Time-dependent volume shrinkage results in a time-dependent increase in modulus when the asphalt cement is held at a constant temperature. This phenomenon, which is well-known for polymers and other organic materials, has significant implications for testing procedures, and repeatability is also of potential significance with respect to field performance. No direct link between low-temperature isothermal physical hardening and field performance was established during the project, and therefore it was necessary to include this phenomenon only as an informational feature in the recommended binder specification. Further research is needed to determine the significance of low-temperature physical hardening with respect to field performance and with respect to the microstructural parameters that affect low-temperature physical hardening.

The rheological studies conducted as part of this project were related to a microstructural model. The observed rheological behavior requires a model that accounts for the overall magnitude and distribution of polarity and molecular weight. The rheological properties of the asphalt cement are, in the main, governed by both molecular weight and polarity as well as their distribution. The rheological properties, as quantified by the rheological model and

the parameters that describe the model, do not require associated domains within the asphalt cement; however, molecular interactions, as well as molecular size, are essential to explain rheological behavior. Fractional free volume was also shown to be an important microstructural consideration in the explanation of the physical behavior of asphalt cement.

The physical property tests defined during the course of the project--dynamic shear rheology, creep rheology, and direct tension failure properties--were used to develop a performance-related binder specification. The binder specification was developed as a means for specifying and controlling asphalt binders and is applicable to both plain and modified binders. Test measurements are conducted on tank material, rolling thin-film oven (RTFO) test (ASTM D 2872) residue, and PAV residue as appropriate for the different performance criteria considered in the specification. Tank material and RTFO test residue are used to determine the contribution offered by the as-placed binder to rutting resistance, with full recognition that the aggregate is the primary mixture component responsible for rutting resistance. Fatigue and low-temperature binder specification criteria are based on PAV residue, once again recognizing that mixture design also plays an important role in each of these distress modes. The rutting criterion is based on the nonrecoverable binder deformation, and the fatigue criterion is based on the energy dissipated in the binder during each loading cycle. Low-temperature thermal cracking is addressed by specifying the stiffness and rate of change of stiffness with time (time dependence) at the lowest pavement service temperature. In addition, the direct tension test was adopted in the specifications as a measure of the extensibility of the asphalt cement at low temperatures. In summary, the rheological and fracture properties of asphalt cements, as selected during the course of the project, can be related successfully to the microstructural model as well as to pavement performance and form the basis for a new asphalt binder specification that is equally applicable to plain and modified asphalts. Thus, the new asphalt binder specification is truly performance-related as well as related to asphalt chemistry.

In the SHRP Binder Characterization and Evaluation Program (A-002A), several separation techniques and analytical methods used in other areas of fossil fuel science were applied to asphalts. Among these techniques are ion exchange chromatography (IEC) and preparative size exclusion chromatography (SEC), as mentioned above. Also developed during the course of the program was a rapid, scaled-down version of the preparative SEC separation method, called *streamlined preparative SEC*. The novel technique of supercritical fluid chromatography was used to determine carbon number distributions of asphalt solvent moieties. Potentiometric titration of asphalts and asphalt fractions was used to verify many aspects of the microstructural model. This technique showed that maltenes, as defined by solvent precipitation of asphaltenes, may not be good models for asphalt solvent moieties.

The above methods were used to develop chemical indexes to predict performance-related physical properties. They were also useful in developing a better understanding of asphalt structure. Correlations of observed physical properties with the observed chemical properties of asphalts were sought throughout this project. Many strong correlations were found; generally, any given physical property was found to be governed by a multiplicity of chemical properties, as is typical in complex mixtures of chemical structures. These correlations are described in detail in chapter 3. Two of the most important chemical parameters were found to be the overall polarity of an asphalt, as defined by polarity factors,

and the number-average molecular weight ( $M_n$ ) of the solvent moiety, as defined by IEC separation. The polarity indexes (volume 2, chapter 5) developed are an improvement over estimations of polar interactions by asphaltene content alone. The neutral fractions isolated by IEC appear to approximate the predicted properties of asphalt solvent moieties better than maltenes obtained by solvent precipitation of asphaltenes. Number-average molecular weight data for IEC neutral fractions can be used as property predictors, whereas  $M_n$  values for whole asphalts are of limited utility. The reason for this is discussed in volume 2.

Properties of defined chemical fractions of asphalts and their effects on rheological properties were verified by model compound studies. Rheological properties of mixtures comprising fractions from different asphalts were observed to vary greatly but could be rationalized by consideration of polarity factors.

The overall chemical makeup of asphalts studied in the Binder Characterization and Evaluation Program did not vary greatly. Nonpolar molecules dominated all asphalts, and polar fractions—including acidic, basic, and amphoteric fractions—were found in varying amounts in the materials studied. Amphoteric materials are the viscosity-enhancing components of asphalts. More than any other class of materials, these polar, aromatic molecules could be reasonably equated with goodies or stickies. Since no asphalts from before 1970 were analyzed, such a judgment cannot be made with confidence. From what is known of the composition data of asphalts of that time, no major chemical species are absent in contemporary asphalt cements. It is, however, the opinion of most participants in the Binder Characterization and Evaluation Program that goodies and stickies, or components having properties attributable to them, are found in asphalts being made today. The quantities probably are more variable, because of the greater variety of crudes.

A great deal was learned about oxidative aging of asphalts. The mechanism of oxidative aging of asphalts was not well understood before the beginning of the SHRP Binder Characterization and Evaluation Program. Knowledge of the details of the oxidation will assist in the design of a realistic aging test, in choosing asphalts to avoid premature age hardening, and in the design of additives to inhibit aging.

Chemiluminescence (CL) was detected in asphalts in the presence of oxygen. This finding demonstrates that components of asphalt react with oxygen to form peroxy radicals. Other asphalt components, almost certainly phenols, are free radical inhibitors, as was demonstrated by measuring the inhibition of cumene oxidation in the presence of asphalts and methylated asphalts. The unmethylated asphalts inhibited cumene oxidation, while the methylated asphalts did not. These observations indicate that asphalt oxidation involves radicals, but is not a radical chain process.

Two major products of asphalt oxidation are ketones and sulfoxides. Sulfur compounds in asphalts were demonstrated to be thiophenes and aliphatic sulfides (thioethers). Sulfoxides form only from aliphatic sulfides, so the ratio of thiophenic to aliphatic sulfur determines the eventual amount of sulfoxides formed in asphalt aging. It also was shown that sulfides do not react with oxygen directly. Sulfides react with reactive intermediates resulting from the direct reaction of asphalt components with oxygen. The reactive intermediates appear to be independent of the aliphatic sulfides and are fairly abundant. When the model compound

dimethyl sulfide (DMS) was heated in the presence of oxygen, no sulfoxide was formed. When DMS was heated in the presence of oxygen and asphalt, dimethyl sulfoxide was formed. Paradoxically, asphalts appear to contain components that inhibit oxidation (phenols) and other components whose nature is not known, but that are highly reactive with oxygen.

Measurements of carbonyl content and sulfoxides formed during asphalt oxidation fell far short of actual oxygen uptake. Apparently, there are oxidation products other than those mentioned above. Oxidation rates, based on oxygen uptake data, vary by only a factor of 2 among several asphalts.

Based on the above findings, it appears that some highly reactive asphalt components combine with oxygen to form peroxy radicals. These radicals then react with aliphatic sulfur compounds to form sulfoxides and also eventually form carbonyl compounds.

The oxidative aging of asphalt is a primary cause of asphalt hardening in pavements, thus contributing to various forms of pavement cracking. Although the changes in asphalt physical properties upon oxidative aging primarily result from the formation of oxygen-containing functional groups in the asphalt and an increase in microstructure, the sensitivity of an asphalt to these oxidation products and the subsequent microstructure formation varies widely with asphalt source (composition). An understanding of the kinetics of oxidation in the pavement temperature range is confounded by both the complex composition of asphalt and its thermally reversible microstructure. To better understand the mechanisms of age hardening, the kinetics of asphalt oxidation were investigated from the pavement temperature range, 60°C (140°F), through the higher temperature range of commonly used accelerated laboratory tests, 130°C (266°F). It was found that asphalts with different component compatibilities may exhibit similar age-hardening kinetics in the low end of the pavement temperature range but quite different kinetics in the high end. This is because the aging kinetics become highly dependent on how temperature affects the molecular microstructure. A new microstructural model of the age hardening of asphalt cement was determined that proposes that the kinetics of aging in the pavement temperature range are largely governed by physical-chemical factors related to the state of dispersion of the molecular microstructure rather than the inherent reactivity of the molecular components with oxygen.

The results from the kinetic aging experiments performed during the Binder Characterization and Evaluation Project and results from pavement aging studies in the literature showed that the changes in physical properties of asphalts with aging time produce a parabolic plot. The magnitude of the long-term change in physical properties is a function of temperature and asphalt composition (source). On the basis of the data from the chemistry and kinetics of asphalt aging, the PAV test for long-term aging of asphalt will effectively rank asphalts according to their inherent tendency to age-harden in the field if the test is conducted as near as possible to the maximum pavement temperature expected and if measurements are not taken until the asphalt has reached a viscosity as near as practical to the plateau region of the parabolic viscosity kinetic curve. It is also important to know the aging characteristics of an asphalt being selected for pavement service as a function of temperature so that the asphalt can be properly matched with the climate in which it will be used.



Statistical analysis of the aging data with other chemical and physical property data indicated that there are group relationships. No obvious correlations with aging were found involving any gross properties of asphalts. This result is not surprising because such a correlation would have been discovered long ago. Aging is dependent on a subtle interplay among many factors, as has been shown previously. Because aging is a combination of oxidation, loss of volatiles, and the response of the system to the first two factors, a complicated dependence is hardly surprising. It was noted during the statistical analysis that each asphalt seemed to be characterized by a response to one predominant factor but that this predominant factor differed among asphalts.

When asphalts were aged after being coated on aggregate surfaces, the amount of oxygen-containing functional groups formed during aging was essentially the same regardless of asphalt-aggregate combinations and was also about the same as the concentrations observed when aging neat asphalts. The largest difference was observed in asphalt AAG-1, for which the carbonyl formed after 144 hours aging on aggregate at 60°C (140°F) was in the range of 0.18 to 0.20 absorbance units on the three aggregates tested, compared with 0.12 absorbance units in the aged neat asphalt.

The viscosity change observed in an asphalt after aging on aggregate and after thermal annealing was also different for some asphalt-aggregate combinations compared with the neat asphalt alone. It appeared that the asphalts most prone to microstructure formation exhibited less viscosity change when aged on aggregate and that the asphalts less prone to microstructure formation showed more viscosity change when aged on aggregate. However, the differences in viscosity change between asphalt-aggregate aging and neat asphalt aging were not large in any of the cases tested. There were also some cases noted in which differences were observed in asphalt aging when different aggregates were compared, but these differences were also relatively small.

By now it should be obvious that a comprehensive model of petroleum asphalt must be rather liberal or broad based. The argument should be yet more convincing after examination of volumes 2 and 3. Asphalts, quite simply, are rather variable from one stock to another, and the description of a given asphalt, in terms of the current model, must include measured parameters that are specific to that asphalt. Major differences in the relative importance of the various chemical properties or physical (performance) properties have been and will continue to be seen. Quite simply, the word *asphalt* refers to a large collection of quite variable materials.

## References

- Al-Jarrah, M.M.F., and A.H. Al-Dujaili (1989). "Characteristics of Some Iraqi Asphalts II: New Findings on the Physical Nature of Asphaltenes," *Fuel Sci. Tech. Intl.*, vol. 7, pp. 69–88.
- Altgelt, K.H., and O.L. Harle (1975). "The Effect of Asphaltenes on Asphalt Viscosity," *Industrial & Engineering Chemistry, Prod. R&D*, vol. 14, pp. 240–246.
- Andersen, S.I., and K.S. Birdi (1991). "Aggregation of Asphaltenes as Determined by Calorimetry," *Colloid Interface Sci.*, vol. 142, pp. 497–502.
- Andersen, S.I. (1992). "Hysteresis in Precipitation and Dissolution of Petroleum Asphaltenes," *Fuel Sci. Tech. Intl.*, vol. 10, pp. 1743–1749.
- Anderson, D.A., E.L. Dukatz, and J.L. Rosenberger (1983). "Properties of Asphalt Cement and Asphaltic Concrete," *Proc. Assoc. Asph. Pav. Technol.*, vol. 52, pp. 291–324.
- Anderson, D.A., D.R. Luhr, C.E. Antle, Z. Siddiqui, E.G. Fernando, T. Chizewick, and J.P. Tarris (1990). *Performance-Related Specification for Hot-Mix Asphaltic Concrete. Final Report, August*, Project No. HR-10-26A, Pennsylvania Trans. Inst., Univ. Park, PA, PTI 8805.
- Anderson, D.A., D.W. Christensen, and H.B. Bahia (1991). "Physical Properties of Asphalt Cement and the Development of Performance Related Specifications," *Proc. Assoc. Asph. Pav. Technol.*, vol. 60, pp. 291–324.
- ASTM. "Standard Test Method for Effect of Heat and Air on Asphaltic Materials (Thin-Film Oven Test)," *Annual Book of ASTM Standards*, D 1754-87, vol. 04.03, Philadelphia, PA, 1991.
- ASTM. "Standard Test Method for Effect of Heat and Air on a Moving Film of Asphalt (Rolling Thin-Film Oven Test)," *Annual Book of ASTM Standards*, D 2872-88, vol. 04.03, Philadelphia, PA, 1991.

- ASTM. "Standard Test Method for Viscosity Determination of Unfilled Asphalts Using the Brookfield Thermosel Apparatus," *Annual Book of ASTM Standards*, D 4402-87, vol. 04.04, Philadelphia, PA, 1988.
- Bahia, H.V., and D.A. Anderson (1992). "Physical Hardening of Paving Grade Asphalts as Related to Compositional Characteristics," *Preprints, Div. Fuel Chem., Am. Chem. Soc.*, vol. 37, pp. 1397-1407.
- Bandurski, E. (1982). "Structural Similarities between Oil-Generating Kerogens and Petroleum Asphaltenes," *Ener. Sources*, vol. 6, pp. 47-64.
- Barth, E.J. (1962). *Asphalt Science and Technology*. Gordon and Breach, New York.
- Behar, F., R. Pelet, and J. Roucache (1984). "Geochemistry of Asphaltenes," *Org. Geoch.*, vol. 6, pp. 587-595.
- Boduszynski, M.M., and C.A. and K.H. Altgelt (1991). "Composition of Heavy Petroleum—Significance of the Extended Atmospheric Boiling Point (AEBP) Scale," Presented at Confab 91, Granby, CO, August 5-9.
- Bukka, K., J.D. Miller, and A.G. Oblad (1991). "Fractionation and Characterization of Utah Tar Sand Bitumens: Influence of Chemical Composition on Bitumen Viscosity," *Ener. Fuels*, vol. 5, pp. 333-340.
- Bunger, J.W., and N.C. Li, eds. (1981). *Chemistry of Asphaltenes*. Adv. Chem. Ser., Am. Chem. Soc., Washington, DC, vol. 195.
- Button, J.W., and J.A. Epps (1985). "Identifying Tender Asphalt Mixtures in the Laboratory," *Trans. Res. Rec.*, vol. 1034, pp. 20-26.
- Chandrasekhar, S. (1982). "Liquid Crystals of Dislike Molecules," in *Advances in Liquid Crystals*, G.H. Brown, ed. Academic Press, Inc., New York, vol. 5, pp. 47-78.
- Christensen, D.W., and D.A. Anderson (1992). "Interpretation of Dynamic Mechanical Test Data for Paving Grade Asphalt," *Proc. Assoc. Asph. Pav. Technol.*, vol. 61, pp. 67-116.
- Corbett, L.W., and H.E. Schweyer (1981). "Composition and Rheology Considerations in Age Hardening of Bitumen," *Proc. Assoc. Asph. Pav. Technol.*, vol. 50, pp. 571-582.
- Desbene, P.L., D. Lambert, J.J. Basselier, and R. Boulet (1988). "Etude Analytique des Produits Lourds du Pétrole IV: Asphaltenes, Réalité ou Fiction?" *Analysis*, vol. 16, pp. 478-483.

- Dickinson, E.J., and H.P. Witt (1974). "The Dynamic Shear of Paving Asphalts as a Function of Frequency," *Transactions Soc. Rheology*, vol. 18, pp. 591–606.
- Dobson, G.R. (1972). "On the Development of Rational Specifications for the Rheological Properties of Bitumens," *Inst. Petrol. Technol.*, vol. 58, pp. 14–24.
- Doolittle, A.K., and D.B. Doolittle (1957). "Studies in Newtonian Flow, V: Further Verification of the Free Space Viscosity Equation," *Appl. Phys.*, vol. 28, pp. 901–905.
- Dwiggins, C.W., Jr. (1978). "Study of the Colloidal Nature of Petroleum with an Automated Bonse-Hart X-Ray Small-Angle Scattering Unit," *Appl. Cryst.*, vol. 11, pp. 615–619.
- Eldib, I.A., H.N. Dunning, and R.J. Bolen (1960). "Nature of Colloidal Materials in Petroleum," *Chem. Eng. Data*, vol. 5, pp. 550–553.
- El-Mohamed, S., M.F. Archard, F. Hardouin, and H. Gasparoux (1986). "Correlations between Diamagnetic Properties and Structural Characters of Asphaltenes and Other Heavy Petroleum Products," *Fuel*, vol. 65, pp. 1501–1504.
- Ensley, Keith E. (1975). "A Kinetic Investigation of Association in Asphalt," *Colloid Interface Sci.*, vol. 53, pp. 452–460.
- Ferry, J.D. (1980). *Viscoelastic Properties of Polymers*, 3rd ed. Wiley, New York.
- Girdler, R.B. (1965). "Constitution of Asphaltenes and Related Studies," *Proc. Assoc. Asph. Pav. Technol.*, vol. 34, pp. 45–79.
- Goulon, J., C. Esselin, P. Friant, C. Berthe, J.F. Muller, J.L. Poncet, R. Guillard, J.C. Escalier, and B. Neff (1984). "Structural Characterization by X-Ray Absorption Spectroscopy (EXAFS/XANES) of the Vanadium Chemical Environment in Various Asphaltenes," in *Symposium on Characterization of Heavy Crude Oils and Petroleum Residues*. Editions Technip, Paris, pp. 158–163.
- Griffin, R.L., T.K. Miles, C.J. Penther, and W.C. Simpson (1956). "Sliding Plate Microviscometer for Rapid Measurement of Asphalt Viscosity in Absolute Units," *Am. Soc. Test. Matl., Special Tech. Publ.*, vol. 212, pp. 36ff.
- Haas, R.C.G., and T.H. Topper (1969). "Thermal Fracture Phenomena in Bituminous Surfaces," *Highway Res. Board Special Rep.*, Nat. Res. Coun., Washington, DC, vol. 101, pp. 136–153.
- Hagen, A.P., R. Jones, R.M. Hofener, B.B. Randolph, and M.P. Johnson (1984). "Characterization of Asphalt by Solvent Profile," *Proc. Assoc. Asph. Pav. Technol.*, vol. 53, pp. 119–137.

- Halstead, W.J., and J.A. Zenewitz (1961). "Changes in Asphalt Viscosities during the Thin Film Oven and Microfilm Durability Tests," *Am Soc. Test. Matl., Special Tech. Publ.*, vol. 309, pp. 133ff.
- Herzog, P., D. Tchoubar, and D. Espinat (1988). "Macrostructure of Asphaltene Dispersions by Small-Angle X-Ray Scattering," *Fuel*, vol. 67, pp. 245–250.
- Heukelom, W. (1966). "Observations on the Rheology and Fracture of Bitumens and Asphalt Mixes," *Proc. Assoc. Asph. Pav. Technol.*, vol. 36, pp. 359–397.
- Jennings, P.W., J.A. Pribanic, B. Faconi, and D.L. van der Hart (1991). *Binder Characterization and Evaluation by Nuclear Magnetic Resonance Spectroscopy*. SHRP Report no. A-335, Washington, DC.
- Jirgensons, B., and M.E. Straumanis (1962). *A Short Textbook of Colloid Chemistry*. Macmillan, New York.
- Jongepier, R., and B. Kuilman (1969). "Characteristics of the Rheology of Bitumens," *Proc. Assoc. Asph. Pav. Technol.*, vol. 38, pp. 98–122.
- Katz, D.L., and K.E. Beau (1945). "Nature of Asphaltic Substances," *Ind. Eng. Chem.*, vol. 37, pp. 195–200.
- Kim, O.K., C.A. Bell, J.E. Wilson, and G. Boyle (1987). "Development of Laboratory Oxidative Aging Procedures for Asphalt Cements and Asphalt Mixtures," *Trans. Res. Rec.*, vol. 1115, pp. 101–112.
- King, G.N., O. Harders, and P. Chaverot (1992). "Influence of Asphalt Grade and Polymer Concentration on the High Temperature Performance of Polymer Modified Asphalt," *Proc. Assoc. Asph. Pav. Technol.*, vol. 61, pp. 98–122.
- Kirk-Othmer Encyclopedia of Chemical Technology* (1981). Wiley, New York.
- Labout, J.W.A. (1950). "Constitution of Asphaltic Bitumen," in *The Properties of Asphaltic Bitumen*, J.P. Pfeiffer, ed. Elsevier, New York, pp. 13–48.
- Lee, D.Y. (1968). "Development of a Laboratory Durability Test for Asphalts," *Hwy. Res. Rec.*, vol. 231, pp. 34–49.
- Long, R.B. (1981). "The Concept of Asphaltenes," in *Chemistry of Asphaltenes*, J.W. Bunge and N.C. Li, eds. Adv. Chem. Ser., Am. Chem. Soc., Washington, DC, vol. 195, pp. 17–27.
- Maccarrone, S. (1987). "Rheological Properties of Weathered Asphalts Extracted from Sprayed Seals Nearing Distress Conditions," *Proc. Assoc. Asph. Pav. Technol.*, vol. 56, pp. 654–687.

- Mack, C.J. (1932). "Colloid Chemistry of Asphalts, *Phys. Chem.*, vol. 36, pp. 2901–2914.
- Majidzadeh, K., and H.E. Schweyer (1965). "Non-Newtonian Behavior of Asphalt Cements," *Proc. Assoc. Asph. Pav. Technol.*, vol. 34, pp. 20–44.
- Maruska, H.P., and B.M.L. Rao (1987). "The Role of Polar Species in the Aggregation of Asphaltenes," *Fuel Sci. Tech. Intl.*, vol. 5, pp. 119–168.
- McGraw-Hill Encyclopedia of Science and Technology* (1982). McGraw-Hill, New York.
- McLeod, N.W. (1972). "A Four Year Survey of Low Temperature Transverse Pavement Cracking on Three Ontario Test Roads," *Proc. Assoc. Asph. Pav. Technol.*, vol. 41, pp. 424–493.
- Moavenzadeh, J., and R.R. Stander, Jr. (1967). "Effect of Aging on Flow Properties of Asphalts," *Hwy. Res. Brd. Rec.*, vol. 178, pp. 1–29.
- Monismith, C.L., G.A. Secor, and K.E. Secor (1965). "Temperature Induced Stresses and Deformations in Asphalt Concrete," *Proc. Assoc. Asph. Pav. Technol.*, vol. 34, pp. 248–285.
- Monismith, C.L., and J.A. Deacon (1969). "Fatigue of Asphalt Paving Mixtures," *Proc. Am. Soc. Civ. Eng., Trans. Eng. J.*, May, TE 2, pp. 317–346.
- Moschopedis, S.E., and J.G. Speight (1976). "Investigation of Hydrogen Bonding by Oxygen Functions in Athabasca Bitumen," *Fuel*, vol. 55, pp. 187–192.
- Moschopedis, S.E., J.F. Fryer, and J.G. Speight (1976). "Investigation of Asphaltene Molecular Weights," *Fuel*, vol. 55, pp. 227–232.
- Nellensteyn, F.J. (1924). "The Constitution of Asphalt," *Inst. Petrol. Technol.*, vol. 10, pp. 311–325.
- Nellensteyn, F.J. (1928). "Relation of the Micelle to the Medium in Asphalt," *Inst. Petrol. Technol.*, vol. 14, pp. 134–138.
- Overfield, R.E., E.Y. Sheu, S.K. Sinha, and K.S. Liang (1989). "SANS Study of Asphaltene Aggregation," *Fuel Sci. Tech. Intl.*, vol. 7, pp. 611–624.
- Park, S.J., and G.A. Mansoori (1988). "Aggregation and Deposition of Heavy Organics in Petroleum Crudes," *Ener. Sources*, vol. 10, pp. 109–125.
- Pell, P.S., and K.E. Cooper (1975). "The Effect of Testing and Mix Variables on the Fatigue Performance of Bituminous Materials," *Proc. Assoc. Asph. Pav. Technol.*, vol. 44, pp. 1–37.

- Pfeiffer, J.P., and P.M. van Doormaal (1936). "The Rheological Properties of Asphaltic Bitumen," *Inst. Petrol. Technol.*, vol. 22, pp. 414ff.
- Pfeiffer, J.P., and R.N.J. Saal (1940). "Asphaltic Bitumen as Colloidal System," *Phys. Chem.*, vol. 44, pp. 139–149.
- Puzinauskas, V.P. (1967). "Evaluation of Properties of Asphalt Cements with Emphasis on Consistencies at Low Temperature," *Proc. Assoc. Asph. Pav. Technol.*, vol. 36, pp. 489–540.
- Puzinauskas, V.P. (1979). "Properties of Asphalt Cements," *Proc. Assoc. Asph. Pav. Technol.*, vol. 48, pp. 646–710.
- Rao, B.M.L., and J.E. Serrano (1986). "Viscometric Study of Aggregation Interactions in Heavy Oil," *Fuel Sci. Tech. Intl.*, vol. 4, pp. 483–500.
- Ravey, J.C., G. Ducouret, and D. Espinat (1988). "Asphaltene Macrostructure by Small Angle Neutron Scattering," *Fuel*, vol. 67, pp. 1560–1567.
- Ray, B.R., P.A. Witherspoon, and R.E. Grim (1957). "A Study of the Colloidal Characteristics of Petroleum Using the Ultracentrifuge," *Phys. Chem.*, vol. 61, pp. 1296–1302.
- Readshaw, E.E. (1972). "Asphalt Specification in British Columbia for Low Temperature Performance," *Proc. Assoc. Asph. Pav. Technol.*, vol. 42, pp. 562–581.
- Reerink, H., and J. Lijzenga (1975). "Gel-Permeation Chromatography Calibration Curve for Asphaltene and Bituminous Resins," *Anal. Chem.*, vol. 47, pp. 2160–2167.
- Robertson, R.E., J.F. Branthaver, and D.A. Anderson (1991). Quarterly Progress Report, June, SHPR A-002A: "Binder Characterization and Evaluation."
- Rogacheva, O.V., R.N. Rimaev, V.Z. Gubaidullin, and D.K. Khakimov (1980). "Investigation of the Surface Activity of the Asphaltenes of Petroleum Residues," *Kolloidnyi Zhurnal*, vol. 42, pp. 586–589.
- Romberg, J.W., and R.N. Traxler (1947). "Rheology of Asphalt," *Colloid Sci.*, vol. 2, pp. 33–47.
- Rostler, F.S., and R.M. White (1962). "Composition and Changes in Composition of Highway Asphalts, 85-100 Penetration Grade," *Proc. Assoc. Asph. Pav. Technol.*, vol. 31, pp. 35–89.
- Schweyer, H.E., L.L. Smith, and G.W. Fish (1976). "A Constant Stress Rheometer for Asphalt Cements," *Proc. Assoc. Asph. Pav. Technol.*, vol. 45, pp. 53–72.

- Senglet, N., C. Williams, D. Faure, T. Des Courieres, and R. Guillard (1990). "Microheterogeneity Study of Heavy Crude Petroleum by U.V.-Visible Spectroscopy and Small Angle X-Ray Scattering," *Fuel*, vol. 69, pp. 72-77.
- Severs, E.T. (1962). *Rheology of Polymers*. Reinhold Publishing Corp., New York, Chapter 4, "Solid Polymers."
- Shapery, R.A. (1973). *A Theory of Crack Growth in Viscoelastic Media*, Research Report MM 2765-73-1, March, Mechanics and Materials Research Center, Texas A&M Univ., College Station.
- Sheu, E.Y., M.M. DeTar, and D.A. Storm (1991). "Rheological Properties of Vacuum Residue Fractions in Organic Solvents," *Fuel*, vol. 70, pp. 1151-1156.
- Speight, J.G., and S.E. Moschopedis (1977). "Asphaltene Molecular Weights by a Cryoscopic Method," *Fuel*, vol. 56, pp. 344-345.
- Speight, J.G., and S.E. Moschopedis (1981). "On the Molecular Nature of Petroleum Asphaltenes," in *Chemistry of Asphaltenes*, J.W. Bunger and N.C. Li, eds. Adv. Chem. Ser., Am. Chem. Soc., Washington, DC, vol. 195, pp. 1-15.
- Speight, J.G., R.B. Long, and T.D. Trowbridge (1984). "Factors Influencing the Separation of Asphaltenes from Heavy Petroleum Feedstocks," *Fuel*, vol. 63, pp. 616-620.
- Storm, D.A., S.J. DeCanio, M.M. DeTar, and V.P. Nero (1990). "Upper Bound on Number Average Molecular Weight of Asphaltene," *Fuel*, vol. 69, pp. 735-737.
- Storm, D.A., R.J. Baressi, and S.J. DeCanio (1991). "Colloidal Nature of Vacuum Residue," *Fuel*, vol. 70, pp. 779-782.
- Storm, D.A. and E.Y. Sheu (1993). "Rheological Studies of Ratawi Vacuum Residue at 366 K," *Fuel*, vol. 72, pp. 233-237.
- Struik, L.C.E. (1978). *Physical Aging in Amorphous Polymers and Other Materials*. Elsevier Scientific, Amsterdam.
- Traxler, R.N., and H.E. Schwyer (1936). "Increase in Viscosity of Asphalts with Time," *Proc. Am. Soc. Test. Matl.*, vol. 36, pp. 544-551.
- Traxler, R.N., and C.E. Coombs (1937). "Development of Internal Structure in Asphalts with Time," *Proc. Am. Soc. Test. Matl.*, vol. 37, pp. 549-555.
- Traxler, R.N., H.E. Schwyer, and H.W. Romberg (1944). "Rheological Properties of Asphalt," *Ind. Eng. Chem.*, vol. 36, pp. 823-829.



- Traxler, R.N. (1947). "A Review of the Rheology of Bituminous Materials," *Colloid Sci.*, vol. 2, pp. 49-68.
- Traxler, R.N. (1961). *Asphalt: Its Composition, Properties and Uses*. Reinhold, New York.
- Vallerga, B.A. (1980). "Pavement Deficiencies Related to Asphalt Durability," *Proc. Assoc. Asph. Pav. Technol.*, vol. 50, pp. 481-491.
- van der Poel, C. (1954). "A General System Describing the Viscoelastic Properties of Bitumens and Its Relation to Routine Test Data," *Appl. Chem.*, vol. 4, pp. 221-236.
- van Dijk, W. (1975). "Practical Fatigue Characterization of Bituminous Mixes," *Proc. Assoc. Asph. Pav. Technol.*, vol. 44, pp. 37-74.
- Vold, R.D., and M.J. Vold (1983). *Colloid and Interface Chemistry*. Addison-Wesley, Reading, MA.
- Yen, T.F., J.G. Erdman, and S.S. Pollack (1961). "Investigation of the Structure of Petroleum Asphaltenes by X-Ray Diffraction," *Anal. Chem.*, vol. 33, pp. 1587-1594.